

Anthropogenic and Natural Disturbances of the Nitrogen Cycle at Multiple Scales from Local to Global: A Modeling Investigation of Nitrous Oxide and Ammonia Emissions

by

Rongting Xu

A dissertation submitted to the Graduate Faculty of
Auburn University
in partial fulfillment of the
requirements for the Degree of
Doctor of Philosophy

Auburn, Alabama
May 5, 2019

Keywords: The nitrogen cycle, Agricultural systems, Nitrous oxide,
Ammonia, Process-based model

Copyright 2019 by Rongting Xu

Approved by

Hanqin Tian, Chair, Solon Dixon Professor of School of Forestry and Wildlife Sciences
Shufen Pan, Co-Chair, Assistant Professor of School of Forestry and Wildlife Sciences
Yucheng Feng, Professor of College of Agriculture
William D. Batchelor, Professor of College of Agriculture
Stephen A Prior, Lead Scientist and Plant Physiologist of USDA-ARS

Abstract

Nitrogen (N) is an essential element that affects natural vegetation and crop growth in terrestrial and aquatic ecosystems. Meanwhile, N is tightly coupled with carbon and other nutrients (e.g., phosphorous) that influence the structure and functioning of ecosystems in the long-term run. However, “Nitrogen Cascade” has been raised by previous scientists as a substantial amount of reactive N has been introduced into almost all ecosystems across land and oceans. Anthropogenic perturbation of the global N cycle contributed approximately two-thirds of the annual flux of reactive N (Nr) into the atmosphere in the early 21st century. The addition of excess reactive N compounds to terrestrial ecosystems plays a significant role in the enormous emissions of N-containing gases, including oxides of nitrogen (NO_x), nitrous oxide (N_2O), and ammonia (NH_3) in the atmosphere. The high output of these N gases remains a matter of great concern to human health and the environment. Thus, it is essential to understand and quantify how natural and human disturbances have affected the N cycle including these N gas emissions at multiple scales from local to global.

A growing amount of N fertilizer and manure has been applied to agricultural systems since the 1960s. This dissertation focuses on three cutting-edge research issues in the field of global N cycle as follows: First, I investigated how much N fertilizer and manure have been introduced into world’s grasslands. Much attention has been paid to N fertilizer and manure N applications to global cropland, however, there is still a lack of spatially-explicit estimates of continuous time-series datasets of manure and fertilizer N inputs in global grasslands. My research has filled a gap

in global N data sets, which provided a critical data set for global land modeling. Second, this dissertation examined how Nr together with other environmental factors have affected the emissions of N-containing gases (N_2O and NH_3) from agricultural systems at multiple scales during the historical period. Finally, this dissertation has projected NH_3 emissions under future climate change scenarios. More specifically, three global N input datasets I developed at a resolution of $0.5^\circ \times 0.5^\circ$ during 1860–2016 (i.e., annual manure N deposition (by grazing animals) rate, synthetic N fertilizer and N manure application rates) showed that total N inputs, sum of manure N deposition, manure and fertilizer N application, to pastures and rangelands increased from 15 to 101 Tg N yr^{-1} from 1860 to 2016. Manure N deposition accounted for 83% of the total N inputs, whereas manure and fertilizer N application accounted for 9% and 8%, respectively, during 2000–2016.

A coupled Dynamic Land Ecosystem Model (DLEM) with the bi-directional NH_3 exchange module in the Community Multiscale Air-Quality (CMAQ) model (DLEM-Bi- NH_3) was used to estimate and predict NH_3 emissions from N fertilizer/manure application at multiple scales. At the global scale, results showed that the annual increase of NH_3 emissions showed large spatial variations. Southern Asia, including China and India, accounted for more than 50% of total global NH_3 emissions since the 1980s, followed by North America and Europe. In addition, results showed that not considering environmental factors in the empirical methods (constant emission factor in the IPCC Tier 1 guideline) could underestimate NH_3 emissions in the context of global warming, with the highest difference (i.e., 6.9 Tg N yr^{-1}) occurring in 2010. Then, we addressed how global warming would affect NH_3 emissions over the 21st century based on the set of Representative Concentration Pathway (RCP) emission scenarios. The results show that compared with the period 1986–2005, NH_3 emissions due to global warming would increase by 15%~31%

by 2099. The Northern Hemisphere would experience a substantial increase of NH_3 emissions due to the future global warming. At the regional scale, results indicated that NH_3 emissions were $21.3 \pm 3.9 \text{ Tg N yr}^{-1}$ from southern Asia agricultural systems with a rapidly increasing rate of $\sim 0.3 \text{ Tg N yr}^{-1}$ per year during 1961–2014. Among the emission sources, $10.8 \text{ Tg N yr}^{-1}$ was released from synthetic N fertilizer use, and $10.4 \pm 3.9 \text{ Tg N yr}^{-1}$ was released from manure production in 2014. Ammonia emissions from China and India together accounted for 64% of the total amount in SA during 2000–2014.

Based on DLEM simulations, the pre-industrial N_2O emissions from terrestrial ecosystems were estimated to be $6.20 \text{ Tg N yr}^{-1}$, with an uncertainty range of 4.76 to $8.13 \text{ Tg N yr}^{-1}$. Among that, global croplands contributed to $0.41 (0.32\text{--}0.55) \text{ Tg N yr}^{-1}$. However, due to agricultural activities, the total emissions increased by 195%, from 1.1 ± 0.2 to $3.3 \pm 0.14 \text{ Tg N yr}^{-1}$, during 1961–2014. Fertilizer N applications accounted for $\sim 70\%$ of the total emissions during 2000–2014. At the regional scale, Europe and North America were two leading regions for N_2O emissions in the 1960s. However, East Asia became the largest emitter amongst all regions after the 1990s.

This dissertation has also identified knowledge gaps and limitations in existing information that need to be investigated in the future to improve our understanding of N dynamics and our ability to evaluate and predict impacts of reactive N enrichment on N-containing gas emissions and ecosystem health.

Acknowledgments

I am so blessed to have this opportunity to study at Auburn University for the past four and half years. It is a beautiful place to study and live. I enjoyed my life here. With a ton of help from many people here, I finally complete my dissertation. My first appreciation will definitely go to Dr. Hanqin Tian, my supervisor who has supported me during these past four and half years. He is one of the smartest persons I have ever known and will always provide me innovative research ideas. Without his supports, I will never finish my PhD. My second appreciation will go to Dr. Shufen Pan, my co-supervisor who gave me many helps in my research and normal lives. She is a wonderful person and always thinks the best for her students. I am so thankful for her kindness and encouragements during my PhD. I also deeply appreciate the support from my committee members: Dr. Yucheng Feng, Dr. William D. Batchelor, and Dr. Stephan A. Prior. I enjoyed Dr. Yucheng Feng's classes and learned a lot from her. Drs. William D. Batchelor and Stephan A. Prior encouraged me a lot and provided many advices for my research. I also thank Dr. Christopher G. Burton for reviewing this dissertation.

Many thanks will go to previous members: Drs. Wei Ren, Bo Tao, Chaoqun Lu, Guangsheng Chen, Xiaofeng Xu, Mingliang Liu, Chi Zhang, Jia Yang, and Bowen Zhang who made great contributions to developing the Dynamic Land Ecosystem Model in the past decade. I specially thank Dr. Chaoqun Lu and Dr. Jia Yang for providing me with precious advices on my research. Also, I specially thank Dr. Wei Ren for giving me great comforts and encouragements. In addition, I will thank Mr. Yuanzhi Yao, Dr. Hao Shi, Mr. Naiqing Pan, and other group members

for all helps in my studies. I am also grateful for all helps from Dr. James Shepard, Dr. Graeme Lockaby, Ms. Audrey Grindle, and all faculty and staff members in School of Forestry and Wildlife Sciences.

I deeply appreciate my parents for supporting me pursuing my PhD abroad. I also thank my husband, Mr. Jian Chen, for his great supports to my studies and lives. He is the person who always stands by my side to encourage me. I also thank my daughter, Christina Chen, who is a big joy for my life. Last but not least, I appreciate funding supports from our school and NOAA-funded project.

Table of Contents

Abstract	ii
Acknowledgments.....	v
Table of Contents	vii
List of Tables	xi
List of Figures.....	xii
Chapter 1. Introduction	1
1. Objectives	7
2. Hypothesis.....	8
3. Approaches	8
4. Dissertation Structure.....	9
References.....	12
Chapter 2. The description of the DLEM N ₂ O processes and DLEM-Bi-NH ₃ module.....	16
2.1. Model description	17
2.1.1. The N ₂ O module	17
2.1.2. NH ₃ fluxes in the DLEM-Bi-NH ₃ module	20
2.2. Model evaluation and validation.....	25
2.2.1. N ₂ O emissions from natural vegetation	25
2.2.2. N ₂ O emissions from agricultural systems.....	28
2.2.3. NH ₃ emissions from agricultural systems.....	29
References.....	31
Chapter 3. Increased nitrogen enrichment and shifted patterns in the world's grassland: 1860-2016.....	36
Abstract	36
1. Introduction.....	37
2. Methods.....	40
2.1. Land use categories.....	40
2.2. Fertilizer N application on global pastures	41
2.3. Global manure N application to pastures.....	43
2.4. Global manure N deposition on pastures and rangelands	46

3. Results.....	47
3.1. Synthetic fertilizer N application to pastures, 1961-2016	47
3.2. Manure N application to pastures, 1860-2016.....	52
3.3. Manure N deposition on pastures and rangelands, 1860-2016.....	54
4. Discussion.....	57
4.1. Overview of global N inputs to pastures and rangelands	57
4.2. Extension of FAO information	58
4.3. Comparison with other studies	58
4.4. Changes in N inputs hotspots.....	61
4.5 Limitations and uncertainties.....	62
5. Conclusion	65
References.....	66
Chapter 4. Preindustrial nitrous oxide emissions from the land biosphere estimated by using a global biogeochemistry model.....	69
Abstract.....	69
1. Introduction.....	70
2. Methodology	72
2.1. Input datasets	72
2.2. Model simulation.....	74
2.3. Estimate of uncertainty	75
3. Results & discussion.....	77
3.1. Magnitude and spatial distribution of N ₂ O emission.....	77
3.2. Revisit preindustrial global N ₂ O emission by incorporating top-down estimates.....	88
3.3. Comparison with estimates by bottom-up methodology	89
3.4. The N ₂ O budget in the pre-industrial era.....	91
3.5. Future research needs.....	92
4. Conclusions.....	93
References.....	94
Chapter 5. Global N ₂ O emissions from croplands driven by environmental factors and management strategies: comparison and uncertainty analysis.....	99
Abstract.....	99
1. Introduction.....	100
2. Material and methods.....	104
2.1. Input data	104
2.2. Experiment design	107

3. Results.....	108
3.1. Environmental changes in global croplands during 1961–2014	108
3.2. Temporal patterns of N ₂ O emissions from global croplands during 1961–2014	109
3.3. Spatial patterns of N ₂ O emissions from global croplands during 1961–2014	112
3.4. Factorial contributions of N ₂ O emissions from global croplands.....	112
4. Discussion.....	114
4.1. The comparison with previous studies.....	114
4.2. The comparison of results from process-based model with EFs	116
4.3. The contribution of multiple environmental changes to N ₂ O emissions	116
4.4. Uncertainties and future work.....	117
5. Conclusions.....	119
References.....	121
Chapter 6. Half-century ammonia emissions from agricultural systems in southern Asia: Magnitude, spatiotemporal patterns and implications for human health.....	126
Abstract.....	126
Plain Language Summary	127
1. Introduction.....	127
2. Material and Method.....	131
2.1. NH ₃ emission from livestock excreta	131
2.2. Input data and simulation setup	131
3. Results.....	132
3.1. Contemporary and historical patterns of NH ₃ emissions.....	132
3.2. Spatial pattern of NH ₃ emissions	135
3.3. NH ₃ emissions from major countries.....	137
4. Discussion.....	139
4.1. The importance of Asia’s contribution to global NH ₃ emissions	139
4.2. Comparison with other studies in SA	140
4.3. Comparison of monthly NH ₃ emissions with other studies in China	141
4.4. Uncertainties	142
4.5. Implications	143
References.....	146
Chapter 7. Global ammonia emissions from synthetic nitrogen fertilizer applications in agricultural systems: empirical and process-based estimates and uncertainty	151
Abstract.....	151
1. Introduction.....	152

2. Methodology and inputs	155
2.1. Input data description.....	155
2.2. Model simulation experiments and implementation.....	156
3. Results.....	158
3.1. Temporal changes in global NH ₃ emissions	158
3.2. Spatial pattern of global NH ₃ emissions	159
3.3. Intra-annual changes of global and regional NH ₃ emissions.....	162
3.4. Crop-specific NH ₃ emissions.....	165
3.5. Comparisons with the estimate by the IPCC Tier1 guideline methodology.....	166
4. Discussion	167
4.1. Comparisons with other studies	167
4.2. Climate effects on NH ₃ emissions at spatiotemporal scales	169
4.3. Causes of intra-annual variations at regional scales	175
4.4. Uncertainties and future work.....	176
References.....	179
Chapter 8. Rise of future ammonia emissions from global croplands	185
Abstract.....	185
1. Introduction.....	185
2. Methodology	187
2.1 Input datasets and experimental design	187
3. Results and discussions.....	189
3.1 Temporal changes of future NH ₃ emissions	189
3.2 Spatial pattern of future NH ₃ emissions	191
3.3 Uncertainty and future work	192
4. Conclusion	195
References.....	196
Chapter 9. Conclusions and future works	198

List of Tables

Table 2-1. The description of field measurements from natural vegetation in different sites.	26
Table 2-2. The comparison of the modeled N ₂ O emissions in response to multiple N fertilizer addition levels with <i>in situ</i> observations.	27
Table 2-3. The comparison of the modeled N ₂ O emissions in response to multiple manure N addition levels with <i>in situ</i> observations.	28
Table 2-4 The comparison of NH ₃ emissions from N fertilizer use using the DLEM-Bi-NH ₃ module with <i>in-situ</i> observations.	30
Table 3-1. The N input rates, applied/deposited area, and total amounts in global pastures and rangelands in 1860, 1961, 2000, 1980, and 2016 (1 km ² = 100 ha). N/A: not available.....	48
Table 3-2 Pasture area changes (Mha) during the period 1860–2016 (adapted from HYDE 3.2, Klein Goldewijk et al. (2017)).	55
Table 3-3 Rangeland area changes (Mha) during the period 1860–2016 (adapted from HYDE 3.2, Klein Goldewijk et al. (2017)).	56
Table 3-4. Comparison of manure and fertilizer N application amounts between this study and published datasets. N/A: not available.....	58
Table 4-1. All results of the global-, continental-, and biome-level N ₂ O emission from 100 sets of DLEM results in 1860. The unit is Tg N yr ⁻¹	79
Table 4-2. Pre-industrial N ₂ O emissions from natural vegetation and croplands in different countries. 1Mha = 10 ⁴ km ²	87
Table 5-1. Design of simulation experiments.....	108
Table 6-1. NH ₃ emissions in major countries of southern Asia during 2000–2014 (1Tg = 10 ³ Gg): the left side represents NH ₃ emissions from synthetic N fertilizer; the right side represents NH ₃ emissions from livestock excreta.	139
Table 6-2. Comparison of NH ₃ emissions from N fertilizer application and livestock excreta between this study and previous estimates.	140
Table 7-1. Simulation experiment design in this study.....	158
Table 7-2. Estimates of global NH ₃ emissions (expressed in Tg N yr ⁻¹) based on different approaches.....	173
Table 7-3. N fertilizer uses in different regions across the globe.	178
Table 8-1. Estimates of global NH ₃ emissions during 1986-2005 and over the 21st century in the three RCP scenarios. Unit: Tg N yr ⁻¹	191

List of Figures

Figure 1-1. The global nitrogen cycle including the input and output of reactive nitrogen and the environmental factors that could affect the whole cycle in atmosphere, terrestrial ecosystems, and Ocean.	7
Figure 2-1. Framework of the Dynamic Land Ecosystem Model (Tian et al., 2010).....	17
Figure 2-2. The N process and C-N coupling in DLEM (Lu et al., 2012).....	19
Figure 2-3. The framework of N biogeochemical processes and fluxes in the DLEM-Bi-NH ₃ module. R _a , R _{soil} , and R _w : aerodynamic, soil, and cuticular resistance; R _b : the quasi laminar boundary layer resistance; R _{bg} : the soil boundary layer resistance; R _{st} : stomatal resistance; R _{inc} : the aerodynamic resistance within the canopy; C _a : the atmospheric NH ₃ concentration; C _c , C _g , and C _{st} : canopy, ground, and stomatal layer compensation point.....	20
Figure 2-4. The comparison of the DLEM-simulated N ₂ O emissions with field observations....	25
Figure 3-1. Diagram of the workflow for developing the database of global annual N fertilizer use rate in pasture during the period 1961–2016.	41
Figure 3-2. Diagram of the workflow for developing the database of global annual manure N use rate in pastures and manure N deposition rate in pastures and rangelands during the period 1860–2016.....	43
Figure 3-3. Temporal patterns of global manure N use, N fertilizer use, and manure deposition in grassland systems: (a) Manure N use and N fertilizer use on global pastures during 1860-2016 and during 1961-2016, respectively; (b) Manure N deposition to global pastures and rangelands during 1860-2016.....	50
Figure 3-4. Spatial patterns of N input rates in global pastures and rangelands in 1860, 1961, and 2016: (a, b, c) N fertilizer application rates; (d, e, f) manure N application rates; (g, h, i) manure N deposition rates.	51
Figure 3-5. Nitrogen fertilizer use (a) and rate (d), manure N use (b) and rate (e), and manure N deposition (c) and rate (f) at regional scales in 1860s, 1960s, 1980s, and 2000-2016. Error bars represent standard deviation within each decade.....	53
Figure 3-6. The temporal patterns of average N input rates (kg N ha ⁻¹) in regional pastures and rangelands during 1860–2016.....	60
Figure 4-1. Global potential natural vegetation map used by DLEM in the pre-industrial era. BNEF: Boreal Needleleaf Evergreen Forest, BNDF: Boreal Needleleaf Deciduous Forest, TBDF: Temperate Broadleaf Deciduous Forest, TBEF: Temperate Broadleaf Evergreen Forest, TNEF: Temperate Needleleaf Evergreen Forest, TNDF: Temperate Needleleaf Deciduous Forest,	

TrBDF: Tropical Broadleaf Deciduous Forest, TrBEF: Tropical Broadleaf Evergreen Forest, Dshrub: Deciduous Shrubland, Eshrub: Evergreen Shrubland.....	73
Figure 4-2. The spatial distribution of cropland area in 1860.....	74
Figure 4-3. The distribution of 100 sets of results from DLEM simulations.	76
Figure 4-4. The 95% confidence intervals of the mean pre-industrial N ₂ O emission using the Bootstrap resampling method with 10,000 replicates.....	76
Figure 4-5. The spatial distribution of N ₂ O emission in the pre-industrial era.....	77
Figure 4-6. Estimated N ₂ O emission rates (a) and emissions (b) with uncertainty ranges at continental-level in 1860. Solid line within each box refers to the median value of N ₂ O emission rate or amount.	84
Figure 4-7. (a) Estimated N ₂ O emission rate at biome-level in 1860 with the median value (solid line), the mean (solid dot), and the uncertainty range of emission rates from different biomes. The emission rate in the tundra was removed because of the extremely small value (less than 0.003g N m ⁻² yr ⁻¹); (b) Estimated N ₂ O emission (Tg N yr ⁻¹) with uncertainty ranges and its percentage (%) at biome-level in 1860.	86
Figure 5-1. Multiple environmental changes in global croplands: (a) Annual mean temperature and precipitation; (b) Annual atmospheric CO ₂ concentration; (c) Annual N deposition.....	103
Figure 5-2. Three datasets of annual N fertilizer application amount in global croplands.....	105
Figure 5-3. Comparison of spatial patterns of multiple fertilizer N application datasets in global croplands in 1961 and 2005.	106
Figure 5-4. The annual N ₂ O emissions from global croplands during 1961–2014: (a) total emissions, (b) N fertilizer application, and (c) N deposition. The uncertainty range is ±1 standard deviation.....	109
Figure 5-5. The decadal N ₂ O emissions at regional scales in the 1960s, 1980s, and 2000–14. We included average N ₂ O emissions from all sources of N inputs and the environmental factors. The uncertainty range is ±1 standard deviation.	110
Figure 5-6. Spatial distributions of total N ₂ O emissions from global croplands in the 1960s and 2000–2014. We included average N ₂ O emissions from all sources of N inputs and the environmental factors.....	111
Figure 5-7. Relative contributions of environmental factors to decadal N ₂ O emissions from global croplands. Fertilizer use causing N ₂ O emissions was based on the average amounts of different synthetic N fertilizer inputs.....	113
Figure 5-8. The impacts of N fertilizer use on regional N ₂ O emissions in the 1960s, 1980s, and 2000–14.	114
Figure 6-1. Annual NH ₃ emissions from N fertilizer application and manure production in southern Asia during the period 1961–2014.....	133
Figure 6-2. Seasonal variation in NH ₃ emissions from N fertilizer application in southern Asia during the periods 2000–2004, 2005–2009, and 2010–2014.	133
Figure 6-3. Spatial distribution of annual NH ₃ emissions from N fertilizer application in southern Asia.	135

Figure 6-4. Decadal NH ₃ emissions in different regions of southern Asia. Emission (y axis of each graph) is reported in Tg N yr ⁻¹	136
Figure 7-1. The spatial distribution of cropland area within each grid in 1961 and 2010.....	156
Figure 7-2 The spatial pattern of simulated NH ₃ emission from global croplands in 1961, 1980, 2000, and 2010.....	159
Figure 7-3. Simulated ammonia (NH ₃) emissions response to application of synthetic nitrogen (N) fertilizer in the 1960s, 1980s, 1990s, and 2000s.	161
Figure 7-4. The contemporary estimation of ammonia (NH ₃) emission at continental scales in the 1960s, 1980s, 1990s, and 2000s. The displayed NH ₃ emissions in the historical period were the mean of simulation results driven by four climate datasets, with uncertainty of 95% confidence interval. All units are Tg N yr ⁻¹	162
Figure 7-5. Simulated seasonal NH ₃ emissions from global croplands during 2000–2010.	163
Figure 7-6. Simulated seasonal mean ammonia (NH ₃) emissions in the 2000s: (a) December–January–February, (b) March–April–May, (c) June–July–August, and (d) September–October–November.	164
Figure 7-7. Crop-specific NH ₃ emissions from synthetic N fertilizer application estimated by the DLEM-Bi-NH ₃ module (a) and the IPCC EF (b).	165
Figure 7-8. Global NH ₃ emissions from DLEM-Bi-NH ₃ simulations (CRUNCEP, PGMFD v.2, GSWP3, and WATCH_WFDEI) and emission factor in the IPCC Tier1 guideline.	166
Figure 7-9. Climate effect on ammonia (NH ₃) emissions during 1961–2010. The temperature impact on annual NH ₃ emissions was calculated through the difference between S2 and S1 experiments; the precipitation impact on annual NH ₃ emissions was calculated through the difference between S3 and S2 experiments; the temperature difference equals annual average temperature during 1961–2010 minus the average temperature during 1901–1930.....	169
Figure 7-10. The spatial pattern of NH ₃ emission based on IPCC EF from global croplands in the 1960s, 1980s, 1990s, and 2000s.....	171
Figure 7-11. The decadal trends of crop-specific NH ₃ emissions during the 1960s to the 2000s: (a) rice, (b) wheat, (c) corn, (d) soybean, and (e) other crops.	172
Figure 8-1. The historical and projected trends of climate changes (i.e., temperature and precipitation) in the RCP projection. Data were obtained from the CRU-NCEP and three Global Circulation Models (GCMs): GFDL-ESM2M, PSL-CM5A-LR, and MIROC5.....	188
Figure 8-2. Projected global annual mean ammonia (NH ₃) emissions over the period 2006-2099 driven by three GCMs. The green, orange, and blue shaded areas are 95% confidence intervals of mean NH ₃ emissions driven by the RCP8.5, RCP6.0, and RCP2.6 emission scenarios, respectively.	190
Figure 8-3. Estimates of NH ₃ emission at continental scales during the period 2006-2099. All units are Tg N yr ⁻¹	193
Figure 8-4. The spatial distribution of annual mean NH ₃ emission (a, b, c) and the difference (d, e, f) between the future prediction and the period 1986-2005 forced by three GCMs in three RCPs emission scenarios.	194

Chapter 1. Introduction

Nitrogen (N) is a fundamental component in controlling primary production in the biosphere and is often a limiting factor for crop growths (Gruber and Galloway, 2008). Diatomic nitrogen (N_2), as a non-reactive N, consists of nearly 78% of the atmosphere, which is unavailable to most organisms until its triple bond is interrupted by chemical reactions. Nitrogen accessible to plants was defined as reactive N (Nr), which includes all biologically active, photo-chemically reactive, and radioactively active N compounds in the atmosphere and biosphere of the Earth (Galloway et al., 2004). Unlike previous definitions, Galloway et al. (2004) defined the Nr in a broader way, that is inorganic reduced forms of N (e.g., NH_3 , NH_4^+), inorganic oxidized forms (e.g., NO_x , HNO_3 , N_2O , NO_3^-), organic compounds (e.g., urea, amines, proteins, nucleic acids). In the pristine biosphere, there are two major processes for fixing non-reactive N into biologically available forms: lightning and biological nitrogen fixation (Figure 1-1). Both processes retain the normality of the terrestrial N cycle (Cleveland et al., 1999).

Fowler et al. (2013) reported that global natural sources of Nr is $203 (\pm 50) \text{ Tg N yr}^{-1}$. Lightning is a natural reaction that produces NO_x and introduces it to remote regions of the troposphere. According to previous studies, the estimate of the global Nr introduced by lightning ranges from 2 to 10 Tg N yr^{-1} (Levy et al., 1996; Tie et al., 2002), with a widely acceptable value of 5 Tg N annually (Fowler et al., 2013; Galloway and Cowling, 2002). Nitrogen fixers have the capacity to break the triple bonds of N_2 and fix it into NH_4^+ , which can be used by most organisms.

The biological N fixation (BNF) is a result of the activity of a phylogenetically diverse list of bacteria, archaea, and symbioses, among which symbiotic nitrogen fixers have the highest rates of nitrogen fixation (Vitousek et al., 2013). Cleveland et al. (1999) provided their “best estimate” of potential BNF in terrestrial ecosystems, which was about 195 Tg N yr⁻¹, with a range of 100–290 Tg N yr⁻¹ using the net primary productivity and evapotranspiration. However, Vitousek et al. (2013) pointed out the overestimate of previous values and provided the estimate of annual pre-industrial BNF in terrestrial ecosystems of 58 Tg N, within a range of 40–100 Tg N. Oceans cover three quarters of the Earth’s surface, which contribute to a substantial amount of Nr to the global N fluxes through the BNF in marine ecosystems. Several studies have focused on the estimates of BNF in marine ecosystems. Duce et al. (2008) estimated the global marine BNF as 125 Tg N yr⁻¹, with a range of 60–200 Tg N yr⁻¹, which is lower than the estimates of 140 Tg N yr⁻¹ from Canfield et al. (2010) and of 145 Tg N yr⁻¹ from Galloway et al. (2004). Voss et al. (2013) reviewed the nitrogen cycle in the oceans and provided the value for marine BNF of 140 Tg N yr⁻¹ (± 50), which had been adopted in Fowler et al. (2015).

Since the pre-industrial era, natural N cycle has been altered as expansion of agricultural lands, biomass burning, the combustion of fossil fuel, and the cultivation of leguminous crops that carry out biological N fixation (Davidson and Kanter, 2014). The Nr creation increased from approximately 15 Tg N in 1860 to 156 Tg N in 1995, and increased further from 156 Tg N yr⁻¹ in 1995 to 187 Tg N yr⁻¹ in 2005 (Galloway et al., 2008). The human-induced creation of Nr in 2010 was ~210 (190–230) Tg N, which is at least two times larger than the rate of natural terrestrial creation through the BNF (Ciais et al., 2014). Food production is known as the major process that has introduced the increasing amount of Nr into terrestrial ecosystems, which has reached as more than 100 Tg N yr⁻¹ in the 2000s (Gruber and Galloway, 2008). In the past century, the Haber-Bosch

process, the chemical process that synthetically transforms atmospheric dinitrogen (N_2) gas into ammonia (NH_3), contributed to the enormous increase in food production, which in turn has fed the rapid increase of the global population (Erisman et al., 2008). Meanwhile, the expansion of leguminous crops, such as soybean, groundnut, etc., has introduced 50–70 Tg N fixed by BNF in global croplands into soils (Herridge et al., 2008). Human induced N deposition is from biomass burning, fossil fuel combustion, human sewage, volatilization, and from landfill, composting and incarnation of solid waste. It is well understood that NO_x emissions are from fossil fuel combustion, but less from biomass burning and soil emissions (Galloway et al., 2008). The atmospheric NO_x and NH_y emitted from anthropogenic activities, about 70 and 80%, respectively, are redeposited to terrestrial ecosystems (Galloway, 1998). The deposition of NO_x and NH_y from the atmosphere was estimated to be 46.9 and 53.1 Tg N yr^{-1} , respectively (Ciais et al., 2014).

The addition of excess anthropogenic N compounds to terrestrial ecosystem plays a role in the enormous emission of N gases, i.e., N_2 , N_2O , NO_x , and NH_3 in the atmosphere, remaining a matter of great concern to human health and the environment (Behera et al., 2013). Reactive nitrogen in the terrestrial ecosystems can be converted back to N_2 through soil cultivation, the burning of crop residue, manure management, and natural wetlands and peatlands. Denitrification rates are dominated by environmental factors, such as temperature, soil moisture, oxygen availability, PH, etc. Thus, anoxia, a carbon to nitrogen ratio greater than 30, and PH-neutral conditions favor complete denitrification to N_2 in soils (Čuhel et al., 2010; Kolb and Horn, 2012). The production of N_2 that is from N_r due to anthropogenic activities and natural sources was estimated as 110 Tg N yr^{-1} , which is nearly 40% of the total inputs (Bouwman et al., 2013).

In soils, N_2O and NO_x production are mainly dominated by nitrification and denitrification (Barnard et al., 2005; Chapuis-Lardy et al., 2007). Nitrification, a process converting NH_4^+ into

NO_3^- , affected by soil temperature, moisture, and NH_4^+ concentrations. Denitrification is the process that converts NO_3^- into three types of nitrogen gases, namely, NO , N_2O , and N_2 . This process was controlled by several environmental factors, such as soil temperature, moisture content, PH, and NO_3^- concentrations (Brotto et al., 2015; Butterbach-Bahl et al., 2013; Firestone and Davidson, 1989; Goldberg and Gebauer, 2009; Rowlings et al., 2015). The continuous inputs of N_r provide a huge amount of available substrate to microbes in soils and oceans, resulting in increasing N-related gas emissions. Nitrous oxide is an important atmospheric trace gas, which has a long lifetime, contributes greatly to the global warming and stratosphere ozone depletion. However, atmospheric N_2O concentration has increased by 20% since 1860, fitting in a linear increasing rate of 0.26% per year during the recent few decades (Ciais et al., 2014). Global N_2O emissions from all sources increase from 16.5 Tg $\text{N}_2\text{O-N yr}^{-1}$ in 2000 to 18.0 (Adapting Mosaic scenario) and 19.7 (Global Orchestration scenario) Tg $\text{N}_2\text{O-N yr}^{-1}$ in 2050 (Butterbach-Bahl et al., 2013).

Nitrogen oxides can cause detrimental effects on human health and crop productivity through catalyzing the photochemical formation of ground-level ozone (Crutzen et al., 1979; Yan et al., 2003). Davidson and Kinglerlee (1997) provided an estimate of 21 Tg $\text{NO}_x\text{-N yr}^{-1}$ from soils through scaling up field flux measurements. Martin et al. (2003) reported that a global posteriori estimate for land surface NO_x emissions are 37.7 Tg $\text{NO}_x\text{-N yr}^{-1}$, which agreed with the GEIA-based a priori (36.4 Tg $\text{NO}_x\text{-N yr}^{-1}$) and with the Emission Database for Global Atmospheric Research (EDGAR) 3.0 bottom-up inventory (36.6 Tg $\text{NO}_x\text{-N yr}^{-1}$). Through analyzing the satellite observations of tropospheric NO_2 columns during 2003–2009, Lamsal et al. (2011) reported that anthropogenic NO_x emission from land surface has increased by 9.2% globally.

There are two major sources for NH₃ emissions: volatilization from livestock manures and mineral fertilizer application, which account for approximately 80–90% of the total anthropogenic NH₃ emission (Bouwman et al., 1997; Zhang et al., 2010). NH₃, as one of main loss of N fertilizer to the atmosphere, would be deposited back on land after a short-distance transport in the atmosphere (Asman et al., 1998). This deposition of reactive N has increased, in large regions of the world, the average atmospheric N deposition twentyfold higher than the pre-industrial times, which has contributed to eutrophication, acidification and loss of biodiversity in the entire ecosystem (Erisman et al., 2008). Bouwman et al. (1997) estimated global NH₃ emission in 1990 was about 54 Tg N yr⁻¹ using a simplified emission factor. Riddick et al. (2016) provided an updated estimate of 33 Tg N yr⁻¹ in 2000 through model simulation and predicted that the global NH₃ emission will increase 1 Tg per year per °C of warming. Sutton et al. (2013) predicted that global NH₃ emission may increase from 65 (48–85) in 2008 to 132 (89–179) Tg N by 2100.

Besides N-containing gas emissions, the additional Nr could also contribute to the leaching and runoff from terrestrial ecosystems to ground water or marine ecosystems. Fowler et al. (2013) described that the transfer of Nr from land to oceans comprises 50–70 Tg N yr⁻¹ leaching in freshwaters and the deposition of an additional 30 Tg N yr⁻¹ from the atmosphere on oceans. Through considering all Nr sources from terrestrial ecosystems (fertilizer and manure management, BNF, and human sewage) and atmosphere deposition, McCrackin et al. (2014) estimated the global DIN export of 10.3 Tg N yr⁻¹ using the NEWS2-DIN-S model; however, this estimate is much lower than previously published NEWS2-DIN output (18.9 Tg N yr⁻¹) (Mayorga et al., 2010), as well as estimates of 20.8 Tg N yr⁻¹ from Seitzinger and Kroeze (1998) and 14 Tg N yr⁻¹ from (Green et al., 2004). In consequence, there exist large uncertainties of the estimates of N-related gas emission from riverine, which is defined as indirect emissions. In the Intergovernmental Panel

on Climate Change (IPCC) AR5, the indirect emission of N₂O was estimated as 0.6 Tg N yr⁻¹, which is much higher than the estimate (0.032 Tg N yr⁻¹) by Hu et al. (2016). Hu et al. (2012) suggests that aquaculture can be an important anthropogenic source of N₂O emission, which could increase to 0.383 Tg by 2030. If the aquaculture industry continues developing, the annual growth rate of N₂O emission will increase about 7.10% annually (Hu et al., 2012).

There remain large uncertainties in the estimates of all forms of Nr involved in the global N budget due to the approaches. For example, the main two approaches for estimating global N₂O fluxes are bottom-up (inventory, statistical extrapolation of local flux measurements, and process-based modeling) and top-down (atmospheric inversion) methodology (Davidson and Kanter, 2014; Tian et al., 2016). Among these approaches, Emission factors (EF) and process-based models are two major approaches to quantify N₂O/NH₃ emissions from N fertilizer/manure at global or regional scales. Emission factor represents the percentage of N fertilizer/manure applied that volatilizes as NH₃, which varies with synthetic N fertilizer/manure types. The constant EFs were used to build emission inventories at global and regional scales, such as Emission Database for Global Atmospheric Research (EDGAR, Olivier et al. (2002)) and National Emission Inventory (NEI, Reis et al. (2009)) of the United States. However, a constant EF might not represent the real NH₃ volatilization or N₂O production and emission process and its interaction with crops during or after N fertilizer/manure application as the conversion of Nr to NH₃ involved with biological and chemical processes is strongly sensitive to environmental conditions (Fowler et al., 2015; Sutton et al., 2013). Thus, a process-based model is an effective tool to estimate N₂O/NH₃ emissions from N fertilizer/manure at the site, regional and global scale.

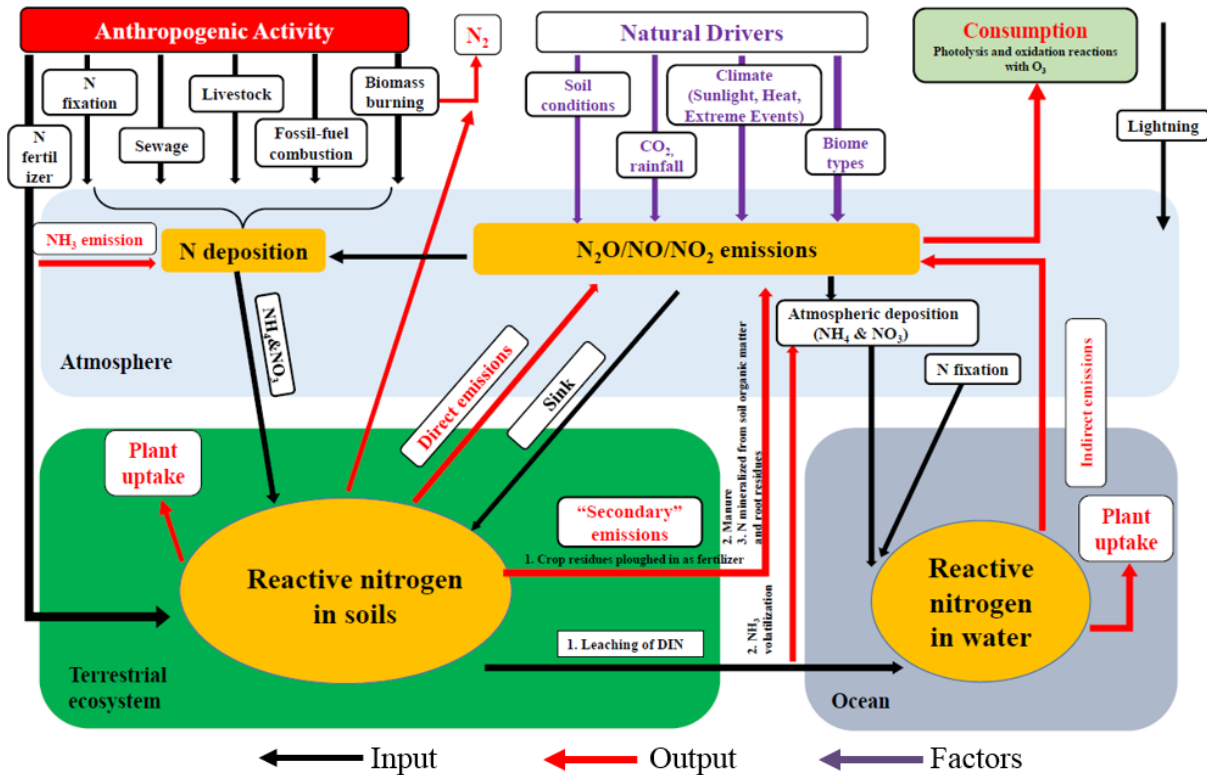


Figure 1-1. The global nitrogen cycle including the input and output of reactive nitrogen and the environmental factors that could affect the whole cycle in atmosphere, terrestrial ecosystems, and Ocean.

1. Objectives

We applied a process-based Dynamic Land Ecosystem Model (DLEM) to study how human activities affected the global and regional N cycle during the past century. In addition, with the condition of global warming, the DLEM model would be used to predict N-related gas emissions in the rest of this century. The specific objectives of this study are to:

1. Apply mathematical expressions of N_2O/NH_3 processes in the DLEM and build a comprehensive modeling approach.
2. Develop time-series gridded datasets for N fertilizer and manure input during 1860-2016 to evaluate how much reactive N was introduced into agricultural systems.

3. Provide a whole picture of N₂O emissions from terrestrial ecosystems in the context of negligible human disturbances.
4. Assess N₂O emissions from agricultural systems during the past half decades at multiple scales under the circumstance of intensive human activities and climate change.
5. Quantify NH₃ emissions from N inputs because of intensive agricultural activities during 1961-2014 at global and regional scales.
6. Predict global NH₃ emissions in the context of global warming for the rest of 21st century and identify hotspot regions for emissions.

2. Hypothesis

1. The tropics was the top one region with high N₂O emissions in the pre-industrial era. Regions with agricultural activities could have produce a slight amount of N₂O gases (Objective 3).
2. The distribution of N₂O emissions could have changed because intensive agricultural activities (i.e., N fertilizer application) and environmental changes (i.e, global warming) (Objective 4).
3. The substantial increase of NH₃ emissions in the atmosphere is due to a huge amount of N fertilizer and manure inputs in agricultural systems (Objective 5).
4. The global warming is an important stimulator for large increase of agricultural NH₃ emissions in the future (Objective 6).

3. Approaches

- Data collection:

- (1) Reconstructed gridded N fertilizer and manure distribution in grassland ecosystems at $0.5^\circ \times 0.5^\circ$ resolution based on FAO and HYDE Land Use datasets.
 - (2) Model input datasets including climate, atmospheric CO₂ concentration, N deposition, N fertilizer, land use and land cover, and topography, etc.
 - (3) Site-level observational data including annual or monthly N₂O/NH₃ emissions.
 - (4) Inventory data for N₂O/NH₃ emissions at the global or national scale, such as NEI, EDGAR, etc.
- Model development:
 - (1) Evaluate soil N₂O emission processes in the DLEM.
 - (2) Improve the DLEM model by coupling a process-based bi-directional NH₃ exchange module in the Community Multiscale Air-Quality (CMAQ) model (DLEM-Bi-NH₃).
 - (3) Calibrate and validate the DLEM-Bi-NH₃ across different sites globally.
 - Model application:
 - (1) Global- and regional-scale evaluations of soil N₂O emission processes in the DLEM.
 - (2) Global- and regional-scale evaluations of the DLEM-Bi-NH₃ module.
 - (3) Predict global NH₃ emissions using the DLEM-Bi-NH₃ module in the context of global warming in the remaining 21st century.

4. Dissertation Structure

Chapter 1 describes the background and significance of this study, research objectives and hypothesis, and approaches to study these research questions.

Chapter 2 provides the detailed description of N₂O flux processes in the DLEM. Observations of natural vegetation during 1970–2009 were collected to test the model performance in the contemporary period. Simulation results of N₂O emissions from agricultural systems were

validated by observational data at different sites. This chapter also thoroughly described the coupled DLEM-Bi-NH₃ module. Site-level validations for the DLEM-Bi-NH₃ module simulations are provided.

Chapter 3 describes the methods to develop gridded datasets of N fertilizer and manure inputs in global grasslands at a resolution of $0.5^\circ \times 0.5^\circ$ during 1860–2016 by combining annual and 5-arc minute spatial data on pasture and rangeland with country-level manure and synthetic fertilizer N data.

Chapter 4 quantifies the preindustrial N₂O emissions from the terrestrial ecosystem. Meanwhile, uncertainties associated with key parameters in the DLEM were also evaluated.

Chapter 5 investigates global N₂O emissions from croplands driven by environmental factors and management strategies. In this study, I examine how annual and decadal climate changes and variability affected N₂O emissions from agricultural systems during 1961-2014. The contributions of different environmental factors have been attributed.

Chapter 6 studies NH₃ emissions from agricultural systems in southern Asia based on the DLEM-Bi-NH₃ module. This chapter presents the magnitude and spatiotemporal patterns of emissions from 1961 to 2014, and implications for human health in the study region.

Chapter 7 studies global NH₃ emissions from synthetic N fertilizer applications in agricultural systems based on process-based estimates, the DLEM-Bi-NH₃ module. In addition, using the same input N fertilizer data, I evaluated NH₃ emission based on the empirical, emission factors, to compare the difference between these two approaches and identify the uncertainties. Besides above, I also applied multiple climate datasets to examine the climate effects on NH₃ emissions during 1960-2010.

Chapter 8 predicts global NH₃ emissions from agricultural systems using the DLEM-Bi-NH₃ module. Three climate datasets obtained from the Global Circulation Models (GCMs) over the period 2006-2099 in three different Representative Concentration Pathway (RCP) emission scenarios (RCP 2.6, RCP 6.0, and RCP 8.5) were used to simulate the impact of future climate change on NH₃ emissions.

Chapter 9 summarizes the significant findings and presents improvements that will be needed in the future work.

References

- Asman, W. A., Sutton, M. A., and Schjørring, J. K.: Ammonia: emission, atmospheric transport and deposition, *New phytologist*, 139, 27-48, 1998.
- Barnard, R., Leadley, P. W., and Hungate, B. A.: Global change, nitrification, and denitrification: a review, *Global biogeochemical cycles*, 19, 2005.
- Behera, S. N., Betha, R., and Balasubramanian, R.: Insights into chemical coupling among acidic gases, ammonia and secondary inorganic aerosols, *Aerosol and Air Quality Research*, 13, 1282-U1414, 2013.
- Bouwman, A., Lee, D., Asman, W., Dentener, F., Van Der Hoek, K., and Olivier, J.: A global high-resolution emission inventory for ammonia, *Global biogeochemical cycles*, 11, 561-587, 1997.
- Bouwman, L., Goldewijk, K. K., Van Der Hoek, K. W., Beusen, A. H., Van Vuuren, D. P., Willems, J., Rufino, M. C., and Stehfest, E.: Exploring global changes in nitrogen and phosphorus cycles in agriculture induced by livestock production over the 1900–2050 period, *Proceedings of the National Academy of Sciences*, 110, 20882-20887, 2013.
- Brotto, A. C., Li, H., Dumit, M., Gabarró, J., Colprim, J., Murthy, S., and Chandran, K.: Characterization and mitigation of nitrous oxide (N₂O) emissions from partial and full-nitrification BNR processes based on post-anoxic aeration control, *Biotechnology and bioengineering*, 112, 2241-2247, 2015.
- Butterbach-Bahl, K., Baggs, E. M., Dannenmann, M., Kiese, R., and Zechmeister-Boltenstern, S.: Nitrous oxide emissions from soils: how well do we understand the processes and their controls?, *Phil. Trans. R. Soc. B*, 368, 20130122, 2013.
- Canfield, D. E., Glazer, A. N., and Falkowski, P. G.: The evolution and future of Earth's nitrogen cycle, *science*, 330, 192-196, 2010.
- Chapuis-Lardy, L., Wrage, N., Metay, A., CHOTTE, J. L., and Bernoux, M.: Soils, a sink for N₂O? A review, *Global Change Biology*, 13, 1-17, 2007.
- Ciais, P., Sabine, C., Bala, G., Bopp, L., Brovkin, V., Canadell, J., Chhabra, A., DeFries, R., Galloway, J., Heimann, M., Jones, C., Le Quere, C., Myneni, R., Piao, S., Thornton, P., Heinze, C., Tans, P., and Vesala, T.: Carbon and other biogeochemical cycles. In: *Climate Change 2013: The Physical Science Basis. Contribution of Working Group I to the Fifth Assessment Report of the Intergovernmental Panel on Climate Change*, Cambridge University Press, 2014.
- Cleveland, C. C., Townsend, A. R., Schimel, D. S., Fisher, H., Howarth, R. W., Hedin, L. O., Perakis, S. S., Latty, E. F., Von Fischer, J. C., and Elseroad, A.: Global patterns of terrestrial biological nitrogen (N₂) fixation in natural ecosystems, *Global Biogeochemical Cycles*, 13, 623-645, 1999.
- Crutzen, P. J., Heidt, L. E., Krasnec, J. P., Pollock, W. H., and Seiler, W.: Biomass burning as a source of atmospheric gases CO, H₂, N₂O, NO, CH₃Cl and COS, *Nature*, 282, 253, 1979.
- Čuhel, J., Šimek, M., Laughlin, R. J., Bru, D., Chêneby, D., Watson, C. J., and Philippot, L.: Insights into the effect of soil pH on N₂O and N₂ emissions and denitrifier community size and activity, *Applied and environmental microbiology*, 76, 1870-1878, 2010.
- Davidson, E. A. and Kanter, D.: Inventories and scenarios of nitrous oxide emissions, *Environmental Research Letters*, 9, 105012, 2014.
- Davidson, E. A. and Kinglerlee, W.: A global inventory of nitric oxide emissions from soils, *Nutrient cycling in agroecosystems*, 48, 37-50, 1997.

- Duce, R., LaRoche, J., Altieri, K., Arrigo, K., Baker, A., Capone, D., Cornell, S., Dentener, F., Galloway, J., and Ganeshram, R.: Impacts of atmospheric anthropogenic nitrogen on the open ocean, *science*, 320, 893-897, 2008.
- Erisman, J. W., Sutton, M. A., Galloway, J., Klimont, Z., and Winiwarter, W.: How a century of ammonia synthesis changed the world, *Nature Geoscience*, 1, 636-639, 2008.
- Firestone, M. K. and Davidson, E. A.: Microbiological basis of NO and N₂O production and consumption in soil, *Exchange of trace gases between terrestrial ecosystems and the atmosphere*, 47, 7-21, 1989.
- Fowler, D., Coyle, M., Skiba, U., Sutton, M. A., Cape, J. N., Reis, S., Sheppard, L. J., Jenkins, A., Grizzetti, B., and Galloway, J. N.: The global nitrogen cycle in the twenty-first century, *Phil. Trans. R. Soc. B*, 368, 20130164, 2013.
- Fowler, D., Steadman, C. E., Stevenson, D., Coyle, M., Rees, R. M., Skiba, U., Sutton, M., Cape, J., Dore, A., and Vieno, M.: Effects of global change during the 21st century on the nitrogen cycle, *Atmospheric Chemistry and Physics*, 15, 13849-13893, 2015.
- Galloway, J. N.: The global nitrogen cycle: changes and consequences. In: *Nitrogen, the Conference*, Elsevier, 1998.
- Galloway, J. N. and Cowling, E. B.: Reactive nitrogen and the world: 200 years of change, *AMBIO: A Journal of the Human Environment*, 31, 64-71, 2002.
- Galloway, J. N., Dentener, F. J., Capone, D. G., Boyer, E. W., Howarth, R. W., Seitzinger, S. P., Asner, G. P., Cleveland, C., Green, P., and Holland, E.: Nitrogen cycles: past, present, and future, *Biogeochemistry*, 70, 153-226, 2004.
- Galloway, J. N., Townsend, A. R., Erisman, J. W., Bekunda, M., Cai, Z., Freney, J. R., Martinelli, L. A., Seitzinger, S. P., and Sutton, M. A.: Transformation of the nitrogen cycle: recent trends, questions, and potential solutions, *Science*, 320, 889-892, 2008.
- Goldberg, S. D. and Gebauer, G.: Drought turns a Central European Norway spruce forest soil from an N₂O source to a transient N₂O sink, *Global Change Biology*, 15, 850-860, 2009.
- Green, P. A., Vörösmarty, C. J., Meybeck, M., Galloway, J. N., Peterson, B. J., and Boyer, E. W.: Pre-industrial and contemporary fluxes of nitrogen through rivers: a global assessment based on typology, *Biogeochemistry*, 68, 71-105, 2004.
- Gruber, N. and Galloway, J. N.: An Earth-system perspective of the global nitrogen cycle, *Nature*, 451, 293-296, 2008.
- Herridge, D. F., Peoples, M. B., and Boddey, R. M.: Global inputs of biological nitrogen fixation in agricultural systems, *Plant and Soil*, 311, 1-18, 2008.
- Hu, M., Chen, D., and Dahlgren, R. A.: Modeling nitrous oxide emission from rivers: a global assessment, *Global change biology*, 22, 3566-3582, 2016.
- Hu, Z., Lee, J. W., Chandran, K., Kim, S., and Khanal, S. K.: Nitrous oxide (N₂O) emission from aquaculture: a review, *Environmental science & technology*, 46, 6470-6480, 2012.
- Kolb, S. and Horn, M. A.: Microbial CH₄ and N₂O consumption in acidic wetlands, *Frontiers in microbiology*, 3, 78, 2012.
- Lamsal, L., Martin, R., Padmanabhan, A., Van Donkelaar, A., Zhang, Q., Sioris, C., Chance, K., Kurosu, T., and Newchurch, M.: Application of satellite observations for timely updates to global anthropogenic NO_x emission inventories, *Geophysical Research Letters*, 38, 2011.
- Levy, H., Moxim, W., and Kasibhatla, P.: A global three-dimensional time-dependent lightning source of tropospheric NO_x, *Journal of Geophysical Research: Atmospheres*, 101, 22911-22922, 1996.

- Martin, R. V., Jacob, D. J., Chance, K., Kurosu, T. P., Palmer, P. I., and Evans, M. J.: Global inventory of nitrogen oxide emissions constrained by space-based observations of NO₂ columns, *Journal of Geophysical Research: Atmospheres*, 108, 2003.
- Mayorga, E., Seitzinger, S. P., Harrison, J. A., Dumont, E., Beusen, A. H., Bouwman, A., Fekete, B. M., Kroeze, C., and Van Drecht, G.: Global nutrient export from WaterSheds 2 (NEWS 2): model development and implementation, *Environmental Modelling & Software*, 25, 837-853, 2010.
- McCrackin, M. L., Harrison, J. A., and Compton, J. E.: Factors influencing export of dissolved inorganic nitrogen by major rivers: A new, seasonal, spatially explicit, global model, *Global Biogeochemical Cycles*, 28, 269-285, 2014.
- Olivier, J. G., Jm, B., Peters, J. A., Bakker, J., Visschedijk, A. J., and Bloos, J. J.: Applications of EDGAR emission database for global atmospheric research, 2002. 2002.
- Reis, S., Pinder, R., Zhang, M., Lijie, G., and Sutton, M.: Reactive nitrogen in atmospheric emission inventories, *Atmospheric Chemistry and Physics*, 9, 7657-7677, 2009.
- Riddick, S., Ward, D., Hess, P., Mahowald, N., Massad, R., and Holland, E.: Estimate of changes in agricultural terrestrial nitrogen pathways and ammonia emissions from 1850 to present in the Community Earth System Model, *Biogeosciences*, 13, 3397-3426, 2016.
- Rowlings, D., Grace, P., Scheer, C., and Liu, S.: Rainfall variability drives interannual variation in N₂O emissions from a humid, subtropical pasture, *Science of The Total Environment*, 512, 8-18, 2015.
- Seitzinger, S. P. and Kroeze, C.: Global distribution of nitrous oxide production and N inputs in freshwater and coastal marine ecosystems, *Global biogeochemical cycles*, 12, 93-113, 1998.
- Sutton, M. A., Reis, S., Riddick, S. N., Dragosits, U., Nemitz, E., Theobald, M. R., Tang, Y. S., Braban, C. F., Vieno, M., and Dore, A. J.: Towards a climate-dependent paradigm of ammonia emission and deposition, *Philosophical Transactions of the Royal Society of London B: Biological Sciences*, 368, 20130166, 2013.
- Tian, H., Lu, C., Ciais, P., Michalak, A. M., Canadell, J. G., Saikawa, E., Huntzinger, D. N., Gurney, K. R., Sitch, S., Zhang, B., Yang, J., Bousquet, P., Bruhwiler, L., Chen, G., Dlugokencky, E., Friedlingstein, P., Melillo, J., Pan, S., Poulter B., Prinn, R., Saunio, M., Schwalm, C., and Wofsy, S.: The terrestrial biosphere as a net source of greenhouse gases to the atmosphere, *Nature*, 531, 225-228, 2016.
- Tie, X., Zhang, R., Brasseur, G., and Lei, W.: Global NO_x production by lightning, *Journal of Atmospheric Chemistry*, 43, 61-74, 2002.
- Vitousek, P. M., Menge, D. N., Reed, S. C., and Cleveland, C. C.: Biological nitrogen fixation: rates, patterns and ecological controls in terrestrial ecosystems, *Philosophical Transactions of the Royal Society of London B: Biological Sciences*, 368, 20130119, 2013.
- Voss, M., Bange, H. W., Dippner, J. W., Middelburg, J. J., Montoya, J. P., and Ward, B.: The marine nitrogen cycle: recent discoveries, uncertainties and the potential relevance of climate change, *Philosophical Transactions of the Royal Society B: Biological Sciences*, 368, 20130121, 2013.
- Yan, X., Akimoto, H., and Ohara, T.: Estimation of nitrous oxide, nitric oxide and ammonia emissions from croplands in East, Southeast and South Asia, *Global Change Biology*, 9, 1080-1096, 2003.

Zhang, Y., Dore, A., Ma, L., Liu, X., Ma, W., Cape, J., and Zhang, F.: Agricultural ammonia emissions inventory and spatial distribution in the North China Plain, *Environmental Pollution*, 158, 490-501, 2010.

Chapter 2. The description of the DLEM N₂O processes and DLEM-Bi-NH₃ module

The DLEM (Figure 2-1) is a highly integrated process-based ecosystem model, which combines biophysical characteristics, plant physiological processes, biogeochemical cycles, vegetation dynamics and land use to make daily, spatially-explicit estimates of carbon, nitrogen and water fluxes and pool sizes in terrestrial ecosystems from site- and regional- to global-scales (Lu and Tian, 2013; Tian et al., 2015; Tian et al., 2012a). Biophysical characteristics component simulates water and energy fluxes in terrestrial ecosystems and their interactions with the environment. The plant physiological process component simulates all essential processes of plant growth, such as photosynthesis, respiration, allocation, and evapotranspiration. The biogeochemical cycle processes component includes processes of decomposition, nitrogen mineralization/immobilization, nitrification/denitrification, fermentation, and other major biochemical processes in soils. The land use and land management component simulates the impact of natural and human disturbances on water and nutrient fluxes and storages in the land biosphere.

The DLEM is characterized of cohort structure, multiple soil layer processes, coupled carbon, water and nitrogen cycles, multiple GHG emissions simulation, enhanced land surface processes, and dynamic linkages between terrestrial and riverine ecosystems (Liu et al., 2013; Tian et al., 2015; Tian et al., 2010). The previous results of GHG emissions from DLEM simulations have been validated against field observations and measurements at various sites (Lu and Tian, 2013; Ren et al., 2011; Tian et al., 2010; Tian et al., 2011; Zhang et al., 2016). The estimates of

water, carbon, and nutrients fluxes and storages were also compared with the estimates from different approaches at regional-, continental-, and global-scales (Pan et al., 2014; Tian et al., 2015; Yang et al., 2015). Different soil organic pools and calculations of decomposition rates were described in Tian et al. (2015). The decomposition and nitrogen mineralization processes in the DLEM were described in other publications (Lu and Tian, 2013; Yang et al., 2015).

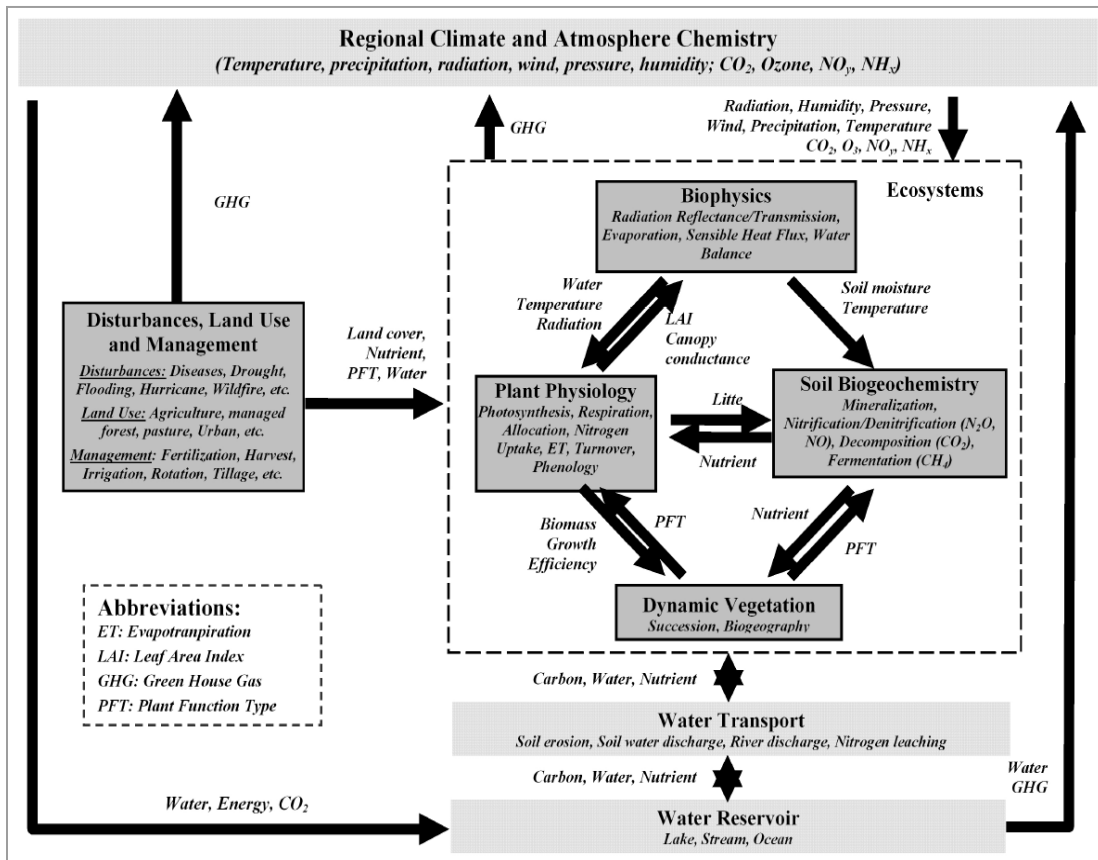


Figure 2-1. Framework of the Dynamic Land Ecosystem Model (Tian et al., 2010).

2.1. Model description

2.1.1. The N₂O module

Previous work provided a detailed description of trace gas modules in the DLEM (Tian et al., 2010). However, both denitrification and nitrification processes have been modified based on the first-order kinetics (Chatskikh et al., 2005; Heinen, 2006).

In the DLEM, the N₂O production and fluxes (Figure 2-2) are determined by soil inorganic N content (NH₄⁺ and NO₃⁻) and environmental factors, such as soil texture, temperature, and moisture:

$$F_{N_2O} = (R_{nit} + R_{den})F(T_{soil})(1 - F(Q_{wfp})) \quad (1)$$

where F_{N_2O} is the N₂O flux from soils to the atmosphere (g N m² d⁻¹), R_{nit} is the daily nitrification rate (g N m² d⁻¹), R_{den} is the daily denitrification rate (g N m² d⁻¹), $F(T_{soil})$ is the function of daily soil temperature on nitrification process (unitless), and $F(Q_{wfp})$ is the function of water-filled porosity (unitless).

Nitrification, a process converting NH₄⁺ into NO₃⁻, is simulated as a function of soil temperature, moisture, and soil NH₄⁺ concentration:

$$R_{nit} = k_{nit}F(T_{soil})F(\psi)C_{NH_4} \quad (2)$$

where k_{nit} is the daily maximum fraction of NH₄⁺ that is converted into NO₃⁻ or gases (d⁻¹), $F(\psi)$ is the soil moisture effect (unitless), and C_{NH_4} is the soil NH₄⁺ content (g N m⁻²). Unlike Chatskikh et al. (2005), who set k_{nit} to 0.10 d⁻¹, it varies with different plant function types (PFTs) in the DLEM with a range of 0.04 to 0.15 d⁻¹. The detailed calculations of $F(T_{soil})$ and $F(\psi)$ were described in Pan et al. (2015) and Yang et al. (2015).

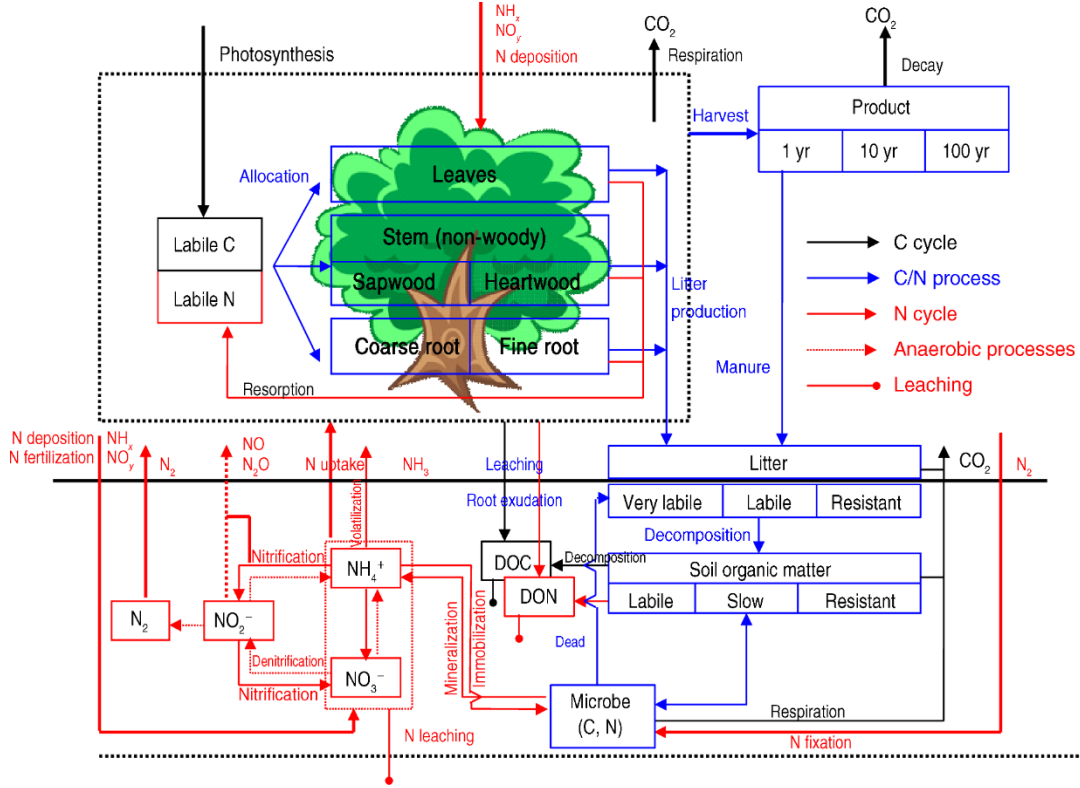


Figure 2-2. The N process and C-N coupling in DLEM (Lu et al., 2012).

Denitrification is the process that converts NO_3^- into three types of gases, namely, nitric oxide, N_2O , dinitrogen. The denitrification rate is simulated as a function of soil temperature, water-filled porosity, and NO_3^- concentration C_{NO_3} (g N g^{-1} soil):

$$R_{\text{den}} = \alpha F(T_{\text{soil}}) F(Q_{\text{wfp}}) F_{\text{N}}(C_{\text{NO}_3}) \quad (3)$$

where $F_{\text{N}}(C_{\text{NO}_3})$ is the dependency of the denitrification rate on NO_3^- concentration (unitless), and α is the maximum denitrification rate ($\text{g N m}^{-2} \text{d}^{-1}$). The detailed calculations of $F(Q_{\text{wfp}})$, $F_{\text{N}}(C_{\text{NO}_3})$ and α were described in (Yang et al., 2015).

In each grid cell, there are four natural vegetation types and one crop type. The sum of N_2O emission in each grid/ d^{-1} is calculated by the following formula:

$$E = \sum_{i=1}^{62481} \sum_{j=1}^5 (N_{ij} \times f_{ij}) \times A_i \times 10^6 / 10^{12}, \quad i = 1, \dots, 62481, j = 1, \dots, 5 \quad (4)$$

where E is the daily sum of N_2O emission from all plant functional types (PFTs) in total grids (Tg $N/yr^{-1} d^{-1}$); N_{ij} ($g N/m^2$) is the N_2O emission in the grid cell i for PFT j ; f_{ij} is the fraction of cell used for PFT j in grid cell i ; and A_i (km^2) is the area of the i th grid cell. 10^6 is to convert km^2 to m^2 and 10^{12} is to convert g to Tg.

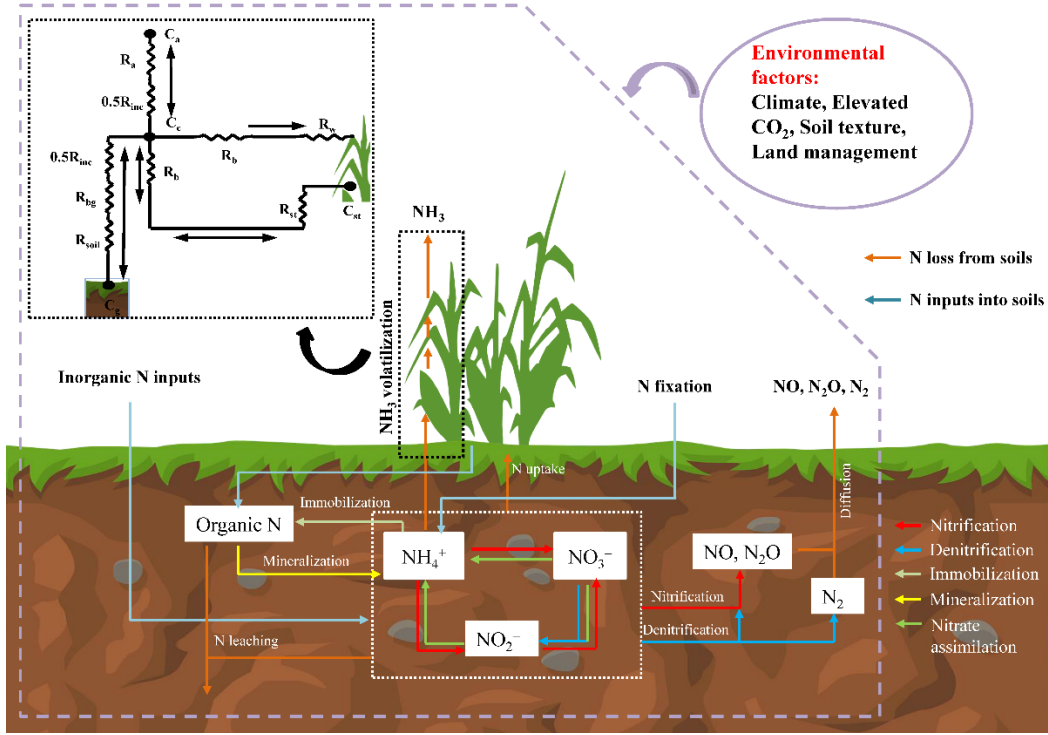


Figure 2-3. The framework of N biogeochemical processes and fluxes in the DLEM-Bi- NH_3 module. R_a , R_{soil} , and R_w : aerodynamic, soil, and cuticular resistance; R_b : the quasi laminar boundary layer resistance; R_{bg} : the soil boundary layer resistance; R_{st} : stomatal resistance; R_{inc} : the aerodynamic resistance within the canopy; C_a : the atmospheric NH_3 concentration; C_c , C_g , and C_{st} : canopy, ground, and stomatal layer compensation point.

2.1.2. NH_3 fluxes in the DLEM-Bi- NH_3 module

Ammonia production is from the transformation of organic compounds and various sources of N inputs. The ammonium (NH_4^+ , $g N m^{-2}$) dynamics in soils:

$$NH_4^+ = NH_4^+_{soil} + NH_4^+_{input} \quad (5)$$

where $\text{NH}_4^+_{\text{soil}}$ (g N m^{-2}) is the soil NH_4^+ pool involved in biogeochemical processes, $\text{NH}_4^+_{\text{input}}$ (g N m^{-2}) is the input of NH_4^+ from N deposition from the atmosphere, N fertilizer application by human, and crop N fixation (Figure 2-3).

In the DLEM, NH_4^+ inputs into soils experience: NH_3 volatilization, plant uptake, nitrification, or N leaching, resulting in variable amounts of NH_4^+ over time. Soil NH_4^+ decreases because of soil immobilization, nitrification, organic and inorganic N leaching and runoff, while NH_4^+ increases due to soil mineralization, crop N fixation, N deposition, and fertilizer/manure N application (Figure 2-3). These processes are regulated by environmental factors (e.g., soil temperature, moisture, pH) and vegetation (e.g., crop type, NH_4^+ uptake).

The overall emission of NH_3 varies daily after chemical N fertilizer was applied to soils and is calculated as follows:

$$F_{\text{emis}} = C_c / (R_a + 0.5 R_{\text{inc}}) \quad (6)$$

where C_c is the canopy NH_3 compensation point as calculated in Eq. (8), R_a is the aerodynamic resistance ranging from 30 to 200, and R_{inc} is the aerodynamic resistance within the canopy. Units of NH_3 fluxes are $\mu\text{g m}^{-3} \text{s}^{-1}$, units of all compensation points are $\mu\text{g m}^{-3}$, and units of all the above resistances are s m^{-1} . For R_{inc} , the following equation was used:

$$R_{\text{inc}} = b_0 \times LAI \times \frac{h_{\text{can}}}{\mu_*} \quad (7)$$

where b_0 is an empirical constant taken as 14 m^{-1} , LAI is the leaf area index, h_{can} is the canopy height (m), and μ_* is the fraction velocity ranging from 0.2 to 0.5 (m s^{-1}). For C_c , the following equation was used:

$$C_c = \frac{\frac{C_{st}}{R_b + R_{st}} + \frac{C_g}{0.5R_{\text{inc}} + R_{bg} + R_{soil}}}{(R_a + 0.5R_{\text{inc}})^{-1} + (R_b + R_{st})^{-1} + (R_b + R_w)^{-1} + (0.5R_{\text{inc}} + R_{bg} + R_{soil})^{-1}} \quad (8)$$

where R_b is the quasi laminar boundary layer resistance at the leaf surface, R_{st} is the stomatal resistance, R_{bg} is the quasi laminar boundary layer resistance at the ground surface, R_w is the cuticular resistance, and R_{soil} is the resistance to diffusion through the soil layer (Cooter et al., 2012; Sakaguchi and Zeng, 2009).

The soil emission potential of NH_3 is regulated by the ratio of NH_4^+ concentration ($[\text{NH}_4^+]$) to H^+ concentration ($[\text{H}^+]$), which is defined as

$$\Gamma_g = \frac{N_{fer}/(\theta_s M_N d_l)}{10^{-\text{pH}}} \quad (9)$$

where N_{fer} is the fertilizer application rate (g N m^{-2}), d_l is the depth of soil layer (m), and pH is the pH of the soil after N fertilizer application (pH = 7.5), M_N is the molar mass of N (14 g mol^{-1}), θ_s is the soil volumetric water content in $\text{m}^3 \text{ m}^{-3}$. The maximum emission potential was found in the first time of fertilization and decreased with passing time. The DLEM deals with loss of N fertilizer at daily step including plant and microbial uptake, nitrification, or N leaching/runoff resulting in variable amounts of NH_4^+ over time.

The ground layer (C_g) compensation points are defined as follows:

$$C_g = M_n/V_m \frac{161500}{T_s} e^{(-\frac{10380}{T_s})} \Gamma_g \quad (10)$$

where $M_n = 1.7 \times 10^7 \text{ } \mu\text{g mol}^{-1}$, $V_m = 1 \times 10^{-3}$ (convert L to m^3), T_s is soil temperature in $^\circ\text{K}$.

The stomatal compensation points are defined as follows:

$$C_{st} = M_n/V_m \frac{161500}{T_{can}} e^{(-\frac{10380}{T_{can}})} \Gamma_s \quad (11)$$

where T_{can} is the canopy temperature in $^\circ\text{K}$, Γ_s is the ratio of $[\text{NH}_4^+]$ to $[\text{H}^+]$ in the apoplast parametrized in Massad et al. (2010).

$$R_b = \frac{v}{D_{NH_3}} \times \left[\frac{c}{(LAI)^2} \times \left(\frac{l \times \mu_*}{v} \right) \right]^{1/3} \quad (12)$$

$$D_{NH_3} = 0.1978 \times \left(\frac{T}{273.13} \right)^{1.81} \times 10^{-4} \quad (13)$$

where D_{NH_3} is the molecular diffusivity of NH_3 in air ($m^2 s^{-1}$, Massman (1998)), c is an empirical constant of order one taken as 3, l is the leaf width (m), v is the kinematic viscosity of air ($1.56 \times 10^{-5} m^2 s^{-1}$ at 25 °C), T is the temperature in °K.

$$R_{st} = (g_s)^{-1} \times \frac{D_x}{D_{NH_3}} \quad (14)$$

where g_s is the stomatal resistance or conductance that controls the flux of gases, D_x is the diffusivity in air of the derived gas ($0.16 \times 10^{-5} m^2 s^{-1}$).

$$R_{bg} = \frac{\frac{v}{D_{NH_3}} - \ln\left(\frac{\delta_0}{z_r}\right)}{k \times \mu_{*g}} \quad (15)$$

where z_r is the top of the logarithmic wind profile layer estimated as 0.1 m, k is the von Karman constant taken as 0.41, δ_0 is the thickness (m) of the laminar layer at the ground surface given by

$$\delta_0 = \frac{v}{k \times \mu_{*g}} \quad (16)$$

where μ_{*g} is the ground level friction velocity given by

$$\mu_{*g} = \mu_* \times \exp(-LAI) \quad (17)$$

$$R_{soil} = L_{dry} / D_p \quad (18)$$

where L_{dry} is the dry layer thickness (m), and D_p is diffuse rate of gas in the soil, defined as,

$$L_{dry} = d_s \times \frac{\exp\left[\left(1 - \theta_s / \theta_{sat}\right)^5\right] - 1}{e - 1} \quad (19)$$

$$D_p = D_{NH_3} \theta_{sat}^2 \left(1 - \frac{\theta_r}{\theta_{sat}}\right)^{(2+3/b)} \quad (20)$$

where d_s is the soil diffusion layer thickness (m), θ_{sat} is the volumetric water content at saturation, θ_s is the soil actual water content, θ_r is the residual water content approaching the soil wilting point, e is the constant taken as 2.718, the b is the slope of the retention curve and is strongly dominated by soil textures, which is estimated in Clapp and Hornberger (1978) and varies according to different soil textures in DLEM-Bi-NH₃ module simulations.

$$R_w = R_{wmin} \times e^{a \times (100 - RH)} \quad (21)$$

$$R_{wmin} = 31.5 \times (AR)^{-1} \quad (22)$$

where a is an empirical factor taken as 0.148 ± 0.113 for arable ecosystem (Sutton et al., 1993), RH is the relative humidity in %, AR is total acid/NH₃ ratio ranging from 0.57 to 2.0 in arable ecosystem.

F_{emis} varies daily after chemical N fertilizer was applied to soils. Here, R_{inc} is also an important factor that controls the overall NH₃ volatilization process. Leaf Index area (LAI) and canopy height (h_{can}) are two dominant variables that determine the value of R_{inc} in this module. Both variables are dependent on crop physiological stages and provided by DLEM physiology simulation module. These related equations and methods for determining crop physiological stages have been described in our previous publications (Pan et al., 2014; Ren et al., 2011). In general, crop physiological stages are highly affected by N supply in soils; i.e., sufficient supply of inorganic N can promote crop growths resulting in larger LAI s and taller crops. Thus, daily-varied NH₃ volatilization amounts from N fertilizer application in this module affects crop growth and N cycling in the DLEM model.

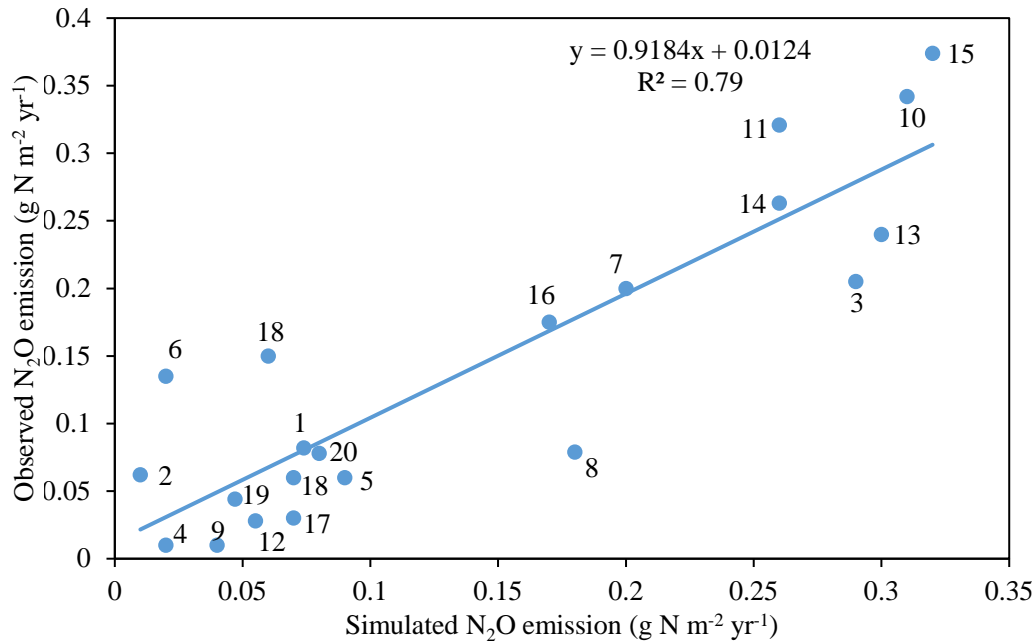


Figure 2-4. The comparison of the DLEM-simulated N₂O emissions with field observations.

2.2. Model evaluation and validation

2.2.1. N₂O emissions from natural vegetation

Observations of annual N₂O emission accumulations (g N m⁻² yr⁻¹) were selected to compare with the simulated emissions in different sites. As there were no field measurements in the pre-industrial era, observations during 1970–2009 were collected to test the model performance in the contemporary period. All environmental factors (climate, CO₂ concentration, soil property, N deposition, LULC) in the exact year were used as input datasets for N₂O simulations. The selected sites include temperate forest, tropical forest, boreal forest, savanna, and grassland globally. As shown in Figure 2-4, the simulated N₂O emissions have a good correlation with field observations ($R^2 = 0.79$). It indicates that the DLEM has the capacity to simulate N₂O emissions in the pre-industrial era driven by environmental factors back then. The detailed information at each site can be found in Table 2-1.

Table 2-1. The description of field measurements from natural vegetation in different sites.

Number	PFT	location		Year	References
		Longitude	Latitude		
1	Forest: Spruce	11°25'E	48°46'N	1993-1995	Butterbach-Bahl et al. (1998)
2	Forest: Spruce	09°34'E	51°46'N	2007-2008	Eickenscheidt and Brumme (2012)
3	Forest: Liana canopy	55°31'W	3°59'S	1998-2000	Davidson et al. (2004)
4	Forest: Douglas-fir	124°30'W	44°00'N	2007-2008	Erickson and Perakis (2014)
5	Grassland	09°42'E	51°46'N	2008-2009	Hoefl et al. (2012)
6	Forest	156°14'W	20°48'N	2000-2001	Holtgrieve et al. (2006)
7	Forest: Spruce & Oak	19°57'–58'E	47°53'N	2002-2003	Horváth et al. (2006)
8	Forest: Beech	16°15'E	48°14'N	2002-2004	Kitzler et al. (2006)
9	Grassland	104°42'W	40°50'N	1997-2000	Mosier et al. (2002)
10	Tropical rain forest	145°30'E	17°30'S	1997-1999	Breuer et al. (2000)
11	Tropical rain forest	63°00'W	10°00'S	–	Stehfest and Bouwman (2006)
12	Savanna	28°30'E	24°30'S	1994	Scholes et al. (1997)
13	Tropical forest	47°30'W	3°00'S	1987	Luizão et al. (1989)
14	Tropical forest	115°30'E	2°00'S	1998-1999	Hadi et al. (2000)
15	Tropical forest	84°00'W	10°26'N	1990-1991	Keller and Reiners (1994)
16	Subtropical forest	66°00'W	18°00'N	1995-1996	Erickson et al. (2001)
17	Temperate forest	116°30'E	39°30'N	1997-1998	Sun and Xu (2001)
18	Temperate forest	89°00'W	43°00'N	1979-1981	Goodroad and Keeney (1984)
19	Grassland	116°04'E	43°26'N	1995	Chen et al. (2000)
20	Temperate forest	126°55'E	41°23'N	1994-1995	

Table 2-2. The comparison of the modeled N₂O emissions in response to multiple N fertilizer addition levels with *in situ* observations.

Crop system	Location	Year	Annual N fertilizer (kg N ha ⁻¹ yr ⁻¹)	Observed N ₂ O emission (kg N ha ⁻¹ yr ⁻¹)	Model simulation (kg N ha ⁻¹ yr ⁻¹)	References
Rice	119°42'E 32°36'N	2005-2007	0	0.38±0.09	0.48±0.02	Yao et al. (2012)
			150	1.33±0.82	1.8±0.06	
			250	2.66±1.49	2.57±0.85	
Rice-wheat	77°12' E 28°40' N	1999-2000	0	0.66±0.05	0.37±0.15	Pathak et al. (2002)
			120	1.57±0.1	1.01±0.31	
	120°55'E 31°32'N	2011-2014	0	1.42±0.35	0.36±0.04	Yang et al. (2015)
Corn	73°57'W 45°50'N	2004	0	0.95±0.21	0.22	Larouche (2006)
			80	2.0±0.28	1.24	
			160	2.5±0.42	2.42	
	133°31'E 47°35'N	2005	0	0.44	0.2	Song and Zhang (2009)
			150	2.0	2.4	
			250	4.84	3.4	
Wheat-corn	117°59'E 36°58'N	2008-2010	0	0.67±0.18	0.19±0.03	Yan et al. (2013)
			400	3.67±1.59	4.84±1.64	
			600	4.64±0.88	5.39±1.05	
Winter wheat	11°21'E 48°30'N	1996-1997	0	0.29±0.29	0.34±0.02	Ruser et al. (2001)
			90	2.7±1.26	1.43±0.79	
			180	3.64±1.21	2.55±1.59	
Barley	10°32'E 52°16'N	1996	0	2.9	0.62	Kaiser et al. (1998)
			73	3.1	1.71	
			146	3.7	2.88	
	6°55'W 52°51'N	2004	0	0.05±0.06	0.12	Abdalla et al. (2010)
			70	0.38±0.16	0.48	
			140	0.89±0.13	1.10	
Soybean	71°19'W 46°46'N	2001-2002	0	0.46-3.08	1.53±0.17	Rochette et al. (2004)
Spring wheat	107°W 50°N	1999	0	0.16±0.09	0.16	Izaurrealde et al. (2004)
			45	0.69±0.21	0.27	
			110	1.62±0.6	0.45	
Cotton	34°55'N 110°43'E	2008	0	1.97	0.89	Liu et al. (2010a)
			66.3	2.6	1.35	
Sorghum	78°27'E 17°53'N	2010	0	0.09	0.23	Ramu et al. (2012)
			90	0.7	0.56	
Pearl millet	Bamako, Mali	2004-2005	0	0.6	0.11±0.04	Dick et al. (2008)
			50	1.54	0.23±0.09	

Table 2-3. The comparison of the modeled N₂O emissions in response to multiple manure N addition levels with *in situ* observations.

Crop system	Location	Year	Annual manure (kg N ha ⁻¹ yr ⁻¹)	Observed N ₂ O emission (kg N ha ⁻¹ yr ⁻¹)	Model simulation (kg N ha ⁻¹ yr ⁻¹)	References
Barley	112°45'E 49°42'N	1993-1994	0	0.7	0.59±0.06	Chang et al. (1998)
			556	11	8.39±3.77	
			1113	23	9.77±1.82	
			1670	56	10.08±1.59	
	116°38'E 36°57'N	2003	0	2.45	1.14	Dong et al. (2005)
			114-138	3.27-3.8	2.02±0.17	
			204-228	3.35-4.7	3.51±0.65	
Corn	5°40'E 51°57'N	2001	0	0.14	0.31	van Groenigen et al. (2004)
			104	0.47	0.7	
			156	1.28	1.02	
			209	1.7	1.45	
			261	1.92	1.98	
			0	1.52	0.18	
			98	2.51	0.45	
			147	3.01	0.76	
	5°48'E 53°12'N		196	3.37	1.01	
			245	6.81	1.46	
Rice	118°50'E 31°52'N	2007	100	0.39±0.08	0.87	Qin et al. (2010)
Alfalfa		2001	0	1.05±0.21	1.12	Ellert and Janzen (2008)
			33	2.91±1.02	1.13	
Wheat	112°46'W 49°42'N,	2002	0	2.74±0.31	1.32	
			33	4.38±0.62	1.34	
Barley		2003	0	1.11±0.18	1.10	
			33	1.36±0.34	1.18	
Winter wheat	75°43'W, 45°22'N	1992	0	0.3	0.1	Lessard et al. (1996)
			170	0.7	0.6	
			339	1.0	0.93	
Sorghum	152°20'E 27°34'S,	2007	0	3.29±0.12	0.84	Dalal et al. (2010)
			186.7	5.09±0.26	2.86	
			373.4	5.52±0.35	5.57	

2.2.2. N₂O emissions from agricultural systems

Previous model validation indicated that the DLEM is capable to accurately simulate site-level and regional N₂O emissions in the context of climate change and human management. Specifically, N₂O emissions from different nature vegetation (temperate forest, tropical forest,

boreal forest, savanna, and grassland) have been selected to compare with the DLEM simulations in those sites. The results showed that DLEM can effectively catch the N₂O fluxes in nature ecosystems (Xu et al., 2017). Lu and Tian (2013) compared the model-estimated fluxes of three GHGs in response to multiple N addition levels with experimental data from two sites in China. It indicated that the DLEM can well simulate the GHG fluxes in control and N added plots during the growing season of marshes and tropical forest. In this study, we obtained the ground-based observations of major crop types (rice, corn, wheat, soybean, cotton, pearl millet, barley, and sorghum) from previous literatures and simulated N₂O fluxes responded to multiple inorganic and organic N addition levels. Then, we compared the model-estimated results with the *in situ* observations (Table 2-2 & 2-3).

2.2.3. NH₃ emissions from agricultural systems

I provided site-level validations of our study with *in situ* observations in Table 2-4.

Table 2-4 The comparison of NH₃ emissions from N fertilizer use using the DLEM-Bi-NH₃ module with *in-situ* observations.

References	Location (Latitude, Longitude)	Year	Crop type	Observed NH ₃ loss (%)	Modeled NH ₃ loss (%)
Bosch-Serra et al. (2014)	41.75, 1.16	2003–2007	Winter cereal	31.98 (7.2~77.9)	32.82 (31.4~34.35)
Cai et al. (2002)	35.07, 114.57	1998–2000	Corn	13.3±1.6/37.4±5.2	11.6 (10.57~13.25)
			Wheat	1.5±0.9/17.5±2.5	
Hayashi et al. (2006)	36.02, 140.12	2006	Rice	8.2	9.4
Hou et al. (2007)	36.2, 139.07	2005	Rice	12.2	12.7
Lin et al. (2007)	31.65, 120.75	2003	Rice	12.2 (9.0~16.7)	10.43
Ma et al. (2010)	45.3, -75.72	2005–2007	Corn	0.13~5.11	10.6 (9.49~11.9)
	43.57, -80.42	2006–2007		0.5-38.3	11.54 (10.39~13.52)
Pacholski et al. (2006)	35.02, 114.07	1998–1999	Winter wheat/ corn	0.6~17.9 14.6~47.9	17.87 (17.68~18.07)
Abalos et al. (2012)	40.53, -3.28	–	Barley	6.7	8.08
Liu et al. (2003)	39.95, 119.5	1998–2000	Winter Wheat/ corn	10.59 (8.33~14.7)	19.32 (18.90~21.26)
Engel et al. (2011)	48.54, -109.91	2008–2010	Winter wheat	8.4	7.65
	48.53, -110.04			11.6	8.2
	48.53, -109.92			10.4	9.11
	45.8, -111.59			44.1	9.89
	48.55, -110.13			14.7	9.84

References

- Abalos, D., Sanz-Cobena, A., Misselbrook, T., and Vallejo, A.: Effectiveness of urease inhibition on the abatement of ammonia, nitrous oxide and nitric oxide emissions in a non-irrigated Mediterranean barley field, *Chemosphere*, 89, 310-318, 2012.
- Abdalla, M., Jones, M., Ambus, P., and Williams, M.: Emissions of nitrous oxide from Irish arable soils: effects of tillage and reduced N input, *Nutrient Cycling in Agroecosystems*, 86, 53-65, 2010.
- Bosch-Serra, À. D., Yagi, M. R., and Teira-Esmatges, M. R.: Ammonia emissions from different fertilizing strategies in Mediterranean rainfed winter cereals, *Atmospheric environment*, 84, 204-212, 2014.
- Breuer, L., Papen, H., and Butterbach-Bahl, K.: N₂O emission from tropical forest soils of Australia, *Journal of Geophysical Research: Atmospheres*, 105, 26353-26367, 2000.
- Butterbach-Bahl, K., Gasche, R., Huber, C., Kreutzer, K., and Papen, H.: Impact of N-input by wet deposition on N-trace gas fluxes and CH₄ oxidation in spruce forest ecosystems of the temperate zone in Europe, *Atmospheric Environment*, 32, 559-564, 1998.
- Cai, G., Chen, D., Ding, H., Pacholski, A., Fan, X., and Zhu, Z.: Nitrogen losses from fertilizers applied to maize, wheat and rice in the North China Plain, *Nutrient Cycling in Agroecosystems*, 63, 187-195, 2002.
- Chang, C., Janzen, H., Nakonechny, E., and Cho, C.: Nitrous oxide emission through plants, *Soil Science Society of America Journal*, 62, 35-38, 1998.
- Chatskikh, D., Olesen, J. E., Berntsen, J., Regina, K., and Yamulki, S.: Simulation of effects of soils, climate and management on N₂O emission from grasslands, *Biogeochemistry*, 76, 395-419, 2005.
- Chen, G. X., Huang, B., Xu, H., Zhang, Y., Huang, G., Yu, K., Hou, A., Du, R., Han, S., and VanCleemput, O.: Nitrous oxide emissions from terrestrial ecosystems in China, *Chemosphere-Global Change Science*, 2, 373-378, 2000.
- Clapp, R. B. and Hornberger, G. M.: Empirical equations for some soil hydraulic properties, *Water Resources Research*, 14, 601-604, 1978.
- Cooter, E., Bash, J., Benson, V., and Ran, L.: Linking agricultural crop management and air quality models for regional to national-scale nitrogen assessments, *Biogeosciences*, 9, 4023-4035, 2012.
- Dalal, R. C., Gibson, I., Allen, D. E., and Menzies, N. W.: Green waste compost reduces nitrous oxide emissions from feedlot manure applied to soil, *Agriculture, ecosystems & environment*, 136, 273-281, 2010.
- Davidson, E. A., Ishida, F. Y., and Nepstad, D. C.: Effects of an experimental drought on soil emissions of carbon dioxide, methane, nitrous oxide, and nitric oxide in a moist tropical forest, *Global Change Biology*, 10, 718-730, 2004.
- Dick, J., Kaya, B., Soutoura, M., Skiba, U., Smith, R., Niang, A., and Tabo, R.: The contribution of agricultural practices to nitrous oxide emissions in semi-arid Mali, *Soil use and management*, 24, 292-301, 2008.
- Dong, Y., Ouyang, Z., Li, Y., and Zhang, L.: Influence of fertilization and environmental factor on CO₂ and N₂O fluxes from agricultural soil, *Journal of Agro-Environmental Science*, 24, 913-918, 2005.

- Eickenscheidt, N. and Brumme, R.: NO_x and N₂O fluxes in a nitrogen-enriched European spruce forest soil under experimental long-term reduction of nitrogen depositions, *Atmospheric Environment*, 60, 51-58, 2012.
- Ellert, B. and Janzen, H.: Nitrous oxide, carbon dioxide and methane emissions from irrigated cropping systems as influenced by legumes, manure and fertilizer, *Canadian Journal of Soil Science*, 88, 207-217, 2008.
- Engel, R., Jones, C., and Wallander, R.: Ammonia volatilization from urea and mitigation by NBPT following surface application to cold soils, *Soil Science Society of America Journal*, 75, 2348, 2011.
- Erickson, H., Keller, M., and Davidson, E. A.: Nitrogen oxide fluxes and nitrogen cycling during postagricultural succession and forest fertilization in the humid tropics, *Ecosystems*, 4, 67-84, 2001.
- Erickson, H. E. and Perakis, S. S.: Soil fluxes of methane, nitrous oxide, and nitric oxide from aggrading forests in coastal Oregon, *Soil Biology and Biochemistry*, 76, 268-277, 2014.
- Goodroad, L. and Keeney, D.: Nitrous oxide emission from forest, marsh, and prairie ecosystems, *Journal of Environmental Quality*, 13, 448-452, 1984.
- Hadi, A., Inubushi, K., Purnomo, E., Razie, F., Yamakawa, K., and Tsuruta, H.: Effect of land-use changes on nitrous oxide (N₂O) emission from tropical peatlands, *Chemosphere-Global Change Science*, 2, 347-358, 2000.
- Hayashi, K., Nishimura, S., and Yagi, K.: Ammonia volatilization from the surface of a Japanese paddy field during rice cultivation, *Soil science and plant nutrition*, 52, 545-555, 2006.
- Heinen, M.: Simplified denitrification models: overview and properties, *Geoderma*, 133, 444-463, 2006.
- Hoefl, I., Steude, K., Wrage, N., and Veldkamp, E.: Response of nitrogen oxide emissions to grazer species and plant species composition in temperate agricultural grassland, *Agriculture, ecosystems & environment*, 151, 34-43, 2012.
- Holtgrieve, G. W., Jewett, P. K., and Matson, P. A.: Variations in soil N cycling and trace gas emissions in wet tropical forests, *Oecologia*, 146, 584-594, 2006.
- Horváth, L., Führer, E., and Lajtha, K.: Nitric oxide and nitrous oxide emission from Hungarian forest soils; linked with atmospheric N-deposition, *Atmospheric Environment*, 40, 7786-7795, 2006.
- Hou, H., Zhou, S., Hosomi, M., Toyota, K., Yosimura, K., Mutou, Y., Nisimura, T., Takayanagi, M., and Motobayashi, T.: Ammonia emissions from anaerobically-digested slurry and chemical fertilizer applied to flooded forage rice, *Water, air, and soil pollution*, 183, 37-48, 2007.
- Izaurrealde, R., Lemke, R. L., Goddard, T. W., McConkey, B., and Zhang, Z.: Nitrous oxide emissions from agricultural toposequences in Alberta and Saskatchewan, *Soil Science Society of America Journal*, 68, 1285-1294, 2004.
- Kaiser, E.-A., Kohrs, K., Kücke, M., Schnug, E., Heinemeyer, O., and Munch, J.: Nitrous oxide release from arable soil: importance of N-fertilization, crops and temporal variation, *Soil Biology and Biochemistry*, 30, 1553-1563, 1998.
- Keller, M. and Reiners, W. A.: Soil-atmosphere exchange of nitrous oxide, nitric oxide, and methane under secondary succession of pasture to forest in the Atlantic lowlands of Costa Rica, *Global Biogeochemical Cycles*, 8, 399-409, 1994.

- Kitzler, B., Zechmeister-Boltenstern, S., Holtermann, C., Skiba, U., and Butterbach-Bahl, K.: Nitrogen oxides emission from two beech forests subjected to different nitrogen loads, *Biogeosciences*, 3, 293-310, 2006.
- Larouche, F.: Émissions de protoxyde d'azote dans une rotation maïs/soya telles qu'influencées par le travail du sol et la fertilisation azotée, 2006. 2006.
- Lessard, R., Rochette, P., Gregorich, E., Pattey, E., and Desjardins, R.: Nitrous oxide fluxes from manure-amended soil under maize, *Journal of Environmental Quality*, 25, 1371-1377, 1996.
- Lin, D.-X., Fan, X.-H., Hu, F., Zhao, H.-T., and Luo, J.-F.: Ammonia volatilization and nitrogen utilization efficiency in response to urea application in rice fields of the Taihu Lake region, China, *Pedosphere*, 17, 639-645, 2007.
- Liu, C., Zheng, X., Zhou, Z., Han, S., Wang, Y., Wang, K., Liang, W., Li, M., Chen, D., and Yang, Z.: Nitrous oxide and nitric oxide emissions from an irrigated cotton field in Northern China, *Plant and Soil*, 332, 123-134, 2010.
- Liu, X., Ju, X., Zhang, F., Pan, J., and Christie, P.: Nitrogen dynamics and budgets in a winter wheat–maize cropping system in the North China Plain, *Field crops research*, 83, 111-124, 2003.
- Liu, X., Zhang, Y., Han, W., Tang, A., Shen, J., Cui, Z., Vitousek, P., Erisman, J. W., Goulding, K., and Christie, P.: Enhanced nitrogen deposition over China, *Nature*, 494, 459-462, 2013.
- Lu, C. and Tian, H.: Net greenhouse gas balance in response to nitrogen enrichment: perspectives from a coupled biogeochemical model, *Global change biology*, 19, 571-588, 2013.
- Lu, C., Tian, H., Liu, M., Ren, W., Xu, X., Chen, G., and Zhang, C.: Effect of nitrogen deposition on China's terrestrial carbon uptake in the context of multifactor environmental changes, *Ecological Applications*, 22, 53-75, 2012.
- Luizão, F., Matson, P., Livingston, G., Luizão, R., and Vitousek, P.: Nitrous oxide flux following tropical land clearing, *Global Biogeochemical Cycles*, 3, 281-285, 1989.
- Ma, B., Wu, T., Tremblay, N., Deen, W., McLaughlin, N., Morrison, M., and Stewart, G.: On-farm assessment of the amount and timing of nitrogen fertilizer on ammonia volatilization, *Agronomy Journal*, 102, 134-144, 2010.
- Massad, R.-S., Nemitz, E., and Sutton, M.: Review and parameterisation of bi-directional ammonia exchange between vegetation and the atmosphere, *Atmospheric Chemistry and Physics*, 10, 10359-10386, 2010.
- Massman, W.: A review of the molecular diffusivities of H₂O, CO₂, CH₄, CO, O₃, SO₂, NH₃, N₂O, NO, and NO₂ in air, O₂ and N₂ near STP, *Atmospheric Environment*, 32, 1111-1127, 1998.
- Mosier, A., Morgan, J., King, J., Lecain, D., and Milchunas, D.: Soil-atmosphere exchange of CH₄, CO₂, NO_x, and N₂O in the Colorado shortgrass steppe under elevated CO₂, *Plant and Soil*, 240, 201-211, 2002.
- Pacholski, A., Cai, G., Nieder, R., Richter, J., Fan, X., Zhu, Z., and Roelcke, M.: Calibration of a simple method for determining ammonia volatilization in the field—comparative measurements in Henan Province, China, *Nutrient Cycling in Agroecosystems*, 74, 259-273, 2006.

- Pan, S., Tian, H., Dangal, S. R., Yang, Q., Yang, J., Lu, C., Tao, B., Ren, W., and Ouyang, Z.: Responses of global terrestrial evapotranspiration to climate change and increasing atmospheric CO₂ in the 21st century, *Earth's Future*, 3, 15-35, 2015.
- Pan, S., Tian, H., Dangal, S. R., Zhang, C., Yang, J., Tao, B., Ouyang, Z., Wang, X., Lu, C., and Ren, W.: Complex Spatiotemporal Responses of Global Terrestrial Primary Production to Climate Change and Increasing Atmospheric CO₂ in the 21 st Century, *PloS one*, 9, e112810, 2014.
- Pathak, H., Bhatia, A., Prasad, S., Singh, S., Kumar, S., Jain, M., and Kumar, U.: Emission of nitrous oxide from rice-wheat systems of Indo-Gangetic plains of India, *Environmental Monitoring and Assessment*, 77, 163-178, 2002.
- Qin, Y., Liu, S., Guo, Y., Liu, Q., and Zou, J.: Methane and nitrous oxide emissions from organic and conventional rice cropping systems in Southeast China, *Biology and Fertility of Soils*, 46, 825-834, 2010.
- Ramu, K., Watanabe, T., Uchino, H., Sahrawat, K. L., Wani, S. P., and Ito, O.: Fertilizer induced nitrous oxide emissions from Vertisols and Alfisols during sweet sorghum cultivation in the Indian semi-arid tropics, *Science of the Total Environment*, 438, 9-14, 2012.
- Ren, W., Tian, H., Xu, X., Liu, M., Lu, C., Chen, G., Melillo, J., Reilly, J., and Liu, J.: Spatial and temporal patterns of CO₂ and CH₄ fluxes in China's croplands in response to multifactor environmental changes, *Tellus B*, 63, 222-240, 2011.
- Rochette, P., Angers, D. A., Bélanger, G., Chantigny, M. H., Prévost, D., and Lévesque, G.: Emissions of N₂O from alfalfa and soybean crops in eastern Canada, *Soil Science Society of America Journal*, 68, 493-506, 2004.
- Ruser, R., Flessa, H., Schilling, R., Beese, F., and Munch, J.: Effect of crop-specific field management and N fertilization on N₂O emissions from a fine-loamy soil, *Nutrient Cycling in Agroecosystems*, 59, 177-191, 2001.
- Sakaguchi, K. and Zeng, X.: Effects of soil wetness, plant litter, and under-canopy atmospheric stability on ground evaporation in the Community Land Model (CLM3.5), *Journal of Geophysical Research: Atmospheres*, 114, 2009.
- Scholes, M., Martin, R., Scholes, R., Parsons, D., and Winstead, E.: NO and N₂O emissions from savanna soils following the first simulated rains of the season, *Nutrient Cycling in Agroecosystems*, 48, 115-122, 1997.
- Song, C. and Zhang, J.: Effects of soil moisture, temperature, and nitrogen fertilization on soil respiration and nitrous oxide emission during maize growth period in northeast China, *Acta Agriculturae Scandinavica Section B–Soil and Plant Science*, 59, 97-106, 2009.
- Stehfest, E. and Bouwman, L.: N₂O and NO emission from agricultural fields and soils under natural vegetation: summarizing available measurement data and modeling of global annual emissions, *Nutrient Cycling in Agroecosystems*, 74, 207-228, 2006.
- Sun, X. and Xu, H.: Emission flux of nitrous oxide from forest soils in Beijing, *Scientia Silvae Sinicae*, 37, 57-63, 2001.
- Sutton, M., Pitcairn, C. E., and Fowler, D.: The exchange of ammonia between the atmosphere and plant communities. In: *Advances in ecological research*, Elsevier, 1993.
- Tian, H., Chen, G., Lu, C., Xu, X., Ren, W., Zhang, B., Banger, K., Tao, B., Pan, S., and Liu, M.: Global methane and nitrous oxide emissions from terrestrial ecosystems due to multiple environmental changes, *Ecosystem Health and Sustainability*, 1, 1-20, 2015.

- Tian, H., Chen, G., Zhang, C., Liu, M., Sun, G., Chappelka, A., Ren, W., Xu, X., Lu, C., and Pan, S.: Century-scale responses of ecosystem carbon storage and flux to multiple environmental changes in the southern United States, *Ecosystems*, 15, 674-694, 2012.
- Tian, H., Xu, X., Liu, M., Ren, W., Zhang, C., Chen, G., and Lu, C.: Spatial and temporal patterns of CH₄ and N₂O fluxes in terrestrial ecosystems of North America during 1979–2008: application of a global biogeochemistry model, *Biogeosciences*, 7, 2673-2694, 2010.
- Tian, H., Xu, X., Lu, C., Liu, M., Ren, W., Chen, G., Melillo, J., and Liu, J.: Net exchanges of CO₂, CH₄, and N₂O between China's terrestrial ecosystems and the atmosphere and their contributions to global climate warming, *Journal of Geophysical Research: Biogeosciences*, 116, 2011.
- van Groenigen, J. W., Kasper, G. J., Velthof, G. L., van den Pol-van Dasselaar, A., and Kuikman, P. J.: Nitrous oxide emissions from silage maize fields under different mineral nitrogen fertilizer and slurry applications, *Plant and Soil*, 263, 101-111, 2004.
- Xu, R., Tian, H., Lu, C., Pan, S., Chen, J., Yang, J., and Bowen, Z.: Preindustrial nitrous oxide emissions from the land biosphere estimated by using a global biogeochemistry model, *Climate of the Past*, 13, 977-990, 2017.
- Yan, G., Zheng, X., Cui, F., Yao, Z., Zhou, Z., Deng, J., and Xu, Y.: Two-year simultaneous records of N₂O and NO fluxes from a farmed cropland in the northern China plain with a reduced nitrogen addition rate by one-third, *Agriculture, ecosystems & environment*, 178, 39-50, 2013.
- Yang, B., Xiong, Z., Wang, J., Xu, X., Huang, Q., and Shen, Q.: Mitigating net global warming potential and greenhouse gas intensities by substituting chemical nitrogen fertilizers with organic fertilization strategies in rice–wheat annual rotation systems in China: A 3-year field experiment, *Ecological Engineering*, 81, 289-297, 2015.
- Yang, Q., Tian, H., Friedrichs, M. A., Hopkinson, C. S., Lu, C., and Najjar, R. G.: Increased nitrogen export from eastern North America to the Atlantic Ocean due to climatic and anthropogenic changes during 1901–2008, *Journal of Geophysical Research: Biogeosciences*, 120, 1046-1068, 2015.
- Yao, Z., Zheng, X., Dong, H., Wang, R., Mei, B., and Zhu, J.: A 3-year record of N₂O and CH₄ emissions from a sandy loam paddy during rice seasons as affected by different nitrogen application rates, *Agriculture, ecosystems & environment*, 152, 1-9, 2012.
- Zhang, B., Tian, H., Ren, W., Tao, B., Lu, C., Yang, J., Banger, K., and Pan, S.: Methane emissions from global rice fields: Magnitude, spatiotemporal patterns, and environmental controls, *Global Biogeochemical Cycles*, 30, 1246-1263, 2016.
- Zhou, M., Zhu, B., Butterbach-Bahl, K., Zheng, X., Wang, T., and Wang, Y.: Nitrous oxide emissions and nitrate leaching from a rain-fed wheat-maize rotation in the Sichuan Basin, China, *Plant and soil*, 362, 149-159, 2013.

Chapter 3. Increased nitrogen enrichment and shifted patterns in the world's grassland: 1860-2016

Abstract

Production and application to soils of manure excreta from livestock significantly perturb the global nutrient balance and result in significant greenhouse gas emissions that warm the earth's climate. Despite much attention paid to synthetic nitrogen (N) fertilizer and manure N applications to croplands, spatially-explicit, continuous time-series datasets of manure and fertilizer N inputs on pastures and rangelands are lacking. We developed three global gridded datasets at a resolution of $0.5^\circ \times 0.5^\circ$ for the period 1860–2016 (i.e., annual manure N deposition (by grazing animals) rate, synthetic N fertilizer and N manure application rates), by combining annual and 5-arc minute spatial data on pastures and rangelands with country-level statistics on livestock manure, mineral and chemical fertilizers, and land use information for cropland and permanent meadows and pastures. Based on the new data products, we estimated that total N inputs, sum of manure N deposition, manure and fertilizer N application to pastures and rangelands increased globally from 15 to 101 Tg N yr⁻¹ during 1860–2016. In particular during the period 2000-2016, livestock manure N deposition accounted for 83% of the total N inputs, whereas manure and fertilizer N application accounted 9% and 8%, respectively. At the regional scale, hotspots of manure N deposition remained largely similar during the period 1860–2016 (i.e., southern Asia, Africa, and South America); however, hotspots of manure and fertilizer N application shifted from Europe to southern Asia in the early 21st century. The new three global datasets contribute to fill previous

data gaps of global and regional N inputs in pastures and rangelands, improving the abilities of ecosystem and earth system models to investigate the global impacts of N enrichment due to agriculture, in terms of associated greenhouse gas emissions and environmental sustainability issues.

1. Introduction

Livestock production has increased substantially in response to growing meat consumption across the globe in the past century (Bouwman et al., 2013; Dangal et al., 2017). Agriculture occupies 37% of Earth's ice-free land surface for use as cropland and permanent meadows and pastures (Tubiello, 2018). Land used by livestock for permanent meadows and pastures is the largest component, using 25% of the total land earth surface (FAOSTAT, 2018) to generate 33%–50% of world total agricultural GDP (Herrero et al., 2013). While livestock is a major source of income for more than 1.3 billion people, it is also a major user of crop and freshwater resources (Dangal et al., 2017; Herrero et al., 2013). Overall, livestock production plays a major role as driver of global change in land use and nutrient cycles (Havlík et al., 2014; Herrero et al., 2013; Zhang et al., 2017). There is a growing recognition that livestock production is linked to increasing global greenhouse gas (GHGs) and ammonia emissions (Tian et al., 2016; Tian et al., 2018b; Tubiello, 2018; Xu et al., 2018a; Xu et al., 2019b). Unsustainable practices, especially in intensive systems, may lead to severe pollution of aquatic systems and soil degradation locally, regional and globally, in particular through nitrate leaching to water bodies (Dangal et al., 2017; Davis et al., 2015; Fowler et al., 2015; Yang et al., 2016). Growing global demand for livestock products has increased grain production for feed in many regions, and has become a global driver of fertilizers trends, through increase in manure availability and synthetic fertilizer N use (FAOSTAT, 2018).

Livestock production systems therefore play an important role in global nutrient cycles. For example, nitrogen excretion from livestock increased from 21 Tg N yr⁻¹ in 1860 to 123 Tg N yr⁻¹ in 2016 (FAOSTAT, 2018; Zhang et al., 2017). Livestock contribute roughly two-thirds of non-CO₂ GHG emissions from agriculture (Smith et al., 2014), with roughly an equal share of CH₄ and N₂O emissions (Dangal et al., 2017; Tubiello et al., 2013). Importantly, about 45% of total anthropogenic N₂O emissions are linked to manure deposited through grazing and manure applied to croplands or left on pasture (Davidson, 2009; FAOSTAT, 2018). Globally, emissions from manure N applied to soils or left on pastures has increased from 0.44 to 0.88 GtCO₂eq yr⁻¹ during 1961–2010 (FAOSTAT, 2018). Increased meat and dairy products consumption worldwide was a major driver behind the documented increase in cattle herds globally (FAOSTAT, 2018), and thus a major cause in the observed atmospheric increase of N₂O and CH₄ over the past several decades (Bai et al., 2018; Bouwman et al., 2013; Dangal et al., 2017; Tubiello, 2018).

While the availability of national-level statistics is a fundamental component of our knowledge base, environmental problems related to nitrogen pollution or emissions are best tackled at local scale and often require finer, geo-spatial information, for example to assess proximity to water bodies and thus pollution risks. In particular, a number of studies have focused on downscaling existing national information to develop geospatially explicit regional and global datasets of nitrogen fertilizer and livestock manure production and use, to better understand their feedback on the climate system. Several datasets of N fertilizer use were used in this study, in particular the FAOSTAT annual, country-specific statistics on mineral and chemical fertilizers and livestock manure over the period 1961-2016 (FAOSTAT, 2018), as well as specific geospatially-downscaled products (e.g., (Bouwman et al., 2005; Lu and Tian, 2017; Mueller et al., 2012; Nishina et al., 2017; Potter et al., 2010; Sheldrick et al., 2002). Further, global manure production

datasets were developed in different studies to achieve various research goals (Bouwman et al., 2009; Bouwman et al., 2013; Holland et al., 2005; Potter et al., 2010; Zhang et al., 2017). Although datasets of manure application in croplands are increasingly available, there is considerable uncertainty in the estimation of total manure application and their spatial distribution across different studies (Gerber et al., 2016; Herrero et al., 2013; Liu et al., 2010b; Zhang et al., 2017).

Although previous studies have provided spatially explicit datasets of N inputs in the form of mineral or chemical and manure N in cropland systems, the spatially explicit datasets on N inputs in grassland systems are still missing (Chang et al., 2016; Lassaletta et al., 2014a; Stehfest and Bouwman, 2006). By grassland systems we mean the FAO livestock land use definition, i.e., land used as permanent meadows and pastures (FAOSTAT, 2018). The same may also be referred to in the literature as ‘pastures and rangelands’. We note that ‘grassland’ is in fact a land cover definition. In order to avoid the confusion often made in the literature between land cover and land use terminology, we will adopt FAO land use terminology of ‘permanent meadows and pastures,’ to which the various national regional and global land use statistics cited in this work refer. Furthermore, using results from the HYDE 3.2 dataset (Klein Goldewijk et al., 2017), we may split the FAO land use category into ‘pastures’ and ‘rangelands’, to highlight differences between managed intensive and unmanaged extensive systems, as needed. To enhance our understanding of the role of livestock on the global GHG balance and nutrient budgets (e.g., ammonia emissions, nitrate leaching), global biogeochemistry models require spatially explicit estimates of N inputs. In this study, we developed datasets for major sources of N inputs in agriculture (i.e., manure and fertilizer application and manure deposition on permanent meadows and pastures), using the recently published FAOSTAT statistics on manure N use in agriculture (FAOSTAT, 2018). The latter are estimates based on IPCC Tier 1 methodology, i.e., they rely on default coefficients

prescribing, among other variables, N excretion rates by animal type and region, as well as regional compositions of manure management systems (FAOSTAT, 2018).

Through combining the land-use dataset HYDE 3.2, FAOSTAT fertilizers N statistics, and gridded manure production data in Zhang et al. (2017), we developed three annual global datasets at a spatial resolution of $0.5^\circ \times 0.5^\circ$, as follows: 1) manure N application rates to pastures (1860–2016); 2) synthetic N fertilizer application rates to pastures (1961–2016); and 3) manure deposition rates by grazing livestock, to rangelands and pastures (1860–2016). We quantified regional variations in N inputs, identified hotspots of N inputs from different N sources from livestock, and discussed their uncertainty. These datasets are developed for global model simulation studies in model inter-comparison projects (e.g., NMIP; (Tian et al., 2018; Tian et al., 2019), and will be updated annually based on regular annual updates of FAO fertilizers and land use statistics and other sources of data such as global land use data products.

2. Methods

2.1. Land use categories

The concepts of grassland, pastures and meadows span several international land cover and land use statistical definitions, specifically those used by FAO (FAOSTAT, 2018). In this paper, we follow the relevant FAO land use definition of ‘permanent meadows and pastures,’ considering our focus on livestock production. Importantly, complete country, regional and global statistics available from FAO refer to this land use category. This land use definition is roughly equivalent to the one adopted by the academic community engaged in global biogeochemical modeling, for which ‘grassland systems’ are thought of as land cover/land use areas dominated by herbaceous and shrub vegetation, including savannas (Africa, South America and India), steppes (Eurasia),

prairies (North America), shrub-dominated areas (Africa), meadows and pastures (United Kingdom and Ireland) and tundra (Breymer, 1990; White et al., 2000).

For mineral and chemical fertilizers, we further split the FAO definition using HYDE 3.2, into ‘pastures’ and ‘rangelands,’ the former representing land use areas managed to support high stocking densities of grass production for hay/silage, whereas the latter represents unmanaged and grazed at low stocking densities. Although FAOSTAT land-use statistics cover in principle these two sub-categories of land use, data coverage needed is insufficient for the consistent global mapping needed herein. The spatial distribution map of pastures and rangelands provided by HYDE are nonetheless based on and normalized to FAOSTAT land use statistics, complemented by additional information (Klein Goldewijk et al., 2017). To investigate N inputs from livestock at a regional level, the global landmass was disaggregated into seven regions: North America, South America, Africa, Europe, southern Asia (i.e., west, south, east, central and southeast Asia), northern Asia, and Oceania.

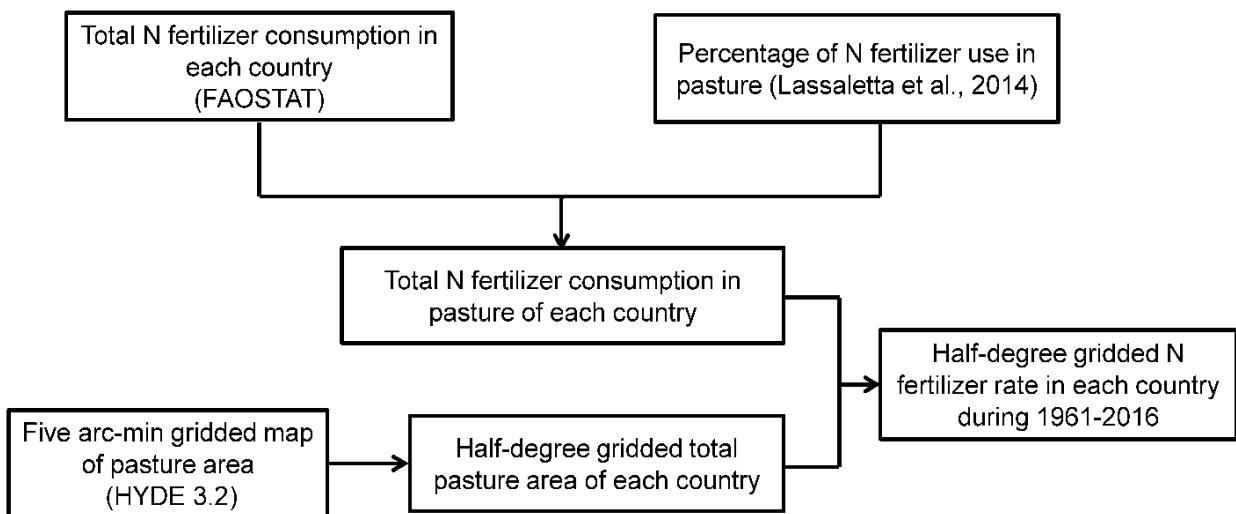


Figure 3-1. Diagram of the workflow for developing the database of global annual N fertilizer use rate in pasture during the period 1961–2016.

2.2. Fertilizer N application on global pastures

We obtained national-level datasets of “Agricultural use of mineral or chemical fertilizers” from the FAOSTAT (2018) ‘Fertilizers by Nutrient’ domain, over the time series 1961–2016. The FAOSTAT statistics of agricultural use include use for both agriculture and forestry, as well as use in aquaculture. Furthermore, agricultural use includes both cropland and permanent meadows and pastures. We assumed that fertilizers use for forestry and aquaculture was zero, as well as fertilizers applications on rangelands. Subsequently, we estimated N application rates to pastures by using the ratio of pasture to cropland N use total published by Lassaletta et al. (2014a). We finally spatialized the pasture N data using HYDE 3.2, obtaining gridded maps of synthetic fertilizers N application rates on pastures in each grid cell area, over the period 1961–2016 (Figure 3-1). We assumed even application rates within each country. Although gridded livestock density maps were available from FAO, these are currently fixed for specific time periods, mainly 2010, so that we deemed their use not particularly relevant to improve estimates for the 1961-2016 time series considered herein. Improved live density map products from FAO will considerably improve our work and reduce uncertainty, and will be used when available.

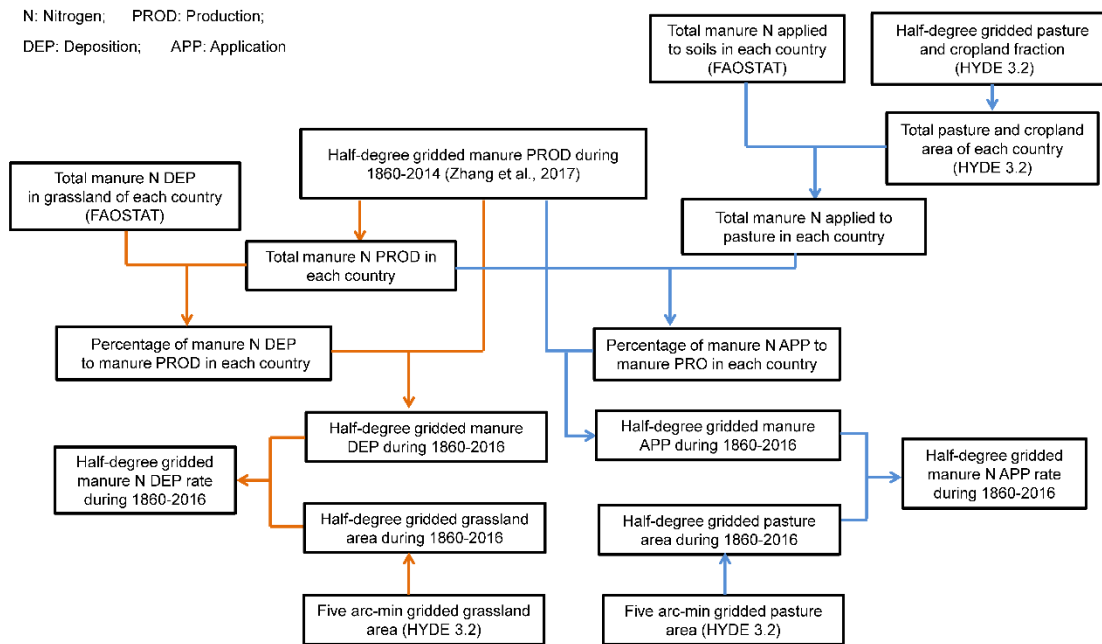


Figure 3-2. Diagram of the workflow for developing the database of global annual manure N use rate in pastures and manure N deposition rate in pastures and rangelands during the period 1860–2016.

2.3. Global manure N application to pastures

We obtained country-level datasets of “manure applied to soils” from the FAOSTAT (2018) ‘Livestock Manure’ domain for the period 1961–2016 (FAO, 2018). Following IPCC guidelines, the data in this domain do not consider N leaching during treatment (FAOSTAT, 2018). Furthermore, the FAOSTAT data do not separate manure application to cropland and pastures and data of manure N application rates to pastures are currently not available. We therefore assumed that manure N application rates in pastures and croplands were the same, considering that the overall uncertainty in the input manure N data would not justify further assumptions at this stage of knowledge. Improved FAO statistics on both use and application rates will be used when available to improve this current work. Through combining land-use data HYDE 3.2, we

calculated the total cropland and pasture areas within each country where manure application amount was larger than zero. We then computed mean manure N application rates on pastures, annually over the period 1961–2016 (Figure 3-2).

We calculated the national-level ratio of manure application to production ($R_{a2p_{y,j}}$) by combining gridded manure production data in Zhang et al. (2017) and the grid cell area. To spatialize the national-level manure N application amounts to gridded maps of application rates in each grid area, we multiplied the $R_{a2p_{y,j}}$ in grids where pasture areas were larger than zero with the time-series gridded spatial distribution maps of manure production rate in Zhang et al. (2017) during 1961–2014 and based on the spatial distributions of global pastures in land-use data HYDE 3.2 (Klein Goldewijk et al., 2017).

The above-mentioned processes are represented by following equations:

$$R_{a2p_{y,j}} = \frac{T_{Mapp_{y,j}}}{\sum_{g=1}^{g=n \text{ in country } j} (R_{Mprod_{y,g}} \times A_g)} \quad (1)$$

where year is from 1961 to 2016, and country number is 165. $R_{a2p_{y,j}}$ is the ratio (unitless) of manure application to production in the year y and country j . $T_{Mapp_{y,j}}$ is the national total manure application amount (kg N yr^{-1}) derived from the FAO database for each year. A_g is the area of each grid (km^2).

$$R_{Mapp_{y,g}} = R_{a2p_{y,j}} \times R_{Mprod_{y,g}} \quad (2)$$

where $R_{Mapp_{y,g}}$ is the gridded manure application rate ($\text{kg N km}^{-2} \text{ yr}^{-1}$) in year y and country j .

As the national-level manure application amount was not available during 1860–1960, we assumed that $R_{a2p_{y,j}}$ is the same as for 1961. Combining with the gridded spatial maps of manure

production rates in Zhang et al. (2017), we generated the datasets of spatialized manure application rates to global pastures during 1860–1960.

Finally, we calculated manure application amounts in each country by combining $R_{Mapp_{y,g}}$ and grid areas to compare with national-level deposition amounts from the FAOSTAT database during 1961–2016. As we calculated national-level manure application amounts during 1860–1960 using $R_{azp_{y,j}}$ in 1961, these data served as national total manure N application amounts to adjust $R_{Mapp_{y,g}}$ during 1860–1960.

The adjustment procedure is represented in the following equations:

$$CT_{Mapp_{y,j}} = \sum_{g=1}^{g=n \text{ in country } j} (R_{Mapp_{y,g}} \times A_g) \quad (3)$$

where year is from 1860–2016. $CT_{Mapp_{y,j}}$ (kg N yr⁻¹) is the calculated national-level manure application amounts in the year y and country j . If $CT_{Mapp_{y,j}}$ is less or more than $T_{Mapp_{y,j}}$, an adjustment is needed to keep calculated national total amounts consistent with amounts from the FAOSTAT database. In this case, $CT_{Mapp_{y,j}}$ is less than $T_{Mapp_{y,j}}$ using Eq. 3, thus an adjustment is needed, using the following equations:

$$R_{a_{y,j}} = \frac{T_{Mapp_{y,j}}}{CT_{Mapp_{y,j}}} \quad (4)$$

where $R_{a_{y,j}}$ is the regulation ratio (unitless) in the year y and country j .

$$R_{Mapp_{y,g(r)}} = R_{Mapp_{y,g}} \times R_{a_{y,j}} \quad (5)$$

where $R_{Mapp_{y,g(r)}}$ is real gridded manure application rate (kg N km⁻² yr⁻¹) in the year y and country j .

2.4. Global manure N deposition on pastures and rangelands

To develop global distribution maps of manure N deposition by grazing animals, we first obtained country-level statistics of “manure left on pasture” over the period 1961–2016 from the FAOSTAT (2018) ‘Livestock manure’ domain of FAOSTAT agri-environmental indicators (FAO, 2018). We then obtained the national-level ratio of manure deposition to production ($R_{d2p_{y,j}}$) by combining country-level FAOSTAT datasets of “Manure left on pasture” and gridded total manure production datasets based on Zhang et al. (2017). Then, we used spatial distributions of global permanent meadows and pastures, including pastures and rangelands, based on HYDE 3.2 grassland data (Klein Goldewijk et al., 2017) and gridded maps of deposition rates, to spatialize the national-level manure N deposition at the global scale. For example, we multiplied the $R_{d2p_{y,j}}$ ratio in grids within which the pastures and rangelands area was larger than zero, with the time-series gridded spatial distribution maps of manure production rates in Zhang et al. (2017) during 1961–2014 (Figure 3-2).

The above-mentioned processes are represented by the following equations:

$$R_{d2p_{y,j}} = \frac{T_{Mdep_{y,j}}}{\sum_{g=1}^{g=n \text{ in country } j} (R_{Mprod_{y,g}} \times A_g)} \quad (6)$$

where year (y) is from 1961 to 2016 and country number (j) is 157. $R_{d2p_{y,j}}$ is the ratio (unitless) of manure deposition to production in the year y and country j . $T_{Mdep_{y,j}}$ is national total manure deposition amount (kg N yr⁻¹) derived from the FAOSTAT database for each year. $R_{Mprod_{y,g}}$ is the gridded manure N production rate (kg N km⁻² yr⁻¹) in the year y and grid g .

$$R_{Mdep_{y,g}} = R_{d2p_{y,j}} \times R_{Mprod_{y,g}} \quad (7)$$

where $R_{Mdep_{y,g}}$ is the gridded manure deposition rate (kg N km⁻² yr⁻¹) in the year y and country j .

Finally, we calculated the manure deposition amount for each country through combining $R_{Mdep_{y,g}}$ and grid area to compare with the national-level deposition amounts from the FAOSTAT database, using the following equation:

$$CT_{Mdep_{y,j}} = \sum_{g=1}^{g=n \text{ in country } j} (R_{Mdep_{y,g}} \times A_g) \quad (8)$$

where $CT_{Mdep_{y,j}}$ (kg N yr⁻¹) is the calculated national-level manure deposition amount in the year y and country j . If $CT_{Mdep_{y,j}}$ is less or more than $T_{Mdep_{y,j}}$, an adjustment was made to keep calculated national total amounts consistent with those from the FAOSTAT database. In this case, $CT_{Mdep_{y,j}}$ is roughly equal to $T_{Mdep_{y,j}}$ using Eq. 8, thus no adjustment was needed.

Since the national-level manure deposition amounts are not available during 1860–1960, we assumed that $R_{d2p_{y,j}}$ is the same as that in 1961. Combining the gridded spatial maps of manure production rates in Zhang et al. (2017), we generated datasets of spatialized manure deposition rates on permanent meadows and pastures globally, for the period 1860–1960.

3. Results

3.1. Synthetic fertilizer N application to pastures, 1961–2016

The FAO data, combined with the geospatial analysis in this work, show that the total amount of synthetic N fertilizer applied to pastures increased from 0.04 to 8.7 Tg N yr⁻¹ during 1961–2016 at an average rate of ~0.18 Tg N yr⁻¹ ($R^2 = 0.98$) per year (Figure 3-3a). Synthetic N fertilizer application rates showed rapid increases across the globe, with large spatial variations during the study period (Figures 8-4b-c). The global average application rate on pastures was 0.07 kg N ha⁻¹ yr⁻¹ in 1961 and reached 10.9 kg N ha⁻¹ yr⁻¹ in 2016 (increased ~154 folds) (Table 3-1).

Table 3-1. The N input rates, applied/deposited area, and total amounts in global pastures and rangelands in 1860, 1961, 2000, 1980, and 2016 (1 km² = 100 ha). N/A: not available.

	1860	1961	1980	2000	2016
Averaged N fertilizer application rate (kg N ha ⁻¹ yr ⁻¹)	N/A	0.07	3.6	7.8	10.9
Total applied area (Mha)	N/A	623.8	725	797.8	803.1
Total amounts (Tg N yr ⁻¹)	N/A	0.04	2.6	6.2	8.7
Average manure N application rate (kg N ha ⁻¹ yr ⁻¹)	5.3	8.1	9.8	9.5	10.7
Total applied area (Mha)	268.2	623.8	725	797.8	803.1
Total amounts (Tg N yr ⁻¹)	1.4	5.0	7.1	7.6	8.6
Average manure N deposition rate (kg N ha ⁻¹ yr ⁻¹)	11.2	15.4	19.0	20.7	25.3
Total deposited area (Mha)	1250.1	3070.7	3194.2	3398.5	3295
Total amounts (Tg N yr ⁻¹)	14.0	47.2	60.7	70.5	83.5

In the 1960s, Europe (0.2 Tg N yr⁻¹) was the largest contributor (67.8%) to the total global N fertilizer use, followed by North America (0.06 Tg N yr⁻¹, 21.8%) and southern Asia (0.03 Tg N yr⁻¹, 9.9%) (Figure 3-5a). The remaining regions accounted for less than 1% of the total N fertilizer application. During 1961–2016, southern Asia showed a continuous increase of N fertilizer consumption and became the largest contributor (3.4 Tg N yr⁻¹, 45%) between 2000 and 2016. In contrast, Europe’s synthetic N fertilizer use and contribution to the global total decreased since the 1980s (Figure 3-5a). This is a well-known trend, linked to EU-wide policy directives aimed at minimizing N pollution (Tubiello, 2018). During 2000–2016, Europe applied 2.1 Tg N yr⁻¹, which accounted for 27% of the total global N fertilizer use on pastures. There was a slight increase in the contribution from North America, and the synthetic fertilizer N use amount increased by 1.6 Tg N yr⁻¹. The remaining regions accounted for roughly 7% of the total N fertilizer application on pastures.

The average synthetic N application rate in Oceania, North America, and southern Asia showed a rapid increase over the period 1961–2016 (Figure 3-5d). Africa and northern Asia showed a slight increase in average N fertilizer application rates during the study period. Europe exhibited a rapid increase of N fertilizer application rates since 1961, then decreased after 2000, and then started to increase in recent five years (Figure 3-6).

We identified the top five countries (India, United States, China, France, and Germany) with highest fertilizer N application to pastures in 2016. These countries consumed 49% to 58% of the total N fertilizer from 1961 to 2016. India (1.5 Tg N yr⁻¹) and the United States (1.5 Tg N yr⁻¹) were the two largest contributors in 2016, at an increasing rate of 45 Gg N yr⁻¹ (R² = 0.98) per year during 1980–2016 and 32 Gg N yr⁻¹ (R² = 0.99) per year during 1961–2016, respectively. China consumed 1.4 Tg N yr⁻¹ in 2016 at an increasing rate of 34 Gg N yr⁻¹ (R² = 0.96) per year during 1977–2016 while there was only a slight increase during 1961–1976. In contrast, fertilizer N use in France peaked in 1999 (0.8 Tg N yr⁻¹), then showed a rapid decrease until 2016 (0.5 Tg N yr⁻¹). Similarly, in Germany, it peaked in 1988 (0.8 Tg N yr⁻¹), and showed a continuous decrease until 2016 (0.3 Tg N yr⁻¹).

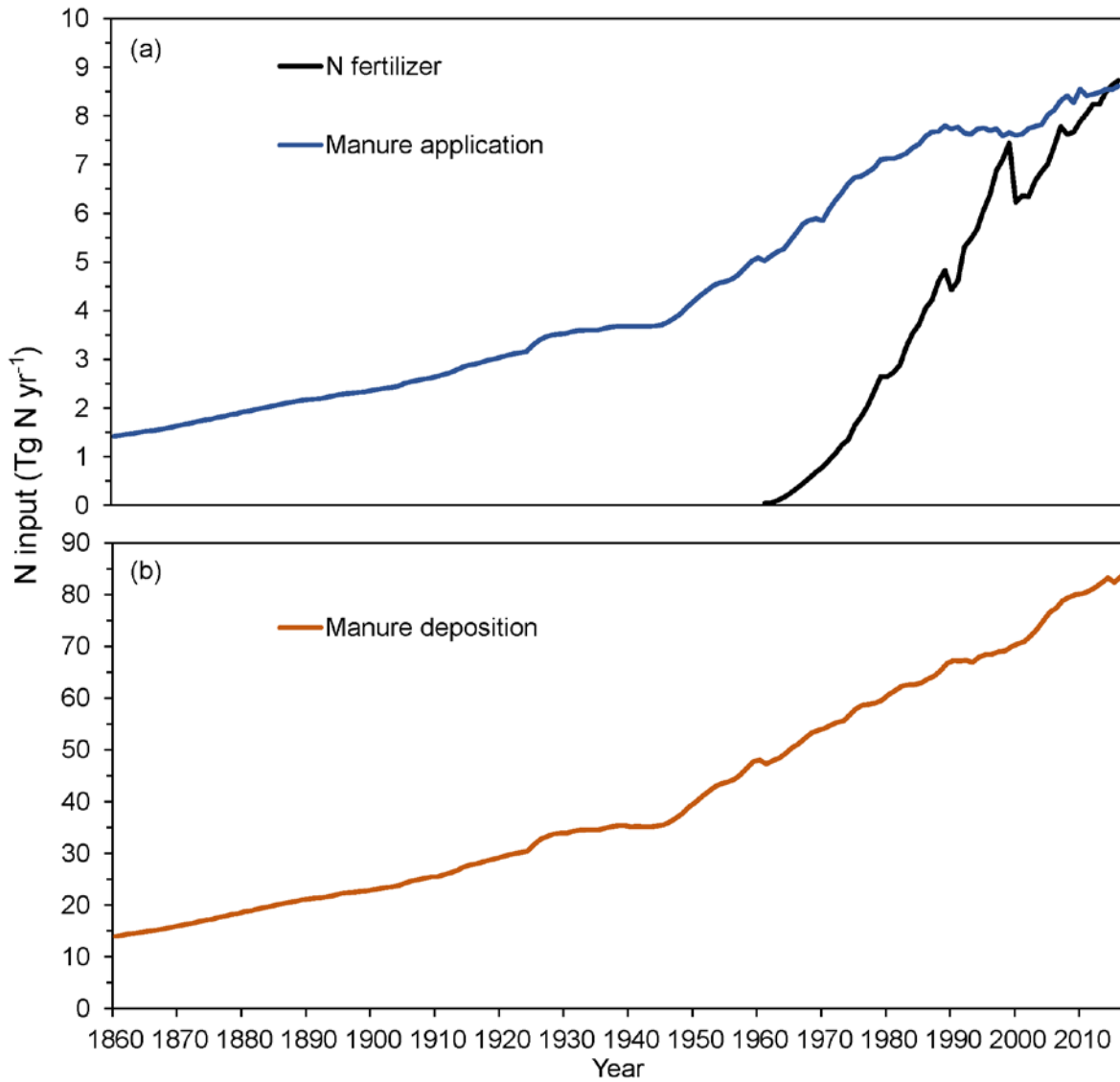


Figure 3-3. Temporal patterns of global manure N use, N fertilizer use, and manure deposition in grassland systems: (a) Manure N use and N fertilizer use on global pastures during 1860-2016 and during 1961-2016, respectively; (b) Manure N deposition to global pastures and rangelands during 1860-2016.

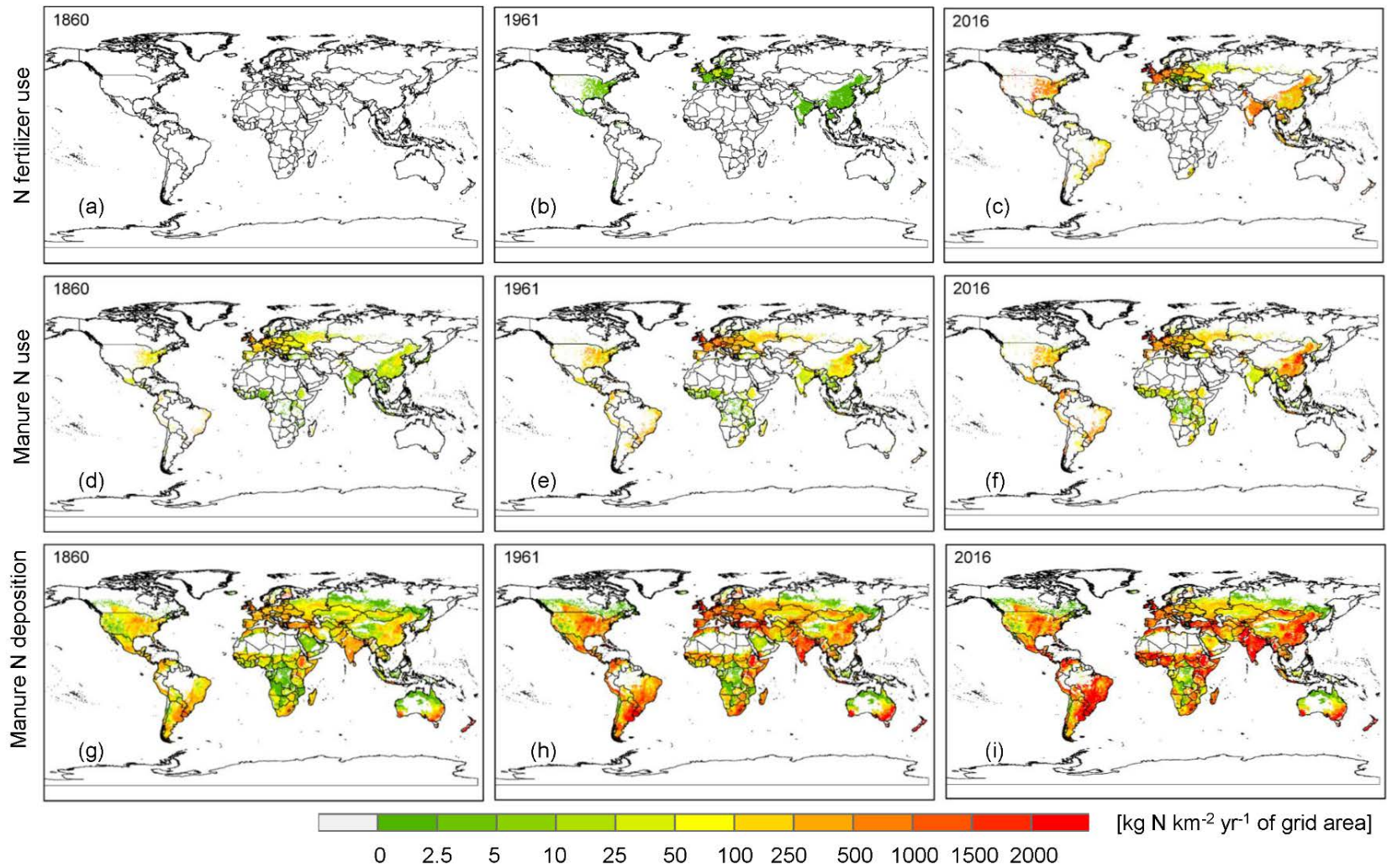


Figure 3-4. Spatial patterns of N input rates in global pastures and rangelands in 1860, 1961, and 2016: (a, b, c) N fertilizer application rates; (d, e, f) manure N application rates; (g, h, i) manure N deposition rates.

3.2. Manure N application to pastures, 1860–2016

Our results showed that the annual manure N application rates on pastures increased from 1.4 to 8.6 Tg N yr⁻¹ during 1860–2016 (Figure 3-3a). Manure N application rates showed rapid increases across the globe and exhibited large spatial variations, shifting the regional use from North America and Europe to Asia, during the study period (Figure 3-4d-f). The global average manure application rate was 5.3 kg N ha⁻¹ yr⁻¹ in the 1860s and roughly doubled by 2016 (10.7 kg N ha⁻¹ yr⁻¹) (Table 3-1).

From the regional perspective (Figure 3-5b), in the 1860s Europe (0.8 Tg N yr⁻¹) was the largest contributor and accounted for 53%, while southern Asia (0.25 Tg N yr⁻¹) accounted for 17% of the global total manure N application on pastures. South and North America shared the same proportion (13%), whereas the remaining regions only shared 4%. Conversely during 2000–2016, manure N application on pastures in southern Asia (2.9 Tg N yr⁻¹) was tenfold higher than that in the 1860s and accounted for 36% of the global total, surpassing Europe, which accounted for 28% of the global total. Manure N application amounts in North America and South America increased, but with different magnitudes. During 2000–2016, North America accounted for 11%, while South America accounted for 17% of the global total. In the remaining regions, significant increases of annual manure N application on pastures also occurred, but their contributions to the global total changed only slightly (8%) compared to the 1860s.

The regional average manure N application rate was increasing in southern Asia and Africa during 1860–2016 (Figure 3-6b). South America, Oceania, and North America exhibited a rapid decreasing trend of manure N application rates from the 1860s to the 1960s and showed continuous increases afterward until 2016 (Figures 8-5e, 8-6b), which was associated with the substantial

expansion of pasture areas (Table 3-2). Europe exhibited a rapid increase of manure N application rates since the 1860s, then decreased after the 1980s (Figure 3-5e).

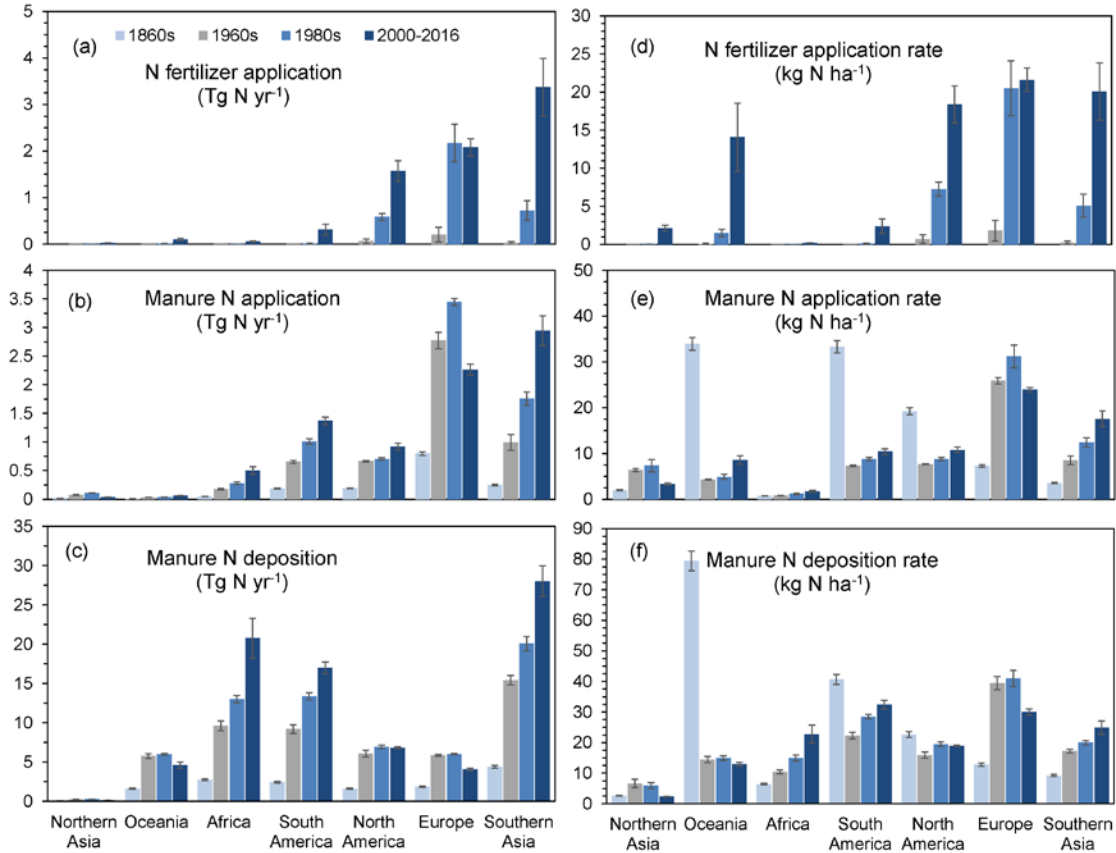


Figure 3-5. Nitrogen fertilizer use (a) and rate (d), manure N use (b) and rate (e), and manure N deposition (c) and rate (f) at regional scales in 1860s, 1960s, 1980s, and 2000-2016. Error bars represent standard deviation within each decade.

In 2016, the top five countries with largest manure N applications on pastures were China, United States, Brazil, Russia, and France. Manure N application in these countries contributed 43% to 52% of global total use from 1961 to 2016. China (2.5 Tg N yr⁻¹) alone accounted for 30% in 2016 at an increasing rate of 42 Gg N yr⁻¹ ($R^2 = 0.98$) per year during 1961–2016. Manure N use on pastures in Brazil and the United States was roughly the same (0.7 Tg N yr⁻¹) in 2016. Both countries showed a slower increasing trend (Brazil: 7 Gg N yr⁻¹ per year and United States: 3 Gg

N yr⁻¹ per year) during 1961–2016. In contrast, Russian manure N application peaked in 1989 (0.7 Tg N yr⁻¹), then showed a rapid decrease until 2016 (0.3 Tg N yr⁻¹). Similarly, in France, it peaked in 1979 (0.45 Tg N yr⁻¹), then showed a continuous decrease until 2016 (0.28 Tg N yr⁻¹).

3.3. Manure N deposition on pastures and rangelands, 1860–2016

Our data show that the total amounts of manure N deposited on pastures and rangelands increased from 14 to 84 Tg N yr⁻¹ during 1860–2016 (Figure 3-3b). Manure N deposition rates increased steeply across the globe, but exhibited large spatial variations during the study period (Figure 3-4g-i). The increase was much larger in the eastern world (typically China and India) and South America compared to the western world. The global average manure deposition rate was 11 kg N ha⁻¹ yr⁻¹ in 1860 and reached 25 kg N ha⁻¹ yr⁻¹ in 2016 (Table 3-1).

At the regional scale (Figure 3-5c), in the 1860s southern Asia was the region with the largest manure N deposition on pastures and rangelands (4.4 Tg N yr⁻¹; 30% of total manure N deposition amounts), followed by Africa (2.8 Tg N yr⁻¹; 19%) and South America (2.4 Tg N yr⁻¹; 16%). Manure N deposition in the remaining regions was estimated to be 5.1 Tg N yr⁻¹, contributing 35% to the total manure N deposition amount. During 2000–2016, southern Asia, Africa, and South America were still the three largest contributors: 27 Tg N yr⁻¹ accounted for 34%, 20 Tg N yr⁻¹ accounted for 26%, and 15 Tg N yr⁻¹ accounted for 20% of the global manure N deposition on pastures and rangelands, respectively. The remaining regions (Oceania, North America, and Europe) contributed to 20% of the global total during 2000–2016. Europe and Oceania saw an increase in manure N deposition amounts from 1860 to 1960, but since 1980 there was a significant decrease, partly explained by the onset of N pollution regulation. Manure N

deposition amounts in North America increased during 1860–1980, but changed slightly since 1960.

Oceania showed a continuously decreasing trend of average manure N deposition rates in pastures and rangelands over the period 1860–2016. Manure N deposition rates in South America decreased between 1860 and 1960 and then increased afterward until 2016 (Fig. 8-6c). The significant contrast of changes in manure N deposition rates in Oceania and South America between the 1860s and the 1960s is due to the substantial and rapid increase of grassland areas (Tables 8-2, 8-3). Africa and southern Asia saw continuous increases in manure N deposition rates from 1860 to 2016, whereas Europe and North America was found with decreasing deposition rates since the 1980s (Figure 3-5f, 8-6c).

Table 3-2 Pasture area changes (Mha) during the period 1860–2016 (adapted from HYDE 3.2, Klein Goldewijk et al. (2017)).

Pasture (Mha)	North America	South America	Europe	Africa	Oceania	Southern Asia	Northern Asia	Total
1860s	9.9	5.6	109.3	60.9	0.2	69.8	7.7	263.4
1880s	18.0	9.0	121.7	69.9	0.5	64.1	10.9	294.1
1900s	38.4	18.0	134.2	79.2	1.1	70.9	16.2	358.0
1920s	46.3	32.5	133.8	92.8	2.6	80.7	16.4	405.1
1940s	66.5	54.3	133.2	123.9	4.4	90.9	24.1	497.3
1960s	86.8	89.4	107.1	213.3	7.4	116.8	12.0	632.8
1980s	83.2	118.7	105.0	258.4	8.1	149.8	13.0	736.2
2000-2016	85.3	131.2	94.6	293.1	7.6	167.9	11.6	791.3

Table 3-3 Rangeland area changes (Mha) during the period 1860–2016 (adapted from HYDE 3.2, Klein Goldewijk et al. (2017)).

Rangeland (Mha)	North America	South America	Europe	Africa	Oceania	Southern Asia	Northern Asia	Total
1860s	61.0	54.1	31.8	372.0	20.1	404.2	33.1	976.3
1880s	89.4	69.7	36.0	402.9	45.6	406.9	37.8	1088.3
1900s	157.5	107.7	37.7	433.8	100.8	472.8	43.2	1353.5
1920s	174.3	158.1	38.7	466.8	178.1	545.4	43.7	1605.1
1940s	242.6	223.0	37.7	526.9	277.8	607.4	51.3	1966.7
1960s	287.9	291.4	31.6	674.2	389.7	734.1	23.2	24312.1
1980s	265.7	312.5	32.8	634.8	394.6	810.3	24.6	2475.3
2000-2016	274.8	335.7	36.4	598.0	353.4	903.3	30.8	2532.4

In this study, we identified the top 10 countries (China, Brazil, India, Ethiopia, United States, Australia, Sudan (former), Pakistan, Argentina, and Nigeria) that together contributed to 48% of the global total manure N deposition on pastures and rangelands in 2016. Among these countries, China (17%) and Brazil (21%) were the two largest contributors, with the similar annual rate of increase of $\sim 125 \text{ Gg N yr}^{-1}$ ($R^2 = 0.99$) per year during 1961–2016. India was the third largest contributor, however, at a small increasing rate of 63 Gg N yr^{-1} ($R^2 = 0.98$) per year during 1961–2016. Annual manure N deposition in Ethiopia was stable during 1961–2000, but since then rapidly increased at a rate of 117 Gg N yr^{-1} ($R^2 = 0.96$) per year. The United States showed a significant increase of annual manure N deposition on pastures and rangelands from 1961 to 1975 and then was stable after 1980. Australia showed a decreasing trend during 1990–2016 at a rate of 62 Gg N yr^{-1} ($R^2 = 0.92$) per year, whereas, in the former Sudan, Pakistan, and Nigeria annual manure N deposition amounts to pastures and rangelands increased at an annual average rate of 68 ($R^2 = 0.8$), 46 ($R^2 = 0.97$), 56 ($R^2 = 0.98$) Gg N yr^{-1} per year, respectively. There was no significant

change in manure N deposition amounts in Argentina; the annual from 1961 to 2016 was 2.6 Tg N yr⁻¹.

4. Discussion

4.1. Overview of global N inputs to pastures and rangelands

The global N cycle has been significantly perturbed by human activity since at least the industrial revolution. Intense agricultural activities, such as synthetic N fertilizer production and use, and intensive livestock production, were identified as major drivers to such change. In this context, improving estimates of global anthropogenic N inputs to pastures and rangelands and their consequences, including on N₂O emissions, is important (Galloway et al., 2008; Tian et al., 2016; Xu et al., 2017). In this study, we generated global datasets of fertilizers N inputs from livestock, both synthetic and from manure, during the period 1860–2016. Pastures and rangelands have experienced substantial land expansion over the period of 1860–1998 (Klein Goldewijk et al., 2017). The total amount of mineral and manure N applied to permanent meadows and pastures increased by 573% over the study period, from 15 to 101 Tg N yr⁻¹ from 1860 to 2016. During 2000–2016, the global mineral N fertilizer application to agriculture was significant, reaching 110 Tg N yr⁻¹ in 2016, while manure N production was 123 Tg N yr⁻¹ (FAO, 2018; FAOSTAT, 2018), resulting in a total input of 233 Tg N yr⁻¹. Our estimate of total N inputs (synthetic N fertilizer: 7.5 Tg N yr⁻¹; manure N application: 8.2 Tg N yr⁻¹; manure N deposition: 78.1 Tg N yr⁻¹) to permanent meadows and pastures (93.8 Tg N yr⁻¹) accounted for 45% of global total N production (manure: 114.2 Tg N yr⁻¹; synthetic N fertilizer: 96.4 Tg N yr⁻¹) during 2000–2016.

Table 3-4. Comparison of manure and fertilizer N application amounts between this study and published datasets. N/A: not available

	Bouwman et al. (2002b) ^α	Stehfest and Bouwman (2006) ^β	Bouwman et al. (2013a) ^γ	Chang et al. (2016) ^α	Liu et al. (2010b) ^γ	Lassaletta et al. (2014a) ^γ	This study ^γ
Manure N application (Tg N yr ⁻¹)	12.4	4.8	57.8	12.4	~2.8	N/A	7.6
Applied area (Mha)	625	N/A	3358 ^η	1231	N/A	N/A	798
N fertilizer application (Tg N yr ⁻¹)	4.3	3.1	N/A	3.1	12.9	6.5	6.2
Applied area (Mha)	103	N/A	N/A	39	N/A	N/A	798

^α estimated in 1995.

^β national-level fertilizer data for 1998. The total grassland area for N fertilizer and manure was 677 Mha.

^γ estimated in 2000.

^η the grassland area includes both mixed and patrol systems.

4.2. Extension of FAO information

Our work extends the relevant FAO national-level statistics in order to provide input drivers for process-based model simulations (e.g., NMIP, (Tian et al., 2018; Tian et al., 2019)). We furthermore separated N application rates between pastures and cropland, based on previous published work. We likewise extended information available in FAOSTAT by providing spatialized manure N application rates to pastures and spatialized national-level manure N deposition dataset from 1860 to 2016.

4.3. Comparison with other studies

We compared our datasets with other existing data sources (Table 3-4). Our estimate of world total manure N use on pastures was 58% and 171% higher than that estimated by Stehfest

and Bouwman (2006) and Liu et al. (2010b), respectively. However, our estimate was 39% and 87% lower than estimates by (Bouwman et al., 2002b; Bouwman et al., 2013). Critically, pasture area data varied significantly across different studies. For example, Bouwman et al. (2013a) divided grasslands into mixed and pastoral systems, and estimated grasslands area based on the country- or regional-level grazing intensity (Table 3-4). In addition, synthetic fertilizers were applied to the area of mixed agricultural systems (grassland and cropland) and manure N was assumed to be applied to both mixed and pastoral systems. The HYDE 3.2 land use dataset divides the global grazing area into intensively managed grasslands (pastures), and less intensive and unmanaged grasslands (rangelands) (Klein Goldewijk et al., 2017). In this study, we rather assumed that all manure N was applied to pastures, the latter estimated from the HYDE database (798 Mha). Hence, pasture area defined in Bouwman et al. (2013a) was more than fourfold higher than the data we used. Consequently, the spatial distribution and annual total N application differed substantially compared with that in Bouwman et al. (2013a).

Similarly, the estimates of N fertilizer use in pastures showed large variations across studies (Table 3-1). This study obtained country-level N fertilizer amounts applied to pastures from the national-level ratios provided by Lassaletta et al. (2014a) and total N amounts applied to soils provided by FAOSTAT. Thus, the global N fertilizer amount in 2000 was consistent with that in Lassaletta et al. (2014a). Liu et al. (2010b) assumed that 16% of fertilizer was applied to global grasslands. Their estimate was roughly twice as high as this study (6.2 Tg N yr^{-1}) for the year 2000. The estimates by Bouwman et al. (2002a) and Stehfest and Bouwman (2006) were 31% and 50%, respectively, lower than our estimates in the corresponding years. Klein Goldewijk et al. (2017) divided land used for grazing into more intensively used pastures, less intensively used or unmanaged rangelands. In this study, we assumed N fertilizer was applied to all global pastures

and therefore the total area of intensively managed grassland was significantly different from the area used in Bouwman et al. (2002a) and Chang et al. (2016).

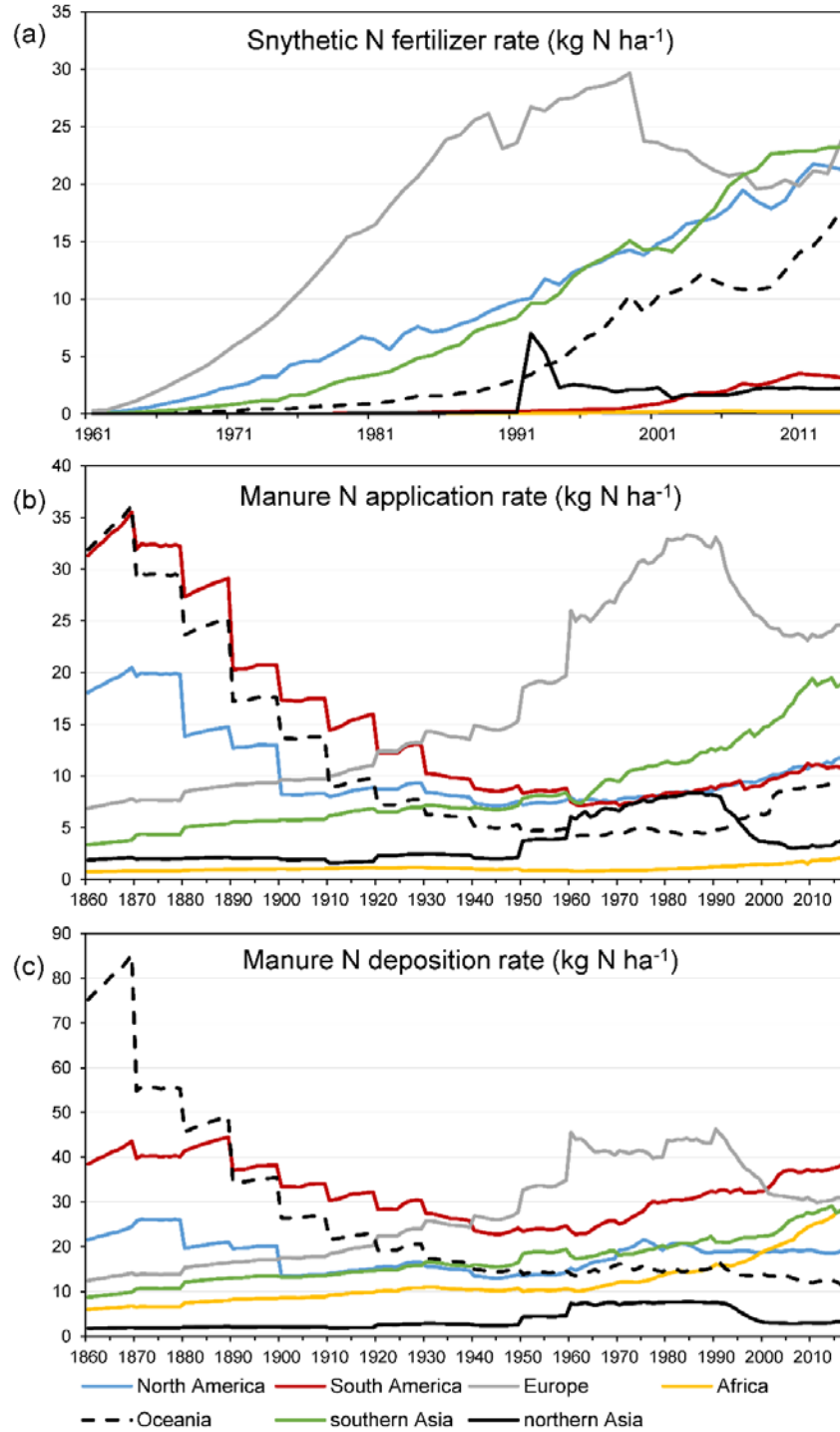


Figure 3-6. The temporal patterns of average N input rates (kg N ha⁻¹) in regional pastures and rangelands during 1860–2016.

4.4. Changes in N inputs hotspots

Overall, southern Asia ranks as a top hotspot of all sources of global N inputs in pastures and rangelands during the past three decades, causing a major threat to environmental sustainability and human health in this region. In the 1860's overall manure N production amounts were similar in Asia and Europe (Zhang et al., 2017). However, manure N deposition was 2.4 times higher than that in Europe, whereas manure N application was roughly three times lower than that in Europe. During 2000–2016, southern Asia accounted for ~42% of global manure N production. Consequently, manure N deposition and application amounts in southern Asia were the highest compared to the rest of the regions between 2000–2016. These increases are due to large increases in animal numbers (e.g., cattle, sheep and goats) since 1950 (Bouwman et al., 2013; Dangal et al., 2017). For the rest of the regions, the increases of livestock numbers were also found in South America and Africa since 1860, whereas livestock numbers in Europe and North America showed a decreasing trend after 1980 (Dangal et al., 2017). Thus, besides southern Asia, South America and Africa were hotspots for manure N deposition during 1860–2016, while manure N deposition amount decreased in Europe and North America since the 1980s.

4.4.1 Shifting hotspots of N fertilizer application

European countries (e.g., Germany, United Kingdom, and Ireland) were identified as top hotspots of global N fertilizer application in 1961 (Figure 3-4b). However, these hotspots have shifted from Western Europe towards southern Asia at the end of the 20th century (Figure 3-4c). Southern Asia was found with the highest N fertilizer application amounts between 2000 and 2016, most concentrated in countries of East and South Asia (e.g., China and India). China and India together applied 36% of global total N fertilizer to pastures and rangelands.

4.4.2 Shifting hotspots of manure N application

Manure application hotspots moved from European countries to southern Asia during the past 155 years. Between 1860 and 1999, Europe accounted for 50% of global total manure N application to pastures and experienced a rapid growth of manure N application, peaked (3.5 Tg N yr⁻¹) in 1986. In 1860, the highest applications were in the United Kingdom, France, and Germany (Figure 3-4d), but by 2016, the highest application was in the North China Plain (Figure 3-4f). China alone applied 29% of global total manure N during 2000–2016.

4.4.3 Hotspots of manure N deposition

Southern Asia, as the hotspot of manure N deposition to pastures and rangelands, contributed 31% of the global total amount during the past 157 years. Also, in Africa and South America substantial increases of manure N deposition during 1860–2016 were observed. In the 1860s, manure N deposition from southern Asia, Africa, and South America contributed to 65%, whereas Europe accounted only for 12% of the global total manure N deposition. In 1860, the highest deposition rates were observed for New Zealand, Australia, and Western Europe (Figure 3-4g). In 2016, except for the above-mentioned regions, the highest deposition rates were in South and West Asia, China, West and East Africa, and South America (Figure 3-4i). During 2000–2016, manure N deposition from southern Asia, Africa, and South America contributed to 80%, while Europe accounted for 5% of the global total amount.

4.5 Limitations and uncertainties

This study attempts to provide an overall estimate of N inputs to global pastures and rangelands, during the period 1860–2016. However, before these data are used in global models, uncertainties of these datasets need to be addressed. First, the different definitions of grassland

systems used by the scientific community introduce uncertainties of the spatial patterns and annual total amounts of N inputs. Chang et al. (2016) generated global maps of grassland management intensity since 1901 based on modeled net primary production and the use of grass biomass generated by Herrero et al. (2013). Their total grassland area substantially differed from pasture area developed by HYDE 3.1 (Chang et al., 2016). In this study, we used HYDE 3.2 to generate N inputs to global grasslands, defined more appropriately by using the FAO land use definition of ‘permanent meadows and pastures’. This dataset exactly followed the FAOSTAT data during 1960–2015, and combined population density data to reconstruct land use prior to 1960. Pastures and rangelands defined in HYDE 3.2 were based on the intensity of human management. Although Bouwman et al. (2013a) indicated that grassland areas in their study were also calculated based on the grazing intensity, their total area (pastures and rangelands) and spatial patterns were obviously different from HYDE 3.2 (Table 3-4). Thus, a better understanding of land use is vital to reduce the uncertainty of estimating N input rates and amounts in pastures and rangelands.

Second, the FAOSTAT database provides country-level manure N applied to soils; however, this dataset could not be directly applied to study N cycles on pastures since applications to cropland and pasture soils are not differentiated. In this study, it remains large uncertainty that we separated national-level manure N application on pastures simply based on pasture area over total agricultural area (cropland, pastures and rangelands). In previous studies, Bouwman et al. (2013a) assumed that 50% and only 5% of the available manure was applied to grasslands in most industrialized countries and in most developing countries, respectively. Liu et al. (2010b) allocated 34% of the national total solid manure to pastures in European countries and Canada, 13% of the national total manure to pastures in the United States, and 10% of the national total manure to pastures in developing countries. Chang et al. (2016) assumed that manure N application rate

changes along with changes in the total ruminant stocking density. Moreover, the spatialization process of N application rates might introduce large uncertainty. The spatial pattern of gridded manure N application rates in our study are correlated with manure production rates in Zhang et al. (2017). The assumptions and uncertainties mentioned in their study, such as without considering livestock migration, might cause uncertainty of spatial distribution.

Third, studies used different data sources and made various assumptions of the annual amount of fertilizer N applied on global pastures (Bouwman et al., 2002b; Chang et al., 2016; Lassaletta et al., 2014a; Liu et al., 2010b; Stehfest and Bouwman, 2006). Thus, there remains large uncertainty of total N application on permanent meadows and pastures globally. Moreover, N fertilizer application rates by crops were highly investigated and documented in previous studies. Hence, N fertilizer application datasets were generated considering crop-specific fertilizer rates and cropland area in each grid (Lu and Tian, 2017; Mueller et al., 2012; Nishina et al., 2017; Potter et al., 2010). In reality, N fertilizer application on pastures of each country is not homogeneous. In this study, we assumed that N fertilizer application rate in each country was constant, which means fertilizer was applied evenly in each grid with pastures area larger than zero. Last, inside each relevant land use cell pastures and rangelands may be characterized by different livestock density and deposition rates, which is not considered in our current datasets. The final manure N deposition would be highly affected by the proportion of each type of management in the grid cell. Thus, it is necessary to consider these in the future research.

Furthermore, other human-induced sources of N inputs to pastures and rangelands were not included in our study, which may underestimate total N received globally. For example, biological N fixation was one of the major N sources in the terrestrial ecosystem in the absence of human influence (Cleveland et al., 1999). Pastures and rangelands occupy 25% of the Earth's ice-

free land surface across different latitudes with divergent biological N fixation abilities. Plant production in temperate grasslands is proximately limited by N supply due to little N via N fixation; however, tropical savannah received a large amount of N through leguminous species (Cleveland et al., 1999; Vitousek et al., 2013). An estimate of potential N fixation amount by global grassland systems is $\sim 46.5 \text{ Tg N yr}^{-1}$, with a range of 26.6–66.5 Tg N yr^{-1} (Cleveland et al., 1999). Atmospheric N deposition is another major source of N input to permanent meadows and pastures globally and increased from 2 to 14 Tg N yr^{-1} for the period 1860–2016 based on the Chemistry–Climate Model Initiative N deposition fields (Eyring et al., 2013; Tian et al., 2018; Tian et al., 2019).

5. Conclusion

In the context of increasing livestock production, manure and fertilizer N inputs to permanent meadows and pastures (pastures and rangelands areas) globally have increased rapidly since the industrial revolution. However, datasets of global N inputs are still incomplete. This is the first study that has attempted to consider major sources of anthropogenic N inputs in permanent meadows and pastures and hence generated time-series gridded datasets of manure and fertilizer N application rates, and manure deposition rate during 1860–2016. Our datasets indicated a rapid increase of total N inputs to pastures and rangelands globally during this period, especially the past half century. The hotspots of grassland N application shifted from European countries to southern Asia, specifically China and India in the early 21st century, which indicated the spatial transformation of environmental problems. In this study, we have obtained N data from various sources to fill the data gap; however, large uncertainties still remain in our datasets (e.g., N application rate within each country, annual manure application amounts). More information is needed to improve these datasets in our further work.

References

- Bai, Z., Lee, M. R., Ma, L., Ledgard, S., Oenema, O., Velthof, G. L., Ma, W., Guo, M., Zhao, Z., and Wei, S.: Global environmental costs of China's thirst for milk, *Global change biology*, 24, 2198-2211, 2018.
- Bouwman, A., Beusen, A. H., and Billen, G.: Human alteration of the global nitrogen and phosphorus soil balances for the period 1970–2050, *Global Biogeochemical Cycles*, 23, 2009.
- Bouwman, A., Boumans, L., and Batjes, N.: Emissions of N₂O and NO from fertilized fields: Summary of available measurement data, *Global Biogeochemical Cycles*, 16, 2002a.
- Bouwman, A., Boumans, L., and Batjes, N.: Estimation of global NH₃ volatilization loss from synthetic fertilizers and animal manure applied to arable lands and grasslands, *Global biogeochemical cycles*, 16, 2002b.
- Bouwman, A., Goldewijk, K. K., Van Der Hoek, K. W., Beusen, A. H., Van Vuuren, D. P., Willems, J., Rufino, M. C., and Stehfest, E.: Exploring global changes in nitrogen and phosphorus cycles in agriculture induced by livestock production over the 1900–2050 period, *Proceedings of the National Academy of Sciences*, 110, 20882-20887, 2013.
- Bouwman, A., Van Drecht, G., Knoop, J., Beusen, A., and Meinardi, C.: Exploring changes in river nitrogen export to the world's oceans, *Global Biogeochemical Cycles*, 19, 2005.
- Chang, J., Ciais, P., Herrero, M., Havlik, P., Campioli, M., Zhang, X., Bai, Y., Viovy, N., Joiner, J., Wang, X., Peng, S., Yue, C., Piao, S., Wang, T., Hauglustaine, D. A., Soussana, J.-F., Peregon, A., Kosykh, N., and Mironycheva-Tokareva, N.: Combining livestock production information in a process-based vegetation model to reconstruct the history of grassland management, *Biogeosciences*, 13, 3757, 2016.
- Cleveland, C. C., Townsend, A. R., Schimel, D. S., Fisher, H., Howarth, R. W., Hedin, L. O., Perakis, S. S., Latty, E. F., Von Fischer, J. C., and Elseroad, A.: Global patterns of terrestrial biological nitrogen (N₂) fixation in natural ecosystems, *Global Biogeochemical Cycles*, 13, 623-645, 1999.
- Dangal, S. R., Tian, H., Zhang, B., Pan, S., Lu, C., and Yang, J.: Methane emission from global livestock sector during 1890–2014: Magnitude, trends and spatiotemporal patterns, *Global change biology*, 2017. 2017.
- Davidson, E. A.: The contribution of manure and fertilizer nitrogen to atmospheric nitrous oxide since 1860, *Nature Geoscience*, 2, 659-662, 2009.
- Davis, K. F., Yu, K., Herrero, M., Havlik, P., Carr, J. A., and D'Odorico, P.: Historical trade-offs of livestock's environmental impacts, *Environmental Research Letters*, 10, 125013, 2015.
- Eyring, V., Lamarque, J.-F., Hess, P., Arfeuille, F., Bowman, K., Chipperfield, M. P., Duncan, B., Fiore, A., Gettelman, A., and Giorgetta, M. A.: Overview of IGAC/SPARC Chemistry-Climate Model Initiative (CCMI) community simulations in support of upcoming ozone and climate assessments, *Sparc Newsletter*, 40, 48-66, 2013.
- FAO: Nitrogen inputs to agricultural soils from livestock manure: New statistics, 2018. 2018. FAOSTAT, 2018. 2018.
- Fowler, D., Steadman, C. E., Stevenson, D., Coyle, M., Rees, R. M., Skiba, U., Sutton, M., Cape, J., Dore, A., and Vieno, M.: Effects of global change during the 21st century on the nitrogen cycle, *Atmospheric Chemistry and Physics*, 15, 13849-13893, 2015.

- Galloway, J. N., Townsend, A. R., Erisman, J. W., Bekunda, M., Cai, Z., Freney, J. R., Martinelli, L. A., Seitzinger, S. P., and Sutton, M. A.: Transformation of the nitrogen cycle: recent trends, questions, and potential solutions, *Science*, 320, 889-892, 2008.
- Gerber, J. S., Carlson, K. M., Makowski, D., Mueller, N. D., Garcia de Cortazar-Atauri, I., Havlík, P., Herrero, M., Launay, M., O'Connell, C. S., and Smith, P.: Spatially explicit estimates of N₂O emissions from croplands suggest climate mitigation opportunities from improved fertilizer management, *Global change biology*, 2016. 2016.
- Havlík, P., Valin, H., Herrero, M., Obersteiner, M., Schmid, E., Rufino, M. C., Mosnier, A., Thornton, P. K., Böttcher, H., and Conant, R. T.: Climate change mitigation through livestock system transitions, *Proceedings of the National Academy of Sciences*, 111, 3709-3714, 2014.
- Herrero, M., Havlík, P., Valin, H., Notenbaert, A., Rufino, M. C., Thornton, P. K., Blümmel, M., Weiss, F., Grace, D., and Obersteiner, M.: Biomass use, production, feed efficiencies, and greenhouse gas emissions from global livestock systems, *Proceedings of the National Academy of Sciences*, 110, 20888-20893, 2013.
- Holland, E., Lee-Taylor, J., Nevison, C., and Sulzman, J.: Global N Cycle: Fluxes and N₂O mixing ratios originating from human activity, Data set. Available on-line: <http://www.daac.ornl.gov> from Oak Ridge National Laboratory Distributed Active Archive Center, Oak Ridge, Tennessee, USA, doi, 10, 2005.
- Klein Goldewijk, K., Beusen, A., Doelman, J., and Stehfest, E.: Anthropogenic land use estimates for the Holocene–HYDE 3.2, *Earth System Science Data*, 9, 927, 2017.
- Lassaletta, L., Billen, G., Grizzetti, B., Anglade, J., and Garnier, J.: 50 year trends in nitrogen use efficiency of world cropping systems: the relationship between yield and nitrogen input to cropland, *Environmental Research Letters*, 9, 105011, 2014.
- Liu, J., You, L., Amini, M., Obersteiner, M., Herrero, M., Zehnder, A. J., and Yang, H.: A high-resolution assessment on global nitrogen flows in cropland, *Proceedings of the National Academy of Sciences*, 107, 8035-8040, 2010.
- Lu, C. and Tian, H.: Global nitrogen and phosphorus fertilizer use for agriculture production in the past half century: shifted hot spots and nutrient imbalance, *Earth System Science Data*, 9, 181, 2017.
- Mueller, N. D., Gerber, J. S., Johnston, M., Ray, D. K., Ramankutty, N., and Foley, J. A.: Closing yield gaps through nutrient and water management, *Nature*, 490, 254, 2012.
- Nishina, K., Ito, A., Hanasaki, N., and Hayashi, S.: Reconstruction of spatially detailed global map of NH₄⁺ and NO₃⁻ application in synthetic nitrogen fertilizer, *Earth System Science Data*, 9, 149, 2017.
- Potter, P., Ramankutty, N., Bennett, E. M., and Donner, S. D.: Characterizing the spatial patterns of global fertilizer application and manure production, *Earth Interactions*, 14, 1-22, 2010.
- Sheldrick, W. F., Syers, J. K., and Lingard, J.: A conceptual model for conducting nutrient audits at national, regional, and global scales, *Nutrient Cycling in Agroecosystems*, 62, 61-72, 2002.
- Smith, P., Clark, H., Dong, H., Elsiddig, E., Haberl, H., Harper, R., House, J., Jafari, M., Masera, O., and Mbow, C.: Agriculture, forestry and other land use (AFOLU), 2014. 2014.
- Stehfest, E. and Bouwman, L.: N₂O and NO emission from agricultural fields and soils under natural vegetation: summarizing available measurement data and modeling of global annual emissions, *Nutrient Cycling in Agroecosystems*, 74, 207-228, 2006.

- Tian, H., Lu, C., Ciais, P., Michalak, A. M., Canadell, J. G., Saikawa, E., Huntzinger, D. N., Gurney, K. R., Sitch, S., Zhang, B., Yang, J., Bousquet, P., Bruhwiler, L., Chen, G., Dlugokencky, E., Friedlingstein, P., Melillo, J., Pan, S., Poulter B., Prinn, R., Saunio, M., Schwalm, C., and Wofsy, S.: The terrestrial biosphere as a net source of greenhouse gases to the atmosphere, *Nature*, 531, 225-228, 2016.
- Tian, H., Yang, J., Lu, C., Xu, R., Canadell, J. G., Jackson, R., Arneeth, A., Chang, J., Chen, G., and Ciais, P.: The global N₂O Model Intercomparison Project (NMIP): Objectives, Simulation Protocol and Expected Products, *Bulletin of the American Meteorological Society*, 99, 1231-1251, 2018.
- Tian, H., Yang, J., Xu, R., Lu, C., Canadell, J. G., Davidson, E. A., Jackson, R. B., Arneeth, A., Chang, J., and Ciais, P.: Global soil nitrous oxide emissions since the preindustrial era estimated by an ensemble of terrestrial biosphere models: Magnitude, attribution, and uncertainty, *Global Change Biology*, 25, 640-659, 2019.
- Tubiello, F. N.: GHG emissions due to agriculture, *Encyclopedia of Food Systems*, reference module in food science, Elsevier, doi: doi: 10.1016/B978-0-08-100596-5.21996-3, 2018. 2018.
- Tubiello, F. N., Salvatore, M., Rossi, S., Ferrara, A., Fitton, N., and Smith, P.: The FAOSTAT database of greenhouse gas emissions from agriculture, *Environmental Research Letters*, 8, 015009, 2013.
- Vitousek, P. M., Menge, D. N., Reed, S. C., and Cleveland, C. C.: Biological nitrogen fixation: rates, patterns and ecological controls in terrestrial ecosystems, *Philosophical Transactions of the Royal Society of London B: Biological Sciences*, 368, 20130119, 2013.
- Xu, R., Pan, S., Chen, J., Chen, G., Yang, J., Dangal, S., Shepard, J., and Tian, H.: Half-Century Ammonia Emissions From Agricultural Systems in Southern Asia: Magnitude, Spatiotemporal Patterns, and Implications for Human Health, *GeoHealth*, 2, 40-53, 2018.
- Xu, R., Tian, H., Lu, C., Pan, S., Chen, J., Yang, J., and Bowen, Z.: Preindustrial nitrous oxide emissions from the land biosphere estimated by using a global biogeochemistry model, *Climate of the Past*, 13, 977-990, 2017.
- Xu, R., Tian, H., Pan, S., Prior, S. A., Feng, Y., Batchelor, W. D., Chen, J., and Yang, J.: Global ammonia emissions from synthetic nitrogen fertilizer applications in agricultural systems: Empirical and process-based estimates and uncertainty, *Global Change Biology*, 25, 314-326, 2019.
- Yang, Q., Tian, H., Li, X., Ren, W., Zhang, B., Zhang, X., and Wolf, J.: Spatiotemporal patterns of livestock manure nutrient production in the conterminous United States from 1930 to 2012, *Science of the Total Environment*, 541, 1592-1602, 2016.
- Zhang, B., Tian, H., Lu, C., Dangal, S. R., Yang, J., and Pan, S.: Global manure nitrogen production and application in cropland during 1860–2014: a 5 arcmin gridded global dataset for Earth system modeling, *Earth System Science Data*, 9, 667-678, 2017.

Chapter 4. Preindustrial nitrous oxide emissions from the land biosphere estimated by using a global biogeochemistry model

Abstract

To accurately assess how increased global nitrous oxide (N₂O) emission has affected the climate system requires a robust estimation of the pre-industrial N₂O emissions since only the difference between current and pre-industrial emissions represents net drivers of anthropogenic climate change. However, large uncertainty exists in previous estimates of pre-industrial N₂O emissions from the land biosphere, while pre-industrial N₂O emissions at the finer scales such as regional, biome, or sector have not yet well quantified. In this study, we applied a process-based Dynamic Land Ecosystem Model (DLEM) to estimate the magnitude and spatial patterns of pre-industrial N₂O fluxes at the biome-, continental-, and global-level as driven by multiple environmental factors. Uncertainties associated with key parameters were also evaluated. Our study indicates that the mean of the pre-industrial N₂O emission was approximately 6.20 Tg N yr⁻¹, with an uncertainty range of 4.76 to 8.13 Tg N yr⁻¹. The estimated N₂O emission varied significantly at spatial- and biome-levels. South America, Africa, and Southern Asia accounted for 34.12%, 23.85%, 18.93%, respectively, together contributing 76.90% of global total emission. The tropics were identified as the major source of N₂O released into the atmosphere, accounting for 64.66% of the total emission. Our multi-scale estimates provide a robust reference for assessing the climate forcing of anthropogenic N₂O emission from the land biosphere.

1. Introduction

Nitrous oxide (N_2O) acts as the third-most important greenhouse gas (GHG) after carbon dioxide (CO_2) and methane (CH_4), largely contributing to the current radiative forcing (Myhre et al., 2013). Nitrous oxide is also the most long-lived reactant, resulting in the destruction of stratospheric ozone (Prather et al., 2015; Ravishankara et al., 2009). The atmospheric concentration of N_2O increased from 275 to 329 parts per billion (ppb) since the pre-industrial era until 2015 at a rate of approximately 0.26% per year, as a result of human activities (Davidson, 2009; Forster et al., 2007; NOAA2006A). The human-induced N_2O emissions from the terrestrial biosphere have offset about 50% of terrestrial CO_2 sink and contributed a net warming effect on the climate system (Tian et al., 2016). In the contemporary period, anthropogenic N_2O emissions are mainly caused by the expansion of agricultural land area and increase in nitrogen (N) fertilizer application, as well as industrial activities, biomass burning and indirect emissions from reactive N (Galloway et al., 2004; Reay et al., 2012). Human-induced biogenic N_2O emissions were calculated by subtracting the pre-industrial emissions (Tian et al., 2016), even though a small amount of anthropogenic N_2O emissions was present before 1860, which was estimated as 1.1 Tg N yr^{-1} in 1850 by Syakila and Kroeze (2011) and 0.7 (0.6–0.8) Tg N yr^{-1} (including anthropogenic biogenic emissions from soils and biomass burning) in 1860 by Davidson (2009). Therefore, it is necessary to provide a robust reference of pre-industrial N_2O emission for assessing the climate forcing of anthropogenic N_2O emission from the land biosphere.

Numerous studies have reported the sources and estimates of N_2O emission since the pre-industrial era (Davidson and Kanter, 2014; Galloway et al., 2004; Kroeze et al., 1999; Prather et al., 2012, 2015; Syakila and Kroeze, 2011). According to the Intergovernmental Panel on Climate Change Guidelines (IPCC, 1997), the global N_2O emission evaluated by Kroeze et al. (1999) is 11

(8–13) Tg N yr⁻¹ (Natural soils: 5.6–6.6 Tg N yr⁻¹, Anthropogenic: 1.4 Tg N yr⁻¹), which is consistent with the estimation from global pre-agricultural N₂O emissions in soils (6–7 Tg N yr⁻¹) (Bouwman et al., 1993). While taking into account the new emission factor from the IPCC 2006 Guidelines (Denman et al., 2007), Syakila and Kroeze (2011) conducted an updated estimate based on the study of Kroeze et al. (1999) and reported that the global pre-industrial N₂O emission is 11.6 Tg N yr⁻¹ (Anthropogenic: 1.1 Tg N yr⁻¹, Natural soils: 7 Tg N yr⁻¹). Based on the IPCC AR5, Davidson and Kanter (2014) indicated that the central estimates of both top-down and bottom-up approaches for pre-industrial natural emissions were in agreement at 11 (10–12) Tg N yr⁻¹, including natural emission from soils at 6.6 (3.3–9.0) Tg N yr⁻¹ (Syakila and Kroeze, 2011). Prather et al. (2015) provided an estimate of the pre-industrial emissions (total natural emission: 10.5 Tg N yr⁻¹) based on the most recent study with a corrected lifetime of 116±9 years. Although these previous estimates intent to provide a baseline of pre-industrial N₂O emission at global-level, information on pre-industrial N₂O emissions on fine resolutions such as biome-, sector- or country-, and regional-levels remains unknown but is needed for climate change mitigation.

Large uncertainties in the estimates of pre-industrial N₂O emission could derive from different approaches (i.e. top-down and bottom-up), as mentioned above. Nitrous oxide, as an important component of the N cycle, is produced by biological processes such as denitrification and nitrification in terrestrial and aquatic systems (Schmidt et al., 2004; Smith and Arah, 1990; Wrage et al., 2001). In order to accurately estimate pre-industrial N₂O emissions using the process-based Dynamic Land Ecosystem Model (DLEM, Tian et al., 2010), uncertainties associated with key parameters, such as maximum nitrification and denitrification rates, biological N fixation (BNF) rates, and the adsorption coefficient for soil ammonium (NH₄⁺) and nitrate (NO₃⁻), were

required to be considered in model simulation. Upper and lower limits of these parameters were used to derive a range of pre-industrial N₂O emissions from terrestrial ecosystems.

In this study, the DLEM was used to simulate global N₂O emission in the pre-industrial era at a resolution of 0.5° × 0.5° latitude/longitude. Since there are no observational data of N₂O emission in the pre-industrial period, the estimates of natural emission from Prather et al. (2012, 2015) were used to validate the simulation results. In addition, site-level N₂O emissions from different natural vegetation was used to test model performance in the contemporary period. The objectives in this study include: (1) providing a global estimation of N₂O emission from terrestrial soils in 1860, (2) offering the continental-, biome-, and country-scale N₂O emission amounts and flux rates, and (3) discussing uncertainties in estimating N₂O budget in the pre-industrial era. Finally, our estimates at global- and biome-scales were compared with previous estimates.

2. Methodology

2.1. Input datasets

Input data to drive DLEM simulation include static and transient data (Tian et al., 2010). Several additional data sets were generated to better represent terrestrial environment in the pre-industrial period as described below. The natural vegetation map was developed based on LUH (Hurtt et al., 2011) and SYNMAP (Jung et al., 2006), which rendered the fractions of 47 vegetation types in each 0.5° grid. These 47 vegetation types were converted to 15 PFTs used in the DLEM through a cross-walk table (Figure 4-1). Cropland distribution in 1860 were developed by aggregating the 5-arc minute resolution HYDE v3.1 global cropland distribution data (Figure 4-2). Half degree daily climate data (including average, maximum, minimum air temperature, precipitation, relative humidity, and shortwave radiation) were derived from CRU-NCEP climate

forcing data (Wei et al., 2014). As global climate dataset was not available prior to the year 1900, long-term average climate datasets from 1901 to 1930 were used to represent the initial climate state in 1860.

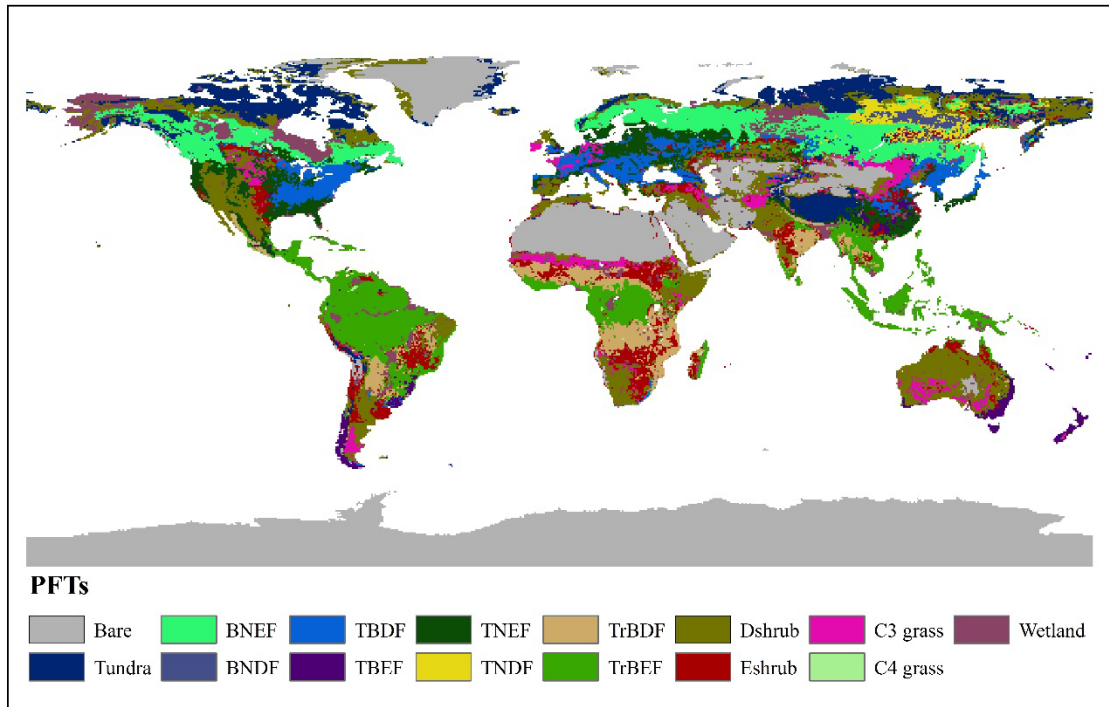


Figure 4-1. Global potential natural vegetation map used by DLEM in the pre-industrial era. BNEF: Boreal Needleleaf Evergreen Forest, BNDF: Boreal Needleleaf Deciduous Forest, TBDF: Temperate Broadleaf Deciduous Forest, TBEF: Temperate Broadleaf Evergreen Forest, TNEF: Temperate Needleleaf Evergreen Forest, TNDF: Temperate Needleleaf Deciduous Forest, TrBDF: Tropical Broadleaf Deciduous Forest, TrBEF: Tropical Broadleaf Evergreen Forest, Dshrub: Deciduous Shrubland, Eshrub: Evergreen Shrubland.

The nitrogen deposition dataset was developed based on the atmospheric chemistry transport model (Dentener, 2006) constrained by the EDGAR-HYDE nitrogen emission data (Aardenne et al., 2001). The nitrogen deposition dataset provided inter-annual variations of $\text{NH}_x\text{-N}$ and $\text{NO}_y\text{-N}$ deposition rates. The manure production dataset (1961–2013) was derived from Food and Agriculture organization of the United Nations statistic website ((FAO),

<http://faostat.fao.org>) and defaulted for N excretion rate referred to IPCC Guidelines (Zhang et al., 2017). Estimates of manure production from 1860 to 1960 were retrieved from the global estimates in (Holland et al., 2005).

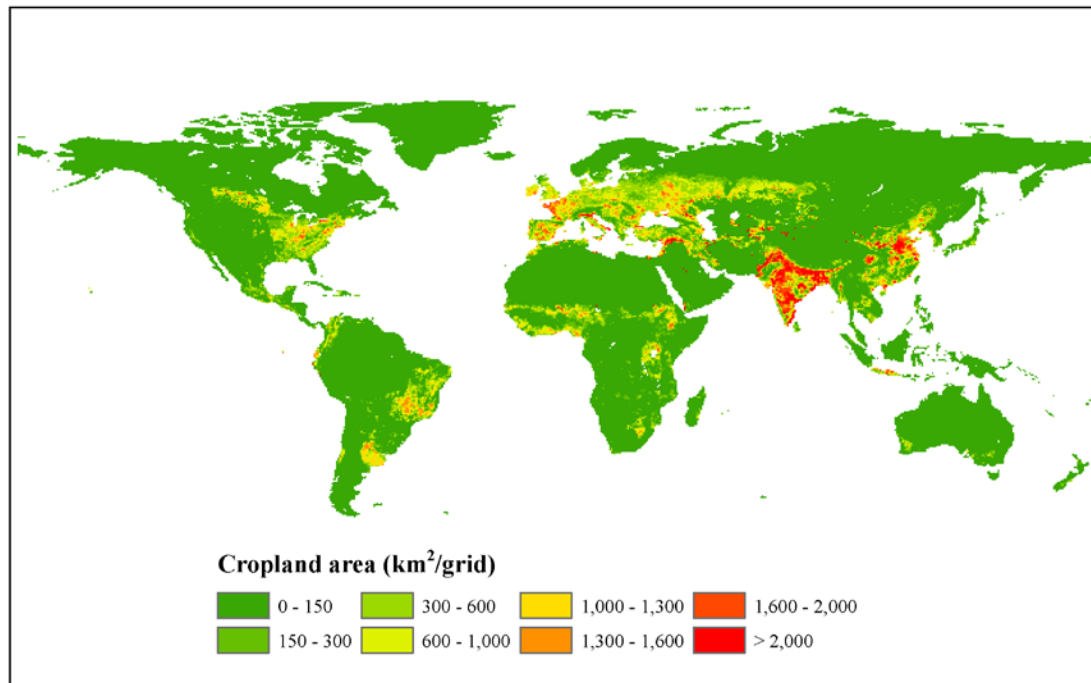


Figure 4-2. The spatial distribution of cropland area in 1860.

2.2. Model simulation

The implementation of the DLEM simulation includes three steps: (1) equilibrium run, (2) spin-up run, and (3) transient run. In this study, we first used land use and land cover (LULC) map in 1860, long-term mean climate during 1901–1930, N input datasets in 1860 (the concentration levels of N deposition and manure application rate), and atmospheric CO₂ in 1860 to run the model to an equilibrium state. In each grid, the equilibrium state was assumed to be reached when the inter-annual variations of carbon, nitrogen, and water storage are less than 0.1 g C/m², 0.1 g N/m² and 0.1 mm, respectively, during two consecutive 50 years. After the model reached equilibrium state, the model was spun up by the detrended climate data from 1901 to 1930 to eliminate system

fluctuation caused by the model mode shift from the equilibrium to transient run (i.e., 3 spins with 10-year climate data each time). Finally, the model was run in the transient mode with daily climate data, annual CO₂ concentration, manure application, and N deposition inputs in 1860 to simulate pre-industrial N₂O emissions. Additional description of model initialization and simulation procedure can be found in previous publications (Tian et al., 2010; Tian et al., 2011).

2.3. Estimate of uncertainty

In this study, uncertainties in the simulated N₂O emission were evaluated through a global sensitivity and uncertainty analysis as described in Tian et al., 2011. Based on sensitivity analyses of key parameters that affect terrestrial N₂O fluxes, the most sensitive parameters were identified to conduct uncertainty simulations with the DLEM. These parameters include potential denitrification and nitrification rates, BNF rates, and the adsorption coefficient for soil NH₄⁺ and NO₃⁻ (Gerber et al., 2010; Tian et al., 2015; Yang et al., 2015). The ranges of five parameters were obtained from previous studies. Chatskikh et al. (2005) set k_{nit} as 0.10 d⁻¹; however, it was set in a range of 0.04 to 0.15 d⁻¹, and varied with different PFTs in the DLEM simulations. The uncertainty ranges of potential nitrification rates were based on previous studies (Hansen, 2002; Heinen, 2006); the global pre-industrial N fixation was estimated as 58 Tg N yr⁻¹, ranging from 50–100 Tg N yr⁻¹ (Vitousek et al., 2013). The spatial distribution of BNF referred to the estimates by Cleveland et al. (1999). Potential denitrification rate was set in an uncertainty range of 0.025–0.74 d⁻¹, and varied with different PFTs in the DLEM. The uncertainty ranges of the adsorption coefficient were referred to the sensitivity analysis conducted in Yang et al. (2015). Parameters used in the DLEM simulations for uncertainty analysis were assumed to follow a normal distribution. The Improved Latin Hypercube Sampling (LHS) approach was used to randomly select an ensemble of 100 sets of parameters (R version 3.2.1) (Tian et al., 2011, 2015).

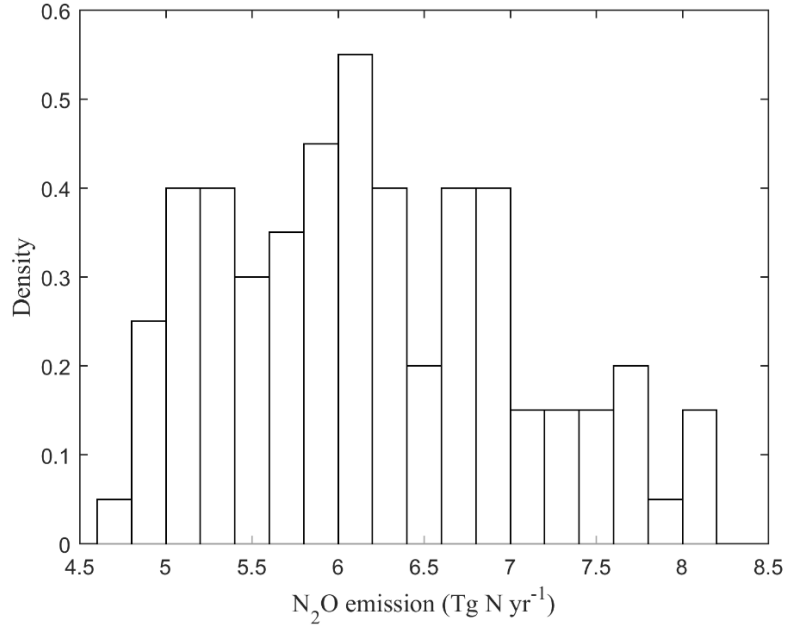


Figure 4-3. The distribution of 100 sets of results from DLEM simulations.

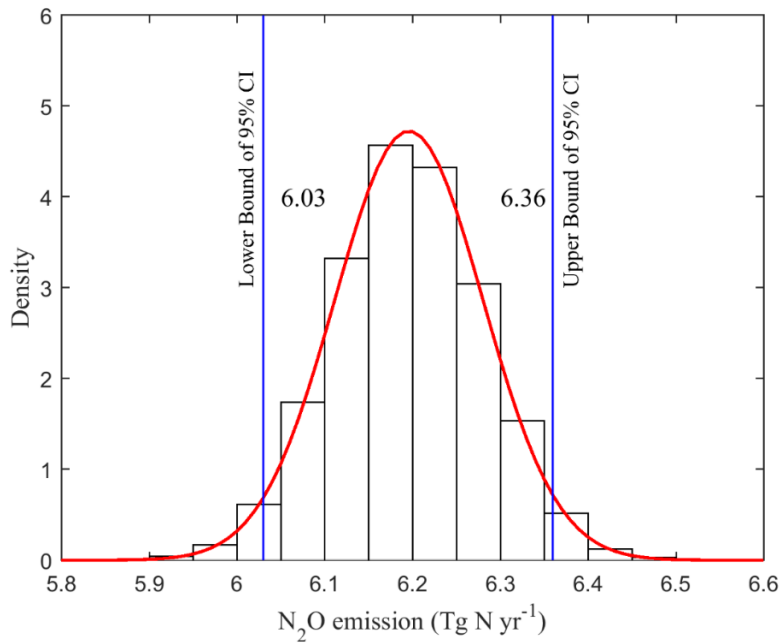


Figure 4-4. The 95% confidence intervals of the mean pre-industrial N₂O emission using the Bootstrap resampling method with 10,000 replicates.

In the DLEM, after the model reached equilibrium state, a spin-up run was implemented using de-trended climate data from 1901 to 1930 for each set of parameter values. Then, each set

of the model was run in transient mode in 1860 to produce the result of the pre-industrial N₂O emissions. All results from 100 groups of simulations are shown in Table 4-1. The Shapiro–Wilk test was used on 100 sets of results to check the normality of DLEM simulations. It turned out that the distribution is not normal (P value < 0.05, R version 3.2.1), as shown in Figure 4-3 & 4-4. Thus, the uncertainty range was represented as the minimum and maximum value of 100 sets of DLEM simulations.

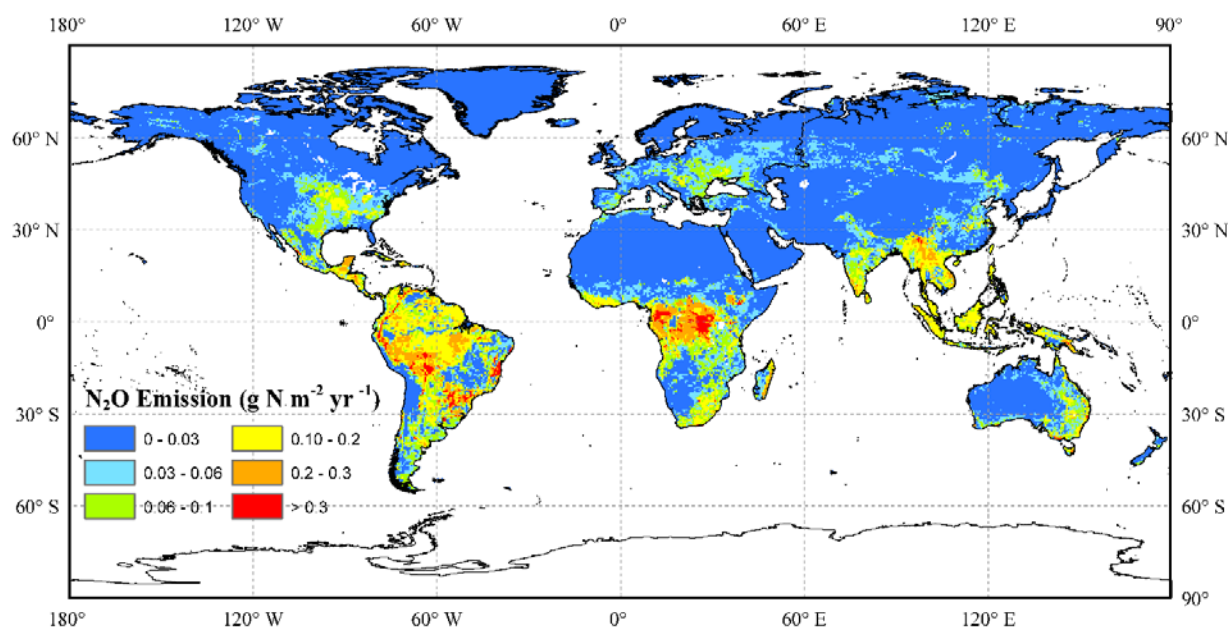


Figure 4-5. The spatial distribution of N₂O emission in the pre-industrial era.

3. Results & discussion

3.1. Magnitude and spatial distribution of N₂O emission

The global mean soil N₂O emission was 6.20 Tg N yr⁻¹. We define the parameter-induced uncertainty of our global estimates as a range between the minimum (4.76 Tg N yr⁻¹) and the maximum (8.13 Tg N yr⁻¹) of 100 sets of DLEM simulations. The terrestrial ecosystem in the pre-industrial period acted as a source of N₂O, and its spatial pattern mostly depends on the biome

distribution across the global land surface. The spatial distribution of annual N₂O emission in a 0.5° × 0.5° grid (Figure 4-5) shows that the strong sources were found near the equator, such as Southeast Asia, Central Africa, and Central America, where N₂O emission reached as high as 0.45 g N m⁻² yr⁻¹. The weak N₂O sources were observed in the northern areas of North America and Asia, where the estimated N₂O emission was less than 0.001 g N m⁻² yr⁻¹. The microbial activity in soils determined the rate of nitrification and denitrification processes, which accounts for approximately 70% of global N₂O emissions (Smith and Arah, 1990; Syakila and Kroeze, 2011). The tropical regions near the equator could provide microbes optimum temperatures and soil moistures to decompose soil organic matter and release more NO_x and CO₂ into the atmosphere (Butterbach-Bahl et al., 2013). Referring to the observational data from field experiments and model simulations in the tropics, it has been supported that the tropics are the main sources within the total N₂O emissions from natural vegetation (Bouwman et al., 1995; Werner et al., 2007; Zhuang et al., 2012).

In this study, Asia is divided into two parts: Southern Asia and Northern Asia, where the PFTs and climate conditions are significantly contrasting. As shown in Figure 4-1, tropical forest and cropland were dominant PFTs in Southern Asia. In contrast, temperate and boreal forests were main PFTs in Northern Asia. The estimates of N₂O emissions from seven land regions are shown in Figure 4-6. At continental scales, the N₂O emission was 2.09 (1.63–2.73) Tg N yr⁻¹ in South America, 1.46 (1.13–1.91) Tg N yr⁻¹ in Africa, and 1.16 (0.90–1.52) Tg N yr⁻¹ in Southern Asia. South America, Africa, and Southern Asia accounted for 33.77%, 23.60%, 18.73%, respectively, together which was 76.10% of global total emission. Europe and Northern Asia contributed to 0.45 (0.32–0.66) Tg N yr⁻¹, which was less than 10% of the total emission.

Table 4-1. All results of the global-, continental-, and biome-level N₂O emission from 100 sets of DLEM results in 1860. The unit is Tg N yr⁻¹.

No.	Total	Europe	North America	South America	Southern Asia	Northern Asia	Oceania	Africa	Boreal Forest	Tropical Forest	Temperate Forest	Shrubland	Grassland	Cropland	Tundra
1	6.986	0.339	0.774	2.323	1.315	0.175	0.348	1.645	0.695	4.467	0.695	0.925	0.225	0.479	0.010
2	6.546	0.292	0.684	2.244	1.225	0.166	0.325	1.545	0.594	4.281	0.594	0.845	0.199	0.428	0.013
3	5.121	0.243	0.554	1.724	0.959	0.124	0.254	1.213	0.504	3.309	0.504	0.672	0.159	0.341	0.005
4	6.699	0.350	0.772	2.167	1.248	0.179	0.339	1.578	0.734	4.180	0.734	0.926	0.219	0.443	0.012
5	5.386	0.257	0.585	1.807	1.004	0.137	0.268	1.275	0.536	3.466	0.536	0.715	0.165	0.347	0.009
6	6.178	0.317	0.701	2.016	1.152	0.163	0.312	1.458	0.661	3.882	0.661	0.846	0.199	0.408	0.011
7	6.029	0.268	0.627	2.073	1.129	0.150	0.298	1.424	0.545	3.953	0.545	0.775	0.182	0.396	0.010
8	6.966	0.303	0.720	2.405	1.306	0.176	0.346	1.643	0.612	4.583	0.612	0.892	0.211	0.455	0.014
9	6.033	0.289	0.659	2.019	1.132	0.150	0.300	1.426	0.595	3.878	0.595	0.796	0.190	0.406	0.008
10	5.666	0.259	0.602	1.932	1.067	0.134	0.278	1.338	0.530	3.703	0.530	0.728	0.175	0.381	0.005
11	5.796	0.267	0.616	1.970	1.088	0.142	0.287	1.369	0.545	3.770	0.545	0.751	0.179	0.389	0.008
12	4.945	0.218	0.508	1.713	0.929	0.117	0.244	1.167	0.442	3.258	0.442	0.628	0.149	0.333	0.006
13	7.677	0.376	0.855	2.536	1.437	0.205	0.386	1.806	0.773	4.873	0.773	1.033	0.246	0.511	0.017
14	5.347	0.236	0.551	1.851	1.003	0.129	0.264	1.263	0.478	3.523	0.478	0.681	0.161	0.355	0.007
15	6.257	0.321	0.709	2.041	1.167	0.168	0.317	1.474	0.667	3.924	0.667	0.859	0.201	0.416	0.013
16	7.443	0.335	0.787	2.540	1.414	0.181	0.371	1.742	0.666	4.847	0.666	0.955	0.237	0.528	0.011
17	6.384	0.287	0.670	2.184	1.188	0.167	0.318	1.509	0.590	4.164	0.590	0.833	0.192	0.404	0.014
18	6.019	0.303	0.675	1.979	1.123	0.158	0.303	1.421	0.629	3.803	0.629	0.818	0.192	0.400	0.011
19	5.520	0.251	0.587	1.886	1.042	0.127	0.269	1.304	0.514	3.615	0.514	0.706	0.171	0.376	0.003

20	6.455	0.291	0.673	2.205	1.206	0.170	0.324	1.523	0.589	4.197	0.589	0.842	0.196	0.422	0.016
21	6.145	0.253	0.580	2.090	1.170	0.128	0.278	1.583	0.480	4.105	0.480	0.805	0.185	0.443	0.015
22	6.886	0.343	0.770	2.266	1.287	0.183	0.347	1.623	0.708	4.354	0.708	0.933	0.221	0.459	0.014
23	6.927	0.300	0.714	2.395	1.313	0.166	0.344	1.627	0.596	4.563	0.596	0.876	0.214	0.480	0.010
24	7.927	0.381	0.866	2.635	1.482	0.221	0.403	1.862	0.774	5.038	0.774	1.067	0.251	0.524	0.024
25	8.045	0.388	0.885	2.669	1.501	0.224	0.407	1.892	0.795	5.117	0.795	1.085	0.253	0.521	0.023
26	4.766	0.219	0.507	1.627	0.898	0.108	0.233	1.129	0.451	3.120	0.451	0.610	0.147	0.323	0.002
27	5.459	0.253	0.578	1.856	1.025	0.134	0.271	1.288	0.514	3.547	0.514	0.708	0.168	0.369	0.007
28	5.181	0.252	0.567	1.730	0.964	0.134	0.260	1.226	0.526	3.314	0.526	0.696	0.160	0.334	0.008
29	6.774	0.314	0.724	2.290	1.267	0.176	0.339	1.597	0.642	4.373	0.642	0.891	0.210	0.447	0.015
30	6.805	0.325	0.741	2.275	1.268	0.184	0.341	1.605	0.671	4.357	0.671	0.911	0.211	0.436	0.016
31	6.258	0.260	0.603	2.121	1.204	0.125	0.282	1.598	0.494	4.168	0.494	0.822	0.191	0.465	0.012
32	7.660	0.370	0.839	2.543	1.438	0.205	0.388	1.802	0.749	4.877	0.749	1.024	0.245	0.517	0.019
33	6.276	0.319	0.711	2.054	1.167	0.167	0.316	1.481	0.670	3.955	0.670	0.860	0.199	0.404	0.012
34	6.591	0.294	0.691	2.261	1.242	0.160	0.326	1.551	0.595	4.315	0.595	0.845	0.204	0.447	0.010
35	5.087	0.224	0.525	1.763	0.963	0.115	0.249	1.198	0.451	3.360	0.451	0.639	0.156	0.354	0.003
36	8.133	0.381	0.878	2.728	1.521	0.222	0.411	1.911	0.772	5.213	0.772	1.081	0.255	0.536	0.024
37	6.066	0.293	0.665	2.026	1.144	0.147	0.301	1.431	0.597	3.895	0.597	0.796	0.194	0.421	0.007
38	4.979	0.243	0.545	1.660	0.930	0.125	0.249	1.178	0.505	3.185	0.505	0.664	0.155	0.331	0.007
39	5.230	0.249	0.569	1.760	0.980	0.124	0.257	1.240	0.519	3.386	0.519	0.685	0.163	0.345	0.004
40	6.075	0.275	0.641	2.076	1.135	0.153	0.301	1.435	0.566	3.964	0.566	0.788	0.185	0.394	0.010

41	6.822	0.266	0.681	2.228	1.223	0.264	0.519	1.577	0.550	4.225	0.550	1.074	0.233	0.440	0.050
42	5.872	0.242	0.582	2.075	1.113	0.135	0.288	1.380	0.477	3.931	0.477	0.724	0.176	0.407	0.006
43	6.743	0.298	0.702	2.317	1.261	0.172	0.335	1.592	0.607	4.416	0.607	0.870	0.204	0.438	0.014
44	7.161	0.380	0.832	2.300	1.338	0.195	0.365	1.682	0.788	4.435	0.788	0.996	0.237	0.483	0.016
45	5.090	0.224	0.525	1.764	0.954	0.121	0.250	1.203	0.457	3.358	0.457	0.647	0.153	0.337	0.006
46	5.912	0.253	0.596	2.061	1.108	0.147	0.294	1.395	0.506	3.908	0.506	0.749	0.176	0.393	0.011
47	6.370	0.332	0.731	2.066	1.191	0.165	0.321	1.502	0.692	3.987	0.692	0.873	0.209	0.428	0.010
48	5.153	0.214	0.513	1.821	0.967	0.120	0.252	1.216	0.432	3.452	0.432	0.640	0.151	0.339	0.006
49	6.057	0.290	0.665	2.030	1.138	0.146	0.298	1.431	0.600	3.906	0.600	0.795	0.192	0.407	0.006
50	4.905	0.217	0.507	1.699	0.922	0.114	0.241	1.158	0.441	3.236	0.441	0.621	0.148	0.331	0.004
51	4.862	0.227	0.521	1.650	0.912	0.115	0.239	1.153	0.470	3.165	0.470	0.631	0.149	0.322	0.004
52	7.706	0.355	0.825	2.603	1.441	0.206	0.387	1.814	0.724	4.972	0.724	1.016	0.239	0.504	0.020
53	6.758	0.306	0.708	2.304	1.266	0.176	0.339	1.593	0.617	4.390	0.617	0.881	0.207	0.448	0.016
54	5.321	0.248	0.565	1.806	0.993	0.136	0.266	1.255	0.508	3.443	0.508	0.699	0.162	0.349	0.009
55	5.758	0.281	0.635	1.914	1.076	0.146	0.288	1.362	0.584	3.678	0.584	0.769	0.181	0.382	0.008
56	5.814	0.247	0.586	2.033	1.078	0.150	0.288	1.375	0.503	3.850	0.503	0.742	0.169	0.362	0.014
57	7.764	0.400	0.887	2.516	1.452	0.215	0.396	1.822	0.823	4.840	0.823	1.070	0.254	0.523	0.020
58	5.386	0.230	0.545	1.884	1.019	0.124	0.265	1.268	0.459	3.581	0.459	0.672	0.162	0.370	0.005
59	5.222	0.232	0.543	1.801	0.970	0.131	0.259	1.236	0.482	3.427	0.482	0.676	0.154	0.328	0.009
60	6.341	0.290	0.667	2.159	1.182	0.168	0.318	1.495	0.589	4.110	0.589	0.832	0.192	0.411	0.016
61	7.150	0.326	0.761	2.430	1.354	0.175	0.356	1.678	0.653	4.645	0.653	0.922	0.227	0.500	0.011

62	5.007	0.229	0.531	1.709	0.947	0.113	0.245	1.183	0.469	3.275	0.469	0.639	0.156	0.348	0.002
63	5.877	0.259	0.610	2.030	1.112	0.138	0.289	1.383	0.521	3.869	0.521	0.744	0.181	0.406	0.006
64	5.175	0.231	0.539	1.786	0.976	0.119	0.254	1.220	0.468	3.409	0.468	0.655	0.158	0.353	0.004
65	6.739	0.324	0.740	2.244	1.255	0.179	0.338	1.591	0.674	4.307	0.674	0.905	0.210	0.433	0.014
66	5.383	0.253	0.577	1.819	1.006	0.134	0.268	1.273	0.521	3.483	0.521	0.706	0.165	0.353	0.008
67	6.911	0.344	0.772	2.276	1.296	0.181	0.347	1.628	0.705	4.376	0.705	0.930	0.223	0.469	0.013
68	5.503	0.219	0.536	1.967	1.031	0.128	0.268	1.299	0.440	3.719	0.440	0.675	0.158	0.357	0.007
69	6.429	0.297	0.684	2.181	1.201	0.166	0.321	1.516	0.606	4.164	0.606	0.843	0.197	0.420	0.013
70	7.045	0.333	0.766	2.361	1.326	0.179	0.351	1.660	0.678	4.531	0.678	0.927	0.223	0.479	0.012
71	6.688	0.309	0.720	2.263	1.268	0.159	0.330	1.573	0.626	4.338	0.626	0.864	0.214	0.470	0.007
72	5.739	0.280	0.633	1.911	1.077	0.141	0.285	1.357	0.579	3.675	0.579	0.760	0.183	0.390	0.006
73	4.956	0.232	0.529	1.679	0.925	0.123	0.247	1.172	0.480	3.207	0.480	0.651	0.152	0.326	0.007
74	5.216	0.252	0.566	1.746	0.974	0.134	0.261	1.233	0.519	3.342	0.519	0.695	0.161	0.345	0.009
75	5.450	0.258	0.592	1.838	1.031	0.125	0.267	1.287	0.529	3.534	0.529	0.704	0.173	0.379	0.002
76	5.734	0.238	0.570	2.021	1.069	0.141	0.282	1.357	0.481	3.828	0.481	0.720	0.167	0.367	0.010
77	5.783	0.273	0.621	1.948	1.086	0.144	0.289	1.366	0.557	3.731	0.557	0.759	0.180	0.391	0.009
78	5.469	0.223	0.541	1.938	1.027	0.127	0.267	1.291	0.450	3.673	0.450	0.676	0.160	0.360	0.007
79	7.412	0.352	0.802	2.480	1.387	0.200	0.374	1.744	0.714	4.743	0.714	0.987	0.233	0.491	0.020
80	5.884	0.281	0.641	1.972	1.107	0.144	0.292	1.390	0.576	3.789	0.576	0.772	0.186	0.402	0.007
81	5.102	0.218	0.519	1.786	0.961	0.116	0.249	1.203	0.442	3.398	0.442	0.637	0.152	0.342	0.003
82	6.319	0.291	0.673	2.144	1.189	0.156	0.314	1.491	0.592	4.101	0.592	0.821	0.197	0.429	0.009

83	5.903	0.276	0.637	1.995	1.120	0.136	0.290	1.391	0.560	3.829	0.560	0.760	0.189	0.418	0.004
84	5.845	0.250	0.599	2.037	1.102	0.136	0.285	1.378	0.508	3.880	0.508	0.734	0.176	0.391	0.006
85	6.217	0.300	0.683	2.075	1.162	0.158	0.309	1.469	0.622	3.986	0.662	0.827	0.195	0.408	0.010
86	6.938	0.312	0.729	2.371	1.307	0.173	0.346	1.633	0.627	4.525	0.627	0.894	0.215	0.471	0.013
87	5.874	0.276	0.631	1.981	1.093	0.154	0.294	1.387	0.572	3.785	0.572	0.779	0.180	0.377	0.012
88	5.571	0.276	0.619	1.847	1.043	0.138	0.277	1.318	0.573	3.556	0.573	0.743	0.177	0.372	0.006
89	5.908	0.260	0.608	2.040	1.099	0.153	0.294	1.396	0.531	3.875	0.531	0.764	0.175	0.375	0.013
90	6.759	0.304	0.708	2.307	1.259	0.181	0.339	1.595	0.619	4.394	0.619	0.885	0.204	0.433	0.018
91	6.084	0.306	0.685	2.002	1.141	0.151	0.303	1.438	0.637	3.862	0.637	0.816	0.197	0.411	0.007
92	5.669	0.279	0.626	1.880	1.058	0.148	0.285	1.339	0.579	3.608	0.579	0.763	0.178	0.372	0.011
93	6.102	0.278	0.644	2.080	1.139	0.157	0.304	1.440	0.570	3.967	0.570	0.797	0.185	0.396	0.012
94	6.085	0.281	0.646	2.065	1.136	0.157	0.304	1.436	0.576	3.939	0.576	0.800	0.186	0.397	0.012
95	8.086	0.378	0.872	2.716	1.519	0.214	0.408	1.899	0.760	5.194	0.760	1.067	0.256	0.547	0.021
96	7.247	0.342	0.784	2.429	1.354	0.195	0.365	1.707	0.700	4.648	0.700	0.964	0.226	0.474	0.018
97	7.495	0.344	0.797	2.537	1.406	0.197	0.377	1.764	0.695	4.845	0.695	0.982	0.234	0.500	0.018
98	7.284	0.365	0.822	2.389	1.358	0.196	0.367	1.716	0.760	4.597	0.760	0.992	0.233	0.476	0.016
99	6.607	0.341	0.756	2.148	1.232	0.175	0.333	1.557	0.714	4.141	0.714	0.908	0.214	0.436	0.012
100	7.233	0.334	0.775	2.446	1.351	0.190	0.361	1.705	0.683	4.678	0.683	0.951	0.223	0.469	0.016

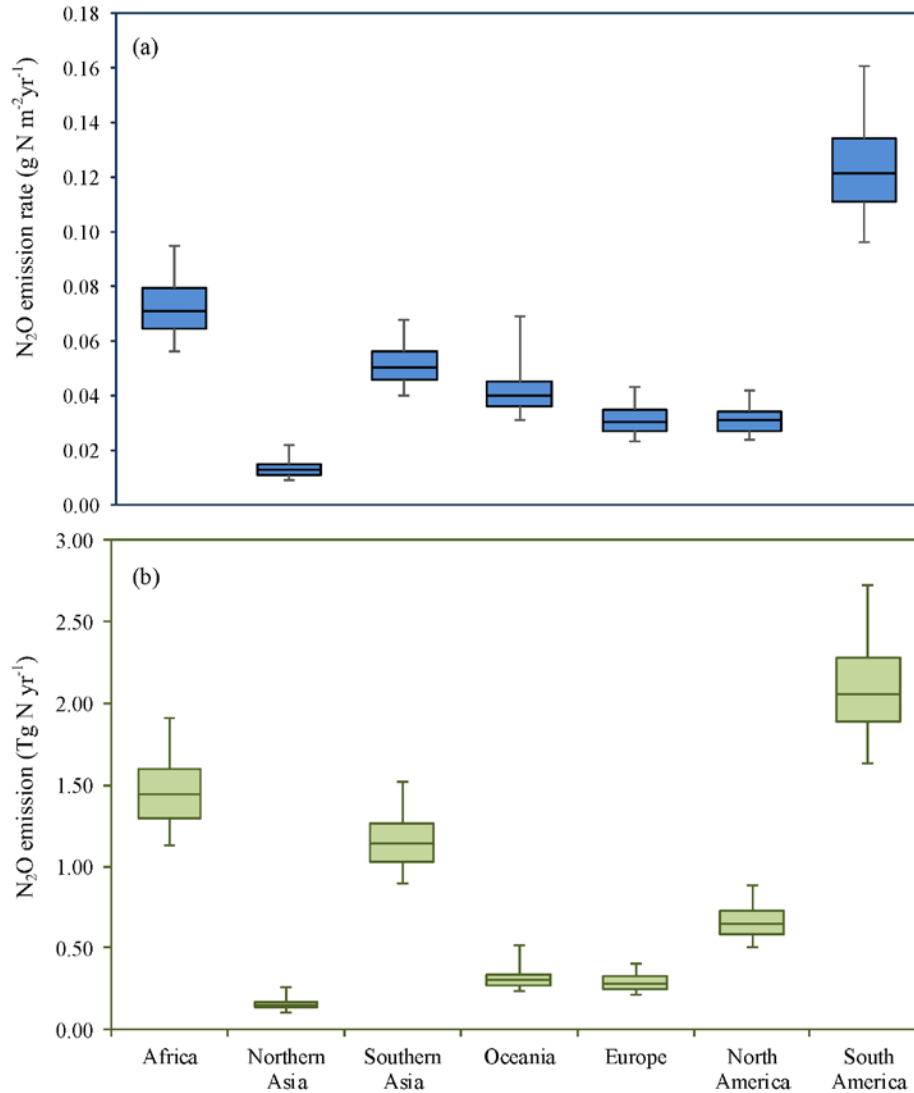


Figure 4-6. Estimated N_2O emission rates (a) and emissions (b) with uncertainty ranges at continental-level in 1860. Solid line within each box refers to the median value of N_2O emission rate or amount.

Nitrous oxide emissions varied remarkably among different ecosystems. Forest, grassland, shrub, tundra and cropland contributed 76.90%, 3.11%, 13.14%, 0.18% and 6.67%, respectively, to the total emission globally (Figure 4-7). In different biomes, the tropics accounted for more than half of the total N_2O emission, which is comparable to the conclusion made by Bouwman et al. (1993). In the pre-industrial era, the major inputs of reactive N to terrestrial ecosystems were from

BNF, which relies on the activity of a phylogenetically diverse list of bacteria, archaea and symbioses (Cleveland et al., 1999; Vitousek et al., 2013). Tropical savannas have been considered as ‘hot spots’ of BNF by legume nodules that provide the major input of available N (Bate and Gunton, 1982). The substantial inputs of N into tropical forests could contribute to higher amount of the gaseous N losses as N₂O or nitrogen gas (Cleveland et al., 2010; Hall and Matson, 1999). In contrast, as the largest terrestrial biome, boreal forests lack of available N because the rate of BNF is restricted by cold temperatures and low precipitation during growing season (Alexander and Billington, 1986). Morse et al. (2015) conducted field experiments in Northeastern North American forests. They found that denitrification does vary coherently with patterns of N availability in forests, and no significant correlations between atmospheric N deposition, potential net N mineralization and nitrification rates. Thus, it is reasonable that boreal forests contributed to the least amount of N₂O emission among different forests.

As shown in Figure 4-2, cropland areas varied spatially. The regions with large areas of cropland were the entire Europe, India, the eastern China, and central-eastern United States. The global N₂O emission from croplands was estimated as 0.41 (0.32–0.55) Tg N yr⁻¹, which is about ten times less than the estimate reported in the IPCC AR5 (Ciais et al., 2014). As no synthetic N fertilizer was applied to the cropland in 1860, leguminous crops were the major source of N₂O emission from croplands, most of which were planted in central-eastern United States (Figure 4-5). Rochette et al. (2004) conducted the experiments on the N₂O emission from soybean without application of N fertilizer. Their work was in agreement with the suggestion that legumes may increase N₂O emissions compared with non-BNF crops (Duxbury et al., 1982) The background emission from ground-based experiments was as high as 0.31–0.42 kg N ha⁻¹ in Canada (Duxbury et al., 1982; Rochette et al., 2004).

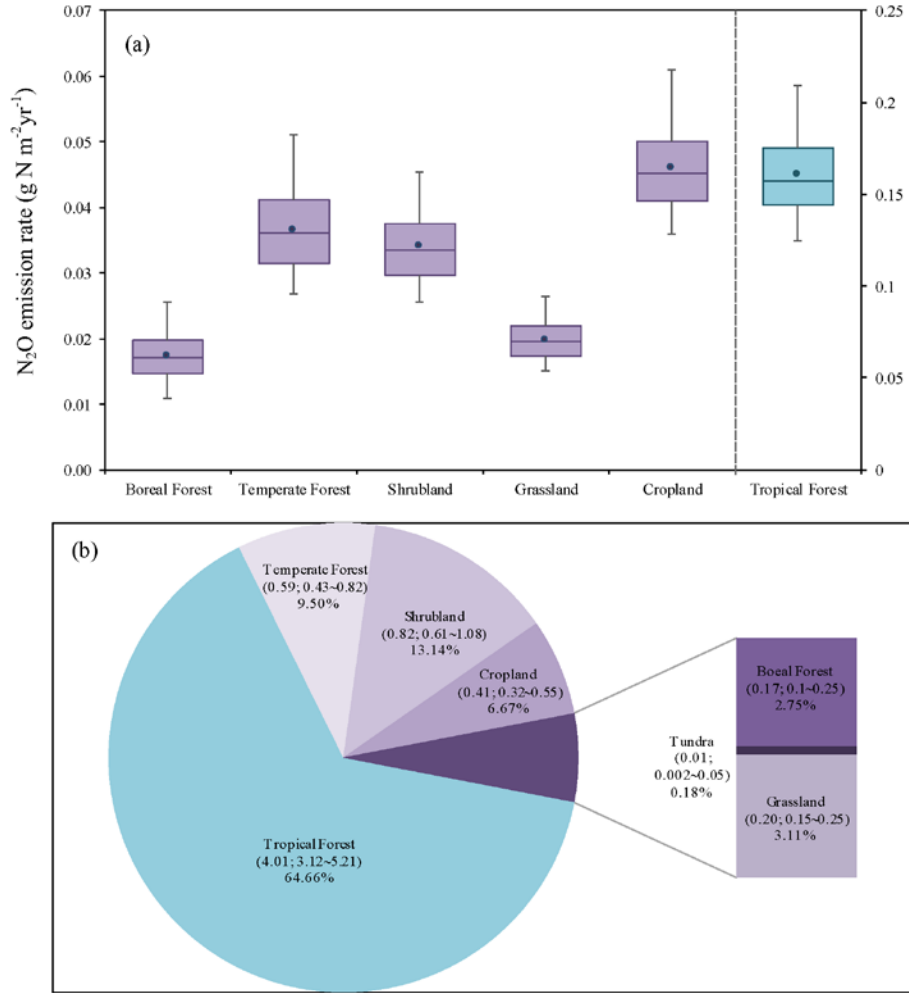


Figure 4-7. (a) Estimated N₂O emission rate at biome-level in 1860 with the median value (solid line), the mean (solid dot), and the uncertainty range of emission rates from different biomes. The emission rate in the tundra was removed because of the extremely small value (less than 0.003g N m⁻²yr⁻¹); (b) Estimated N₂O emission (Tg N yr⁻¹) with uncertainty ranges and its percentage (%) at biome-level in 1860.

Table 4-2. Pre-industrial N₂O emissions from natural vegetation and croplands in different countries.
1Mha = 10⁴ km²

Country	Vegetation area (Mha)	Natural soils (Gg N yr ⁻¹)	Cropland (Gg N yr ⁻¹)	Total (Gg N yr ⁻¹)
China	756.3	188	62	250
India	306.8	121	64	185
United States	913.9	296	81	377
Pakistan	65.1	5	6	11
Indonesia	174.1	181	2	183
France	52.3	7	9	16
Brazil	835.1	1017	11	1028
Canada	914.6	94	2	96
Germany	36.0	9	4	13
Turkey	74.3	17	11	28
Mexico	191.0	118	3	121
Vietnam	31.7	41	2	43
Spain	48.2	14	6	20
Russian Federation	1575.3	234	19	253
Bangladesh	12.4	2	5	7
Thailand	49.3	56	3	59

Pre-industrial N₂O emission at country-level could serve as a reference for calculating human-induced N₂O emission in today's nations. We estimated pre-industrial N₂O emissions from seventeen countries that are "hot spots" of N₂O sources in the contemporary period (Table 4-2). The order of countries was referred to Gerber et al. (2016) that indicated the top seventeen countries in terms of total N application in 2000. Pre-industrial N₂O emissions from natural soils and croplands varied significantly at country-scales. The United States, China, and India were top countries accounted for emissions from pre-industrial croplands. Countries close to or located in the tropics, such as Mexico, Indonesia, and Brazil, accounted for negligible emissions from croplands, but substantial amount from natural vegetation in the pre-industrial era. Previous studies indicated that agriculture produces the majority of anthropogenic N₂O emissions (Ciais et al.,

2014; Davidson and Kanter, 2014). Our estimate at country-scales could be used as a reference to quantify the net increase of N₂O emissions from agriculture activities in countries of “hot spots”.

There is a debate that the natural wetlands and peatlands act as sinks or sources of N₂O. Previous studies showed that N₂O emissions from natural peatlands are usually negligible; however, the drained peatlands with lower water tables might act as sources of N₂O (Augustin et al., 1998; Martikainen et al., 1993). High water tables in wetlands might block the activity of nitrifiers and limit the denitrification (Bouwman et al., 1993). The fluxes of N₂O were negligible in the pelagic regions of boreal ponds and lakes due to the limitation of nitrification and/or nitrate inputs (Huttunen et al., 2003). Couwenberg et al. (2011) mentioned that N₂O emissions always decreased after rewetting when conducting field experiments, which had been excluded from their future analysis of GHG emissions in peatlands. Hadi et al. (2005) pointed out that tropical peatlands ranged from sources to sinks of N₂O, highly affected by land-use and hydrological zone. We were incapable to examine N₂O fluxes from wetlands and peatlands in 1860 as human-induced land-use in those ecosystems was unknown. Thus, we excluded the N₂O emissions from wetlands and peatlands in this study.

3.2. Revisit preindustrial global N₂O emission by incorporating top-down estimates

“Top-down” methodology used to estimate N₂O emissions is based on atmospheric measurements and inversion modeling (Thompson et al. 2014). Prather et al. (2012) provided an estimate of 9.1 ± 1.0 Tg N yr⁻¹ of natural emission in the pre-industrial era using observed pre-industrial abundances of 270 ppb and model estimates of lifetime decreased from 142 years in the pre-industrial era to 131 ± 10 years in the present-day. Later, Prather et al. (2015) re-evaluated N₂O lifetime based on Microwave Limb Sounder satellite measurements of stratospheric, which was consistent with modeled values in the present-day. The lifetime in the pre-industrial era and

present-day was estimated to be 123 and 116 ± 9 years, respectively. The current lifetime increases the pre-industrial natural emission from 9.1 ± 1.0 to $10.5 \text{ Tg N yr}^{-1}$.

Natural sources for N_2O include soil under natural vegetation, oceans, and atmospheric chemistry (Ciais et al., 2014). The emission from atmospheric chemistry was estimated as 0.6 with an uncertainty range of $0.3\text{--}1.2 \text{ Tg N yr}^{-1}$. Syakila and Kroeze (2011) estimated global natural emissions from oceans as 3.5 Tg N yr^{-1} . Oceanic emission was estimated as 3.8 with an uncertainty range of $1.8\text{--}5.8 \text{ Tg N yr}^{-1}$ in the IPCC AR4. However, the uncertainty range became larger ($1.8\text{--}9.4 \text{ Tg N yr}^{-1}$) in the IPCC AR5. In our study, the simulated N_2O emission was from agricultural and natural soils. The natural emission was estimated as $5.78 (4.4\text{--}7.72) \text{ Tg N yr}^{-1}$. Combining the atmospheric chemistry and the ocean emissions in the IPCC AR5 with the natural emissions from our study, the global total natural N_2O emissions were $10.18 (6.5\text{--}18.32) \text{ Tg N yr}^{-1}$. The large uncertainty range was attributed to the uncertainty from oceanic emission, atmospheric chemistry emission, and our estimation. The estimated global total amount ($10.18 \text{ Tg N yr}^{-1}$) in this study was comparable to the estimate ($10.5 \text{ Tg N yr}^{-1}$) by Prather et al. (2015) using the top-down approach.

3.3. Comparison with estimates by bottom-up methodology

“Bottom-up” approach includes the estimations based on inventory, statistical extrapolation of local flux measurements, and process-based modeling (Tian et al., 2016). The global pre-agricultural N_2O emission was estimated as 6.8 Tg N yr^{-1} based on the regression relationship between measured N_2O fluxes and modeled N_2O production indices (Bouwman et al., 1993). This estimate was adopted to retrieve the trends of atmospheric N_2O concentration in Syakila and Kroeze (2011). In our study, the pre-industrial N_2O emission from natural vegetation was estimated as $5.78 (4.4\text{--}7.72) \text{ Tg N yr}^{-1}$, which is about 1 Tg N yr^{-1} lower than the estimate

from Bouwman et al. (1993). Estimate from the tropics ($\pm 30^\circ$ of the equator) was about 4.57 Tg N yr⁻¹, which is 0.83 Tg N yr⁻¹ lower than the estimate from Bouwman et al. (1993). For the rest of natural vegetation, our estimate was 1.21 Tg N yr⁻¹, which is close to 1.4 Tg N yr⁻¹ estimated in Bouwman et al. (1993).

Although Bouwman et al. (1993) has studied the potential N₂O emission from natural soils, our study provided a first estimate of spatially distributed N₂O emission in 1860 using the biogeochemical process-based model. Bouwman et al. (1993) provided 1° × 1° monthly N₂O emission using the monthly controlling factors without considering the impact of N deposition. In their study, the soil fertility and carbon content were constant for every month, which could not reflect the monthly dynamic changes of carbon and N pools in natural soils. Moreover, although their study has represented a spatial distribution of potential N₂O emission from natural soils, they had not provided the estimate at biome-, continent-, and country-scales. Thus, their result was hardly to be used as a regional reference for the net human-induced N₂O emissions from some “hot spots”, such as Southern Asia. In contrast, in our study, using daily climate and N deposition dataset could better reflect the real variation of N₂O emission through the growing season in natural ecosystems. The comparison with field observations during 1997–2001 indicated that the DLEM can catch the daily peak N₂O emissions in Hubbard Brook Forest (Tian et al., 2010) and Inner-Mongolia (Tian et al., 2011).

As far as the N₂O emission from croplands, our estimate is comparable to the estimate of 0.3 (0.29–0.35) Tg N yr⁻¹ extracted from Syakila and Kroeze (2011) by digitizing graphs using the Getdata Graph Digitizer. In their study, the estimation was based on the relationship between the crop production and human population during 1500–1970. In contrast, the result in our study was

estimated based on the cropland area of specific crop type, mainly soybean, rice, corn, and wheat in 1860.

Thus, the DLEM is capable to provide the estimate of N₂O emission from natural ecosystems at regional- and biome-scales with a higher spatial resolution. This could be a useful reference for quantifying effects of human activities such as the LULC change, N fertilizer and manure application, and increasingly atmospheric N deposition on N₂O emissions in different terrestrial ecosystems or sectors in the contemporary period.

3.4. The N₂O budget in the pre-industrial era

The observed N₂O concentration is the result of dynamic production and consumption processes in soils as soils act as sources or sinks of N₂O through denitrification and nitrification (Chapuis-Lardy et al., 2007). There was a slight increase of atmospheric N₂O concentration during 1750–1860 according to the ice core records, but showed a rapid increase from 1860 to present (Ciais et al., 2014). Nature sources of N₂O emissions have been discussed in section 3.2 & 3.3. Previous studies found that there were some anthropogenic N₂O emissions along with the natural sources in the pre-industrial era (Davidson, 2009; Syakila and Kroeze, 2011). Syakila and Kroeze (2011) found anthropogenic N₂O emission began since 1500 because of the biomass burning and agriculture. The total anthropogenic N₂O emission in their study was estimated as 1.1 Tg N in 1850. In addition, Davidson (2009) derived a time-course analysis of sources and sinks of atmospheric N₂O since 1860. The pre-industrial anthropogenic N₂O sources in his study included biomass burning, agriculture (e.g. manure and fertilizer application, and the cultivation of legume) and human sewage, the sum of which was 0.7 (0.6–0.8) Tg N yr⁻¹ (Davidson, 2009). Thus, anthropogenic N₂O emission has already existed in 1860, but in a small magnitude as compared with the contemporary amount.

Davidson (2009) mentioned that there was possibly a certain amount of N₂O loss in the pre-industrial period through atmospheric sink and the reduced emission from tropical deforestation. He estimated the anthropogenic sink as 0.26 Tg N in 1860. In addition, the deforestation of tropical forest might have caused a loss of N₂O emissions in 1860, which was estimated as 0.03 Tg N (Davidson, 2009). However, studies have shown that the conversion of forest to pasture and cropland could increase or have no effect on N₂O emissions because the effects depended on disturbance intensity of human activities on soil conditions (van Lent et al., 2015). For instance, N₂O emissions tended to increase during the first 5–10 years after conversion and thereafter might decrease to average upland forest or low canopy forest levels in the non-fertilized croplands and pastures. In contrast, emissions were at a high level during and after fertilization in fertilized croplands (van Lent et al., 2015). Thus, more work is needed to study how forest degradation affects N₂O fluxes (Mertz et al., 2012).

3.5. Future research needs

Large uncertainty still exists in the DLEM simulation associated with the quality of input datasets and parameters applied in simulations. Although input datasets could play a significant role in the variety of the model output, it is difficult to obtain accurate datasets back to the year 1860. Average climate data from 1901 to 1930 was used to run model simulation, which could raise the uncertainty in estimating N₂O emission in 1860. The datasets of LULC, N deposition, and manure application in 1860 could introduce uncertainties to this estimate. The average oceanic and atmospheric chemistry emissions cited from the IPCC AR5 could introduce the uncertainty into calculation of the total natural emissions in 1860 when comparing with the estimate done by Prather et al. (2015). Thus, more accurate estimate of oceanic N₂O emission is significant to narrow

the confidence estimate of the pre-industrial terrestrial sources. The N₂O fluxes from wetlands and peats needed to be included in the future study.

4. Conclusions

Using the process-based land ecosystem model DLEM, this study provides a spatially-explicit estimate of pre-industrial N₂O emissions for major PFTs across global land surface. Improved LHS was performed to analyze uncertainty ranges of the estimates. We estimated that pre-industrial N₂O emission is 6.20 Tg N yr⁻¹. The modeled results showed a large spatial variability due to variations in climate conditions and PFTs. Tropical ecosystem was the dominant contributor of global N₂O emissions. In contrast, boreal regions contributed less than 5% to the total emission. China, India and United States are top countries accounted for emissions from croplands in 1860. While uncertainties still exist in the N₂O emission estimation in the pre-industrial era, this study offered a relatively reasonable estimate of the pre-industrial N₂O emission from land soils. Meanwhile, this study provided a spatial estimate for N₂O emission from the global hot spots, which could be used as a reference to estimate net human-induced emissions in the contemporary period.

References

- Aardenne, J. V., Dentener, F., Olivier, J., Goldewijk, C., and Lelieveld, J.: A 1×1 resolution data set of historical anthropogenic trace gas emissions for the period 1890–1990, *Global Biogeochemical Cycles*, 15, 909-928, 2001.
- Alexander, V., and Billington, M.: Nitrogen fixation in the Alaskan taiga, in: *Forest ecosystems in the Alaskan taiga*, Springer, 112-120, 1986.
- Augustin, J., Merbach, W., Steffens, L., and Snelinski, B.: Nitrous oxide fluxes of disturbed minerotrophic peatlands, *Agribiological Research*, 51, 47-57, 1998.
- Bate, G., and Gunton, C.: Nitrogen in the *Burkea* savanna, in: *Ecology of tropical savannas*, Springer, 498-513, 1982.
- Bouwman, A., Fung, I., Matthews, E., and John, J.: Global analysis of the potential for N_2O production in natural soils, *Global Biogeochemical Cycles*, 7, 557-597, 1993.
- Bouwman, A., Van der Hoek, K., and Olivier, J.: Uncertainties in the global source distribution of nitrous oxide, *Journal of Geophysical Research: Atmospheres*, 100, 2785-2800, 1995.
- Butterbach-Bahl, K., Baggs, E. M., Dannenmann, M., Kiese, R., and Zechmeister-Boltenstern, S.: Nitrous oxide emissions from soils: how well do we understand the processes and their controls?, *Phil. Trans. R. Soc. B*, 368, 20130122, 2013.
- Chapuis-Lardy, L., Wrage, N., Metay, A., CHOTTE, J. L., and Bernoux, M.: Soils, a sink for N_2O ? A review, *Global Change Biology*, 13, 1-17, 2007.
- Chatskikh, D., Olesen, J. E., Berntsen, J., Regina, K., and Yamulki, S.: Simulation of effects of soils, climate and management on N_2O emission from grasslands, *Biogeochemistry*, 76, 395-419, 2005.
- Ciais, P., Sabine, C., Bala, G., Bopp, L., Brovkin, V., Canadell, J., Chhabra, A., DeFries, R., Galloway, J., Heimann, M., Jones, C., Le Quere, C., Myneni, R., Piao, S., Thornton, P., Heinze, C., Tans, P., and Vesala, T.: Carbon and other biogeochemical cycles. In *Climate Change 2013: The Physical Science Basis. Contribution of Working Group I to the Fifth Assessment Report of the Intergovernmental Panel on Climate Change*. Cambridge University Press, 465-570, 2014.
- Cleveland, C. C., Townsend, A. R., Schimel, D. S., Fisher, H., Howarth, R. W., Hedin, L. O., Perakis, S. S., Latty, E. F., Von Fischer, J. C., and Elseroad, A.: Global patterns of terrestrial biological nitrogen (N_2) fixation in natural ecosystems, *Global Biogeochemical Cycles*, 13, 623-645, 1999.
- Cleveland, C. C., Houlton, B. Z., Neill, C., Reed, S. C., Townsend, A. R., and Wang, Y.: Using indirect methods to constrain symbiotic nitrogen fixation rates: a case study from an Amazonian rain forest, *Biogeochemistry*, 99, 1-13, 2010.
- Couwenberg, J., Thiele, A., Tanneberger, F., Augustin, J., Bärtsch, S., Dubovik, D., Liashchynskaya, N., Michaelis, D., Minke, M., and Skuratovich, A.: Assessing greenhouse gas emissions from peatlands using vegetation as a proxy, *Hydrobiologia*, 674, 67-89, 2011.
- Davidson, E. A.: The contribution of manure and fertilizer nitrogen to atmospheric nitrous oxide since 1860, *Nature Geoscience*, 2, 659-662, 2009.
- Davidson, E. A., and Kanter, D.: Inventories and scenarios of nitrous oxide emissions, *Environmental Research Letters*, 9, 105012, 2014.
- Dentener, F.: Global maps of atmospheric nitrogen deposition, 1860, 1993, and 2050, Data set. Available on-line (<http://daac.ornl.gov/>) from Oak Ridge National Laboratory Distributed Active Archive Center, Oak Ridge, TN, USA, 2006.

- Denman K., Brasseur G., Chidthaisong A., Ciais P. M., Cox P., Dickinson R., Hauglustaine D., Heinze C., Holland E., Jacob D., Lohmann U., Ramachandran S., da Silva Dias P., Wofsy S. and Zhang X.: Couplings Between Changes in the Climate System and Biogeochemistry. In: *Climate Change 2007: The Physical Science Basis. Contribution of Working Group I to the Fourth Assessment Report of the Intergovernmental Panel on Climate Change* [Solomon S., Qin D., Manning M., Chen Z., Marquis M., Averyt K. B., Tignor M., and Miller H. (eds.)]. Cambridge University Press, Cambridge, United Kingdom and New York, NY, USA, 501-566, 2007.
- Duxbury, J., Bouldin, D., Terry, R., and Tate, R. L.: Emissions of nitrous oxide from soils, 1982.
- Forster, P., Ramaswamy, V., Artaxo, P., Bernsten, T., Betts, R., Fahey, D. W., Haywood, J., Lean, J., Lowe, D. C., and Myhre, G.: Changes in atmospheric constituents and in radiative forcing. Chapter 2, in: *Climate Change 2007. The Physical Science Basis*, 2007.
- Galloway, J. N., Dentener, F. J., Capone, D. G., Boyer, E. W., Howarth, R. W., Seitzinger, S. P., Asner, G. P., Cleveland, C., Green, P., and Holland, E.: Nitrogen cycles: past, present, and future, *Biogeochemistry*, 70, 153-226, 2004.
- Gerber, S., Hedin, L. O., Oppenheimer, M., Pacala, S. W., and Shevliakova, E.: Nitrogen cycling and feedbacks in a global dynamic land model, *Global Biogeochemical Cycles*, 24, 2010.
- Gerber, J. S., Carlson, K. M., Makowski, D., Mueller, N. D., Garcia de Cortazar-Atauri, I., Havlík, P., Herrero, M., Launay, M., O'Connell, C. S., and Smith, P.: Spatially explicit estimates of N₂O emissions from croplands suggest climate mitigation opportunities from improved fertilizer management, *Global Change Biology*, 2016.
- Hadi, A., Inubushi, K., Purnomo, E., Razie, F., Yamakawa, K., and Tsuruta, H.: Effect of land-use changes on nitrous oxide (N₂O) emission from tropical peatlands, *Chemosphere-Global Change Science*, 2, 347-358, 2000.
- Hall, S. J., and Matson, P. A.: Nitrogen oxide emissions after nitrogen additions in tropical forests, *Nature*, 400, 152-155, 1999.
- Hansen, S.: Daisy, a flexible soil-plant-atmosphere system model, Report. Dept. Agric, 2002.
- Heinen, M.: Simplified denitrification models: overview and properties, *Geoderma*, 133, 444-463, 2006.
- Holland, E., Lee-Taylor, J., Nevison, C., and Sulzman, J.: Global N Cycle: Fluxes and N₂O mixing ratios originating from human activity, Data set. Available on-line: [http://www. daac. ornl. gov](http://www.daac.ornl.gov) from Oak Ridge National Laboratory Distributed Active Archive Center, Oak Ridge, Tennessee, USA, doi, 10, 2005.
- Hu, M., Chen, D., and Dahlgren, R. A.: Modeling nitrous oxide (N₂O) emission from rivers: A global assessment, *Global Change Biology*, 2016.
- Hurt, G., Chini, L. P., Frolking, S., Betts, R., Feddema, J., Fischer, G., Fisk, J., Hibbard, K., Houghton, R., and Janetos, A.: Harmonization of land-use scenarios for the period 1500–2100: 600 years of global gridded annual land-use transitions, wood harvest, and resulting secondary lands, *Climatic Change*, 109, 117-161, 2011.
- Huttunen, J. T., Alm, J., Liikanen, A., Juutinen, S., Larmola, T., Hammar, T., Silvola, J., and Martikainen, P. J.: Fluxes of methane, carbon dioxide and nitrous oxide in boreal lakes and potential anthropogenic effects on the aquatic greenhouse gas emissions, *Chemosphere*, 52, 609-621, 2003.
- Intergovernmental Panel on Climate Change (IPCC) Revised 1996 IPCC Guidelines for National Greenhouse Gas Inventories vol 1/3 ed J T Houghton, L G Meira Filho, B Lim, K Treanton,

- I Mamaty, Y Bonduki, D J Griggs and B A Callander (London: IPCC, OECD and IEA), 1997.
- Jung, M., Henkel, K., Herold, M., and Churkina, G.: Exploiting synergies of global land cover products for carbon cycle modeling, *Remote Sensing of Environment*, 101, 534-553, 2006.
- Kroeze, C., Mosier, A., and Bouwman, L.: Closing the global N₂O budget: a retrospective analysis 1500–1994, *Global Biogeochemical Cycles*, 13, 1-8, 1999.
- van Lent, J., Hergoualc'h, K., and Verchot, L.: Reviews and syntheses: Soil N₂O and NO emissions from land use and land use change in the tropics and subtropics: a meta-analysis, *Biogeosciences*, 12, 2015.
- Liu, M., Tian, H., Yang, Q., Yang, J., Song, X., Lohrenz, S. E., and Cai, W. J.: Long-term trends in evapotranspiration and runoff over the drainage basins of the Gulf of Mexico during 1901–2008, *Water Resources Research*, 49, 1988-2012, 2013.
- Lu, C., and Tian, H.: Net greenhouse gas balance in response to nitrogen enrichment: perspectives from a coupled biogeochemical model, *Global Change Biology*, 19, 571-588, 2013.
- Machida, T., Nakazawa, T., Fujii, Y., Aoki, S., and Watanabe, O.: Increase in the atmospheric nitrous oxide concentration during the last 250 years, *Geophysical Research Letters*, 22, 2921-2924, 1995.
- Martikainen, P. J., Nykänen, H., Crill, P., and Silvola, J.: Effect of a lowered water table on nitrous oxide fluxes from northern peatlands, *Nature*, 366, 51-53, 1993.
- Mertz, O., Müller, D., Sikor, T., Hett, C., Heinemann, A., Castella, J.-C., Lestrelin, G., Ryan, C. M., Reay, D. S., Schmidt-Vogt, D., Danielsen, F., Theilade, I., Noordwijk, M. v., Verchot, L. V., Burgess, N. D., Berry, N. J., Pham, T. T., Messerli, P., Xu, J., Fensholt, R., Hostert, P., Pflugmacher, D., Bruun, T. B., Neergaard, A. d., Dons, K., Dewi, S., Rutishauser, E., Sun, and Zhanli: The forgotten D: challenges of addressing forest degradation in complex mosaic landscapes under REDD+, *Geografisk Tidsskrift-Danish Journal of Geography*, 112, 63-76, 10.1080/00167223.2012.709678, 2012.
- Morse, J. L., Durán, J., Beall, F., Enanga, E. M., Creed, I. F., Fernandez, I., and Groffman, P. M.: Soil denitrification fluxes from three northeastern North American forests across a range of nitrogen deposition, *Oecologia*, 177, 17-27, 2015.
- Myhre, G., Shindell, D., Bréon, F., Collins, W., Fuglestedt, J., Huang, J., Koch, D., Lamarque, J., Lee, D., and Mendoza, B.: Anthropogenic and natural radiative forcing, *Climate Change*, 423, 2013.
- NOAA2006A: Combined Nitrous Oxide data from the NOAA/ESRL Global Monitoring Division, 2016.
- Pan, S., Tian, H., Dangal, S. R., Zhang, C., Yang, J., Tao, B., Ouyang, Z., Wang, X., Lu, C., and Ren, W.: Complex Spatiotemporal Responses of Global Terrestrial Primary Production to Climate Change and Increasing Atmospheric CO₂ in the 21 st Century, *PloS one*, 9, e112810, 2014.
- Pan, S., Tian, H., Dangal, S. R., Yang, Q., Yang, J., Lu, C., Tao, B., Ren, W., and Ouyang, Z.: Responses of global terrestrial evapotranspiration to climate change and increasing atmospheric CO₂ in the 21st century, *Earth's Future*, 3, 15-35, 2015.
- Prather, M. J., and Hsu, J.: Coupling of nitrous oxide and methane by global atmospheric chemistry, *Science*, 330, 952-954, 2010.
- Prather, M. J., Holmes, C. D., and Hsu, J.: Reactive greenhouse gas scenarios: Systematic exploration of uncertainties and the role of atmospheric chemistry, *Geophysical Research Letters*, 39, 2012.

- Prather, M. J., Hsu, J., DeLuca, N. M., Jackman, C. H., Oman, L. D., Douglass, A. R., Fleming, E. L., Strahan, S. E., Steenrod, S. D., and Søvde, O. A.: Measuring and modeling the lifetime of nitrous oxide including its variability, *Journal of Geophysical Research: Atmospheres*, 120, 5693-5705, 2015.
- Ravishankara, A., Daniel, J. S., and Portmann, R. W.: Nitrous oxide (N₂O): the dominant ozone-depleting substance emitted in the 21st century, *Science*, 326, 123-125, 2009.
- Reay, D. S., Davidson, E. A., Smith, K. A., Smith, P., Melillo, J. M., Dentener, F., and Crutzen, P. J.: Global agriculture and nitrous oxide emissions, *Nature Climate Change*, 2, 410-416, 2012.
- Rochette, P., Angers, D. A., Bélanger, G., Chantigny, M. H., Prévost, D., and Lévesque, G.: Emissions of N O from Alfalfa and Soybean Crops in Eastern Canada, *Soil Science Society of America Journal*, 68, 493-506, 2004.
- Schmidt, I., van Spanning, R. J., and Jetten, M. S.: Denitrification and ammonia oxidation by *Nitrosomonas europaea* wild-type, and NirK- and NorB-deficient mutants, *Microbiology*, 150, 4107-4114, 2004.
- Smith, K. A., and Arah, J.: Losses of nitrogen by denitrification and emissions of nitrogen oxides from soils, *Proceedings-Fertiliser Society*, 1990.
- Syakila, A., and Kroeze, C.: The global nitrous oxide budget revisited, *Greenhouse Gas Measurement and Management*, 1, 17-26, 2011.
- Thompson, R. L., Ishijima, K., Saikawa, E., Corazza, M., Karstens, U., Patra, P. K., Bergamaschi, P., Chevallier, F., Dlugokencky, E., and Prinn, R. G.: TransCom N₂O model inter-comparison–Part 2: Atmospheric inversion estimates of N₂O emissions, *Atmospheric chemistry and physics*, 14, 6177-6194, 2014.
- Tian, H., Xu, X., Liu, M., Ren, W., Zhang, C., Chen, G., and Lu, C.: Spatial and temporal patterns of CH₄ and N₂O fluxes in terrestrial ecosystems of North America during 1979–2008: application of a global biogeochemistry model, *Biogeosciences*, 7, 2673-2694, 2010.
- Tian, H., Xu, X., Lu, C., Liu, M., Ren, W., Chen, G., Melillo, J., and Liu, J.: Net exchanges of CO₂, CH₄, and N₂O between China's terrestrial ecosystems and the atmosphere and their contributions to global climate warming, *Journal of Geophysical Research: Biogeosciences*, 116, 2011.
- Tian, H., Chen, G., Lu, C., Xu, X., Ren, W., Zhang, B., Banger, K., Tao, B., Pan, S., and Liu, M.: Global methane and nitrous oxide emissions from terrestrial ecosystems due to multiple environmental changes, *Ecosystem Health and Sustainability*, 1, 1-20, 2015.
- Tian, H., Lu, C., Ciais, P., Michalak, A. M., Canadell, J. G., Saikawa, E., Huntzinger, D. N., Gurney, K. R., Sitch, S., Zhang, B., Yang, J., Bousquet, P., Bruhwiler, L., Chen, G., Dlugokencky, E., Friedlingstein, P., Melillo, J., Pan, S., Poulter B., Prinn, R., Saunio, M., Schwalm, C., and Wofsy, S.: The terrestrial biosphere as a net source of greenhouse gases to the atmosphere, *Nature*, 531, 225-228, 2016.
- Vitousek, P. M., Menge, D. N., Reed, S. C., and Cleveland, C. C.: Biological nitrogen fixation: rates, patterns and ecological controls in terrestrial ecosystems, *Philosophical Transactions of the Royal Society of London B: Biological Sciences*, 368, 20130119, 2013.
- Wei, Y., Liu, S., Huntzinger, D. N., Michalak, A., Viovy, N., Post, W., Schwalm, C. R., Schaefer, K., Jacobson, A., and Lu, C.: The North American Carbon Program Multi-scale Synthesis and Terrestrial Model Intercomparison Project–Part 2: Environmental driver data, *Geoscientific Model Development*, 7, 2875-2893, 2014.

- Werner, C., Butterbach-Bahl, K., Haas, E., Hickler, T., and Kiese, R.: A global inventory of N₂O emissions from tropical rainforest soils using a detailed biogeochemical model, *Global Biogeochemical Cycles*, 21, 2007.
- Wrage, N., Velthof, G., Van Beusichem, M., and Oenema, O.: Role of nitrifier denitrification in the production of nitrous oxide, *Soil biology and Biochemistry*, 33, 1723-1732, 2001.
- Yang, Q., Tian, H., Friedrichs, M. A., Hopkinson, C. S., Lu, C., and Najjar, R. G.: Increased nitrogen export from eastern North America to the Atlantic Ocean due to climatic and anthropogenic changes during 1901–2008, *Journal of Geophysical Research: Biogeosciences*, 120, 1046-1068, 2015.
- Zhang, B., Tian, H., Lu, C., Dangal, S. R. S., Yang, J., and Pan, S.: Manure nitrogen production and application in cropland and rangeland during 1860–2014: A 5-minute gridded global data set for Earth system modeling, *Earth System Science Data*, 9, 667-678, 2017.
- Zhang, B., Tian, H., Ren, W., Tao, B., Lu, C., Yang, J., Banger, K., and Pan, S.: Methane emissions from global rice fields: Magnitude, spatiotemporal patterns, and environmental controls, *Global Biogeochemical Cycles*, 30, 1246-1263, 2016.
- Zhuang, Q., Lu, Y., and Chen, M.: An inventory of global N₂O emissions from the soils of natural terrestrial ecosystems, *Atmospheric Environment*, 47, 66-75, 2012.

Chapter 5. Global N₂O emissions from croplands driven by environmental factors and management strategies: comparison and uncertainty analysis

Abstract

Human activities have caused significant perturbations of the nitrogen (N) cycle, resulting in an ~21% increase in atmospheric N₂O concentration since the pre-industrial era. Substantial efforts have been made to quantify global and regional N₂O emissions from agricultural soils in the last three decades using a wide variety of approaches with large uncertainties. Moreover, how annual and decadal climate changes and variability affected N₂O emissions from agricultural systems is unknown. Herein, a process-based Dynamic Land Ecosystem Model (DLEM) was applied to estimate global N₂O emissions from croplands driven by environmental factors and management strategies. Total emissions increased by 180% (from 1.1±0.2 to 3.3±0.1 Tg N yr⁻¹) during 1961–2014. Fertilizer N applications accounted for ~70% of total emissions during 2000–2014. At the regional scale, Europe and North America were two leading regions for N₂O emissions in the 1960s. However, East Asia became the largest emitter amongst all regions after the 1990s. Compared with estimates based on linear and nonlinear emission factors, our results were 150% and 186% higher, respectively, at the global scale during 2000–2014. This study considered various N input sources and environmental factors to provide a time-series estimate of N₂O emissions. This information could prompt future N₂O mitigation strategies by countries with higher emission rates.

1. Introduction

The accumulation of terrestrial biogenic methane (CH_4) and nitrous oxide (N_2O) induced by anthropogenic activities has offset the cooling effect due to carbon dioxide (CO_2) uptake by plants, resulting in a net warming effect on the climate system (Tian et al., 2016). Although atmospheric N_2O content is least among the three primary greenhouse gases (GHGs), the warming effect of N_2O is 265 times higher than CO_2 at a 100-year time horizon (Myhre et al., 2013). In addition, N_2O resides in the atmosphere for 116 ± 9 years and is also a reactant that can deplete stratospheric ozone (Nevison and Holland, 1997; Prather et al., 2015). Compared to the pre-industrial era, atmospheric N_2O concentration has increased from 275 to 329 parts per billion (ppb) as of 2015 (NOAA2006A, 2016).

As of 2010, human-induced inputs of reactive nitrogen (Nr) were at least two times larger than the naturally-fixed N (Ciais et al., 2014). Reactive nitrogen creation increased from approximately 15 Tg N ($\text{Tg} = 10^{12} \text{ g}$) in 1900 to 156 Tg N in 1995, with further increase from 156 Tg N yr^{-1} in 1995 to 187 Tg N yr^{-1} in 2005 (Galloway et al., 2008). Due to rapid Nr increases (e.g., agriculture, industry, biomass burning activities), anthropogenic N_2O emissions have increased steadily and were estimated to be 6.9 (2.7 to 11.1) Tg N yr^{-1} in 2006 (Ciais et al., 2014; Reay et al., 2012). Global N_2O emissions from all sources are projected to increase from 16.5 in 2000 to 18.0 (Adapting Mosaic scenario) and 19.7 (Global Orchestration scenario) Tg N yr^{-1} in 2050 (Butterbach-Bahl et al., 2013). Among increased anthropogenic N_2O emissions, agricultural activities are the dominant source due to widespread N fertilizer and manure usage in croplands (Davidson, 2009; Reay et al., 2012; Syakila and Kroeze, 2011). Between 2001 and 2011, annual N_2O emissions from synthetic fertilizers increased by 37% based on data from FAOSTAT (Gerber et al., 2016). Tremendous efforts have been made to estimate global and regional N_2O emissions

from agricultural systems; however, the proportion of N₂O emissions associated with fertilizer remains largely uncertain (Davidson, 2009; Tian et al., 2018; Tian et al., 2019). For instance, N₂O emissions from application of N fertilizer in agriculture were reported as 1.7–4.8 Tg N yr⁻¹ in 2006 (Ciais et al., 2014). However, different estimates with large uncertainty ranges appeared in other studies (Crutzen et al., 2007; Davidson, 2009; Gerber et al., 2016; Mosier et al., 1998; Reay et al., 2012; Saikawa et al., 2014).

The large uncertainties of these estimates are associated with approaches that were used to identify and quantify globally important sources of N₂O (Davidson, 2009). The main two approaches were bottom-up (inventory, statistical extrapolation of local flux measurements, and process-based modeling) and top-down (atmospheric inversion) methodologies (Davidson and Kanter, 2014; Tian et al., 2016). For example, Tian et al. (2016) synthesized estimates of global N₂O fluxes derived from different top-down and bottom-up studies for agriculture and waste during 1981–2010. Their results indicated that estimates from bottom-up methods (4.6±0.2, 5.5±0.7 Tg N yr⁻¹) were much higher than top-down estimates (4.1±0.6, 4.4±0.6 Tg N yr⁻¹) in the 1990s and 2000s.

Emission factors (EFs), which vary in different sectors of N₂O emission sources, were developed by the Intergovernmental Panel on Climate Change (IPCC) as a common means to evaluate emissions at country scales, and were applied to develop several bottom-up inventories (e.g., Emission Database for Global Atmospheric Research (EDGAR, Olivier et al. (2002)), Global Emission Inventory Activity (GEIA, <http://www.geiacenter.org/>), and Food and Agriculture Organization of the United Nations Statistics database (FAO, <http://www.fao.org/faostat/en/#home>)). However, it should be noted that there are large uncertainties in these N₂O emission estimates when default EFs are applied at the global scale

(Crutzen et al., 2007; Davidson, 2009; Smith et al., 2012). Ground-based observations are an important approach to estimate N₂O emissions from specific sites, which could provide relatively accurate estimates for developing EFs models and validating results from process-based models (Rapson and Dacres, 2014). In addition, process-based models are essential tools in assessing and predicting feedbacks of terrestrial ecosystems related to climate change (Reynolds and Acock, 1997). Nitrous oxide is biologically produced in soils during denitrification, nitrification and nitrifier denitrification (Schmidt et al., 2004; Smith and Arah, 1990; Wrage et al., 2001); these processes are mainly driven by soil conditions, such as soil temperature, moisture content, pH, and substrate availability (mineral N and organic carbon) (Brotto et al., 2015; Butterbach-Bahl et al., 2013; Firestone and Davidson, 1989; Goldberg and Gebauer, 2009; Rowlings et al., 2015), as well as human management practices, such as synthetic N fertilizer, manure application, irrigation, and tillage (Cai et al., 1997; Ding et al., 2010; Rice and Smith, 1982). Compared to constant EFs in the IPCC methodology, process-based models are extremely necessary for their capability to study the spatiotemporal variability of N₂O emissions under changing circumstances, such as environmental factors and human management strategies in global croplands.

Previous studies were mainly focused on estimating fertilizer/manure N-induced N₂O emissions through EFs regardless of environmental factors (Gerber et al., 2016; Shcherbak et al., 2014; Yan et al., 2003), or based on statistical models (Bouwman et al., 2002a; Davidson, 2009; Zhou et al., 2015). Large uncertainties remain in understanding how annual and decadal climate changes and variabilities affected N₂O emissions from croplands at global, regional, and country scales. In this study, we applied the Dynamic Land Ecosystem Model (DLEM) to investigate long-term N₂O emissions at global and sectoral scales driven by environmental factors and human management strategies during 1961–2014. The objectives in this study were to: (1) provide a time-

series estimate of N₂O emissions from global croplands; (2) examine the spatial variability of cropland N₂O emissions during 1961–2014; (3) attribute the factorial contributions to increases in N₂O emissions; and (4) investigate uncertainties associated with various N input datasets. The global change factors evaluated in this study included climate variability, elevated atmospheric CO₂ concentration, N deposition, and fertilizer N application in croplands.

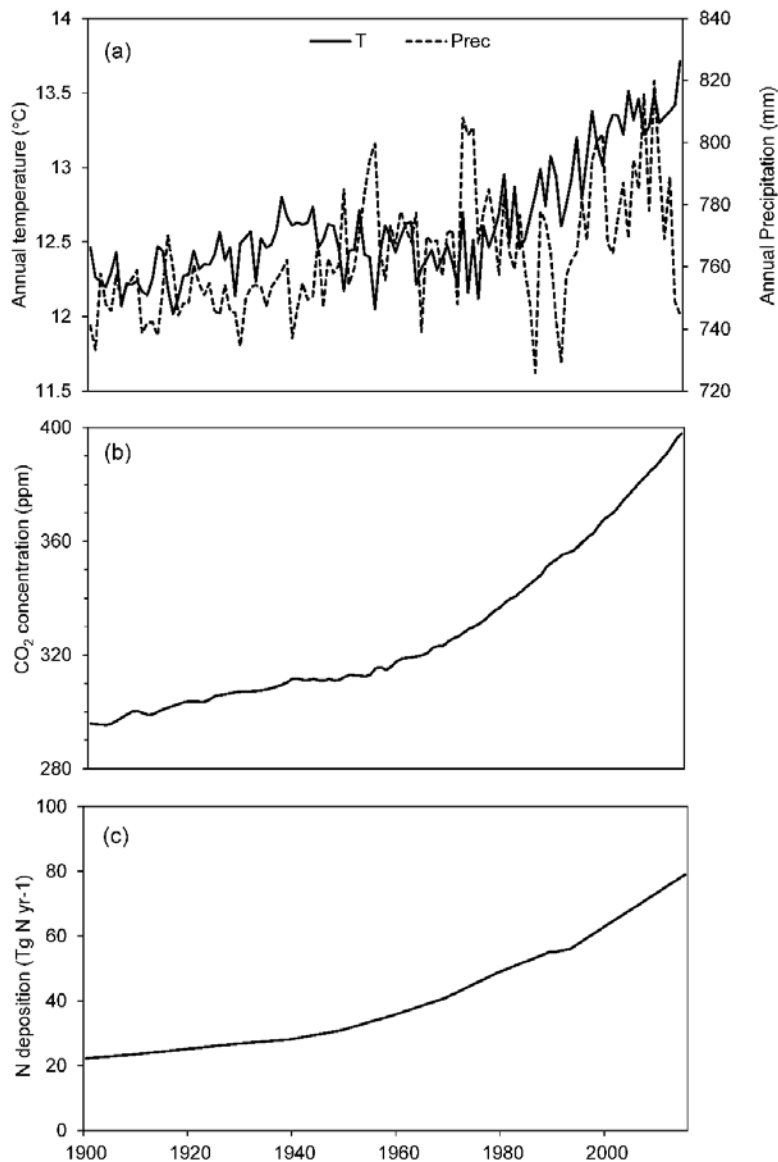


Figure 5-1. Multiple environmental changes in global croplands: (a) Annual mean temperature and precipitation; (b) Annual atmospheric CO₂ concentration; (c) Annual N deposition.

2. Material and methods

2.1. Input data

Datasets included in this study were time-series of climate, atmospheric CO₂ concentration, N deposition, fertilizer N application and the gridded cropland fraction at a spatial resolution of 0.5°.

Climate data was a fusion of the CRU and NCEP/NCAR reanalyzed data sets at the global scale between 1901 and 2014. The monthly CO₂ concentration dataset was obtained from NOAA extended GLOBALVIEW-CO₂ (<http://www.esrl.noaa.gov/gmd/ccgg/globalview/co2/>), spanning from 1900–2015. The N deposition dataset provides NH_x-N and NO_y-N deposition rate with inter-annual variations, which was obtained from the atmospheric chemistry transport model (Wei et al., 2014) and constrained by EDGAR-HYDE N emission data (van Aardenne et al., 2001). Temporal changes of environmental factors are shown in Figure 5-1. Elevation, slope and aspect were derived from global 30 arc-second elevation products (GTOPO30; <https://lta.cr.usgs.gov/GTOPO30>), and soil texture was derived from Food and Agricultural Organization (FAO) Soil Database System (Reynolds et al., 2000).

We obtained three spatially-explicit time-series datasets of agricultural N fertilizer use at a resolution of 0.5° × 0.5° from Lu and Tian (2017), Nishina et al. (2017), and Zaehle et al. (2011). Lu and Tian (2017) developed the datasets through spatializing IFA-based country-level N fertilizer consumption amount according to crop specific N fertilizer application rates, distribution of crop types, and historical cropland distribution during 1960–2013. Nishina et al. (2017) generated datasets by incorporating country-level annual total N fertilizer consumption and fraction of ammonium (and nitrate) in N fertilizer inputs from FAOSTAT during 1960–2010.

Zaehle et al. (2011) developed their dataset based on country-level annual N fertilizer use from FAOSTAT during 1961–2005. Comparisons of temporal and spatial pattern differences are described in the supplementary material (Figures 4-2, 4-3, & 4-4).

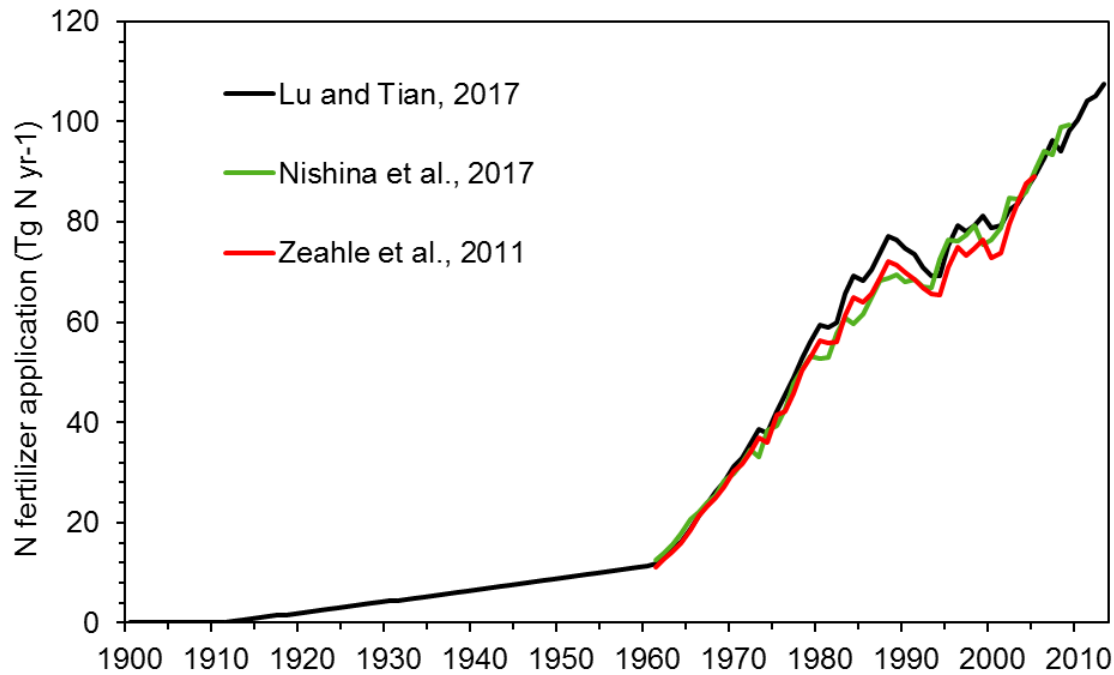


Figure 5-2. Three datasets of annual N fertilizer application amount in global croplands.

All above mentioned datasets assumed that country-level N fertilizer amounts obtained from FAOSTAT were applied to croplands rather than agricultural systems (croplands and pastures). Based on the country-scale data of N fertilizer application to pastures (Lassaletta et al., 2014a), we separated cropland N fertilizer application from pastures in these three N fertilizer datasets. Since data provided by Lassaletta et al. (2014a) was from 1960 to 2009, we assumed that there was no N fertilizer used in pastures before 1960 and that applications of N to pastures during 2010–2014 remained similar to 2009.

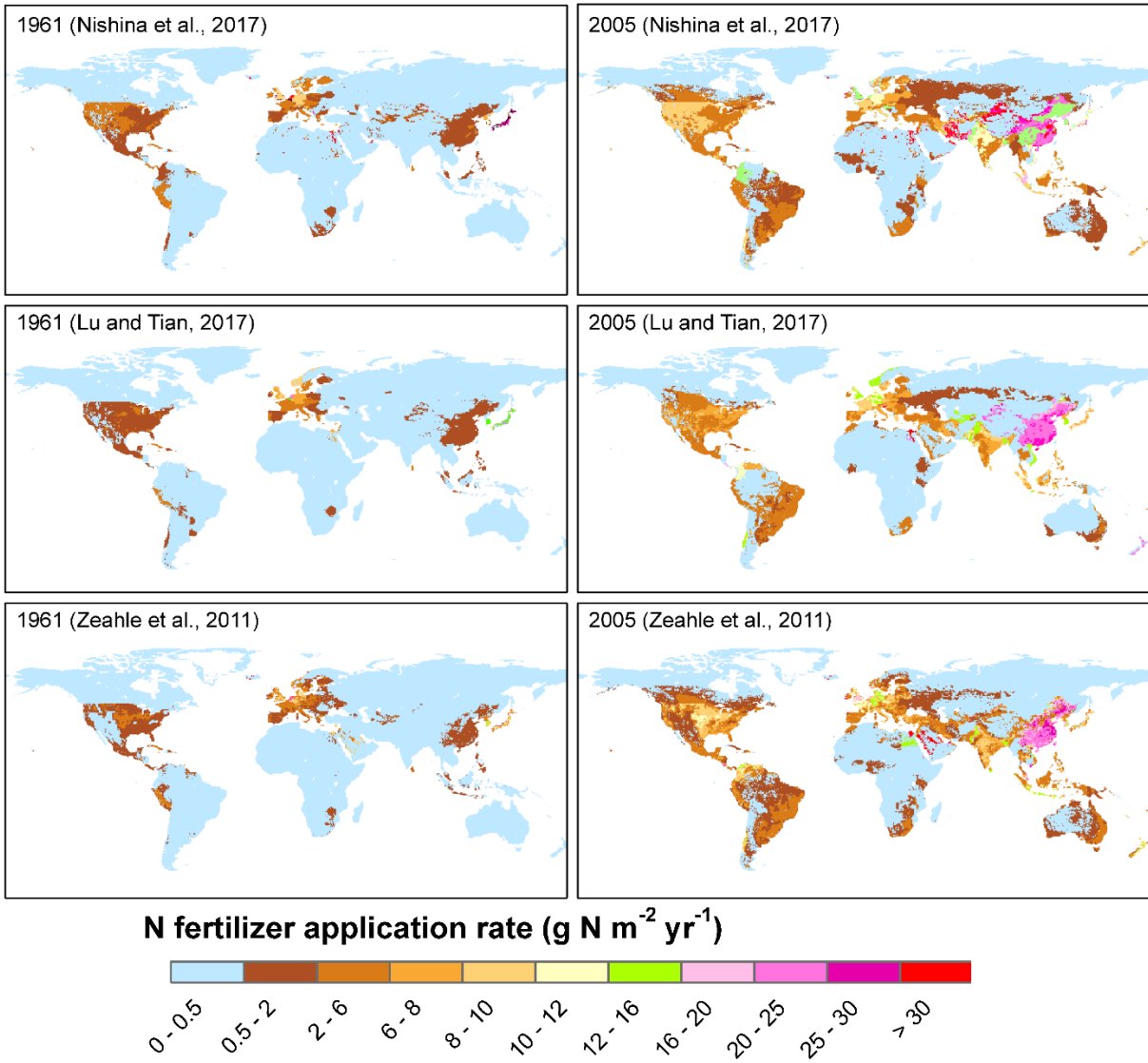


Figure 5-3. Comparison of spatial patterns of multiple fertilizer N application datasets in global croplands in 1961 and 2005.

Cropland distribution datasets (0.5° per grid) developed by aggregating the $5'$ resolution HYDE v3.2 global cropland distribution data during 1860–2016 (Klein Goldewijk et al., 2017) were used to develop gridded datasets of fertilizer N application rates in Lu and Tian (2017). The cropland distribution dataset at a resolution of $0.5^\circ \times 0.5^\circ$ used to generate N fertilizer application

rates in Nishina et al. (2017) and Zaehle et al. (2011) was obtained from the Harmonized Global Land Use map (LUHa) v 1.0 for 1860–2005 (Hurtt et al., 2011).

2.2. Experiment design

Implementation of DLEM simulations included three steps: (1) equilibrium run; (2) spin-up run; and (3) transient run. In the first stage of DLEM simulation, we applied long-term mean climate data from 1901–1920 and other datasets in 1900 as inputs (including CO₂ concentration and N deposition) to run the model to reach an equilibrium state. The equilibrium state was assumed to be reached when inner-annual variations of carbon, nitrogen, and water storage were less than 0.1 g C/m², 0.1 g N/m², and 0.1 mm, respectively, during two consecutive 50 years in each grid. After this stage, the model was spun up driven by detrended climate data (1901 to 1920) to eliminate system fluctuations due to model shifting from equilibrium to transient runs (i.e., 3 spins with 20-year climate data each time). Finally, the model was run in transient mode. At this stage, seven simulation experiments were designed to evaluate N₂O emissions under various scenarios to identify contributions of environmental factors (Table 5-1).

The DLEM simulation is from 1900–2014. However, in this study, we mainly focused on analyses of the period when N fertilizer use became widespread (i.e., 1961–2014). In the reference run (S0), all driving forces were kept at the 1900 level in to track model drift and internal fluctuations, which provided background N₂O emissions with little human perturbation. All essential datasets were considered as inputs in the all combined run (S1), which can provide N₂O emissions due to human management and changing environmental factors. In the remaining simulations (S2–S5), temporal changes of input factors were included, while one specific factor was set as the 1900 level. The difference between S1 and any simulation in S2–S5 represents the

factorial impact on N₂O emissions during 1900–2014 (Table 5-1). For example, all combined without climate change (S2), where climate data was kept constant at the 1900 level while all other factors changed. The difference between S1 and S2 represents the impact of climate change and its interactions with other environmental changes on N₂O emissions.

Table 5-1. Design of simulation experiments

Experiments	Climate	CO ₂	N deposition	N fertilizer
Reference (S0)	1900	1900	1900	1900
All Combined (S1)*	1901–2014	1900–2014	1900–2014	1900–2014
Without Climate (S2)	1900	1900–2014	1900–2014	1900–2014
Without CO ₂ (S3)	1900–2014	1900	1900–2014	1900–2014
Without N deposition (S4)	1900–2014	1900–2014	1900	1900–2014
Without N fertilizer (S5)	1900–2014	1900–2014	1900–2014	1900

* Experiments designed to study impacts of different fertilizer datasets in global croplands on N₂O emissions are included in S1 simulation: S1-1: N fertilizer use from Lu and Tian (2017); S1-2: N fertilizer use from Nishina et al. (2017); and S1-3: N fertilizer use from Zaehle et al. (2011).

3. Results

3.1. Environmental changes in global croplands during 1961–2014

In this study, simulation experiments were driven by various environmental factors including climate, atmospheric CO₂ concentration, N deposition, and N fertilizer application. The time-series climate data showed large inter-annual variations, while an overall increasing trend of annual temperature and precipitation was found during 1961–2014 (Figure 5-1a). Atmospheric CO₂ concentration increased from 319 to 398 ppm at a rate of 1.5 ppm/yr (Figure 5-1b). Compared to the year 1961, N deposition increased by approximately 10 Tg N in 2014 (Figure 5-1c). Reactive N inputs due to human activities showed a rapid increasing trend during 1961–2014.

Specifically, N fertilizer application in global croplands increased from 12 to 108 Tg N yr⁻¹ (Figure 5-2).

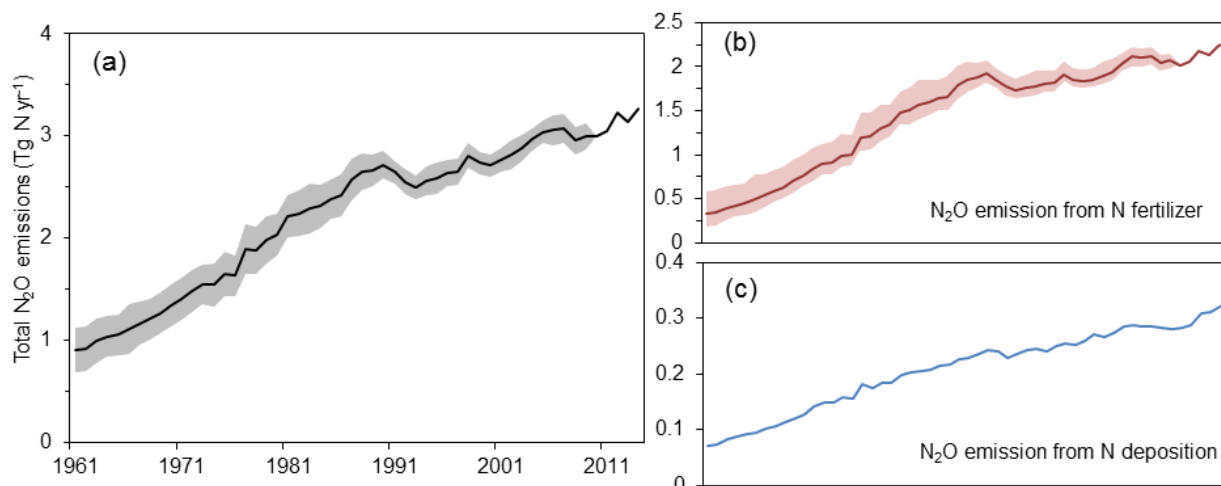


Figure 5-4. The annual N₂O emissions from global croplands during 1961–2014: (a) total emissions, (b) N fertilizer application, and (c) N deposition. The uncertainty range is ± 1 standard deviation.

3.2. Temporal patterns of N₂O emissions from global croplands during 1961–2014

Overall, N₂O emissions from global croplands showed a rapid increasing trend since 1961 (Figure 5-4). Between 2000 and 2014, N₂O emissions increased 180% compared to the 1960s. Global N₂O emissions increased from 1.1 ± 0.2 to 2.6 ± 0.1 Tg N yr⁻¹ at a rate of 0.07 Tg N yr⁻² ($R^2 = 0.99$) during 1961–1990. This was followed by a slight increase from 2.6 ± 0.14 to 3.3 ± 0.18 at a rate of 0.03 Tg N yr⁻¹ ($R^2 = 0.91$) during 1991–2014.

In this study, we divided the Earth land surface into seven parts: Africa, South America, North America, Europe, Northern Asia, Southern Asia, and Oceania. In addition, Southern Asia was portioned into five regions including South Asia, East Asia, West Asia, Central Asia, and

Southeast Asia (Figure 5-5). From a regional perspective, Europe and North America were the two leading continents for N₂O emissions, and contributed 57% of total emissions in the 1960s, followed by South America, East Asia, and South Asia. In total, East Asia and South Asia contributed less than 20% of total emissions. Nitrous oxide emissions for North America and Europe showed a slight increase between 1960 and 1989, with an obvious decrease found in Europe after the 1980s. A slight decrease was also found in Northern and Central Asia during 1980–2014. All remaining regions showed a fast-growing trend of N₂O emissions since the 1960s, especially South and East Asia. During 2000–2014, N₂O emissions in both regions accounted for 37% of total emissions, which was roughly equivalent to contributions from both North America and Europe (38%).

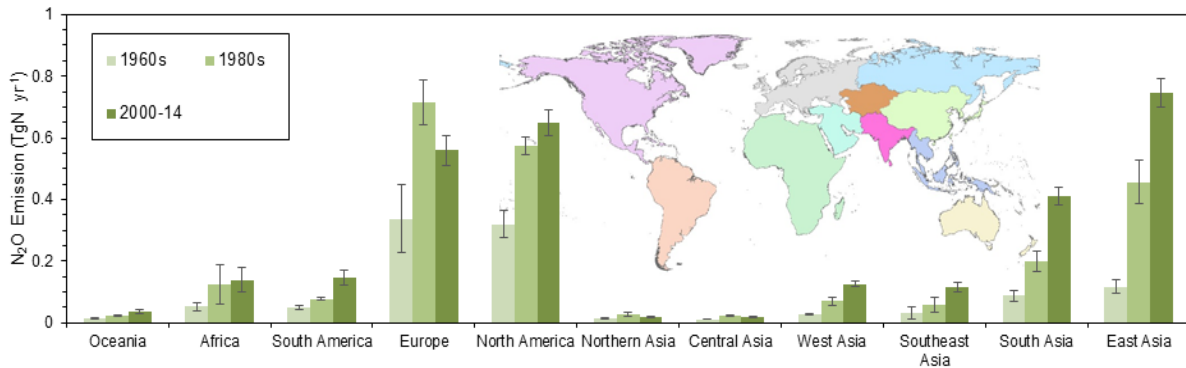


Figure 5-5. The decadal N₂O emissions at regional scales in the 1960s, 1980s, and 2000–14. We included average N₂O emissions from all sources of N inputs and the environmental factors. The uncertainty range is ± 1 standard deviation.

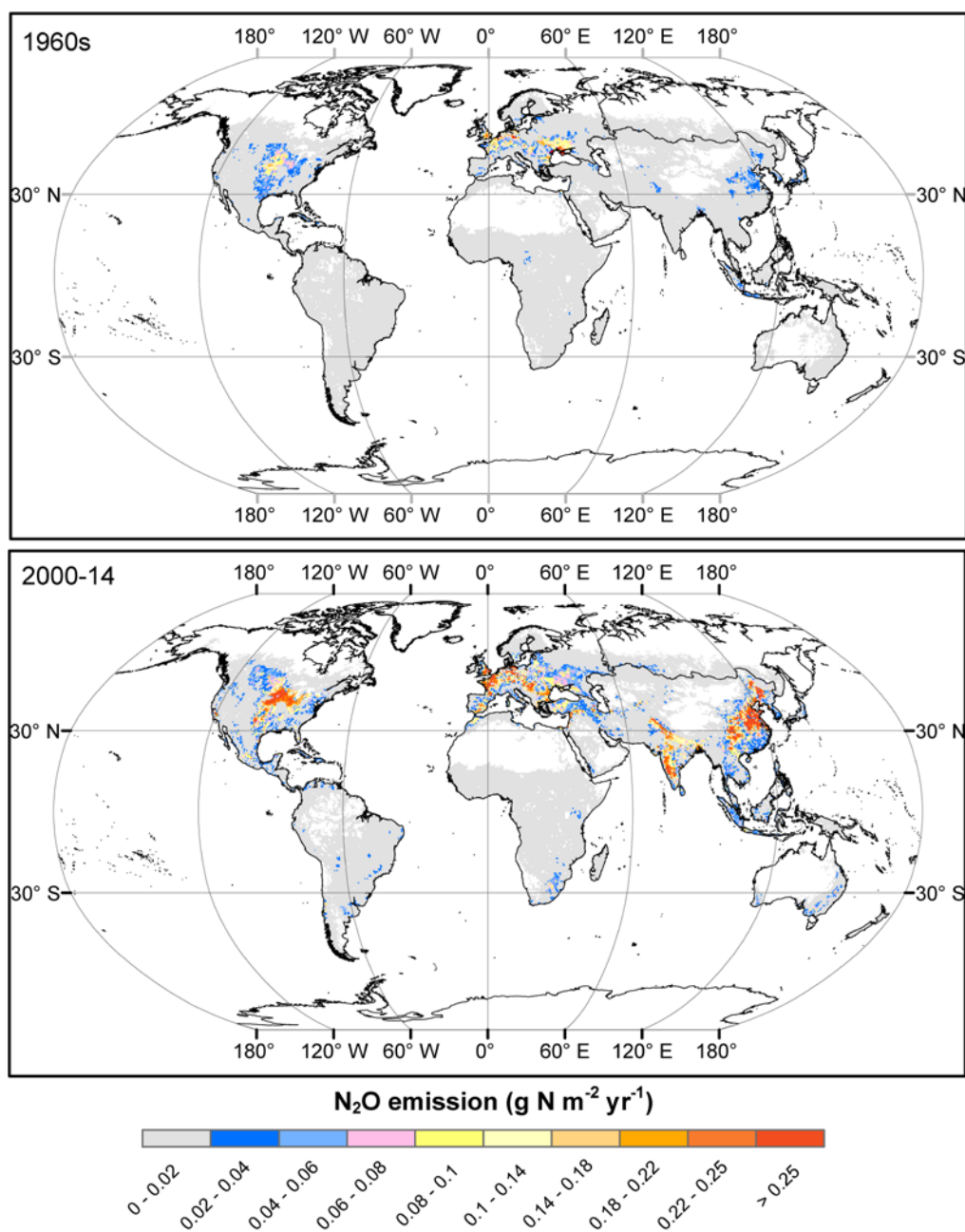


Figure 5-6. Spatial distributions of total N_2O emissions from global croplands in the 1960s and 2000–2014. We included average N_2O emissions from all sources of N inputs and the environmental factors.

3.3. Spatial patterns of N₂O emissions from global croplands during 1961–2014

The spatial pattern of N₂O emissions showed large discrepancies in the past five decades (Figure 5-6). In the 1960s, N₂O emission rates as high as 0.25 g N m⁻² yr⁻¹ were found in North America and Europe. In contrast, N₂O emission rates in most regions of East and South Asia were as low as 0.04 g N m⁻² yr⁻¹. The North China Plain and central India showed slightly higher emission rates which were still lower than 0.22 g N m⁻² yr⁻¹. Relatively higher emission rates were also found in Argentina in the 1960s. During 2000–2014, N₂O emission rates increased in most regions of the world. East and South Asia showed a large increase in N₂O emission rates (higher than 0.35 g N m⁻² yr⁻¹), and a similar increase was also noted in North America, Europe, and West Asia.

3.4. Factorial contributions of N₂O emissions from global croplands

Globally speaking, the application of N fertilizer is a dominant factor accounting for the large emission increase in the past five decades (Figure 5-7). Background emissions represent N₂O emissions from global cropland regardless of impacts induced by all factors, and were kept constant (approximately 0.4 Tg N yr⁻¹) during 1961–2014. Climate variability exerted a significant inter-annual variation in N₂O emissions, with a slightly increasing rate of 5.6 Gg N yr⁻¹ (R² = 0.72; 1 Gg = 10⁹ g) during 1961–2014. Rising atmospheric CO₂ concentration continuously accelerated N₂O emissions in global croplands, which was at an increasing rate of 9.4 Gg N yr⁻¹ (R² = 0.96). Nitrogen deposition increased at a rate of 4.4 (R² = 0.96) during 1961–2014, respectively. Nitrogen fertilizer application grew at a rate of 60.3 (R² = 0.99) and 20.9 Gg N yr⁻¹ (R² = 0.85) during 1961–1990 and 1991–2014, respectively.

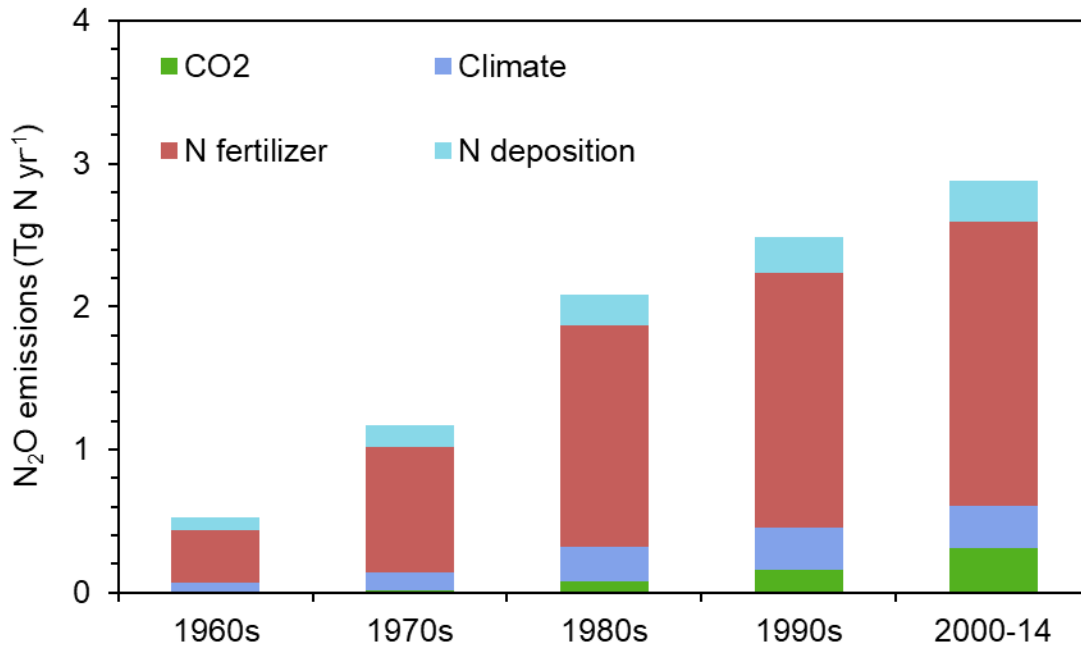


Figure 5-7. Relative contributions of environmental factors to decadal N₂O emissions from global croplands. Fertilizer use causing N₂O emissions was based on the average amounts of different synthetic N fertilizer inputs.

From the regional perspective, N₂O emissions due to N fertilizer varied significantly during 1961–2014. Southern Asia, Europe, and North America are top three regions accounted for fertilizer N-induced emissions during the past five decades. Europe and Northern Asia showed a declining trend of N₂O emissions after the 1980s, while all regions in Asia except Central Asia showed a rapid increasing trend since the 1960s. Southern Asia accounted for 51% of global total emissions during 2000–2014. East and South Asia were two dominant emitters contributing to more than 82% of total emissions in southern Asia. Compared to the 1960s, N₂O emissions in southern Asia increased by 1460% during 2000–2014 (Figure 5-8).

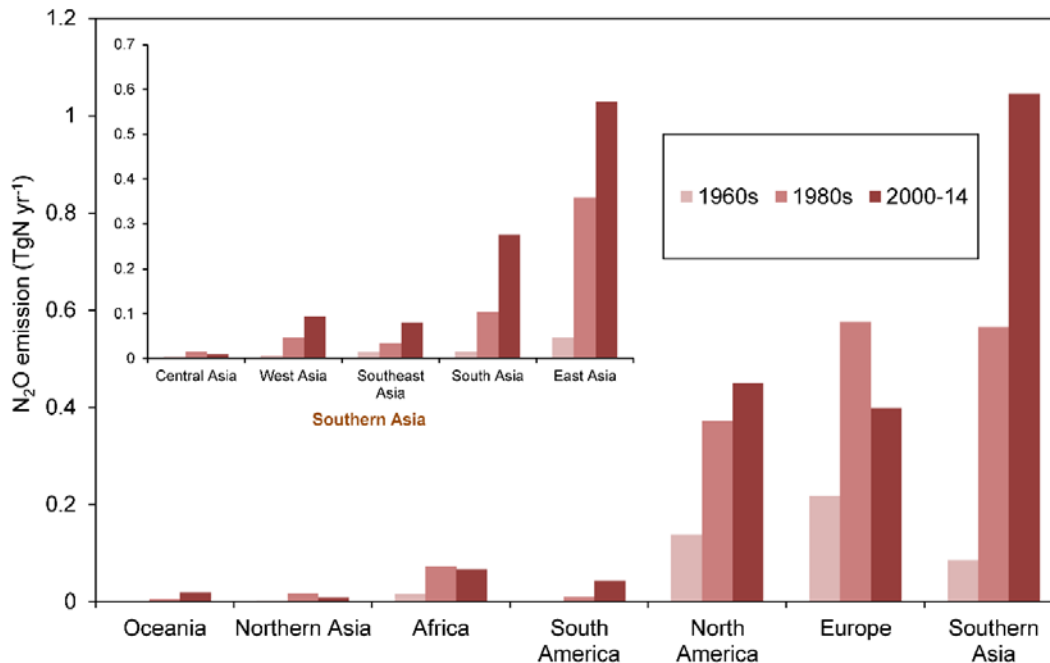


Figure 5-8. The impacts of N fertilizer use on regional N₂O emissions in the 1960s, 1980s, and 2000–14.

4. Discussion

4.1. Comparison with previous studies

Emission factors were one of the major approaches for estimating N₂O emissions from global and regional croplands in the past several decades. The EF in the IPCC Tier 1 Guideline (1% for upland soils and 0.3% for rice paddy) has been widely used. However, recent studies have argued that the IPCC approach underestimates direct emissions from global soils (Smith et al., 2012). Davidson (2009) provided a new EF for N₂O emissions from N fertilizer and manure, which was 2.5% and 2.0%, respectively, based on the entire pattern of increasing N₂O concentrations since 1860. Moreover, Smith et al. (2012) suggested that an overall EF of 4% would be better suited for use in agricultural systems. In addition, site-to-global/regional extrapolation based on field experiments was also used to estimate direct N₂O emissions from croplands. Bouwman et al.

(2002a) provided a global-scale estimate of N₂O emissions from fertilized soils using 846 measurements in agricultural fields. Later, Stehfest and Bouwman (2006) updated their previous estimate using more agricultural field observations. However, large uncertainties remained in these previous estimates.

For the global-scale comparison, Davidson (2009) estimated N₂O emissions averaging 5.0 Tg N yr⁻¹ from both N fertilizer and manure in 2005, where N fertilizer and manure accounted for 2.2 and 2.8 Tg N yr⁻¹, respectively. Since our study only considered direct soil emission from N fertilizer applications, total emissions from our study were 2.1 Tg N for 2005, which was quite similar to their estimate. Reay et al. (2012) estimated that direct emissions from global agricultural soils were 4.0, 4.1, and 4.7 Tg N in 1990, 2000, and 2010, respectively. All numbers were extracted from Reay et al. (2012) by digitizing graphs using the Getdata Graph Digitizer. In our study, modeled N₂O emissions from global agricultural soils were lesser than their estimates in corresponding years. Differences were attributable to two factors: 1) Reay et al. (2012) included direct and indirect N₂O emissions from agricultural soils, while our study only considered direct N₂O emissions; and 2) Reay et al. (2012) used values from US EPA (2011) that were based on EFs. In contrast, results from our study were from model simulations that considered environmental factors. A recent estimate of global direct N₂O emissions provided by Gerber et al. (2016) was 0.66 Tg N yr⁻¹ for N fertilizer and manure applications in 2000. In their assessment, Gerber et al. (2016) applied super-linear crop-specific EFs, while the average EFs for major countries or crops were less than 1%. Our estimate of N₂O emissions from N fertilizer in 2000 was 1.8±0.1 Tg N yr⁻¹, which was three-fold higher than their estimates. The higher estimate in our study was due to higher N fertilizer in global croplands. Moreover, we applied a process-based

model and calibrated site-level N₂O emission for major crops worldwide that included different levels of N fertilizer application.

4.2. Comparison of results from process-based model with EFs

In the IPCC Tier 1 Guideline, EF values (0.3% for paddy rice, 1% for all other crops) were assumed to remain constant across all countries across the globe. Shcherbak et al. (2014) found a nonlinear response of N₂O emissions to N additions in most crops. Gerber et al. (2016) applied linear (0.89%) and nonlinear EFs (0.77%) to compare fertilizer and manure N-induced N₂O emissions at global, country, and crop-type scales in 2000. Based on linear and nonlinear EFs provided in Gerber et al. (2016) and three N fertilizer application datasets, global emissions were calculated as 0.8 and 0.7 Tg N, respectively, during 2000–2014. In contrast, our study found that the effect of N fertilizer on N₂O emissions was 2.0 ± 0.1 Tg N yr⁻¹ over the same period, which was nearly three times higher than estimates by EFs.

However, recent studies including field experiments and meta-analysis indicated that EFs were varying because of N additions, cultivation practice, and environmental conditions (Grace et al., 2011; Saikawa et al., 2014; Zhou et al., 2015). Zhou et al. (2017) found that manure application could significantly increase N₂O emissions compared to application of mineral fertilizer alone. The proposed EF in their study was 1.87% for upland soils and 0.24% for paddy rice soils, while the EF was set as 0.3% for flooded rice fields and 1% for the rest crops in the context of all types of N additions in IPCC Tier 1 guidelines (Zhou et al., 2017). In contrast, Davidson (2009) suggested that N fertilizer and manure could convert 2.5% and 2% to respective N₂O emissions between 1860–2005. Thus, a large uncertainty remains inherent to EF methodology. Through comparisons to the aforementioned studies, total emissions in this study were higher than the EF

methodology, and could serve as the upper boundary in assessing impacts of N fertilizer and manure on N₂O emissions.

4.3. Contributions of multiple environmental changes to N₂O emissions

When studying fertilizer N-induced N₂O emissions from croplands, impacts from environmental factors and human management practices must be considered (Gerber et al., 2016; Stehfest and Bouwman, 2006) since these factors can impact soil conditions and processes that control N₂O emissions (Bouwman et al., 2002a). The inter-annual variability of terrestrial N₂O flux is driven by climate and terrestrial net CO₂ fluxes (Zaehle et al., 2011). Environmental factors included in this study had a positive impact on N₂O emissions, but with different magnitudes. A quantitative assessment that synthesized the effect of elevated CO₂ on GHGs emissions found that increased concentrations of atmospheric CO₂ stimulated N₂O emissions by 18.8% (van Groenigen et al., 2011). Our study found that the impact of CO₂ on N₂O emissions was 0.31 Tg N yr⁻¹ during 2000–2014 (increasing rate of 9.4 Gg N yr⁻¹ ($R^2 = 0.96$) since 1961), which was significantly correlated with the accelerating increase of atmospheric CO₂ concentration. This impact contributed to almost a 10% increase in N₂O emissions over the contemporary period. In the context of global warming, the benefit of carbon sequestration in terrestrial ecosystems has been offset by the increase of Nr inputs (Tian et al., 2016; Zaehle et al., 2011). The effects of climatic variability and change caused an increase of 0.3 Tg N yr⁻¹ in the terrestrial ecosystem (Zaehle et al., 2011), which was similar to the climate effect on N₂O emissions in our study. Previous studies have shown that N deposition could degrade aquatic ecosystems and human health, and increase GHGs emissions (Goulding et al., 1998; Liu et al., 2013; Lu et al., 2012; Xu et al., 2012). In our study, N deposition accounted for 8% of N₂O emissions over the contemporary period. Overall, elevated CO₂, N deposition, and climate had positive impacts on N₂O emissions in global

croplands during the past five decades. Merely applying an empirical EF may not catch the inter-annual variability of N₂O emissions since EFs do not account for N₂O production and diffusion processes in soils.

4.4. Uncertainties and future work

Due to the different land use datasets and methodologies used to generate these three datasets (Lu and Tian, 2017; Nishina et al., 2017; Zaehle et al., 2011), spatial variations in N fertilizer use rates were significant (Figure 5-3). Concentrations of ammonium (NH₄⁺) and nitrate (NO₃⁻) are significant factors that affect N₂O production in agricultural soils since they are necessary substrates for activities of denitrifiers and nitrifiers. The ratio of NH₄⁺ to NO₃⁻ varied with different N fertilizer types. In DLEM simulations, this ratio was set constant when the N fertilizer was applied to croplands. In contrast, Nishina et al. (2017) generated N fertilizer application datasets during 1961–2010 and indicated that the NH₄⁺/NO₃⁻ ratio increased as urea consumption increased over the study period. Simulation results using their datasets were generally higher than results driven by N fertilizer datasets from Lu and Tian (2017) and Zaehle et al. (2011). Thus, data harmonization of existing datasets of N fertilizer application rates may be a better approach to reduce N₂O emission uncertainties due to fertilizer N inputs.

In DLEM simulations, uncertainties associated with five key parameters (i.e., maximum nitrification and denitrification rates, N fixation rate, and adsorption coefficients for soil NH₄⁺ and NO₃⁻) that dominated N₂O production and fluxes in pre-industrial soils were described and quantified in Xu et al. (2017). However, these factors were not considered in long-term runs of our model. Thus, our future work with DLEM simulations should account for key parameters that affect N₂O flux calculations and different sets of input data. In addition, soil condition (specifically soil water, oxygen, and pH) is a key factor that regulates the production and diffusion of N₂O in

soils (Bouwman et al., 2002a). Therefore, future work should also simulate cropland N₂O emissions through use of multiple sets of climate and irrigation data.

An important missing aspect when studying N₂O emission centers on indirect emissions associated with agricultural N inputs. For 2006, global indirect emissions due to agricultural activities based on 1996 and 2006 IPCC Guidelines estimated by Mosier et al. (1998) and Syakila and Kroeze (2011) were 2.6 and 1.3 Tg N, respectively. By examining indirect N₂O emissions from US corn belt streams, Turner et al. (2015) found that indirect EF in the IPCC Tier 1 Guideline underestimated total emissions by 40%. However, this newer study noted that previous work overestimated indirect emissions, which should be 29.6–35.3 Gg N yr⁻¹. In order to comprehensively estimate all sources of N₂O emissions attributable to agricultural activities, a process-based model is needed to simulate indirect N₂O emissions from riverine systems within/beside global croplands.

5. Conclusions

The globally increasing food demand has boosted N₂O emissions to the atmosphere due to intensive inorganic/organic agricultural N inputs by humans. A robust estimate of N₂O emissions from global croplands is vital for assessing environmental and human health impacts. Global N₂O emissions from agricultural systems showed an overall increasing trend with a rate of 56 Gg N yr⁻¹ while its spatial pattern displayed large discrepancies from 1961 to 2014. Although North America was a leading emitter in the 1960s (0.32 Tg N yr⁻¹), this value has been surpassed by southern Asia since the 1980s. During 2000–2014, the highest emission amongst all regions was 1.4 Tg N yr⁻¹ in southern Asia. Nitrogen fertilizer application was the major factor accounting for this substantial increase. Globally speaking, N₂O emissions due to N fertilizer application averagely increased from 0.3 to 2.3 Tg N yr⁻¹ during 1961–2014. In addition, elevated CO₂, N

deposition, and climate change caused increased N₂O emissions of different magnitudes. Our study revealed that anthropogenic activities are responsible for this rapid increase of N₂O emissions to the atmosphere. Effective strategies within agricultural systems should be implemented to help mitigate any future climatic change.

References

- Berdanier, A. B. and Conant, R. T.: Regionally differentiated estimates of cropland N₂O emissions reduce uncertainty in global calculations, *Global change biology*, 18, 928-935, 2012.
- Bouwman, A., Boumans, L., and Batjes, N.: Emissions of N₂O and NO from fertilized fields: Summary of available measurement data, *Global Biogeochemical Cycles*, 16, 2002.
- Bouwman, A., Goldewijk, K. K., Van Der Hoek, K. W., Beusen, A. H., Van Vuuren, D. P., Willems, J., Rufino, M. C., and Stehfest, E.: Exploring global changes in nitrogen and phosphorus cycles in agriculture induced by livestock production over the 1900–2050 period, *Proceedings of the National Academy of Sciences*, 110, 20882-20887, 2013.
- Brotto, A. C., Li, H., Dumit, M., Gabarró, J., Colprim, J., Murthy, S., and Chandran, K.: Characterization and mitigation of nitrous oxide (N₂O) emissions from partial and full-nitrification BNR processes based on post-anoxic aeration control, *Biotechnology and bioengineering*, 112, 2241-2247, 2015.
- Butterbach-Bahl, K., Baggs, E. M., Dannenmann, M., Kiese, R., and Zechmeister-Boltenstern, S.: Nitrous oxide emissions from soils: how well do we understand the processes and their controls?, *Phil. Trans. R. Soc. B*, 368, 20130122, 2013.
- Cai, Z., Xing, G., Yan, X., Xu, H., Tsuruta, H., Yagi, K., and Minami, K.: Methane and nitrous oxide emissions from rice paddy fields as affected by nitrogen fertilisers and water management, *Plant and Soil*, 196, 7-14, 1997.
- Ciais, P., Sabine, C., Bala, G., Bopp, L., Brovkin, V., Canadell, J., Chhabra, A., DeFries, R., Galloway, J., Heimann, M., Jones, C., Le Quere, C., Myneni, R., Piao, S., Thornton, P., Heinze, C., Tans, P., and Vesala, T.: Carbon and other biogeochemical cycles. In: *Climate Change 2013: The Physical Science Basis. Contribution of Working Group I to the Fifth Assessment Report of the Intergovernmental Panel on Climate Change*, Cambridge University Press, 2014.
- Crutzen, P. J., Mosier, A. R., Smith, K. A., and Winiwarter, W.: N₂O release from agro-biofuel production negates global warming reduction by replacing fossil fuels. In: Paul J. Crutzen: A Pioneer on Atmospheric Chemistry and Climate Change in the Anthropocene, Springer International Publishing, 2007.
- Davidson, E. A.: The contribution of manure and fertilizer nitrogen to atmospheric nitrous oxide since 1860, *Nature Geoscience*, 2, 659-662, 2009.
- Davidson, E. A. and Kanter, D.: Inventories and scenarios of nitrous oxide emissions, *Environmental Research Letters*, 9, 105012, 2014.
- Del Grosso, S. J., Wirth, T., Ogle, S. M., and Parton, W. J.: Estimating agricultural nitrous oxide emissions, *EOS, Transactions American Geophysical Union*, 89, 529-529, 2008.
- Ding, W., Yagi, K., Cai, Z., and Han, F.: Impact of long-term application of fertilizers on N₂O and NO production potential in an intensively cultivated sandy loam soil, *Water, Air, & Soil Pollution*, 212, 141-153, 2010.
- Firestone, M. K. and Davidson, E. A.: Microbiological basis of NO and N₂O production and consumption in soil, *Exchange of trace gases between terrestrial ecosystems and the atmosphere*, 47, 7-21, 1989.
- Galloway, J. N., Townsend, A. R., Erismann, J. W., Bekunda, M., Cai, Z., Freney, J. R., Martinelli, L. A., Seitzinger, S. P., and Sutton, M. A.: Transformation of the nitrogen cycle: recent trends, questions, and potential solutions, *Science*, 320, 889-892, 2008.

- Gerber, J. S., Carlson, K. M., Makowski, D., Mueller, N. D., Garcia de Cortazar-Atauri, I., Havlík, P., Herrero, M., Launay, M., O'Connell, C. S., and Smith, P.: Spatially explicit estimates of N₂O emissions from croplands suggest climate mitigation opportunities from improved fertilizer management, *Global change biology*, 2016. 2016.
- Goldberg, S. D. and Gebauer, G.: Drought turns a Central European Norway spruce forest soil from an N₂O source to a transient N₂O sink, *Global Change Biology*, 15, 850-860, 2009.
- Goulding, K., Bailey, N., Bradbury, N., Hargreaves, P., Howe, M., Murphy, D., Poulton, P., and Willison, T.: Nitrogen deposition and its contribution to nitrogen cycling and associated soil processes, *New Phytologist*, 139, 49-58, 1998.
- Grace, P. R., Robertson, G. P., Millar, N., Colunga-Garcia, M., Basso, B., Gage, S. H., and Hoben, J.: The contribution of maize cropping in the Midwest USA to global warming: A regional estimate, *Agricultural Systems*, 104, 292-296, 2011.
- Heffer, P.: Assessment of fertilizer use by crop at the global level, International Fertilizer Industry Association, Paris, www.fertilizer.org/ifa/Home-Page/LIBRARY/Publication-database.html/Assessment-of-Fertilizer-Use-by-Crop-at-the-Global-Level-2006-07-2007-08.html2, 2013. 2013.
- Herrero, M., Havlík, P., Valin, H., Notenbaert, A., Rufino, M. C., Thornton, P. K., Blümmel, M., Weiss, F., Grace, D., and Obersteiner, M.: Biomass use, production, feed efficiencies, and greenhouse gas emissions from global livestock systems, *Proceedings of the National Academy of Sciences*, 110, 20888-20893, 2013.
- Hurt, G., Chini, L. P., Frohling, S., Betts, R., Feddema, J., Fischer, G., Fisk, J., Hibbard, K., Houghton, R., and Janetos, A.: Harmonization of land-use scenarios for the period 1500–2100: 600 years of global gridded annual land-use transitions, wood harvest, and resulting secondary lands, *Climatic Change*, 109, 117-161, 2011.
- Klein Goldewijk, K., Beusen, A., Doelman, J., and Stehfest, E.: Anthropogenic land use estimates for the Holocene–HYDE 3.2, *Earth System Science Data*, 9, 927, 2017.
- Lassaletta, L., Billen, G., Grizzetti, B., Anglade, J., and Garnier, J.: 50 year trends in nitrogen use efficiency of world cropping systems: the relationship between yield and nitrogen input to cropland, *Environmental Research Letters*, 9, 105011, 2014.
- Liu, J., You, L., Amini, M., Obersteiner, M., Herrero, M., Zehnder, A. J., and Yang, H.: A high-resolution assessment on global nitrogen flows in cropland, *Proceedings of the National Academy of Sciences*, 107, 8035-8040, 2010.
- Liu, X., Zhang, Y., Han, W., Tang, A., Shen, J., Cui, Z., Vitousek, P., Erisman, J. W., Goulding, K., and Christie, P.: Enhanced nitrogen deposition over China, *Nature*, 494, 459-462, 2013.
- Lu, C. and Tian, H.: Global nitrogen and phosphorus fertilizer use for agriculture production in the past half century: shifted hot spots and nutrient imbalance, *Earth System Science Data*, 9, 181, 2017.
- Lu, C., Tian, H., Liu, M., Ren, W., Xu, X., Chen, G., and Zhang, C.: Effect of nitrogen deposition on China's terrestrial carbon uptake in the context of multifactor environmental changes, *Ecological Applications*, 22, 53-75, 2012.
- Mosier, A., Kroeze, C., Nevison, C., Oenema, O., Seitzinger, S., and Van Cleemput, O.: Closing the global N₂O budget: nitrous oxide emissions through the agricultural nitrogen cycle, *Nutrient cycling in Agroecosystems*, 52, 225-248, 1998.
- Mueller, N. D., Gerber, J. S., Johnston, M., Ray, D. K., Ramankutty, N., and Foley, J. A.: Closing yield gaps through nutrient and water management, *Nature*, 490, 254, 2012.

- Myhre, G., Shindell, D., Bréon, F., Collins, W., Fuglestedt, J., Huang, J., Koch, D., Lamarque, J., Lee, D., and Mendoza, B.: Anthropogenic and natural radiative forcing, *Climate change*, 423, 2013.
- Nevison, C. and Holland, E.: A reexamination of the impact of anthropogenically fixed nitrogen on atmospheric N₂O and the stratospheric O₃ layer, *Journal of Geophysical Research: Atmospheres*, 102, 25519-25536, 1997.
- Nishina, K., Ito, A., Hanasaki, N., and Hayashi, S.: Reconstruction of spatially detailed global map of NH₄⁺ and NO₃⁻ application in synthetic nitrogen fertilizer, *Earth System Science Data*, 9, 149, 2017.
- Olivier, J. G., Jm, B., Peters, J. A., Bakker, J., Visschedijk, A. J., and Bloos, J. J.: Applications of EDGAR emission database for global atmospheric research, 2002. 2002.
- Potter, P., Ramankutty, N., Bennett, E. M., and Donner, S. D.: Characterizing the spatial patterns of global fertilizer application and manure production, *Earth Interactions*, 14, 1-22, 2010.
- Prather, M. J., Hsu, J., DeLuca, N. M., Jackman, C. H., Oman, L. D., Douglass, A. R., Fleming, E. L., Strahan, S. E., Steenrod, S. D., and Søvde, O. A.: Measuring and modeling the lifetime of nitrous oxide including its variability, *Journal of Geophysical Research: Atmospheres*, 120, 5693-5705, 2015.
- Rapson, T. D. and Dacres, H.: Analytical techniques for measuring nitrous oxide, *TrAC Trends in Analytical Chemistry*, 54, 65-74, 2014.
- Reay, D. S., Davidson, E. A., Smith, K. A., Smith, P., Melillo, J. M., Dentener, F., and Crutzen, P. J.: Global agriculture and nitrous oxide emissions, *Nature Climate Change*, 2, 410-416, 2012.
- Reynolds, C., Jackson, T., and Rawls, W.: Estimating soil water-holding capacities by linking the Food and Agriculture Organization soil map of the world with global pedon databases and continuous pedotransfer functions, *Water Resources Research*, 36, 3653-3662, 2000.
- Reynolds, J. F. and Acock, B.: Modularity and genericness in plant and ecosystem models, *Ecological Modelling*, 94, 7-16, 1997.
- Rice, C. W. and Smith, M. S.: Denitrification in no-till and plowed soils, *Soil Science Society of America Journal*, 46, 1168-1173, 1982.
- Rowlings, D., Grace, P., Scheer, C., and Liu, S.: Rainfall variability drives interannual variation in N₂O emissions from a humid, subtropical pasture, *Science of The Total Environment*, 512, 8-18, 2015.
- Saikawa, E., Prinn, R., Dlugokencky, E., Ishijima, K., Dutton, G., Hall, B., Langenfelds, R., Tohjima, Y., Machida, T., and Manizza, M.: Global and regional emissions estimates for N₂O, *Atmospheric Chemistry and Physics*, 14, 4617-4641, 2014.
- Schmidt, I., van Spanning, R. J., and Jetten, M. S.: Denitrification and ammonia oxidation by *Nitrosomonas europaea* wild-type, and NirK- and NorB-deficient mutants, *Microbiology*, 150, 4107-4114, 2004.
- Shcherbak, I., Millar, N., and Robertson, G. P.: Global metaanalysis of the nonlinear response of soil nitrous oxide (N₂O) emissions to fertilizer nitrogen, *Proceedings of the National Academy of Sciences*, 111, 9199-9204, 2014.
- Smil, V.: Nitrogen in crop production: An account of global flows, *Global Biogeochemical Cycles*, 13, 647-662, 1999.
- Smith, K. A. and Arah, J.: Losses of nitrogen by denitrification and emissions of nitrogen oxides from soils, *Proceedings-Fertiliser Society*, 1990. 1990.

- Smith, K. A., Mosier, A. R., Crutzen, P. J., and Winiwarter, W.: The role of N₂O derived from crop-based biofuels, and from agriculture in general, in Earth's climate, *Philosophical Transactions of the Royal Society of London B: Biological Sciences*, 367, 1169-1174, 2012.
- Stehfest, E. and Bouwman, L.: N₂O and NO emission from agricultural fields and soils under natural vegetation: summarizing available measurement data and modeling of global annual emissions, *Nutrient Cycling in Agroecosystems*, 74, 207-228, 2006.
- Syakila, A. and Kroeze, C.: The global nitrous oxide budget revisited, *Greenhouse Gas Measurement and Management*, 1, 17-26, 2011.
- Tian, H., Lu, C., Ciais, P., Michalak, A. M., Canadell, J. G., Saikawa, E., Huntzinger, D. N., Gurney, K. R., Sitch, S., Zhang, B., Yang, J., Bousquet, P., Bruhwiler, L., Chen, G., Dlugokencky, E., Friedlingstein, P., Melillo, J., Pan, S., Poulter B., Prinn, R., Saunio, M., Schwalm, C., and Wofsy, S.: The terrestrial biosphere as a net source of greenhouse gases to the atmosphere, *Nature*, 531, 225-228, 2016.
- Tian, H., Yang, J., Lu, C., Xu, R., Canadell, J. G., Jackson, R., Arneeth, A., Chang, J., Chen, G., and Ciais, P.: The global N₂O Model Intercomparison Project (NMIP): Objectives, Simulation Protocol and Expected Products, *Bulletin of the American Meteorological Society*, 1231-1251, 2018.
- Tian, H., Yang, J., Xu, R., Lu, C., Canadell, J. G., Davidson, E. A., Jackson, R. B., Arneeth, A., Chang, J., and Ciais, P.: Global soil nitrous oxide emissions since the preindustrial era estimated by an ensemble of terrestrial biosphere models: Magnitude, attribution, and uncertainty, *Global Change Biology*, 25, 640-659, 2019.
- Turner, K. H., Wessel, A. K., Palmer, G. C., Murray, J. L., and Whiteley, M.: Essential genome of *Pseudomonas aeruginosa* in cystic fibrosis sputum, *Proceedings of the National Academy of Sciences*, 112, 4110-4115, 2015.
- van Aardenne, J., Dentener, F., Olivier, J., Goldewijk, C. K., and Lelieveld, J.: A 1×1 resolution data set of historical anthropogenic trace gas emissions for the period 1890–1990, *Global Biogeochemical Cycles*, 15, 909-928, 2001.
- van Groenigen, K. J., Osenberg, C. W., and Hungate, B. A.: Increased soil emissions of potent greenhouse gases under increased atmospheric CO₂, *Nature*, 475, 214-216, 2011.
- Wei, Y., Liu, S., Huntzinger, D. N., Michalak, A., Viovy, N., Post, W., Schwalm, C. R., Schaefer, K., Jacobson, A., and Lu, C.: The North American Carbon Program Multi-scale Synthesis and Terrestrial Model Intercomparison Project–Part 2: Environmental driver data, *Geoscientific Model Development*, 7, 2875-2893, 2014.
- Wrage, N., Velthof, G., Van Beusichem, M., and Oenema, O.: Role of nitrifier denitrification in the production of nitrous oxide, *Soil biology and Biochemistry*, 33, 1723-1732, 2001.
- Xu, R., Tian, H., Lu, C., Pan, S., Chen, J., Yang, J., and Bowen, Z.: Preindustrial nitrous oxide emissions from the land biosphere estimated by using a global biogeochemistry model, *Climate of the Past*, 13, 977-990, 2017.
- Xu, R., Tian, H., Pan, S., Dangal, S. R., Chen, J., Chang, J., Lu, Y., Skiba, U. M., Tubiello, F. N., and Zhang, B.: Increased nitrogen enrichment and shifted patterns in the world's grassland: 1860–2016, *Earth System Science Data*, 11, 175-187, 2019.
- Xu, X., Tian, H., Chen, G., Liu, M., Ren, W., Lu, C., and Zhang, C.: Multifactor controls on terrestrial N₂O flux over North America from 1979 through 2010, *Biogeosciences*, 9, 1351-1366, 2012.

- Yan, X., Akimoto, H., and Ohara, T.: Estimation of nitrous oxide, nitric oxide and ammonia emissions from croplands in East, Southeast and South Asia, *Global Change Biology*, 9, 1080-1096, 2003.
- Zaehle, S., Ciais, P., Friend, A. D., and Prieur, V.: Carbon benefits of anthropogenic reactive nitrogen offset by nitrous oxide emissions, *Nature Geoscience*, 4, 601-605, 2011.
- Zhang, B., Tian, H., Lu, C., Dangal, S. R., Yang, J., and Pan, S.: Global manure nitrogen production and application in cropland during 1860–2014: a 5 arcmin gridded global dataset for Earth system modeling, *Earth System Science Data*, 9, 667-678, 2017.
- Zhou, F., Shang, Z., Zeng, Z., Piao, S., Ciais, P., Raymond, P. A., Wang, X., Wang, R., Chen, M., and Yang, C.: New model for capturing the variations of fertilizer-induced emission factors of N₂O, *Global Biogeochemical Cycles*, 29, 885-897, 2015.
- Zhou, M., Zhu, B., Wang, S., Zhu, X., Vereecken, H., and Brüggemann, N.: Stimulation of N₂O emission by manure application to agricultural soils may largely offset carbon benefits: a global meta-analysis, *Global Change Biology*, 23, 4068-4083, 2017.

Chapter 6. Half-century ammonia emissions from agricultural systems in southern Asia: Magnitude, spatiotemporal patterns and implications for human health

Abstract

Much concern has been raised about the increasing threat to air quality and human health due to ammonia (NH_3) emissions from agricultural systems, which is associated with the enrichment of reactive nitrogen (N) in southern Asia (SA), home of more than 60% the world's population (i.e. the people of West, Central, East, South, and Southeast Asia). Southern Asia consumed more than half of the global synthetic N fertilizer and was the dominant region for livestock waste production since 2004. Excessive N application could lead to a rapid increase of NH_3 in the atmosphere, resulting in severe air and water pollution in this region. However, there is still a lack of accurate estimates of NH_3 emissions from agricultural systems. In this study, we simulated the agricultural NH_3 fluxes in SA by coupling the Bi-directional NH_3 exchange module (Bi- NH_3) from the Community Multi-scale Air Quality (CMAQ) model with the Dynamic Land Ecosystem Model (DLEM). Our results indicated that NH_3 emissions were $21.3 \pm 3.9 \text{ Tg N yr}^{-1}$ from SA agricultural systems with a rapidly increasing rate of $\sim 0.3 \text{ Tg N yr}^{-2}$ during 1961–2014. Among the emission sources, $10.8 \text{ Tg N yr}^{-1}$ was released from synthetic N fertilizer use, and $10.4 \pm 3.9 \text{ Tg N yr}^{-1}$ was released from manure production in 2014. Ammonia emissions from China and India together accounted for 64% of the total amount in SA during 2000–2014. Our results imply that the increased NH_3 emissions associated with high N inputs to croplands would likely

be a significant threat to the environment and human health unless mitigation efforts are applied to reduce these emissions.

Plain Language Summary

Farming practices in southern Asia (SA), including synthetic fertilizer and manure application, have resulted in the emission of tremendous amounts of ammonia, an atmospheric constituent that has been linked to human respiratory and cardiovascular ailments, and also to atmospheric haze. Ammonia emission is expected to increase due to population growth and increased demand for animal products. Ammonia emission is a critically important environmental issue that needs to be addressed collaboratively by farmers and policy-makers in the SA region.

1. Introduction

Anthropogenic perturbation of the global nitrogen (N) cycle has contributed approximately two-thirds of the annual flux of reactive N (Nr) into the atmosphere in the early 21st century (Fowler et al., 2015; Galloway et al., 2004). This substantial enrichment of Nr is mainly caused by combustion, industrial ammonia (NH₃) production (by the Haber-Bosch process), and leguminous crop cultivation (Erisman et al., 2008; Fowler et al., 2015). Ammonia, as one of the major forms of Nr loss from agricultural soils, has produced adverse impacts on the environment and human health. High N fertilizer use and production of livestock wastes have resulted in a substantial increment of NH₃ in the atmosphere (Sutton et al., 2013; Yan et al., 2003). Ammonia is one of the key precursors for aerosol formation in the atmosphere and has caused severe air pollution in East and South Asia, which could have adverse effects on human respiratory and cardiovascular systems and might contribute to visibility reduction and regional haze (Pinder et al., 2007; Seinfeld and Pandis, 1998). For example, the NH₃-induced secondary inorganic aerosol was found as a main contributing factor to haze days in China (Fu et al., 2015). Due to the significant increase of

NH₃ in the atmosphere, more ammonium (NH₄⁺) is returned to terrestrial and aquatic ecosystems through dry and wet deposition, introducing excessive amount of Nr into natural ecosystems, which has resulted in the perturbation of the global N and carbon cycles (Lü and Tian, 2007; Tian et al., 2003). To better assess the potential impact of NH₃ emissions on human health and the environment, it is critical to have robust estimates of the spatial and temporal patterns of NH₃ emissions from agricultural activities in the Southern Asia (SA), home of more than 60% the world's population (i.e. the people of West, Central, East, South, and Southeast Asia) (Food and Agriculture Organization statistics (FAOSTAT), 2016).

The southern Asia region has experienced rapid expansion of agricultural activities (Liu and Tian, 2010; Tian et al., 2014) and has become a hotspot for studies of N-related gas emissions (Tian et al., 2016). The Haber-Bosch process produced approximately 109 Tg N fertilizer per year globally in 2014, of which more than 50% was consumed in Asia since 2004 (FAOSTAT, 2016). Nitrogen fertilizer is applied to agricultural systems to increase crop yield to meet the rising demand for food. In addition, higher demand for livestock products has stimulated the rapid growth of livestock production in the past century (Bouwman et al., 2013; Dangal et al., 2017). Meat consumption in major countries of Asia has grown substantially since 1990 and this trend is expected to continue (OECD/FAO, 2016). Consequently, annual livestock waste production has increased substantially and reached approximately 44.3±0.7 Tg N in the 2010s (Zhang et al., 2017). Increases in both N fertilizer use and livestock excreta have resulted in increased NH₃ emissions, but the magnitude and spatio-temporal pattern of NH₃ emissions from the agricultural sector in SA countries have not been thoroughly investigated.

Estimating NH₃ volatilization from N fertilizer application and livestock excreta has been a research topic of continuous interest for atmospheric and environmental scientists. Previous

studies have used numerous approaches to achieve this research goal. The most common methodology to estimate NH₃ emissions was based on emission factors (EFs). Zhao and Wang (1994) generated an inventory of NH₃ emissions using source-based EFs with considerations of various emission sources from livestock, energy consumption, and N fertilizer use in Asia. Using two constant EFs in upland and rice paddy soils, Zheng et al. (2002) found that the amount of NH₃ volatilization was 13.8 Tg N yr⁻¹ in 2000 and is expected to approach ~18.9 Tg N yr⁻¹ in 2030 in Asia, mainly from increased anthropogenic Nr. Streets et al. (2003) developed an emission inventory for Asia in 2000 using source-based EFs and provided emission estimates for each country in the region. In their study, NH₃ emission was estimated to be 27.5 Tg N yr⁻¹ from all major anthropogenic sources in Asia, among which 45% and 38% were from fertilizer application and animal productions, respectively. Later, Kurokawa et al. (2013) updated the regional emission inventory using country/sub-regional-source-based EFs. They estimated NH₃ emissions to be 32.8 Tg N yr⁻¹ in 2008, of which 57% was from fertilizer application, and 20% was from manure management.

A constant EF might not provide an accurate measure of NH₃ volatilization and its variability in relation to crops growth or N fertilizer application practices because the conversion of Nr to NH₃ involves several biological and chemical processes that are strongly sensitive to environmental conditions (Fowler et al., 2015; Sutton et al., 2014). For example, Gilliland et al. (2003) indicated that static emission factors are inadequate to reflect seasonal variability in NH₃ emissions. Fu et al. (2015) pointed out that environmental factors could strongly affect the NH₃ volatilization from N fertilizer application. Process-based modeling could therefore address this deficiency by considering climatic variables that are not explicitly considered in the EF approach (Fu et al., 2015; Sutton et al., 2014). The single-layer version of the bi-directional NH₃ exchange

model (Bi-NH₃) was developed in the late 1990s, and only simulated gas exchange processes occurring on leaf surface (Sutton et al., 1995). Later, a two-layer model was developed by also considering NH₃ exchange between the soil surface and the atmosphere (Nemitz et al., 2001). Currently, the two-layer Bi-NH₃ model is capable of simulating NH₃ emissions caused by N fertilizer application in agricultural systems under various environmental conditions (Sutton et al., 2014). Further, the Bi-NH₃ model has been fully coupled with various ecosystem/agricultural models to simulate NH₃ emissions at the global, regional, and country scale (Bash et al., 2013; Fu et al., 2015; Riddick et al., 2016). For example, the Bi-NH₃ module in the Community Multi-scale Air Quality model (CMAQ, Foley et al. (2010)) was coupled with the United States Department of Agriculture's (USDA) Environmental Policy Integrated Climate (EPIC) agroecosystem model (Bash et al., 2013; Massad et al., 2010; Nemitz et al., 2000) to simulate NH₃ emissions from N fertilizer application in the United States and China. The simulated results showed that the Bi-NH₃ module can be applied to other regions and even at the global scale. However, previous studies using the CMAQ-EPIC approach have provided only one-year estimates of NH₃ emissions.

No previous study has specifically assessed NH₃ fluxes on a decadal scale and captured the influence of reactive N sources (synthetic N fertilizer and manure) on regional NH₃ emissions. In this study, we have incorporated the Bi-NH₃ module into the process-based Dynamic Land Ecosystem Model (DLEM version 2.0) to estimate NH₃ emission from agricultural systems in SA. Our research objectives are to: (1) quantify the magnitude of NH₃ emissions during the 1961–2014 period at the country level and across the SA subcontinent; (2) investigate spatial and temporal variations in NH₃ emissions from agricultural ecosystems during that period; (3) quantify the relative contribution of synthetic N fertilizer use and manure application on NH₃ emissions; and (4) discuss potential threats of increasing NH₃ emissions to air quality and human health.

2. Material and Method

2.1. NH₃ emission from livestock excreta

Emission factors for estimating NH₃ emissions from livestock excreta were adopted from previous studies. Bouwman et al. (2002) provided a median value of EF (23%) to estimate the global NH₃ loss from animal manure. The range of EF in Bouwman et al. (2002) was 19–29%. Based on the work by Beusen et al. (2008), Riddick et al. (2016) applied a revised EF (17%) to estimate NH₃ emissions from animal manure. In this study, we adopted the minimum EF (17%) from Riddick et al. (2016) and the maximum EF (29%) from Bouwman et al. (2002). Then, we calculated the mean value (23%), the same as the median value in Bouwman et al. (2002), to estimate NH₃ loss from livestock excreta. The uncertainty range of EFs is 17–29%.

2.2. Input data and simulation setup

The input datasets for the DLEM-Bi-NH₃ simulation included gridded-crop fraction data, dynamic crop distribution maps, topography and soil properties, climate data, carbon dioxide (CO₂) concentration, and N fertilizer application. The procedure for developing time series data of crop distribution maps was described in detail by Ren et al. (2012). Cropland distribution datasets were developed by aggregating the 5-arc minute resolution History Database of the Global Environment (HYDE v3.2) global cropland distribution data (Klein Goldewijk et al., 2017). Half degree daily climate data (including average, maximum, and minimum air temperature; precipitation; relative humidity; shortwave radiation) were derived from CRU-NCEP climate forcing data. The monthly CO₂ concentration dataset was obtained from NOAA GLOBALVIEW-CO₂ dataset derived from atmospheric measurements. Spatially-explicit time-series data set of agricultural N fertilizer use was developed through spatializing IFA-based country-level N

fertilizer consumption data according to crop specific N fertilizer application rates, distribution of crop types, and historical cropland distribution during the 1961–2013 period (Lu and Tian, 2017). All mentioned datasets were applied to drive model simulations during the 1961–2014 period and estimate NH₃ emissions from N fertilizer application in SA agricultural systems.

The manure production dataset was derived from Food and Agriculture Organization of the United Nations statistics website (FAO, <http://faostat.fao.org>) and defaulted for N excretion rate as described in the IPCC 2006 Guidelines Tier1 (Zhang et al., 2017). We used the gridded manure production dataset to estimate NH₃ emissions from livestock excreta during 1961–2014.

3. Results

3.1. Contemporary and historical patterns of NH₃ emissions

In this study, we estimated NH₃ emissions from N fertilizer application and livestock excreta in SA between 2000 and 2014. Our results indicated that the mean NH₃ emission was 19.1 ± 3.5 Tg N yr⁻¹. Ammonia emissions from N fertilizer application and livestock excreta were 9.7 and 9.4 ± 3.5 Tg N yr⁻¹, respectively, during that period.

In SA, our results indicated that NH₃ emissions were 21.3 ± 3.9 Tg N yr⁻¹ in 2014 with a rapidly increasing rate of ~ 0.3 Tg N yr⁻² during 1961–2014 (Figure 6-1). Nitrogen fertilizer application increased from 2.6 to 71 Tg N yr⁻¹ at a rate of ~ 1.4 Tg N yr⁻² during 1961–2013. Consequently, NH₃ emissions from synthetic N fertilizer increased from 0.4 to 10.8 Tg N yr⁻¹ in SA. Livestock excreta increased from 19 to 45 Tg N yr⁻¹ at a rate of ~ 0.5 Tg N yr⁻² during 1961–2014. The NH₃ emission from manure increased from 4.3 ± 1.6 to 10.4 ± 3.9 Tg N yr⁻¹ in SA.

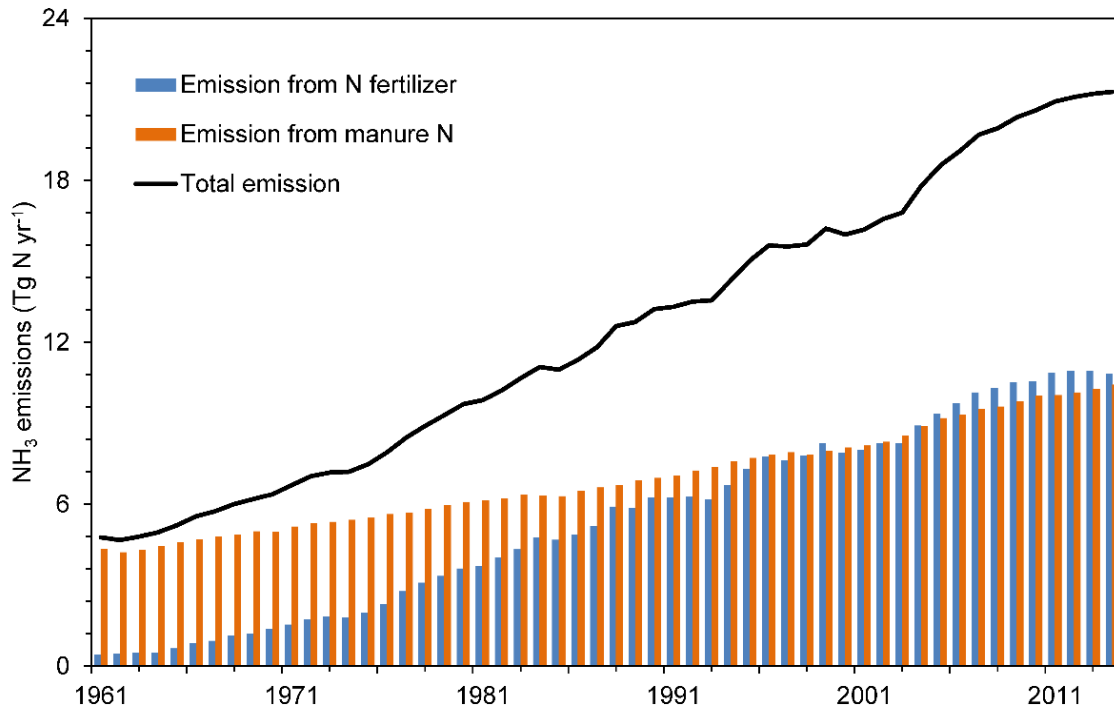


Figure 6-1. Annual NH₃ emissions from N fertilizer application and manure production in southern Asia during the period 1961–2014.

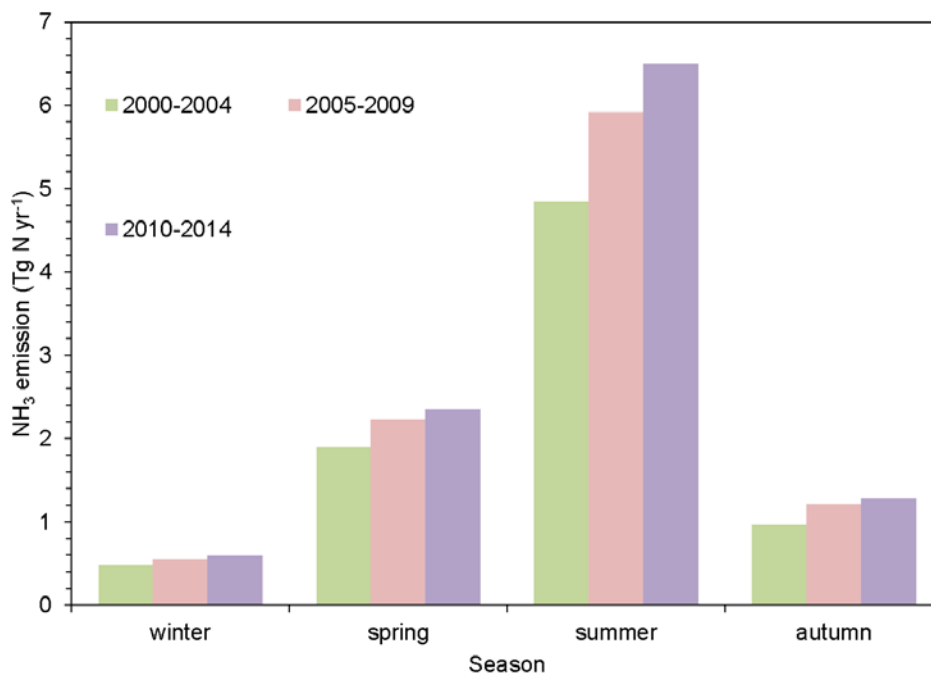


Figure 6-2. Seasonal variation in NH₃ emissions from N fertilizer application in southern Asia during the periods 2000–2004, 2005–2009, and 2010–2014.

Ammonia emissions from N fertilizer application during 2000–2014 showed a substantial seasonal variation (Figure 6-2), which was highly correlated with monthly emission variations. On average, the summer season accounted for 59.8%, while the winter season accounted for 5.6% of annual total emissions. The highest amount of NH₃ emission was recorded in July, followed by June and August (Figure 6-2). The lowest amount of NH₃ emission was found in January. Spring and autumn accounted for 22.5% and 12% of annual total emissions, respectively. Both seasons had an increase of NH₃ emissions during 2010–2014 compared with emissions during 2000–2004, but with different magnitudes. In comparison to the 2000–2004 period, summer emission grew substantially during 2010–2014. The increase in emission between these two periods was of a lesser magnitude when one considers the spring and autumn months (Figure 6-2).

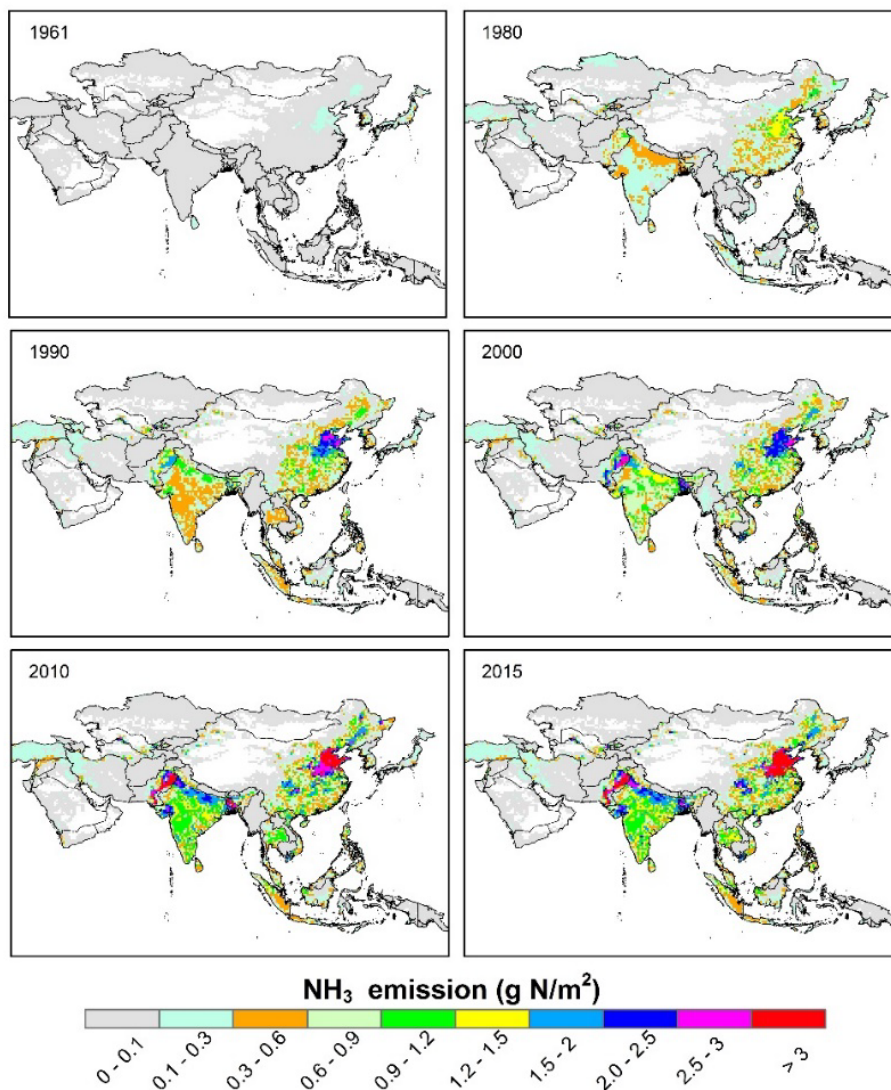


Figure 6-3. Spatial distribution of annual NH₃ emissions from N fertilizer application in southern Asia.

3.2. Spatial pattern of NH₃ emissions

Ammonia emissions from croplands varied significantly across the SA region during the past half-century (Figure 6-3). In this study, SA was divided into five regions: Southeast, East, South, West, and Central Asia. As shown in Figure 6-4, East and South Asia were two regions exhibiting the largest emissions and experiencing the most rapid increase in NH₃ emissions.

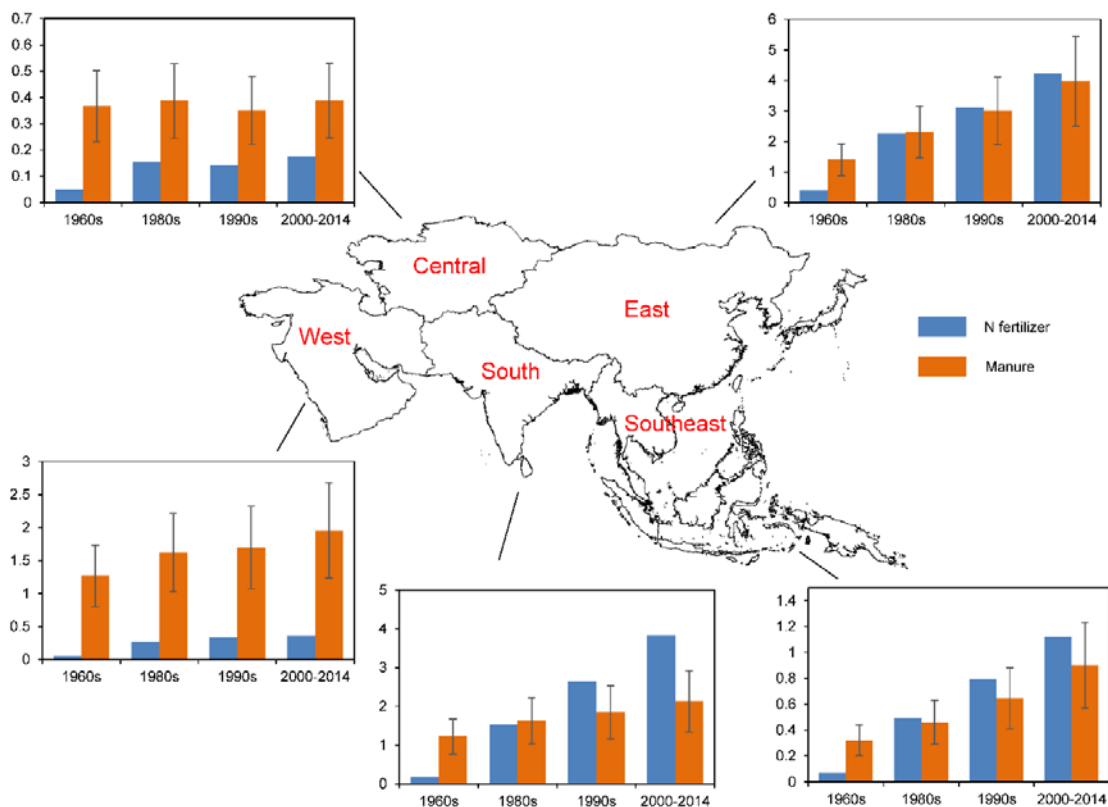


Figure 6-4. Decadal NH_3 emissions in different regions of southern Asia. Emission (y axis of each graph) is reported in Tg N yr^{-1} .

In 1961, as a small amount of N fertilizer was applied to croplands in East Asia (e.g., China, South Korea, and Japan), NH_3 emissions were concentrated in the north and northeast regions of China, but uniform across Japan and South Korea. A substantial amount of N fertilizer was applied in East and South Asia since the 1980s. There was a clear trend of increased NH_3 emissions in most grids of Pakistan and India especially in the northern regions, and China, especially in the North China Plain during 1980–2000. After 2000, more intense NH_3 emissions entirely covered India and a majority of arable land in China. A significant increase of NH_3 emissions was detected in West Asia especially in Turkey and western Iran, and Southeast Asia especially in Thailand during 1961–2014.

In the 1960s, East Asia emitted more than 50% of the SA's total emissions, while South Asia accounted approximately for 25%. However, a faster rate of NH₃ emission increases was found in South Asia during the past half century. During 2010–2014, South Asia accounted for more than 40% of the total emission. In Southeast Asia, NH₃ emissions increased from 35 Gg N yr⁻¹ to 1.3 Tg N yr⁻¹ during 1961–2014 (1 Gg = 10⁻³ Tg). Compared to South and East Asia, there was a slight increase in NH₃ emission in Central and West Asia during the observation period (1961–2014). NH₃ emissions increased sharply from 25 Gg N yr⁻¹ to 0.4 Tg N yr⁻¹ in West Asia during the 1961–2000 period, but only moderately during the last decade (2001–2014). In Central Asia, NH₃ emission was estimated to be 0.2 Tg N yr⁻¹ in 2014, which was approximately seven-fold higher than the emission amount in 1961 (Figure 6-4).

Similar to N fertilizer-induced NH₃ emissions, South and East Asia were two dominant regions that accounted for more than 50% of the total NH₃ emission from manure during 1961–2014. Ammonia emission from South Asia grew from 1.2 to 2.12 Tg N yr⁻¹, while emission from East Asia increased from 1.4 to 4.0 Tg N yr⁻¹ during that period (Figure 6-4). West Asia was the third largest source of manure-induced NH₃ emission, and showed an increasing trend (Figure 6-4). A moderate trend of increased NH₃ emission was found in Southeast Asia. There was no significant increase in manure-related NH₃ emission in Central Asia, a sub-region that contributed to less than 10% of the total emission from manure in SA.

3.3. NH₃ emissions from major countries

Eleven countries from SA (Table 6-1) contributed to ~65% of global total N application. China and India together contributed ~77% of total N application among these eleven countries, as shown in Table 6-1. In consequence, ~75% of total NH₃ emissions were from both countries

during 2000–2014. Ammonia emissions from Chinese croplands increased from 0.2 in 1961 to 4.5 Tg N yr⁻¹ in 2014. Similarly, in India, NH₃ emission rose from 60 Gg N yr⁻¹ in 1961 to 3.3 Tg N yr⁻¹ in 2014. Compared to China and India, the remaining countries contributed less than 25% of total N application, among which Pakistan had the highest N application and NH₃ emission. Turkey, Vietnam, Bangladesh, Thailand, and Iran showed similar total amounts of N fertilizer application; however, Turkey and Iran showed much less NH₃ emissions compared to the south and southeast Asia countries noted above.

We identified eleven countries that showed large manure production amounts during 1961–2014 (Table 6-1). China and India were the two top producing countries and accounted for approximately 67% of the total manure production during 2000–2014. Ammonia emissions from Chinese livestock wastes increased from 1.0±0.4 in 1961 to 4.1±1.5 Tg N yr⁻¹ in 2014. In contrast, NH₃ emissions did not show a rapid increase in India. In the remaining countries, Pakistan produced the highest amount of manure, followed by Turkey and Iran. West Asian countries (Turkey, Iran, Syria, and Jordan) and Southeast Asian countries (Indonesia, Vietnam, and Myanmar) were identified as hotspots for NH₃ emissions from manure.

Table 6-1. NH₃ emissions in major countries of southern Asia during 2000–2014 (1Tg = 10³ Gg): the left side represents NH₃ emissions from synthetic N fertilizer; the right side represents NH₃ emissions from livestock excreta.

Countries	N fertilizer application (Tg N yr ⁻¹)	NH ₃ emissions (Gg N yr ⁻¹)	Countries	Livestock excretes (Tg N yr ⁻¹)	NH ₃ emissions (Gg N yr ⁻¹)
China	30.8	4148	China	16.2	3736±1378
India	14.5	2840	India	6.2	1435±530
Pakistan	3.1	716	Pakistan	2.3	517±165
Indonesia	2.9	365	Turkey	1.8	406±120
Thailand	1.5	264	Iran	1.8	406±109
Vietnam	1.4	253	Jordan	1.3	296±83
Bangladesh	1.1	246	Syria	1.2	280±89
Turkey	1.4	143	Indonesia	1.0	228±73
Iran	1.2	105	Vietnam	0.8	188±53
Philippines	0.6	105	Myanmar	0.7	153±51
Uzbekistan	0.8	97	Afghanistan	0.5	116±35

*The uncertainty of NH₃ emissions from livestock excreta was ± 26%.

4. Discussion

4.1. The importance of Asia's contribution to global NH₃ emissions

Previous studies have presented global estimates of NH₃ emissions from agricultural systems (Beusen et al., 2008; Bouwman et al., 1997; Dentener and Crutzen, 1994; Riddick et al., 2016; Sutton et al., 2014; van Aardenne et al., 2001). In 2000, the mean estimate of global NH₃ emission was 29.9±5.2 Tg N yr⁻¹. In this study, the estimated NH₃ emission from southern Asian agricultural systems was 16.0±3.0 Tg N yr⁻¹, which accounted for ~55% of the total global emissions. Although gaseous NH₃ has a short lifetime and low emission height (Clarisse et al., 2009), the transport of deposited NH₄⁺ from one ecosystem to another could lead to widespread environmental pollution (Liu et al., 2013).

Table 6-2. Comparison of NH₃ emissions from N fertilizer application and livestock excreta between this study and previous estimates.

Country	Year	Method	NH ₃ emissions			References
			Fertilizer	Manure	Total	
China	2010	DLEM-Bi-NH ₃	4.3	4.1±1.5	8.4±1.5	This study
	2000	for N fertilizer;	3.3	3.2±1.2	6.5±1.2	
	1990	EF for manure	2.8	2.5±0.9	5.3±0.9	
	2011	EPIC-CMAQ	3.0	-	-	Fu et al. (2015)
	2010		4.5	5.1	9.6	Xu et al. (2015)
	2008	Correction EFs	3.3	-	-	Xu et al. (2016)
	2006		3.2	5.3	8.5	Huang et al. (2012)
	2005		3.6	-	-	Zhang et al. (2011)
	2005-2008	Region-specific EFs	3.0	4.8	7.8	Paulot et al. (2014)
	2005		3.5	2.8	6.3	Wang et al. (2009)
	2000	EPA	6.8	5.2	12	Streets et al. (2003)
	1995	EEA	3.6	2.0	5.6	Yan et al. (2003)
	1994		6.3	1.8	8.1	Zhao and Wang (1994)
	1990	IPCC	3.7	3.2	6.9	Olivier et al. (1998)
	India	2010	DLEM-Bi-NH ₃	3.3	1.5±0.6	4.8±0.6
2000		for N fertilizer;	2.2	1.3±0.5	3.5±0.5	
1990		EF for manure	1.5	1.3±0.5	2.8±0.5	
2003		Region-specific EFs	2.1	1.7	3.8	Aneja et al. (2012)
2000		EPA	3.3	2.8	6.1	Streets et al. (2003)
1995		EEA	1.5	1.6	3.1	Yan et al. (2003)
1990		IPCC	2.0	3.8	5.8	Olivier et al. (1998)

4.2. Comparison with other studies in SA

There are few regional-scale reports on NH₃ emissions in SA, and large uncertainties exist in the regional estimates of NH₃ emissions (Table 6-2). The research on NH₃ emissions from Asia conducted by Zhao and Wang (1994) and Streets et al. (2003) provided comprehensive estimates in different countries in Asia. Their estimates of total NH₃ emission from N fertilizer in 1990 and 2000 were 8.3 and 12.4 Tg N yr⁻¹, which were 32% and 57%, respectively, higher than our estimates (Figure 6-1). Yan et al. (2003) provided a total estimate of NH₃ emissions in South,

Southeast, and East Asia in 1995 from N fertilizer use, which was 8% lower than our estimate (6.3 Tg N yr⁻¹). There are two primary reasons why our estimates differ from previous estimates. First, we applied a process-based model to simulate NH₃ emissions that considered environmental factors, while the previous studies mentioned above applied an empirical EF. Second, the N fertilizer application data used in this study and previous studies were quite different. For example, the dataset of N fertilizer application rates used in our estimate was developed by Lu and Tian (2017), while the dataset used in Streets et al. (2003) was adopted from International Fertilizer Industry Association (IFA, 1998). The comparisons of NH₃ emission from N fertilizer with other studies in China and India are listed in Table 2.

For NH₃ emission from livestock excreta, the estimate by Yan et al. (2003) for 1995 was 4.7 Tg N yr⁻¹, which was 17% lower than our estimate (5.6 Tg N yr⁻¹, Figure 6-1). However, the estimate (10.5 Tg N yr⁻¹) from Streets et al. (2003) was 29% higher than our estimate (8.1 Tg N yr⁻¹) for 2000. The differences could be associated with the application of different EFs and different livestock excreta amount. In this study, we adopted a mean EF of 23% (17~29%) to estimate NH₃ emissions from livestock excreta, while Yan et al. (2003) adopted the European Environment Agency (EEA) EFs based on the animal types with an average EF less than 20%. Streets et al. (2003) conceded that the use of European-based EFs in their study might have introduced uncertainty in their estimates of NH₃ emission from Asian countries. Thus, future work is needed to better constrain the uncertainties associated with NH₃ emission from livestock excreta. The comparisons of NH₃ emission from manure with other studies in China and India are listed in Table 2.

4.3. Comparison of monthly NH₃ emissions with other studies in China

The uncertainty on monthly NH₃ emissions was associated with the input climate datasets, the cropland area, and N fertilizer application dates and ratios. Large uncertainties appeared in the estimate of monthly NH₃ emissions from N fertilizer application. Similar to the result of Xu et al. (2016), NH₃ emission peaked in July, and was followed by secondary peaks in June and August. Our estimates of NH₃ emission in September and October were different from Xu et al. (2016). Ammonia emissions in summer contributed nearly 60% of the annual total, which was consistent with the results in Zhang et al. (2011). As shown in Fu et al. (2015), NH₃ emission in September was low because of the lower amount of N fertilizer application during that time of the year.

4.4. Uncertainties

As discussed in Xu et al. (2017), uncertainties in modelled NH₃ emission are due to parameters and input datasets. Fertilizer application rates are a major factor that may have affected the accuracy of NH₃ emission estimates. The input datasets of soil properties and climate are two other important factors that might affect the spatial pattern and total amount of NH₃ emissions in SA. In the DLEM, we assumed that the applied N fertilizer could be used, stored, or lost within 30 days, and these assumptions could introduce uncertainties in the simulations. In addition, DLEM used empirical methods to calculate model parameters Γ_s and Γ_g , which might result in some uncertainties due to a lack of observational data to evaluate the validity of this approach (Bash et al., 2013; Fu et al., 2015). Different N fertilizer types have different EFs, and thus could result in different rates of NH₃ emissions. For example, urea, a major form of N fertilizer applied to croplands in developing countries, contributed more than 50% of the total NH₃ emitted from N fertilizer (Zhang et al., 2011). The EF of urea was estimated as 0.2–0.25 (Bouwman et al., 1997; Matthews, 1994). In this study, we did not differentiate between N fertilizer types. Instead, all types of N fertilizer were considered as total N inputs for model simulation, and that may have

reduced the accuracy of the NH_3 estimates. A constant EF for NH_3 emissions from manure was used in this study, which might introduce more uncertainty in our estimate compared to other studies that have used region-based or animal species-based EFs. In addition, although NH_3 emissions from livestock excreta are affected by climate, soil properties, and plant phenology (Hansen et al., 2017; Massad et al., 2010), the timing and rates of animal manure application were not considered in this study. This may also have added to the uncertainty of our estimates.

4.5. Implications

More than half of the N added to croplands can be lost in various ways (Lassaletta et al., 2014b; Tian et al., 2012c). This study indicated that NH_3 volatilization was one of the major outlets for Nr losses. As a significant source of NH_3 and other precursor gases that lead to the generation of $\text{PM}_{2.5}$, agriculture not only affects the Earth's radiation budget, but causes adverse health effects (Aneja et al., 2008; Cao et al., 2009; de Leeuw et al., 2003; Fowler et al., 1998; Seinfeld and Pandis, 2016). First, NH_3 can react with other air pollutants and form aerosols (e.g., $\text{PM}_{2.5}$) in the atmosphere, thus lead to the reduction of visibility (Cheng et al., 2014). Second, the increasing concentration of $\text{PM}_{2.5}$ is positively related to the rates of premature mortality, which increased by 21% and 85%, respectively, in East Asia and South Asia from 1990 to 2010 (Wang et al., 2017). Last, the dry and wet deposition of NH_4^+ from NH_3 emissions may alter soil and water chemistry (e.g., eutrophication), and reduce biological diversity (Clark and Tilman, 2008; Vitousek and Farrington, 1997).

Using a global atmospheric chemistry model (Lelieveld et al., 2015), a recent study reported that outdoor air pollution, mainly by $\text{PM}_{2.5}$, could lead to 3.3 (1.61–4.81) million premature deaths per year worldwide, predominantly in Asia. That study considered agriculture as the largest contributor to global premature deaths due to the releases of NH_3 from livestock wastes

and N fertilizer. Although Jerrett (2015) argued that Lelieveld et al. (2015) may have overestimated the toxicity of PM_{2.5} from agricultural sources, he suggested that scientists and policy-makers should pay much more attention to PM_{2.5} formed by agricultural sources and its adverse effects on human health. Recently, Wang et al. (2017) indicated that reduction of NH₃ emissions could maximize the effectiveness of nitrogen oxides emission controls and potentially provided some health benefits. Thus, effective farming strategies should be adopted by farmers in order to minimize NH₃ loss from N fertilizer or manure application, and mitigate associated threats to human health.

How can we reduce N losses from Nr? One effective strategy is to reduce the application of N fertilizer, and to rotate legume crops (e.g., soybean, alfalfa) with other cereal crops (e.g., wheat, maize). Nitrogen use efficiency (NUE) was found to be generally higher in agricultural systems with a higher proportion of N inputs from symbiotic N fixation (Lassaletta et al., 2014b). The second strategy is to identify the optimal crop-specific N needs to avoid excessive N application to soils (Chen et al., 2011). Mueller et al. (2017) applied N input-yield response functions to investigate regional- or country-scale NUE based on the historical N budget data (1961–2009). Their studies provided an overview of the optimal N input rates in major agricultural countries, and showed that East, South, and Southeast Asia received excessive N inputs up to 10 g N m² greater than needed for optimal crop yield. The third strategy is to minimize the loss of N through improved management techniques (Bouwman et al., 1997; Chen et al., 2011; Chen et al., 2014; Fowler et al., 2015). In addition, some strategies have been approved to be effective for reducing N losses from animal manure in SA. In comparison with composting, solid manure storages via compaction and covering could substantially decline NH₃ emissions (Chadwick, 2005;

Hou et al., 2015). Compared to surface application, manure application through band spreading, incorporation, and injection could significantly reduce NH_3 emissions (Hou et al., 2015).

Asia, whose population could increase by 0.9 billion by 2050, has been projected to be the second largest contributor to future population growth (World Population Prospects, 2015). Valin et al. (2014) reported that food demands would increase by 59–98% between 2005 and 2050 in the reference scenario (the GDP and population pathways of the “middle of the road” Shared Socio-economic Pathway (SSP2) developed by the climate change impacts research community). In the projection of FAO and agriculture models, South and East Asia are expected to experience a rapid increase in crop foods and livestock products during the first-half of the 21st century (Alexandratos and Bruinsma, 2012; Valin et al., 2014). Under this scenario, N fertilizer application to global croplands would double by 2100 (Stocker et al., 2013), while manure production may increase 50% by 2050 compared to 2000 (Bouwman et al., 2013). China and India are the top two countries with the largest N fertilizer consumption, and are expected to remain so in the foreseeable future. Unfortunately, NUE has rapidly decreased in these countries (Tian et al., 2012b; Zhang et al., 2015). The decrease in NUE and increase in N fertilizer use would translate into greater emission of fertilized N as NH_3 and other N gases (Zhang et al., 2015). Thus, farmers as well as policy-makers in Asian countries ought to consider using N fertilizer more efficiently for the benefits of environmental quality and human health (Tian et al., 2016; Zhang, 2017). Moreover, livestock excreta in SA increased from 19 to 45 Tg N yr^{-1} during 1961–2014 (Zhang et al., 2017). In 2000, Southeast, East, and South Asia contribute ~30% of global GHG emissions from ruminants (Herrero et al., 2013). In order to reduce both GHG and NH_3 emissions from livestock systems, it is important to implement an effective strategy for managing animal manure (Bouwman et al., 2013; Fowler et al., 2015).

References

- Alexandratos, N. and Bruinsma, J.: World agriculture towards 2030/2050: the 2012 revision, ESA Working paper Rome, FAO, 2012.
- Aneja, V. P., Schlesinger, W. H., and Erisman, J. W.: Farming pollution, *Nature Geoscience*, 1, 409, 2008.
- Aneja, V. P., Schlesinger, W. H., Erisman, J. W., Behera, S. N., Sharma, M., and Battye, W.: Reactive nitrogen emissions from crop and livestock farming in India, *Atmospheric Environment*, 47, 92-103, 2012.
- Bash, J., Cooter, E., Dennis, R., Walker, J., and Pleim, J.: Evaluation of a regional air-quality model with bidirectional NH₃ exchange coupled to an agroecosystem model, *Biogeosciences*, 10, 1635-1645, 2013.
- Beusen, A., Bouwman, A., Heuberger, P., Van Drecht, G., and Van Der Hoek, K.: Bottom-up uncertainty estimates of global ammonia emissions from global agricultural production systems, *Atmospheric Environment*, 42, 6067-6077, 2008.
- Bouwman, A., Boumans, L., and Batjes, N.: Estimation of global NH₃ volatilization loss from synthetic fertilizers and animal manure applied to arable lands and grasslands, *Global biogeochemical cycles*, 16, 2002.
- Bouwman, A., Lee, D., Asman, W., Dentener, F., Van Der Hoek, K., and Olivier, J.: A global high-resolution emission inventory for ammonia, *Global biogeochemical cycles*, 11, 561-587, 1997.
- Bouwman, A., Goldewijk, K. K., Van Der Hoek, K. W., Beusen, A. H., Van Vuuren, D. P., Willems, J., Rufino, M. C., and Stehfest, E.: Exploring global changes in nitrogen and phosphorus cycles in agriculture induced by livestock production over the 1900–2050 period, *Proceedings of the National Academy of Sciences*, 110, 20882-20887, 2013.
- Cao, J.-J., Zhang, T., Chow, J. C., Watson, J. G., Wu, F., and Li, H.: Characterization of atmospheric ammonia over Xi'an, China, *Aerosol and Air Quality Research*, 9, 277-289, 2009.
- Chadwick, D.: Emissions of ammonia, nitrous oxide and methane from cattle manure heaps: effect of compaction and covering, *Atmospheric environment*, 39, 787-799, 2005.
- Chen, X.-P., Cui, Z.-L., Vitousek, P. M., Cassman, K. G., Matson, P. A., Bai, J.-S., Meng, Q.-F., Hou, P., Yue, S.-C., and Römheld, V.: Integrated soil–crop system management for food security, *Proceedings of the National Academy of Sciences*, 108, 6399-6404, 2011.
- Chen, X., Cui, Z., Fan, M., Vitousek, P., Zhao, M., Ma, W., Wang, Z., Zhang, W., Yan, X., and Yang, J.: Producing more grain with lower environmental costs, *Nature*, 514, 486, 2014.
- Cheng, Z., Wang, S., Fu, X., Watson, J., Jiang, J., Fu, Q., Chen, C., Xu, B., Yu, J., and Chow, J.: Impact of biomass burning on haze pollution in the Yangtze River delta, China: a case study in summer 2011, *Atmospheric Chemistry and Physics*, 14, 4573-4585, 2014.
- Clarisse, L., Clerbaux, C., Dentener, F., Hurtmans, D., and Coheur, P.-F.: Global ammonia distribution derived from infrared satellite observations, *Nature Geoscience*, 2, 479, 2009.
- Clark, C. M. and Tilman, D.: Loss of plant species after chronic low-level nitrogen deposition to prairie grasslands, *Nature*, 451, 712-715, 2008.
- Dangal, S. R., Tian, H., Zhang, B., Pan, S., Lu, C., and Yang, J.: Methane emission from global livestock sector during 1890–2014: Magnitude, trends and spatiotemporal patterns, *Global change biology*, 2017. 2017.

- de Leeuw, G., Skj oth, C. A., Hertel, O., Jickells, T., Spokes, L., Vignati, E., Frohn, L., Frydendall, J., Schulz, M., and Tamm, S.: Deposition of nitrogen into the North Sea, *Atmospheric Environment*, 37, 145-165, 2003.
- Dentener, F. J. and Crutzen, P. J.: A three-dimensional model of the global ammonia cycle, *Journal of Atmospheric Chemistry*, 19, 331-369, 1994.
- Erisman, J. W., Sutton, M. A., Galloway, J., Klimont, Z., and Winiwarter, W.: How a century of ammonia synthesis changed the world, *Nature Geoscience*, 1, 636-639, 2008.
- Foley, K., Roselle, S., Appel, K., Bhave, P., Pleim, J., Otte, T., Mathur, R., Sarwar, G., Young, J., and Gilliam, R.: Incremental testing of the Community Multiscale Air Quality (CMAQ) modeling system version 4.7, *Geoscientific Model Development*, 3, 205, 2010.
- Fowler, D., Pitcairn, C., Sutton, M., Flechard, C., Loubet, B., Coyle, M., and Munro, R.: The mass budget of atmospheric ammonia in woodland within 1 km of livestock buildings, *Environmental Pollution*, 102, 343-348, 1998.
- Fowler, D., Steadman, C. E., Stevenson, D., Coyle, M., Rees, R. M., Skiba, U., Sutton, M., Cape, J., Dore, A., and Vieno, M.: Effects of global change during the 21st century on the nitrogen cycle, *Atmospheric Chemistry and Physics*, 15, 13849-13893, 2015.
- Fu, X., Wang, S., Ran, L., Pleim, J., Cooter, E., Bash, J., Benson, V., and Hao, J.: Estimating NH₃ emissions from agricultural fertilizer application in China using the bi-directional CMAQ model coupled to an agro-ecosystem model, *Atmospheric Chemistry and Physics*, 15, 6637-6649, 2015.
- Galloway, J. N., Dentener, F. J., Capone, D. G., Boyer, E. W., Howarth, R. W., Seitzinger, S. P., Asner, G. P., Cleveland, C., Green, P., and Holland, E.: Nitrogen cycles: past, present, and future, *Biogeochemistry*, 70, 153-226, 2004.
- Gilliland, A. B., Dennis, R. L., Roselle, S. J., and Pierce, T. E.: Seasonal NH₃ emission estimates for the eastern United States based on ammonium wet concentrations and an inverse modeling method, *Journal of Geophysical Research: Atmospheres*, 108, 2003.
- Hansen, K., Personne, E., Skj oth, C., Loubet, B., Ibrom, A., Jensen, R., S orensen, L. L., and B ogh, E.: Investigating sources of measured forest-atmosphere ammonia fluxes using two-layer bi-directional modelling, *Agricultural and Forest Meteorology*, 237, 80-94, 2017.
- Herrero, M., Havl ik, P., Valin, H., Notenbaert, A., Rufino, M. C., Thornton, P. K., Bl ummel, M., Weiss, F., Grace, D., and Obersteiner, M.: Biomass use, production, feed efficiencies, and greenhouse gas emissions from global livestock systems, *Proceedings of the National Academy of Sciences*, 110, 20888-20893, 2013.
- Hou, Y., Velthof, G. L., and Oenema, O.: Mitigation of ammonia, nitrous oxide and methane emissions from manure management chains: a meta-analysis and integrated assessment, *Global change biology*, 21, 1293-1312, 2015.
- Huang, X., Song, Y., Li, M., Li, J., Huo, Q., Cai, X., Zhu, T., Hu, M., and Zhang, H.: A high-resolution ammonia emission inventory in China, *Global biogeochemical cycles*, 26, 2012.
- Jerrett, M.: Atmospheric science: the death toll from air-pollution sources, *Nature*, 525, 330-331, 2015.
- Klein Goldewijk, K., Beusen, A., Doelman, J., and Stehfest, E.: Anthropogenic land use estimates for the Holocene–HYDE 3.2, *Earth System Science Data*, 9, 927, 2017.
- Kurokawa, J., Ohara, T., Morikawa, T., Hanayama, S., Janssens-Maenhout, G., Fukui, T., Kawashima, K., and Akimoto, H.: Emissions of air pollutants and greenhouse gases over

- Asian regions during 2000–2008: Regional Emission inventory in ASia (REAS) version 2, *Atmospheric Chemistry and Physics*, 13, 11019-11058, 2013.
- Lassaletta, L., Billen, G., Grizzetti, B., Garnier, J., Leach, A. M., and Galloway, J. N.: Food and feed trade as a driver in the global nitrogen cycle: 50-year trends, *Biogeochemistry*, 118, 225-241, 2014.
- Lelieveld, J., Evans, J., Fnais, M., Giannadaki, D., and Pozzer, A.: The contribution of outdoor air pollution sources to premature mortality on a global scale, *Nature*, 525, 367-371, 2015.
- Liu, M. and Tian, H.: China's land cover and land use change from 1700 to 2005: Estimations from high-resolution satellite data and historical archives, *Global biogeochemical cycles*, 24, 2010.
- Liu, X., Zhang, Y., Han, W., Tang, A., Shen, J., Cui, Z., Vitousek, P., Erisman, J. W., Goulding, K., and Christie, P.: Enhanced nitrogen deposition over China, *Nature*, 494, 459-462, 2013.
- Lu, C. and Tian, H.: Global nitrogen and phosphorus fertilizer use for agriculture production in the past half century: shifted hot spots and nutrient imbalance, *Earth System Science Data*, 9, 181, 2017.
- Lü, C. and Tian, H.: Spatial and temporal patterns of nitrogen deposition in China: synthesis of observational data, *Journal of Geophysical Research: Atmospheres*, 112, 2007.
- Massad, R.-S., Nemitz, E., and Sutton, M.: Review and parameterisation of bi-directional ammonia exchange between vegetation and the atmosphere, *Atmospheric Chemistry and Physics*, 10, 10359-10386, 2010.
- Matthews, E.: Nitrogenous fertilizers: global distribution of consumption and associated emissions of nitrous oxide and ammonia, *Global biogeochemical cycles*, 8, 411-439, 1994.
- Mueller, N. D., Lassaletta, L., Runck, B. C., Billen, G., Garnier, J., and Gerber, J. S.: Declining spatial efficiency of global cropland nitrogen allocation, *Global biogeochemical cycles*, 31, 245-257, 2017.
- Nemitz, E., Milford, C., and Sutton, M. A.: A two-layer canopy compensation point model for describing bi-directional biosphere-atmosphere exchange of ammonia, *Quarterly Journal of the Royal Meteorological Society*, 127, 815-833, 2001.
- Nemitz, E., Sutton, M. A., Schjoerring, J. K., Husted, S., and Wyers, G. P.: Resistance modelling of ammonia exchange over oilseed rape, *Agricultural and Forest Meteorology*, 105, 405-425, 2000.
- Olivier, J., Bouwman, A., Van der Hoek, K., and Berdowski, J.: Global air emission inventories for anthropogenic sources of NO_x, NH₃ and N₂O in 1990, *Environmental Pollution*, 102, 135-148, 1998.
- Paulot, F., Jacob, D. J., Pinder, R., Bash, J., Travis, K., and Henze, D.: Ammonia emissions in the United States, European Union, and China derived by high-resolution inversion of ammonium wet deposition data: Interpretation with a new agricultural emissions inventory (MASAGE_NH₃), *Journal of Geophysical Research: Atmospheres*, 119, 4343-4364, 2014.
- Pinder, R. W., Adams, P. J., and Pandis, S. N.: Ammonia emission controls as a cost-effective strategy for reducing atmospheric particulate matter in the eastern United States, *Environmental science & technology*, 41, 380-386, 2007.

- Riddick, S., Ward, D., Hess, P., Mahowald, N., Massad, R., and Holland, E.: Estimate of changes in agricultural terrestrial nitrogen pathways and ammonia emissions from 1850 to present in the Community Earth System Model, *Biogeosciences*, 13, 3397-3426, 2016.
- Seinfeld, J. and Pandis, S.: *Atmospheric Chemistry and Physics*, 1326 pp, John Wiley, Hoboken, NJ, 1998.
- Seinfeld, J. H. and Pandis, S. N.: *Atmospheric chemistry and physics: from air pollution to climate change*. John Wiley & Sons, 2016.
- Stocker, B. D., Roth, R., Joos, F., Spahni, R., Steinacher, M., Zaehle, S., Bouwman, L., and Prentice, I. C.: Multiple greenhouse-gas feedbacks from the land biosphere under future climate change scenarios, *Nature Climate Change*, 3, 666-672, 2013.
- Streets, D. G., Bond, T., Carmichael, G., Fernandes, S., Fu, Q., He, D., Klimont, Z., Nelson, S., Tsai, N., and Wang, M. Q.: An inventory of gaseous and primary aerosol emissions in Asia in the year 2000, *Journal of Geophysical Research: Atmospheres*, 108, 2003.
- Sutton, M., Schjorring, J., Wyers, G., Duyzer, J., Ineson, P., and Powlson, D.: Plant-atmosphere exchange of ammonia [and discussion], *Philosophical Transactions of the Royal Society of London A: Mathematical, Physical and Engineering Sciences*, 351, 261-278, 1995.
- Sutton, M. A., Mason, K. E., Sheppard, L. J., Sverdrup, H., Haeuber, R., and Hicks, W. K.: *Nitrogen deposition, critical loads and biodiversity*, Springer Science & Business Media, 2014.
- Sutton, M. A., Reis, S., Riddick, S. N., Dragosits, U., Nemitz, E., Theobald, M. R., Tang, Y. S., Braban, C. F., Vieno, M., and Dore, A. J.: Towards a climate-dependent paradigm of ammonia emission and deposition, *Philosophical Transactions of the Royal Society of London B: Biological Sciences*, 368, 20130166, 2013.
- Tian, H., Banger, K., Bo, T., and Dadhwal, V. K.: History of land use in India during 1880–2010: Large-scale land transformations reconstructed from satellite data and historical archives, *Global and planetary change*, 121, 78-88, 2014.
- Tian, H., Lu, C., Chen, G., Tao, B., Pan, S., Del Grosso, S. J., Xu, X., Bruhwiler, L., Wofsy, S. C., and Kort, E. A.: Contemporary and projected biogenic fluxes of methane and nitrous oxide in North American terrestrial ecosystems, *Frontiers in Ecology and the Environment*, 10, 528-536, 2012a.
- Tian, H., Lu, C., Ciais, P., Michalak, A. M., Canadell, J. G., Saikawa, E., Huntzinger, D. N., Gurney, K. R., Sitch, S., Zhang, B., Yang, J., Bousquet, P., Bruhwiler, L., Chen, G., Dlugokencky, E., Friedlingstein, P., Melillo, J., Pan, S., Poulter, B., Prinn, R., Saunio, M., Schwalm, C., and Wofsy, S.: The terrestrial biosphere as a net source of greenhouse gases to the atmosphere, *Nature*, 531, 225-228, 2016.
- Tian, H., Lu, C., Melillo, J., Ren, W., Huang, Y., Xu, X., Liu, M., Zhang, C., Chen, G., and Pan, S.: Food benefit and climate warming potential of nitrogen fertilizer uses in China, *Environmental Research Letters*, 7, 044020, 2012b.
- Tian, H., Melillo, J. M., Kicklighter, D. W., Pan, S., Liu, J., McGuire, A. D., and Moore, B.: Regional carbon dynamics in monsoon Asia and its implications for the global carbon cycle, *Global and planetary change*, 37, 201-217, 2003.
- Valin, H., Sands, R. D., van der Mensbrugge, D., Nelson, G. C., Ahammad, H., Blanc, E., Bodirsky, B., Fujimori, S., Hasegawa, T., and Havlik, P.: The future of food demand: understanding differences in global economic models, *Agricultural Economics*, 45, 51-67, 2014.

- van Aardenne, J., Dentener, F., Olivier, J., Goldewijk, C. K., and Lelieveld, J.: A 1×1 resolution data set of historical anthropogenic trace gas emissions for the period 1890–1990, *Global Biogeochemical Cycles*, 15, 909-928, 2001.
- Vitousek, P. M. and Farrington, H.: Nutrient limitation and soil development: experimental test of a biogeochemical theory, *Biogeochemistry*, 37, 63-75, 1997.
- Wang, J., Xing, J., Mathur, R., Pleim, J. E., Wang, S., Hogrefe, C., Gan, C.-M., Wong, D. C., and Hao, J.: Historical trends in PM_{2.5}-related premature mortality during 1990–2010 across the northern hemisphere, *Environmental health perspectives*, 125, 400, 2017.
- Wang, S., Liao, Q., Hu, Y., and Yan, X.: A preliminary inventory of NH₃ emission and its temporal and spatial distribution of China, *Journal of Agro-Environment Science*, 28, 619-626, 2009.
- Xu, P., Liao, Y., Lin, Y., Zhao, C., Yan, C., Cao, M., Wang, G., and Luan, S.: High-resolution inventory of ammonia emissions from agricultural fertilizer in China from 1978 to 2008, *Atmospheric Chemistry and Physics*, 16, 1207-1218, 2016.
- Xu, P., Zhang, Y., Gong, W., Hou, X., Kroeze, C., Gao, W., and Luan, S.: An inventory of the emission of ammonia from agricultural fertilizer application in China for 2010 and its high-resolution spatial distribution, *Atmospheric Environment*, 115, 141-148, 2015.
- Xu, R., Tian, H., Lu, C., Pan, S., Chen, J., Yang, J., and Bowen, Z.: Preindustrial nitrous oxide emissions from the land biosphere estimated by using a global biogeochemistry model, *Climate of the Past*, 13, 977-990, 2017.
- Yan, X., Akimoto, H., and Ohara, T.: Estimation of nitrous oxide, nitric oxide and ammonia emissions from croplands in East, Southeast and South Asia, *Global change biology*, 9, 1080-1096, 2003.
- Zhang, B., Tian, H., Lu, C., Dangal, S. R., Yang, J., and Pan, S.: Global manure nitrogen production and application in cropland during 1860–2014: a 5 arcmin gridded global dataset for Earth system modeling, *Earth System Science Data*, 9, 667-678, 2017.
- Zhang, X.: Biogeochemistry: A plan for efficient use of nitrogen fertilizers, *Nature*, 543, 322-323, 2017.
- Zhang, X., Davidson, E. A., Mauzerall, D. L., Searchinger, T. D., Dumas, P., and Shen, Y.: Managing nitrogen for sustainable development, *Nature*, 528, 51-59, 2015.
- Zhang, Y., Luan, S., Chen, L., and Shao, M.: Estimating the volatilization of ammonia from synthetic nitrogenous fertilizers used in China, *Journal of environmental management*, 92, 480-493, 2011.
- Zhao, D. and Wang, A.: Estimation of anthropogenic ammonia emissions in Asia, *Atmospheric Environment*, 28, 689-694, 1994.
- Zheng, X., Fu, C., Xu, X., Yan, X., Huang, Y., Han, S., Hu, F., and Chen, G.: The Asian nitrogen cycle case study, *AMBIO: A Journal of the Human Environment*, 31, 79-87, 2002.

Chapter 7. Global ammonia emissions from synthetic nitrogen fertilizer applications in agricultural systems: empirical and process-based estimates and uncertainty

Abstract

Excessive ammonia (NH_3) emitted from nitrogen fertilizer applications in global croplands plays an important role in atmospheric aerosol production, resulting in visibility reduction and regional haze. However, large uncertainties exist in the estimate of NH_3 emissions from global and regional croplands, which utilize different data and methods. In this study, we coupled a process-based Dynamic Land Ecosystem Model (DLEM) with the bi-directional NH_3 exchange module in the Community Multiscale Air-Quality (CMAQ) model (DLEM-Bi- NH_3) to quantify NH_3 emissions at the global and regional scale, and crop-specific NH_3 emissions globally at a spatial resolution of $0.5^\circ \times 0.5^\circ$ during 1961–2010. This study indicated that global NH_3 emissions increased from 1.9 ± 0.03 to 16.7 ± 0.5 Tg N yr^{-1} between 1961 and 2010. The annual increase of NH_3 emissions showed large spatial variations. Southern Asia, including China and India, accounted for more than 50% of total global NH_3 emissions since the 1980s, followed by North America and Europe. In addition, results showed that not considering environmental factors in the empirical methods (constant emission factor in the IPCC Tier 1 guideline) could underestimate NH_3 emissions in the context of global warming, with the highest difference (i.e., 6.9 Tg N yr^{-1}) occurring in 2010. Estimates by DLEM-Bi- NH_3 module provided a scientific understanding of global and regional NH_3 emissions over the past 50 years, which offers a reference for assessing

air quality consequences of future nitrogen enrichment as well as nitrogen use efficiency improvement.

1. Introduction

Over the past century, a large quantity of chemical N fertilizer was produced using the Haber-Bosch process that converts atmospheric dinitrogen gas (N_2) to ammonia (NH_3). Mineral fertilizer application in cropland contributed to the rapid increase in food production, which supported the fast global population growth (Erisman et al., 2008; Gruber and Galloway, 2008). Human-caused reactive N (typically from agricultural systems) was at least twice the rate of naturally created terrestrial N in 2010 (Ciais et al., 2014). These excess reactive N compounds in terrestrial ecosystems play a role in the emission of N-containing gases, including oxides of nitrogen (N_2O and NO_x), and NH_3 (Tian et al., 2016). The high output of these N-containing gases remains a matter of great concern to human and environmental health (Behera et al., 2013).

Agricultural activities account for approximately 80~90% of total anthropogenic NH_3 emissions (Bouwman et al., 1997; Zhang et al., 2010). There are two major sources for NH_3 emissions: volatilization from livestock manure and mineral fertilizer application (Asman et al., 1998; Bouwman et al., 1997). A large amount of NH_3 from synthetic N fertilizer is emitted to the atmosphere while short-distance transport can return it to the land by wet or dry deposition (Asman et al., 1998). With substantial increases in manure production and chemical N fertilizer consumption, deposition of reactive N has increased across many regions of the globe. For example, the average atmospheric N deposition in this century was twenty-fold higher than that in the pre-industrial period (Dentener, 2006). This increased N deposition has contributed to eutrophication, acidification, and loss of biodiversity in the global ecosystem (Erisman et al., 2008). Moreover, NH_3 is one of key precursors for aerosol ($PM_{2.5}$) formation in the atmosphere

that could adversely affect respiratory and cardiovascular systems, and contribute to visibility reduction and regional haze (Pinder et al., 2007; Seitzinger and Kroeze, 1998). For these reasons, a robust understanding of the magnitude and spatiotemporal patterns of global NH₃ emissions from agricultural activities is essential.

This study mainly focused on NH₃ emissions from synthetic N fertilizer application. Mineral N fertilizer contributed 10–15% of the total estimated NH₃ emissions (45~75 Tg N annually) from terrestrial ecosystems at the end of the last century (Matthews, 1994). Bouwman et al. (1997) estimated global NH₃ emissions in 1990 as ~54 Tg N yr⁻¹ with synthetic N fertilizer application accounting for ~16.7% (9 Tg N yr⁻¹). This estimate was comparable to the 8.5 Tg N yr⁻¹ of Schlesinger and Hartley (1992). Riddick et al. (2016) provided an estimate of global NH₃ emission of 12 Tg N yr⁻¹ from N fertilizer for the year 2000. Previous studies have mainly focused on NH₃ emission in one single year. Although Riddick et al. (2016) presented seasonal estimates of global NH₃ emissions, their simplification of agricultural practices (e.g., no double cropping) along with not considering rice cultivations introduces large uncertainties in their estimates. Thus, studies of global inter-annual and crop-specific NH₃ emissions are still needed.

Emission factors (EF) and process-based models are two major approaches for quantifying global or regional NH₃ emissions from N fertilizer use. The EF represents the percentage of applied N fertilizer that volatilizes as NH₃, which varies with synthetic N fertilizer types. Constant values are often assumed for EFs used to build emission inventories at global and regional scales, such as the Emission Database for Global Atmospheric Research (EDGAR, Olivier et al. (2002)) and the National Emission Inventory (NEI, Reis et al. (2009)) of the United States. Numerous efforts have been made to determine EFs for NH₃ emissions at regional scales (e.g., Europe, United States, and China). However, robust estimations at the global scale and on crop-specific NH₃ emissions

globally over historical time series are lacking. Moreover, large uncertainties still exist for monthly and annual NH_3 emission estimates in previous studies (Riddick et al., 2016; Xu et al., 2016; Zhou et al., 2016). The most widely applied EF of 10% was reported in the Intergovernmental Panel on Climate Change (IPCC) Tier 1 guidelines. Other studies provided global mean EFs ranging from 14 to 21% (Beusen et al., 2008; Bouwman et al., 2002b; report, 2001). However, these studies based on constant EFs were one-year estimates that did not consider how NH_3 emissions respond to climate change and variability.

Process-based models are another popular approach for estimating NH_3 emissions. For instance, the bi-directional NH_3 exchange module has been incorporated into the US Environmental Protection Agency's (EPA) Community Multiscale Air-Quality model (CMAQ, Byun and Schere (2006)) and coupled with the United States Department of Agriculture's (USDA) Environmental Policy Integrated Climate (EPIC) agroecosystem model (Bash et al., 2013; Massad et al., 2010; Nemitz et al., 2000) to estimate seasonal and annual NH_3 emissions from synthetic N fertilizer applications. The Flow of Agricultural Nitrogen (FAN) process model has been combined within the Community Land Model 4.5 to compute the reactive N flows and NH_3 emissions (Riddick et al., 2016). Our previous study incorporated the bi-directional NH_3 exchange module in CMAQ within the Dynamic Land Ecosystem Model (DLEM, Tian et al. (2011)) (DLEM-Bi- NH_3) and applied this model to estimate NH_3 emissions from Asian agricultural systems for 1961–2014 (Xu et al., 2018).

The current study applied the DLEM-Bi- NH_3 module to estimate NH_3 emissions from synthetic N fertilizer application in global croplands from 1961 to 2010. The objectives of this paper were to: (1) investigate spatial and temporal variations of NH_3 emissions; (2) examine the impact of climate factors on NH_3 emissions driven by four historical climate datasets; (3) analyze

crop-specific NH₃ emissions from global croplands; and (4) compare global NH₃ emissions from model simulations with estimates from EFs in the IPCC Tier 1 guideline.

2. Methodology and inputs

2.1. Input data description

Input datasets for the DLEM-Bi-NH₃ simulations include a natural vegetation map, land use change (LUC), synthetic N fertilizer application, atmospheric CO₂ concentration, and time series of climate at a spatial resolution of 0.5° × 0.5°. The developed natural vegetation map was based on SYNMAP (Jung et al., 2006), which rendered fractions of 47 vegetation types in each 0.5° grid. These 47 vegetation types were converted to 15 plant functional types for use in the DLEM through a cross-walk table with a spatial pattern that can be found in Pan et al. (2015) and Xu et al. (2017). Cropland distribution datasets were developed by aggregating 5-arc minute resolution HYDE v.3.2 global cropland distribution data (Klein Goldewijk et al., 2017) to the resolution of 0.5° × 0.5° latitude/longitude. Spatially-explicit LUC data for 1900–2005 was retrieved from high-resolution remotely sensed data, field surveys and contemporary LUC patterns reported in China’s National Land Cover Datasets (Liu and Tian, 2010; Lu et al., 2012; Ren et al., 2012); this dataset has been updated to the year 2010. The land-use change dataset for India was developed from remote sensing datasets available from the Advanced Wide-Field Sensor of Resourcesat-1 during 2005–2009 in combination with three inventory datasets during 1880–2010 to reconstruct LUC at 5-arc minute resolution during 1880–2010 (Tian et al., 2014). Land-use change datasets of China and India were aggregated to 0.5° to replace HYDE v.3.2 for both regions from 1900 to 2010. Cropland spatial distribution within each grid for 1961 and 2010 are shown in Figure 7-1. A spatially-explicit time-series dataset of agricultural N fertilizer use was developed

through spatializing IFA-based country-level N fertilizer consumption according to crop specific N fertilizer application rates, crop type distribution, and historical cropland distribution during 1960–2013 (Lu and Tian, 2017).

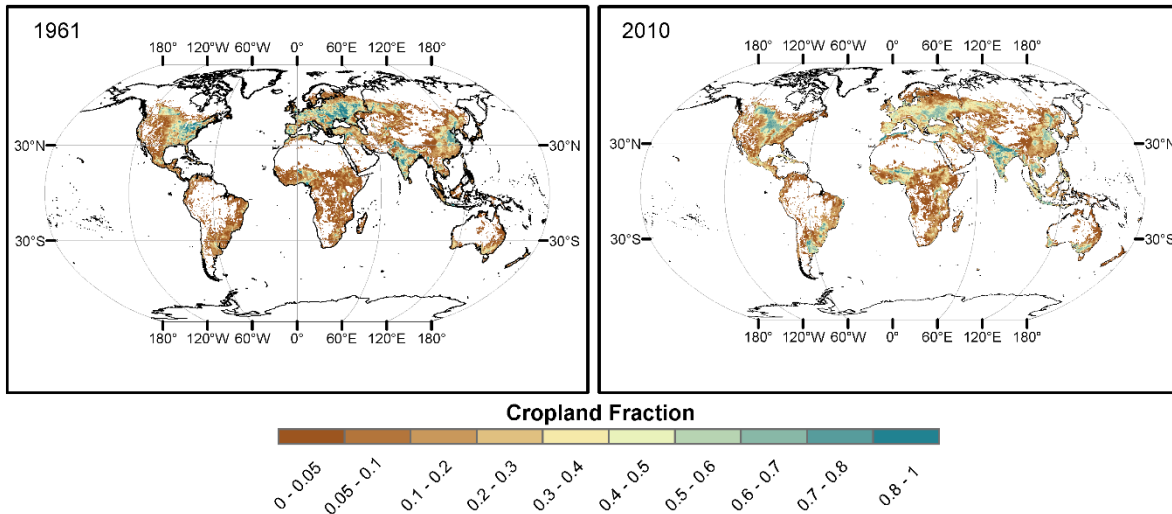


Figure 7-1. The spatial distribution of cropland area within each grid in 1961 and 2010.

Half-degree daily climate data (e.g., average, maximum, minimum air temperature, precipitation, relative humidity, and shortwave radiation) were derived from CRUNCEP climate forcing data (Wei et al., 2013). Long-term average climate datasets (1901 to 1930) were used to represent the initial climate state in 1900. Three additional climate datasets (PGMFD v.2, GSWP3, and WFDEI_WFDEI) with $0.5^\circ \times 0.5^\circ$ resolution of daily climate data were obtained from the Inter-Sectoral Impact Model Integration and Intercomparison Project (ISI-MIP 2.1). All data are available at the ISI-MIP website (www.isimip.org). The monthly CO_2 concentration dataset obtained from NOAA extended GLOBALVIEW- CO_2 spanned the time period of 1900 to 2010 (<http://www.esrl.noaa.gov/gmd/ccgg/globalview/co2/>).

2.2. Model simulation experiments and implementation

Six simulation experiments were conducted to achieve our objectives. Implementation of the DLEM-Bi-NH₃ simulation included three steps: (1) equilibrium run, (2) spin-up run, and (3) transient run. All datasets used to drive the model in the equilibrium run were in 1900. The equilibrium state was assumed to be reached when intra-annual variations of carbon, nitrogen, and water storage were less than 0.1 g C/m², 0.1 g N/m² and 0.1 mm, respectively, during two consecutive 50 years in each grid. The long-term mean climate data for 1901 to 1930 were used to represent 1900 climate. Following the equilibrium run, the model was spun-up by de-trended climate data (1901 to 1930) to allow smoother model mode transitions from equilibrium runs to transient runs more smoothly (i.e., three spins with 10-year climate data each time). Finally, the model was run in the transient mode using daily climate data, CO₂ concentration, N fertilizer application, and LUC inputs for the 1901 to 2010 time period. We conducted three simulation experiments (S1, S2, and S3) driven by CRUNCEP climate forcing data to investigate the response of global NH₃ emissions to temperature and precipitation changes in the historical period (Table 7-1). The difference in NH₃ emissions simulated by S3 and S1 experiments refers to the climate effects: the difference between S2 and S1 experiments reflected temperature effects and precipitation effects was from the difference between S3 and S2 experiments. To estimate the NH₃ emission response to different climate datasets, four simulation experiments (S3–S6) were conducted, driven by different climate datasets during 1901–2010.

Table 7-1. Simulation experiment design in this study.

Experiments	Climate			Nitrogen Fertilizer	CO ₂	LUC
	Source	Temperature	Precipitation			
Initial simulation	CRUNCEP	Averaged (1901–1930)	Averaged (1901–1930)	1900	1900	1900
S1	CRUNCEP	Averaged (1901–1930)	Averaged (1901–1930)	1901–2010	1901–2010	1901–2010
S2	CRUNCEP	1901–2010	Averaged (1901–1930)	1901–2010	1901–2010	1901–2010
S3	CRUNCEP	1901–2010	1901–2010	1901–2010	1901–2010	1901–2010
S4	WFDEI.GPCC	1901–2010	1901–2010	1901–2010	1901–2010	1901–2010
S5	GSWP3	1901–2010	1901–2010	1901–2010	1901–2010	1901–2010
S6	PGMFD v.2	1901–2010	1901–2010	1901–2010	1901–2010	1901–2010

3. Results

3.1. Temporal changes in global NH₃ emissions

We quantified NH₃ emissions from global croplands associated with synthetic N fertilizer application during 1961–2010. Model simulations showed a significant increase in annual mean global NH₃ emissions (Figure 7-9). Compared to the 1960s (2.76 ± 1.50 Tg N yr⁻¹), we estimated an increase of 12.03 ± 0.82 Tg N yr⁻¹ (436%) in NH₃ emissions associated with a 71.38 Tg N yr⁻¹ increase in mean N fertilizer applied to croplands in the 2000s driven by four different climate datasets (S3–S6). Error bars, ± 2 standard deviation (s.d.) calculated from simulation results based on four different climate datasets. The highest global mean NH₃ emission was estimated at 16.72 ± 0.47 Tg N yr⁻¹ in 2010. Total NH₃ emissions associated with different climate datasets varied significantly with a maximum value for WFDEI.GPCC (16.95 Tg N yr⁻¹) and a minimum value for CRUNCEP (16.48 Tg N yr⁻¹) in 2010. Global NH₃ emissions positively responded to increased N fertilization whose temporal trends were similar to N fertilizer input trends. Thus, although climate is an important factor that affects NH₃ emissions from global croplands, the rapid

increase in synthetic N fertilizer applications was the more dominant factor impacting the rise in global NH₃ emissions in the past half century.

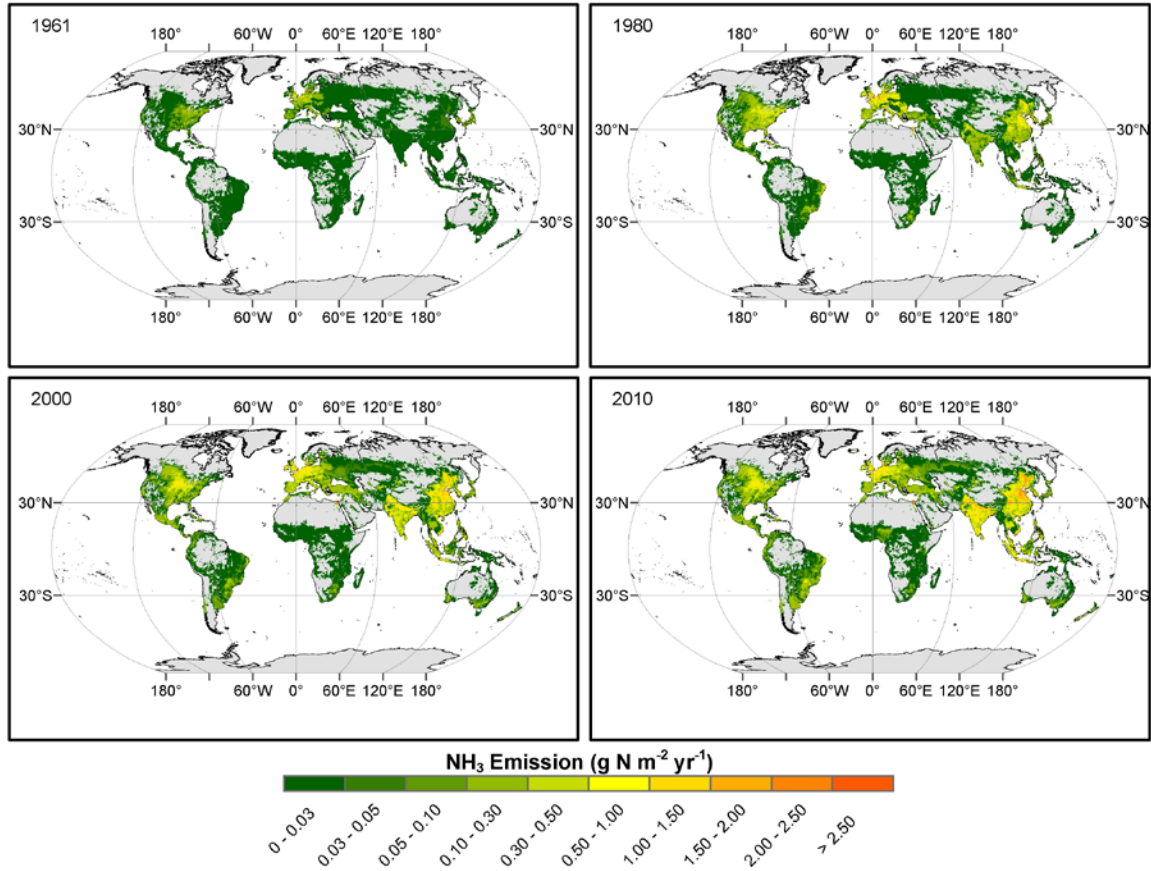


Figure 7-2 The spatial pattern of simulated NH₃ emission from global croplands in 1961, 1980, 2000, and 2010.

3.2. Spatial pattern of global NH₃ emissions

Ammonia emissions varied widely across countries and regions. The magnitude of differences between regions became larger with the increase in global NH₃ emissions during 1961–2010 (Figure 7-2). In the 1960s, major sources were North America and Europe, which contributed to 70% of total annual emissions at an estimated rate of 0.3 to 0.5 g N m⁻² yr⁻¹ (Figure 7-3). Emission rates from remaining grids of different continents stayed within 0~0.05 g N m⁻² yr⁻¹. In the 1980s and 1990s, a large NH₃ emission increases were found in all continents of the

Northern Hemisphere, especially in southern Asia, where NH_3 emission rates were as high as $1.5\text{--}2.0 \text{ g N m}^{-2} \text{ yr}^{-1}$. Total contributions from North America and Europe was 43.2% in the 1980s and 34.2% in the 1990s. The largest variation in spatial patterns were in the 2000s (Figure 7-3). Southern Asia contributed 61.14% of total emissions. The highest emission rate was found in the North Plain of China, which was greater than $3.0 \text{ g N m}^{-2} \text{ yr}^{-1}$ (Figure 7-2). With expansion of cropland and increased N fertilizer consumption in the Southern Hemisphere, all continents showing substantial increases in NH_3 emission rates (within a mean range of $0\text{--}0.05 \text{ g N m}^{-2} \text{ yr}^{-1}$ in the 1960s) shifted to a range of $1.0\text{--}1.5 \text{ g N m}^{-2} \text{ yr}^{-1}$ in the 2000s.

From a continental perspective, North America, Europe, and southern Asia were the three major NH_3 emissions regions in the 1960s (i.e., 1.01 ± 0.46 , 0.91 ± 0.44 , and $0.60\pm 0.48 \text{ Tg N yr}^{-1}$, respectively). Only Europe showed a declining emission trend since the 1980s, with a mean decrease rate of $\sim 0.6 \text{ Gg N yr}^{-2}$ ($1 \text{ Gg} = 1 \times 10^3 \text{ Tg}$). The decadal change in NH_3 emissions from North America was slight since the 1980s. In contrast, southern Asia became the leading emitter with a mean increase rate of $\sim 225.8 \text{ Gg N yr}^{-2}$ (Figure 7-4) during 1980–2010. In the 1960s, NH_3 emissions from South America, Africa, and Oceania were 0.06 ± 0.05 , 0.08 ± 0.04 , and $0.014\pm 0.012 \text{ Tg N yr}^{-1}$, respectively. South America and Africa showed a large increase in NH_3 emissions since the 1990s, with a mean rate of ~ 42.4 and $\sim 10 \text{ Gg N yr}^{-2}$, respectively. Oceania showed an increasing trend with a mean rate of $\sim 7.5 \text{ Gg N yr}^{-2}$. Ammonia emissions have been highly concentrated since 1988, with more than 50% of emissions sourced from southern Asia. The highest emission in North America, southern Asia, and Europe was estimated as 2.46 ± 0.09 in 1991, 10.21 ± 0.5 in 2009, and $2.30\pm 0.03 \text{ Tg N yr}^{-1}$ in 1990, respectively.

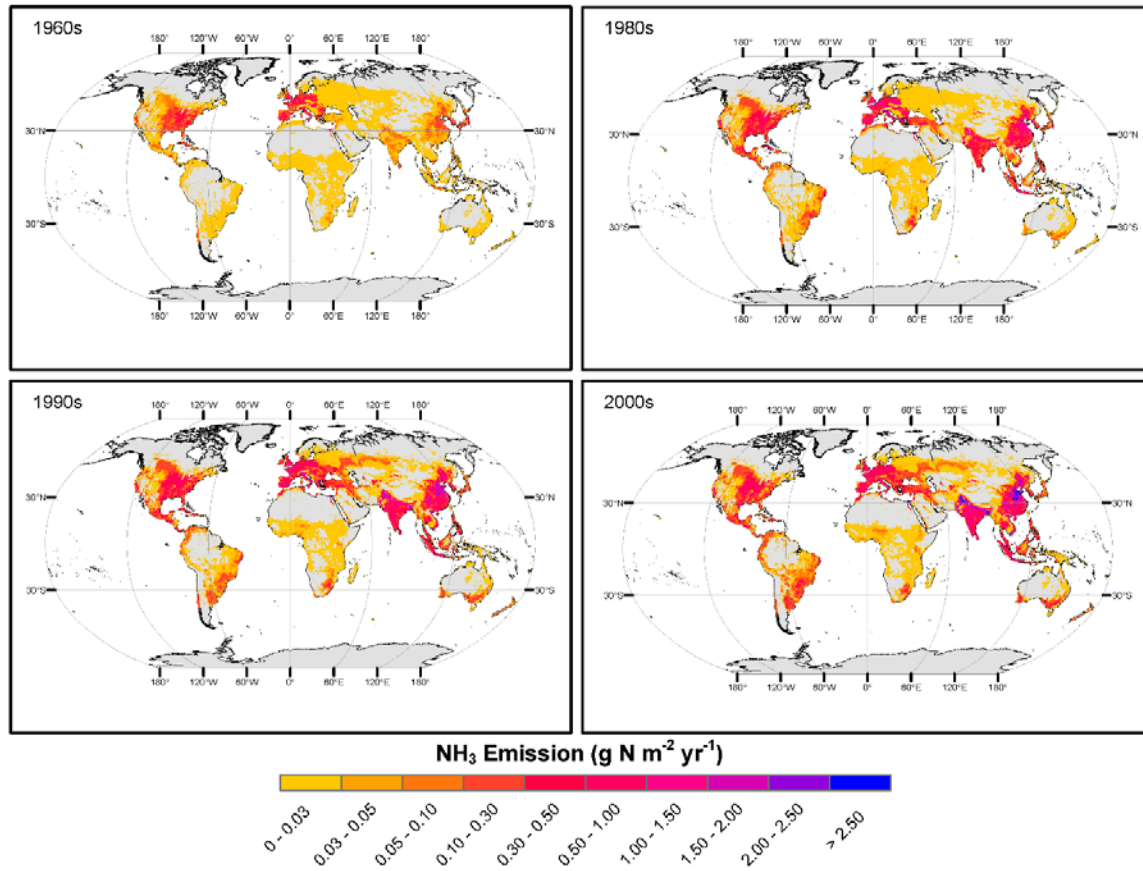


Figure 7-3. Simulated ammonia (NH₃) emissions response to application of synthetic nitrogen (N) fertilizer in the 1960s, 1980s, 1990s, and 2000s.

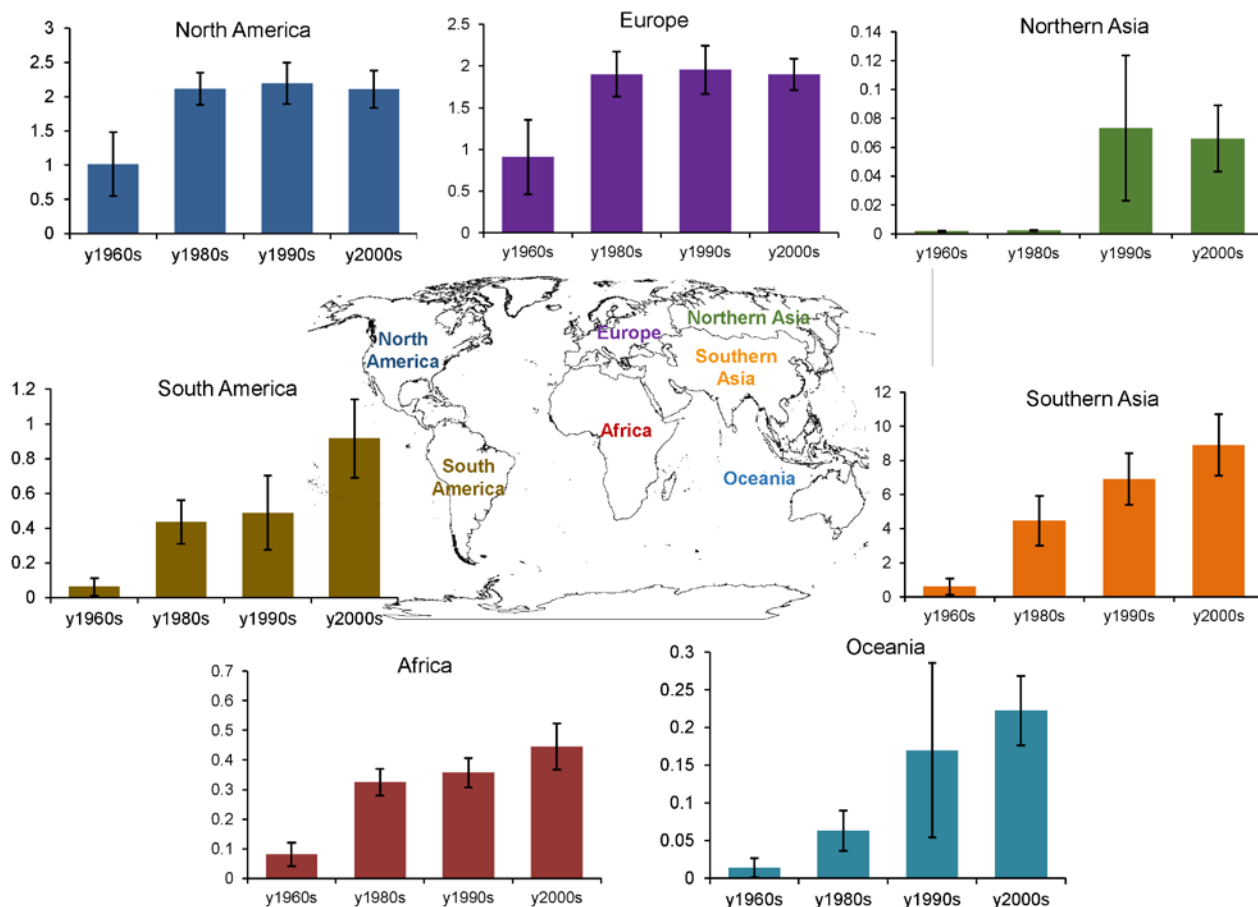


Figure 7-4. The contemporary estimation of ammonia (NH₃) emission at continental scales in the 1960s, 1980s, 1990s, and 2000s. The displayed NH₃ emissions in the historical period were the mean of simulation results driven by four climate datasets, with uncertainty of 95% confidence interval. All units are Tg N yr⁻¹.

3.3. Intra-annual changes of global and regional NH₃ emissions

In terms of intra-annual variation, we only focused on emissions in the 2000s driven by one climate dataset (CRUNCEP). There were two peaks (March–April–May and June–July–August) of global NH₃ emissions from N fertilizer applications during 2000–2010 (Figure 7-5), which contributed about 72% of total N fertilizer-induced emissions. In contrast, December–January–February contributed least and accounted for less than 10% of total emissions. The NH₃ emissions during June–July–August showed an increasing trend during 2000–2010.

Meanwhile, the seasonal contribution of NH₃ emissions varied for the different continents (Figure 7-6). In Asia, the estimated NH₃ emissions in winter (December to February), spring (March to May), summer (June to August), and autumn (September to November) accounted for 5.9%, 22.2%, 56.6%, 15.3% of the annual emission, respectively. In North America, the estimated NH₃ emissions in winter, spring, summer, and autumn accounted for 3.7%, 64.9%, 19.2%, 12.2% of the annual emission, respectively. In Europe, the estimated NH₃ emissions in winter, spring, summer, and autumn accounted for 1.6%, 63.2%, 0.3%, 34.9% of the annual emission, respectively.

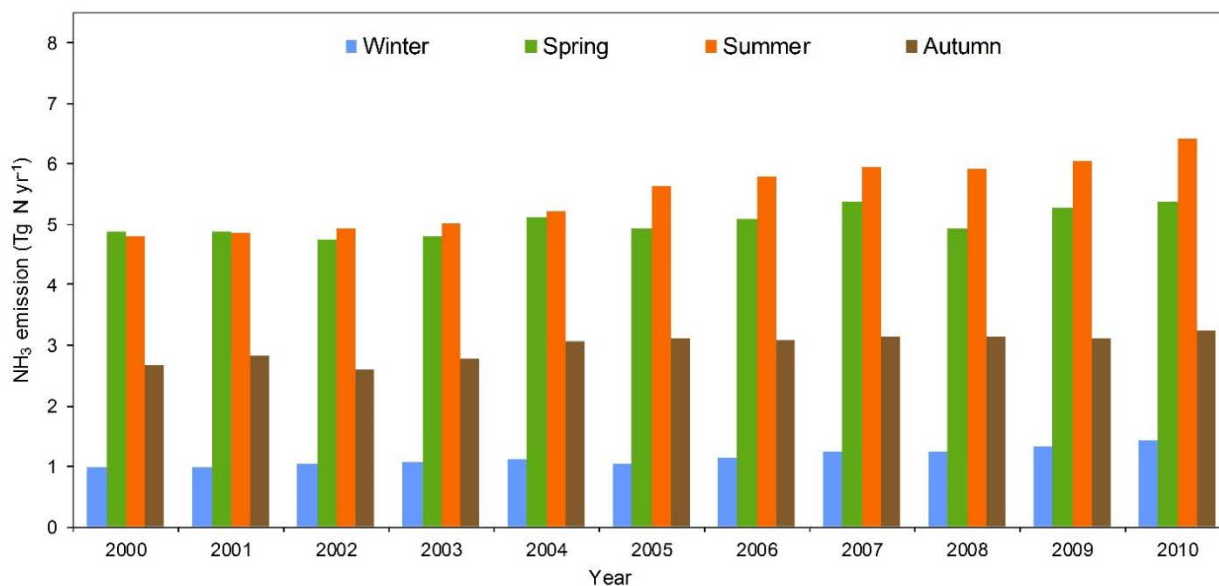


Figure 7-5. Simulated seasonal NH₃ emissions from global croplands during 2000–2010.

From December to February, regions close to the tropics ($\pm 30^\circ$) were significant sources of NH₃ emissions (e.g., Northeast and South India, South Africa, and Brazil; Figure 7-6). From March to May, the emissions shifted to the Northern Hemisphere, where North America, Europe, and southern Asia were the largest sources of global NH₃ emission; this was especially true for the Midwestern United States, Europe, North Plain of China, and North India (Figure 7-6). In addition,

regions within the northern tropics acted as NH_3 sources (e.g., Mexico and Southeast Asia). In summer, the Northern Hemisphere continuously acted as the largest NH_3 source. Moreover, NH_3 emission were substantial the entire area of India and the North, Northeast, and Southeast Plain of China, and most countries in Southeast Asia. However, there was a slight emission associated with Europe and the Midwestern United States. During autumn, NH_3 emissions covered all continents of the Earth's surface.

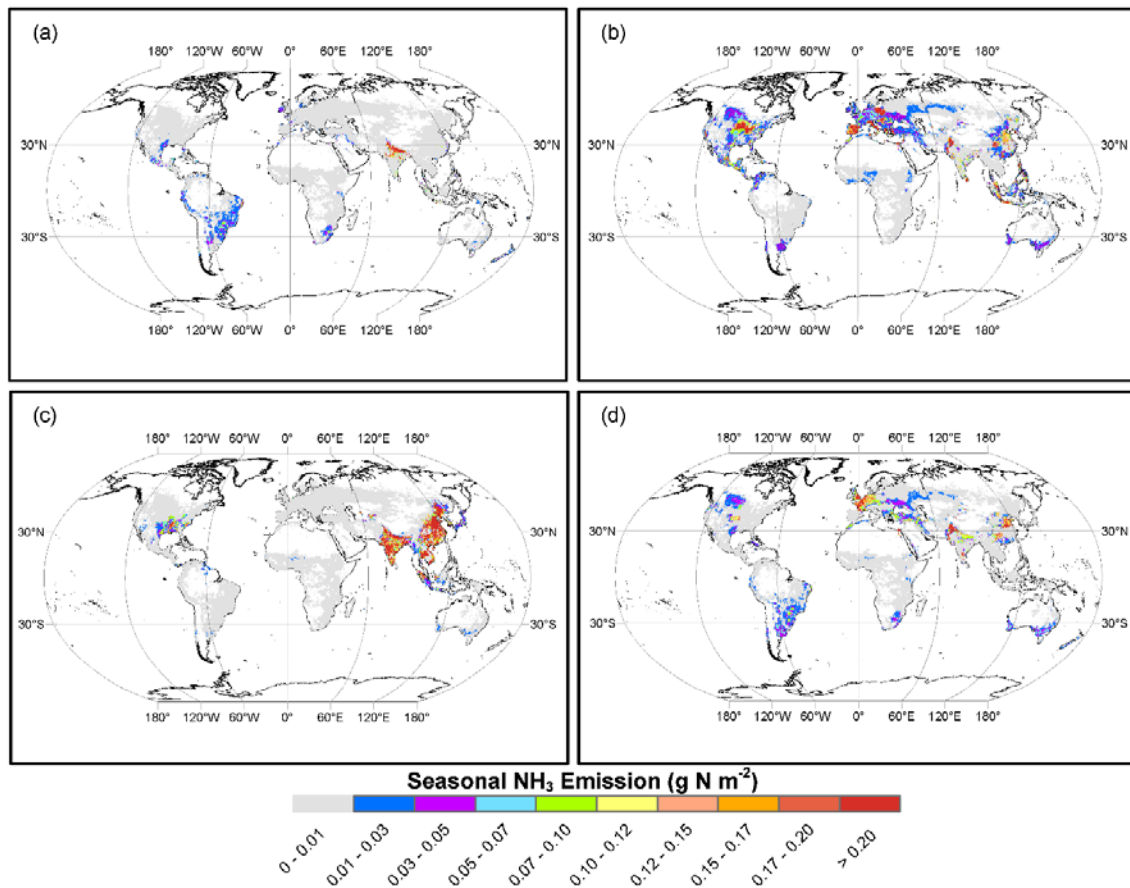


Figure 7-6. Simulated seasonal mean ammonia (NH_3) emissions in the 2000s: (a) December–January–February, (b) March–April–May, (c) June–July–August, and (d) September–October–November.

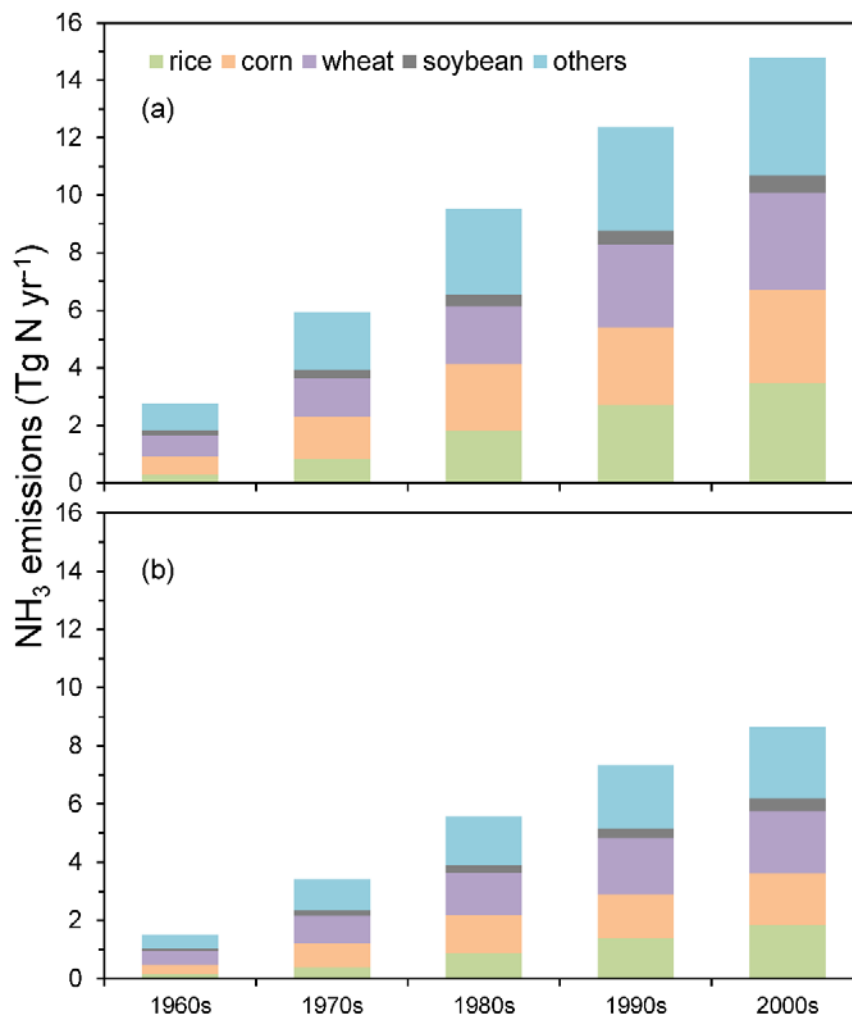


Figure 7-7. Crop-specific NH₃ emissions from synthetic N fertilizer application estimated by the DLEM-Bi-NH₃ module (a) and the IPCC EF (b).

3.4. Crop-specific NH₃ emissions

From a crop-type perspective, we identified four major global crops (rice, corn, wheat, and soybean) and estimated NH₃ emissions from these crops due to synthetic N fertilizer application during 1961–2010. These four crops accounted for 67% of the total emission during the 1960s, among which wheat and corn were the two main sources (Figure 7-7). In the 2000s, the largest source of NH₃ emissions was from rice (23.5%), followed by wheat (22.8%), and corn (21.9%) (Figure 7-8). Soybean only accounted for less than 10% of the global annual total NH₃ emissions

from 1961 to 2010 (Figure 7-7). The transition of global NH₃ emissions from wheat and corn to rice, wheat, and corn was due to area expansion and increased fertilizer use in rice cultivation from 1961 to 2010 in the context of global warming.

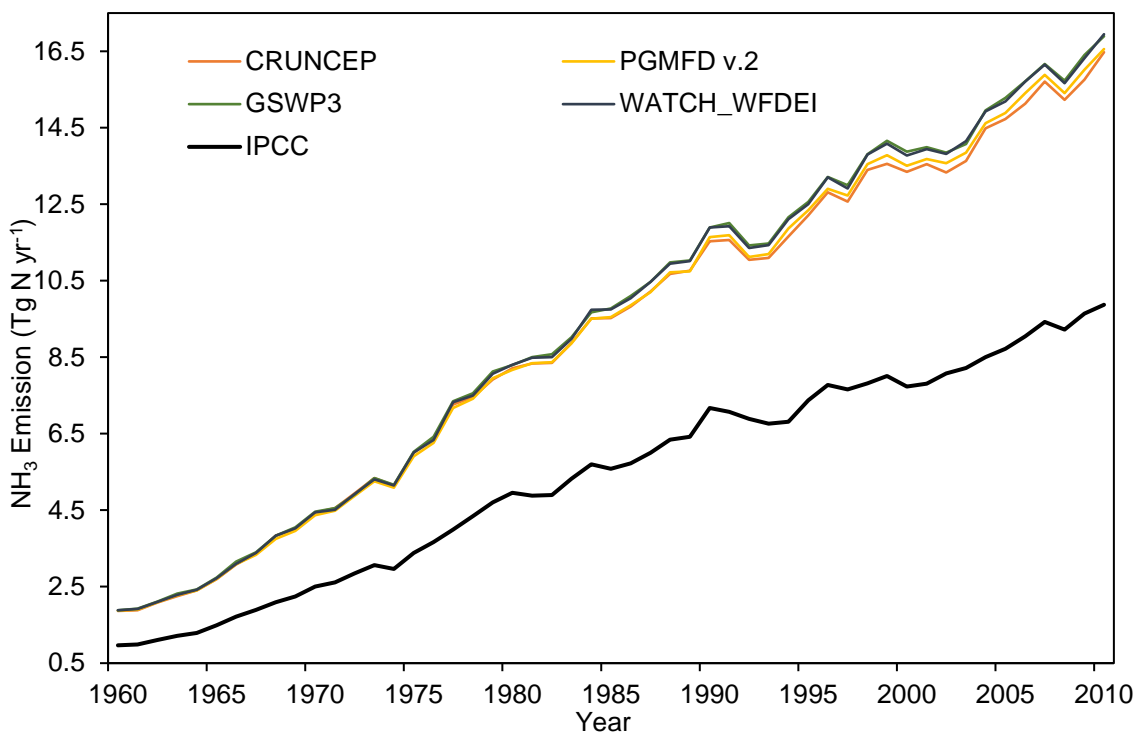


Figure 7-8. Global NH₃ emissions from DLEM-Bi-NH₃ simulations (CRUNCEP, PGMFD v.2, GSWP3, and WATCH_WFDEI) and emission factor in the IPCC Tier1 guideline.

3.5. Comparisons with the estimate by the IPCC Tier1 guideline methodology

The IPCC Tier1 guideline methodology used a constant EF of 10% to estimate global NH₃ emissions from synthetic N fertilizer use; i.e., emissions are equal to 10% of annual applied fertilizer amounts. Herein, global NH₃ emission from synthetic N fertilizer use was estimated to be 1.0 and 9.9 Tg N yr⁻¹ in 1961 and 2010, respectively, based on the EF proposed in the IPCC Tier1 guideline methodology. In contrast, the simulated results from the DLEM in both years were nearly two times higher than the IPCC EF estimates (Figure 7-8). The spatial patterns of EF-based

results differed from those of our model simulations (Figures 5-3 & 5-10). In the 1960s, NH₃ emissions from most regions based on DLEM simulations were slightly larger than IPCC EF estimates (mean range of 0–0.3 g N m⁻² yr⁻¹) except for northern Europe and western United States. During the 1980s and 1990s, DLEM results were far larger than EF-based results in most regions across the globe (i.e., the upper and eastern Midwest of the United States and southern Asia, especially China, India, and Pakistan). The negative difference between EF-based and DLEM NH₃ emissions became much larger in some regions (i.e., northern and the upper eastern Europe, and the western United States) compared to differences in the 1960s. Also, negative differences appeared in western China (where most drylands are located), which was as low as 1.0 g N m⁻² yr⁻¹. The largest difference in NH₃ emissions (i.e., per grid) appeared in the 2000s in northern India (> 5.0 g N m⁻² yr⁻¹). In the Southern Hemisphere, DLEM results were continuously higher than IPCC EF estimates and the positive differences between these two approaches became larger during 1961–2010.

We compared crop-specific NH₃ emissions estimated by DLEM and IPCC EF during 1961–2010 (Figure 7-7). Rice, wheat, and corn were three dominant crops responsible for the significant increase in NH₃ emissions from global croplands due to application of synthetic N fertilizer. Overall, DLEM NH₃ emissions from rice cultivation tended to increase faster than wheat and corn during 1961–2010 (Figure 7-10). During the 1960s, the increasing rate of NH₃ emissions from rice, wheat, and corn according to DLEM were 0.83, 0.65, and 0.68 Tg N decade⁻², respectively. In contrast, the increased rate for these crops based on the IPCC EF was 0.43, 0.36, and 0.44 Tg N decade⁻², respectively.

4. Discussion

4.1. Comparisons with other studies

We compared our model results against previous studies based on EFs and process-based models at global and regional scales. In our study, a general EF was calculated as modeled emissions divided by total N fertilizer applied across the global. At the global scale, the DLEM-simulated mean NH₃ emission in 2000 was 13.63±0.48 Tg N, which was ~14% higher than the FAN model estimates of Riddick et al. (2016) (Table 7-2). In comparison, the DLEM-simulated mean EF was 17.6%, which is slightly lower than their simulation (EF: 19%) in 2000. Although both studies are based on model simulations, our estimates are different for two major reasons: 1) model structures and parameters in both studies differed significantly; and 2) input datasets and fertilization timings were from various sources. For example, total synthetic N inputs and spatial patterns in our study were generated by Lu and Tian (2017), while Riddick et al. (2016) determined synthetic fertilizer application rates based on data provided by Potter et al. (2010). The estimated global NH₃ emission from synthetic N fertilizer was ~9 Tg N yr⁻¹ in 1995 based on the EF calculated by Bouwman et al. (2002), which was 27% lower than our estimate (12.4 Tg N yr⁻¹; Table 7-2). Consequently, the estimated EF in Bouwman et al. (2002b) was lower than the EF in our study for the same year. Differences between these studies were due to the synthetic N fertilizer dataset and estimate methodology. Generally, process-based model estimates of this study and previous estimate by Riddick et al. (2016) are higher than EF-based estimates (Table 7-2).

At the country scale, several studies have estimated NH₃ emissions from hot regions (e.g., China, India, and United States) using various approaches; however, there are large uncertainties with these estimates. Comparisons of estimated NH₃ emissions from synthetic N fertilizer applications in China and India from different studies were listed in Xu et al. (2018a). Calculated 2002 NH₃ emissions in the United States (based on the CMAQ-EPIC model) were 73.68% lower

than our estimates (Bash et al., 2013). However, our 2008 estimate was similar to the NEI 2008 value.

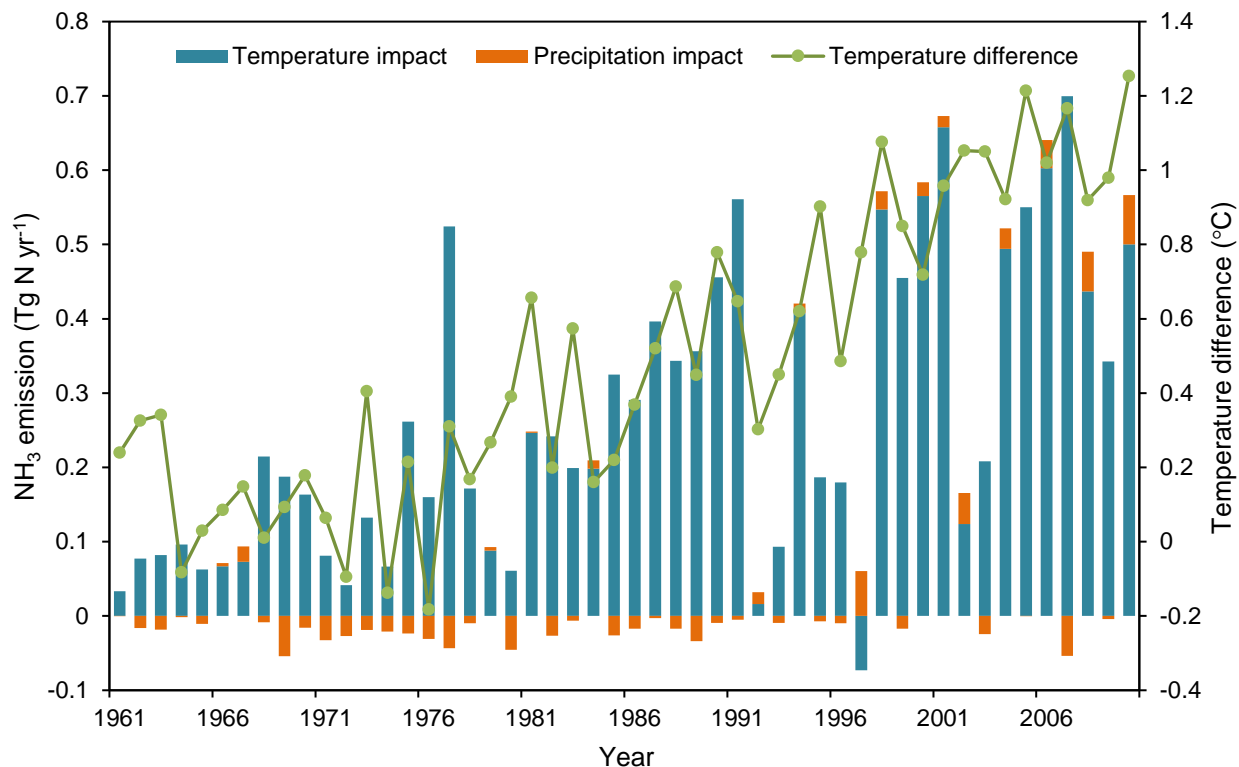


Figure 7-9. Climate effect on ammonia (NH₃) emissions during 1961–2010. The temperature impact on annual NH₃ emissions was calculated through the difference between S2 and S1 experiments; the precipitation impact on annual NH₃ emissions was calculated through the difference between S3 and S2 experiments; the temperature difference equals annual average temperature during 1961–2010 minus the average temperature during 1901–1930.

4.2. Climate effects on NH₃ emissions at spatiotemporal scales

By performing DLEM simulations based on four climate datasets from 1961–2010, we found that annual differences between various climate datasets were the primary factors affecting heterogeneity of simulation results. Annual estimates from CRUNCEP were lowest among all results driven by the other three climate forcing datasets. Additionally, differences rose with

increasing temperature during 1980–2010. Our simulated results show that climate effects on NH₃ emissions increased largely from 33.1 Gg N yr⁻¹ in 1961 to 566.5 Gg N yr⁻¹ in 2010, with substantial year-to-year variations. The average impact of climate variation is about 3%, ranging from 0% to 7% of annual total NH₃ emissions due to inter-annual variations during the period of 1961–2010. The increasing trend and variations in NH₃ is closely associated with increasing global annual temperature with large inter-annual variations. We found that annual NH₃ emissions increased with rising temperature and exhibited large inter-annual variations (Figure 7-9). Temperature increase was a dominant factor that promoted climate effects in global NH₃ emissions. In most years, precipitation had a negative impact on increasing annual emissions to a small extent. This highlights the necessity to consider climate factors when estimating NH₃ emissions from agricultural soils.

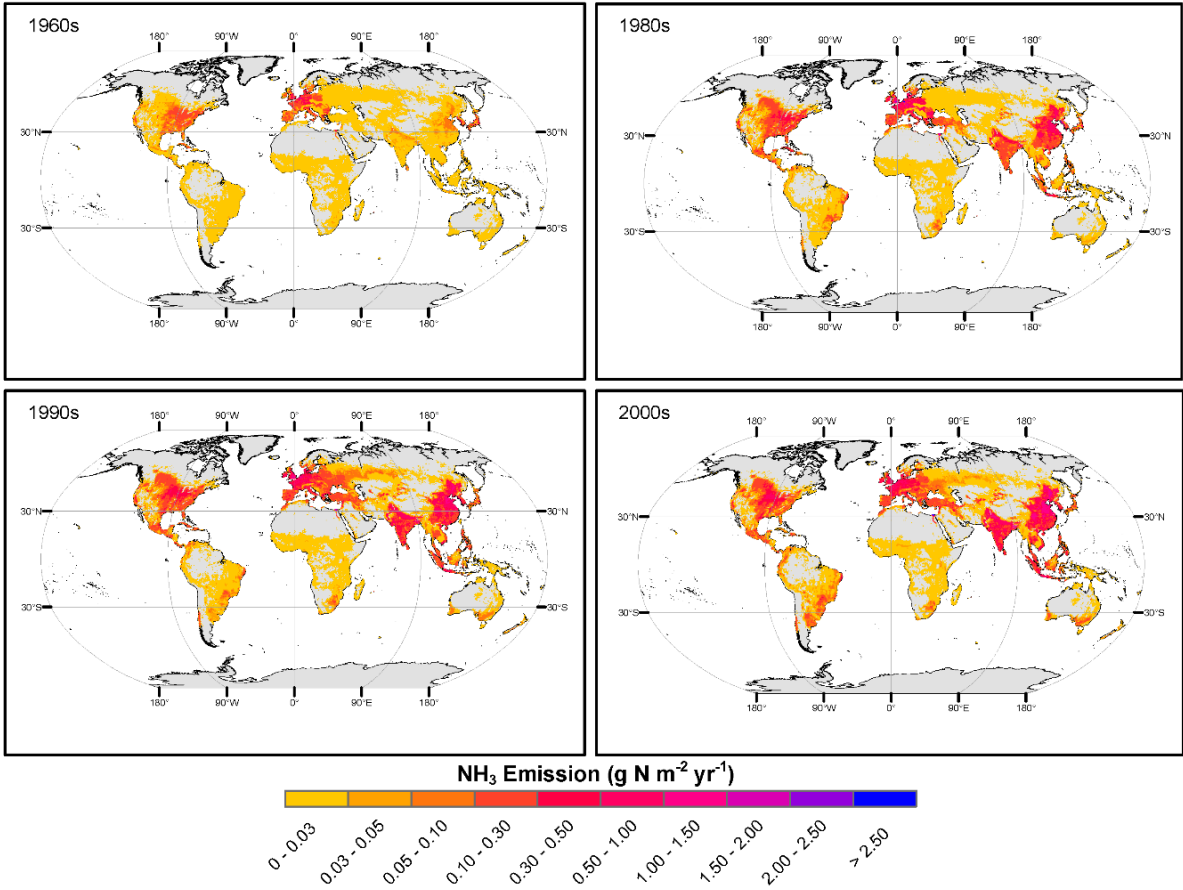


Figure 7-10. The spatial pattern of NH₃ emission based on IPCC EF from global croplands in the 1960s, 1980s, 1990s, and 2000s.

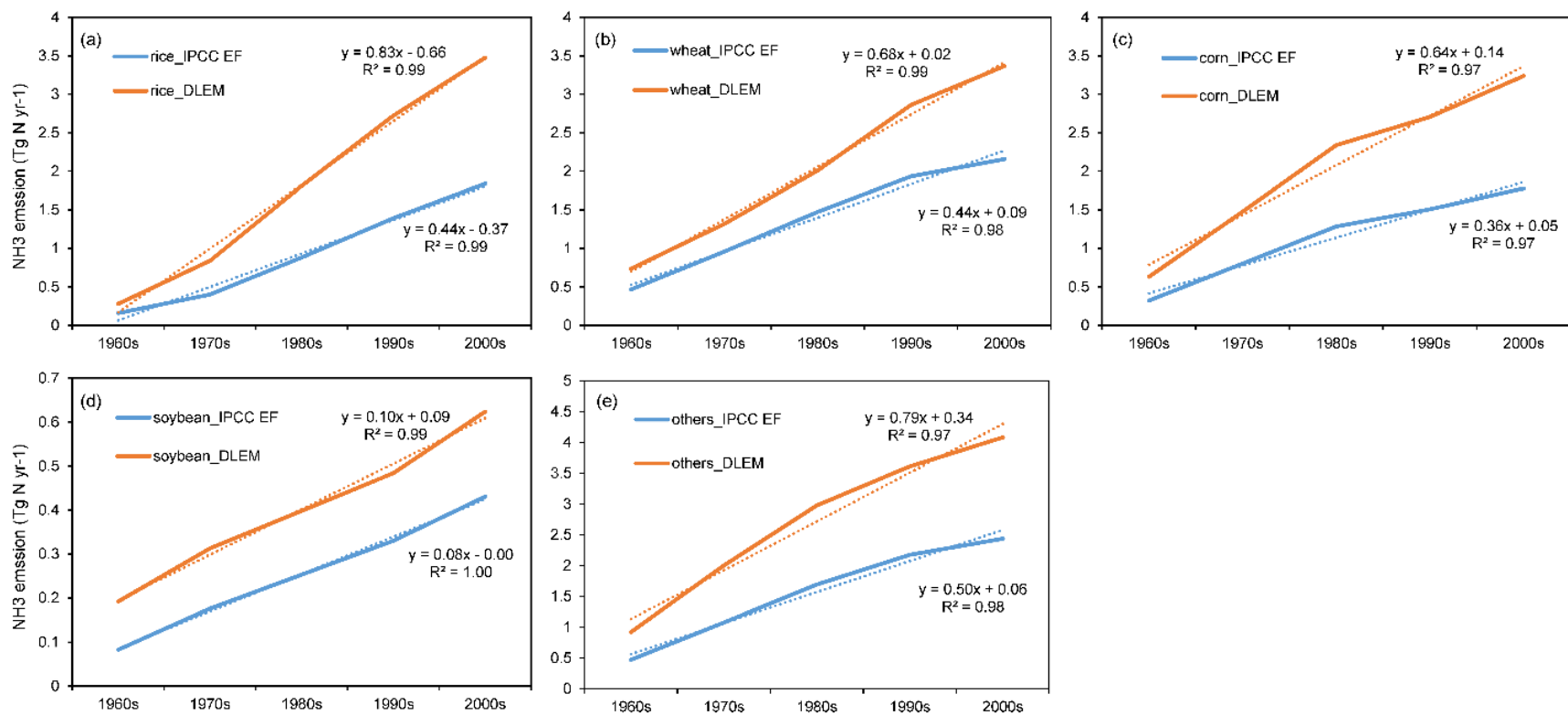


Figure 7-11. The decadal trends of crop-specific NH₃ emissions during the 1960s to the 2000s: (a) rice, (b) wheat, (c) corn, (d) soybean, and (e) other crops.

Table 7-2. Estimates of global NH₃ emissions (expressed in Tg N yr⁻¹) based on different approaches.

Region	Year	Method	NH ₃ emission	Reference
Global	2000	DLEM-Bi-NH ₃	13.63 ± 0.48	This study
	1995		12.41 ± 0.32	
	2000	IPCC Tier 1 guideline	7.74	IPCC, 2006
	2000	Process-based model	12.0	Riddick et al. (2016)
	1995	Constant EF	9.0	Bouwman et al. (2002b)

Previous studies emphasized that NH₃ volatilization from N fertilizer application depends strongly on localized environmental factors; however, this impact has not been investigated at the global and regional scale, and on crop-specific emissions globally (Fu et al., 2015; Huang et al., 2012; Zhang et al., 2011). Agricultural systems are more complex due to the combination of human management and climate effects. Thus, process-based models could be an effective approach to address NH₃ exchange processes (Sutton et al., 2013). However, the EF used in the IPCC Tier 1 guideline was a constant value regardless of regional variations affected by environmental factors. Our study provides comprehensive comparisons of crop-specific NH₃ emissions from global croplands between a constant EF and process-based models at the global and regional scale. Results showed that differences between the two approaches increased from 1.0 Tg N yr⁻¹ to 6.9 Tg N yr⁻¹ during 1961–2010. The largest positive difference was found in regions with warmer climates and/or with higher N fertilizer applications (e.g., southern Asia and North America; Figure 7-6). Negative differences were found in regions with dry or cold climates (e.g., Northern Europe and western North America), which indicates that climate effects in these regions could retard NH₃ emissions. In our simulations, environmental factors (i.e., climate, soil properties, and cropland management strategies) were applied to simulate NH₃ emissions in each grid to better

reflect NH_3 emission processes in real agricultural systems. Utilizing a constant EF without considering environmental factors could, to some extent, underestimate NH_3 emissions in the context of global warming. Similarly, Zhou et al. (2016) found that the estimated annual NH_3 emission in China using a nonlinear model was 40% greater than that derived from the IPCC Tier 1 guideline.

Crop-type scale comparisons demonstrated the importance of environmental impacts on NH_3 emissions. Our study provides evidence that NH_3 emissions were crop-type dependent and were dominated by location and N fertilizer requirements. Crops such as barley grown at high latitudes where temperatures were much lower than in the tropics contributed half of total emissions compared to calculations based on the IPCC EF. In our study, emissions from rice-cultivated regions (primarily in East, South, and Southeast Asia) were two times higher than IPCC EF estimates and showed an increasing trend (Figures 5-7 & 5-11). Although not the largest receiver of global N fertilization in 2010 (Zhang et al., 2015), rice was the top-ranking crop contributing to global NH_3 emissions, followed by corn and wheat. A possible explanation is that high temperature is the dominant factor that accelerates NH_3 emissions from rice cultivation. However, Bouwman et al. (2002b) mentioned that NH_3 volatilization from rice paddy is complicated since it is dependent on rice height, aquatic biota growth that regulates floodwater pH, and N fertilizer application timing and approaches.

Climate effects are of great importance and should be considered when estimating NH_3 emissions. By performing with/without climate and temperature-only simulations, we were able to evaluate the contribution of different climate factors to the increase in global NH_3 emissions during the historical period. Simulation results indicated that temperature was the dominant factor behind increased emissions (Figure 7-9).

4.3. Causes of intra-annual variations at regional scales

Intra-annual NH₃ emissions are highly correlated to dates and N fertilizer application amounts. Overall, rice, corn, and wheat received more than 50% of the world's synthetic N fertilizer (Heffer, 2013) and were the three major NH₃ emission sources that account for ~65% of total emissions during 1961–2010 in this study. In Asia, the estimated NH₃ emissions were highest from summer (June to August), accounting for 56.6% of the annual emission. Higher summer emissions were associated with cultivation periods and N fertilizer application timings (see detailed description in (Xu et al., 2018a) Text S1). Rice cultivation areas in East, South, and Southeast Asia contributed 89% of the world total (Yan et al., 2003). In this study, rice fields were the largest contributor to total Asian emissions since rice is the major cereal crop cultivated in subtropical and tropical regions of Asia (East, South, and Southeast Asia) that use large amounts of fertilizer each summer (Aulakh et al., 2001; Mahajan et al., 2012; Zou et al., 2005). For example, rice cultivation in China, India, Indonesia, Vietnam, Thailand, Bangladesh, and Philippines represented 16%, 30%, 45%, 60%, 45%, 83%, and 48% of total N fertilizer applied to all crops for each country, respectively (Heffer, 2013). As discussed above, warmer temperature during summer can stimulate NH₃ emissions in these regions thereby resulting in higher NH₃ emissions from fertilizer use.

In contrast, spring (March to May) accounted for about 60% of annual emissions in North America and Europe due to high fertilizer use for corn and winter/spring wheat. Corn is generally cultivated in April and May in northern mid-latitudes, winter wheat is usually planted in the fall (September and October), and spring wheat is generally planted in late spring (NASS, 2010; Sacks et al., 2010). We identified fertilizer timings according to field experiments, where N fertilizer was applied to corn and spring wheat at or before planting in spring, and the following March for winter

wheat (Alluvione et al., 2010; Guy and Gareau, 1998; Kurokawa et al., 2013; Lopez-Bellido et al., 2007). For example, corn and wheat cultivations represented 47% and 13%, respectively, of total N fertilizer applied to all crops in the United States, and 13% and 29%, respectively, of total N fertilizer applied to all crops in European countries (Heffer, 2013).

4.4. Uncertainties and future work

Although other studies focused on regional and global estimates of NH_3 emissions from synthetic N fertilizer application, large uncertainties associated with estimation approaches still remain. A process-based dynamic ecosystem model is a fundamental means to investigate agricultural system response to N fertilizer inputs as impacted by all environmental factors. Compared to static EFs in the IPCC Tier 1 guideline, results from our DLEM-Bi- NH_3 model could provide estimates of annual NH_3 emission fluctuations as affected by climate factors to better reflect real NH_3 volatilization processes. However, uncertainties in this study should be associated with N fertilizer datasets and timing of N fertilizer applications should be addressed in future work.

Ammonia volatilization from croplands is sourced from biological degradation of organic compounds and from synthetic and organic fertilizers yielding NH_4^+ (Bouwman et al., 2002b). Thus, nitrogen fertilizer types can have significant impacts on NH_3 volatilization processes. As indicated in Nishina et al. (2017), synthetic N fertilizer consists of NH_4^+ and nitrate (NO_3^-), but the $\text{NH}_4^+/\text{NO}_3^-$ ratio in N fertilizer inputs shows obvious differences at spatiotemporal scales. Our study treated N fertilizer as a total input for NH_3 volatilization regardless of the fraction of NH_4^+ and did not distinguish N fertilizer type (Bash et al., 2013; Fu et al., 2015). In future studies, identifying N fertilizer types and treating them as different N sources would be desirable since our assumption could overestimate global NH_3 emissions.

Timing of N fertilizer application can also be a major factor that controls NH₃ volatilization from soils. Pinder et al. (2004) indicated that the greatest uncertainty in NH₃ emissions are attributable to farming practices. In the DLEM, fertilizer was applied one to four times per year based on field experiments and literature review (Xu et al., 2018a). Except for China and North America, most regions had a one-time fertilizer application, which could introduce large uncertainties in global NH₃ emission estimates (Table 7-3). Furthermore, variation in N fertilizer application timing could affect monthly NH₃ emissions at regional scales. Xu et al. (2015) indicated higher NH₃ emissions in China during summer (June to August) and autumn (September to November) with a peak observed in July that was in agreement with findings of (Zhang et al., 2011). However, those results were inconsistent with the seasonal emission patterns reported by Fu et al. (2015) and Huang et al. (2012). Fu et al. (2015) pointed out that difficulties capturing exact fertilization dates could cause the large discrepancy among studies on seasonal NH₃ estimates in China. Gilliland et al. (2003, 2006) investigated seasonal NH₃ emissions for the continental United States and found that emissions were highest in summer followed by spring since fertilizer application activity peaks during these seasons. Thus, since seasonal NH₃ emissions are heavily dependent on fertilizer application date, more information on fertilization timing from field operations is needed to minimize uncertainties.

This study provided evidence that climate change could significantly accelerate NH₃ emissions from agricultural systems. However, few studies have focused on NH₃ emissions under future conditions. Sutton et al. (2013) predicted that a 5°C warming could increase global NH₃ emissions by 40%. Sensitivity tests conducted by Riddick et al. (2016) also support potential accelerated global NH₃ emissions due to warming. However, those studies did not consider other factors that could affect NH₃ emissions from soils when attempting to predict the responses of NH₃

emissions to global warming. In future work, a multi-factor environmental change framework is required to more accurately predict NH₃ emissions at global and regional scales.

Table 7-3. N fertilizer uses in different regions across the globe.

Region	Crop types	Fertilizer timing	References
North America	corn, soybean, rice, wheat, cotton, barley,	Two to four times	(Beard and Hoover, 1971; Cooter et al., 2012; Fehr et al., 1971; Guy and Gareau, 1998; Karlen et al., 1996; Ottman, 2012; Reese and Buss, 1992; Schmitt et al., 2001; Wood et al., 1993)
Europe	wheat, corn, barley, potato	Two to three times	(Alluvione et al., 2010; Brentrup et al., 2004; Kunzová and Hejcman, 2009; Lopez-Bellido et al., 2007)
South America	corn, barley, rice, soybean, sugarcane, sunflower, millet, pulses, wheat	Zero to three times	(Brentrup et al., 2004; Carvalho et al., 2007; Galantini et al., 2000; Gutiérrez-Boem et al., 2004; Hungria et al., 2006; Jantalia et al., 2008; Melaj et al., 2003; Piva et al., 2012; Rozas et al., 2004)
Africa	corn, millet, sorghum, rice, groundnut, cassava, wheat	Zero to one time	(Becker et al., 2003; Kaizzi et al., 2012; Morris et al., 2007; Nyi et al., 2014)
Australia	wheat, corn, pulses, rice	One to two times	(Afza et al., 1987)

References

- Afza, R., Hardarson, G., Zapata, F., and Danso, S.: Effects of delayed soil and foliar N fertilization on yield and N₂ fixation of soybean, *Plant and Soil*, 97, 361-368, 1987.
- Alluvione, F., Bertora, C., Zavattaro, L., and Grignani, C.: Nitrous oxide and carbon dioxide emissions following green manure and compost fertilization in corn, *Soil Science Society of America Journal*, 74, 384-395, 2010.
- Asman, W. A., Sutton, M. A., and Schjørring, J. K.: Ammonia: emission, atmospheric transport and deposition, *New phytologist*, 139, 27-48, 1998.
- Aulakh, M. S., Khera, T. S., Doran, J. W., and Bronson, K. F.: Denitrification, N₂O and CO₂ fluxes in rice-wheat cropping system as affected by crop residues, fertilizer N and legume green manure, *Biology and Fertility of Soils*, 34, 375-389, 2001.
- Bash, J., Cooter, E., Dennis, R., Walker, J., and Pleim, J.: Evaluation of a regional air-quality model with bidirectional NH₃ exchange coupled to an agroecosystem model, *Biogeosciences*, 10, 1635-1645, 2013.
- Beard, B. H. and Hoover, R. M.: Effect of Nitrogen on Nodulation and Yield of Irrigated Soybeans 1, *Agronomy journal*, 63, 815-816, 1971.
- Becker, M., Johnson, D. E., Wopereis, M. C., and Sow, A.: Rice yield gaps in irrigated systems along an agro-ecological gradient in West Africa, *Journal of Plant Nutrition and Soil Science*, 166, 61-67, 2003.
- Behera, S. N., Betha, R., and Balasubramanian, R.: Insights into chemical coupling among acidic gases, ammonia and secondary inorganic aerosols, *Aerosol and Air Quality Research*, 13, 1282-U1414, 2013.
- Beusen, A., Bouwman, A., Heuberger, P., Van Drecht, G., and Van Der Hoek, K.: Bottom-up uncertainty estimates of global ammonia emissions from global agricultural production systems, *Atmospheric Environment*, 42, 6067-6077, 2008.
- Bouwman, A., Boumans, L., and Batjes, N.: Estimation of global NH₃ volatilization loss from synthetic fertilizers and animal manure applied to arable lands and grasslands, *Global biogeochemical cycles*, 16, 2002.
- Bouwman, A., Lee, D., Asman, W., Dentener, F., Van Der Hoek, K., and Olivier, J.: A global high-resolution emission inventory for ammonia, *Global biogeochemical cycles*, 11, 561-587, 1997.
- Brentrup, F., Küsters, J., Lammel, J., Barraclough, P., and Kuhlmann, H.: Environmental impact assessment of agricultural production systems using the life cycle assessment (LCA) methodology II. The application to N fertilizer use in winter wheat production systems, *European Journal of Agronomy*, 20, 265-279, 2004.
- Byun, D. and Schere, K. L.: Review of the governing equations, computational algorithms, and other components of the Models-3 Community Multiscale Air Quality (CMAQ) modeling system, *Applied Mechanics Reviews*, 59, 51-77, 2006.
- Carvalho, J., Cerri, C., Cerri, C., Feigl, B., Piccolo, M., Godinho, V., and Herpin, U.: Changes of chemical properties in an Oxisol after clearing of native Cerrado vegetation for agricultural use in Vilhena, Rondonia State, Brazil, *Soil and Tillage Research*, 96, 95-102, 2007.
- Ciais, P., Sabine, C., Bala, G., Bopp, L., Brovkin, V., Canadell, J., Chhabra, A., DeFries, R., Galloway, J., Heimann, M., Jones, C., Le Quere, C., Myneni, R., Piao, S., Thornton, P., Heinze, C., Tans, P., and Vesala, T.: Carbon and other biogeochemical cycles. In:

- Climate Change 2013: The Physical Science Basis. Contribution of Working Group I to the Fifth Assessment Report of the Intergovernmental Panel on Climate Change, Cambridge University Press, 2014.
- Cooter, E., Bash, J., Benson, V., and Ran, L.: Linking agricultural crop management and air quality models for regional to national-scale nitrogen assessments, *Biogeosciences*, 9, 4023-4035, 2012.
- Dentener, F.: Global maps of atmospheric nitrogen deposition, 1860, 1993, and 2050, Data set. Available on-line (<http://daac.ornl.gov/>) from Oak Ridge National Laboratory Distributed Active Archive Center, Oak Ridge, TN, USA, 2006. 2006.
- Erisman, J. W., Sutton, M. A., Galloway, J., Klimont, Z., and Winiwarter, W.: How a century of ammonia synthesis changed the world, *Nature Geoscience*, 1, 636-639, 2008.
- Fehr, W. R., Caviness, C. E., Burmood, D., and Pennington, J.: Stage of development descriptions for soybeans, *Glycine max (L.) Merrill*, *Crop science*, 11, 929-931, 1971.
- Fu, X., Wang, S., Ran, L., Pleim, J., Cooter, E., Bash, J., Benson, V., and Hao, J.: Estimating NH₃ emissions from agricultural fertilizer application in China using the bi-directional CMAQ model coupled to an agro-ecosystem model, *Atmospheric Chemistry and Physics*, 15, 6637-6649, 2015.
- Galantini, J., Landriscini, M., Iglesias, J., Miglierina, A., and Rosell, R.: The effects of crop rotation and fertilization on wheat productivity in the Pampean semiarid region of Argentina: 2. Nutrient balance, yield and grain quality, *Soil and Tillage Research*, 53, 137-144, 2000.
- Gruber, N. and Galloway, J. N.: An Earth-system perspective of the global nitrogen cycle, *Nature*, 451, 293-296, 2008.
- Gutiérrez-Boem, F. H., Scheiner, J. D., Rimski-Korsakov, H., and Lavado, R. S.: Late season nitrogen fertilization of soybeans: effects on leaf senescence, yield and environment, *Nutrient Cycling in Agroecosystems*, 68, 109-115, 2004.
- Guy, S. O. and Gareau, R. M.: Crop rotation, residue durability, and nitrogen fertilizer effects on winter wheat production, *Journal of Production Agriculture*, 11, 457-461, 1998.
- Heffer, P.: Assessment of fertilizer use by crop at the global level, International Fertilizer Industry Association, Paris, www.fertilizer.org/ifa/Home-Page/LIBRARY/Publication-database.html/Assessment-of-Fertilizer-Use-by-Crop-at-the-Global-Level-2006-07-2007-08.html2, 2013. 2013.
- Huang, X., Song, Y., Li, M., Li, J., Huo, Q., Cai, X., Zhu, T., Hu, M., and Zhang, H.: A high-resolution ammonia emission inventory in China, *Global biogeochemical cycles*, 26, 2012.
- Hungria, M., Franchini, J. C., Campo, R. J., Crispino, C. C., Moraes, J. Z., Sibaldelli, R. N., Mendes, I. C., and Arihara, J.: Nitrogen nutrition of soybean in Brazil: contributions of biological N₂ fixation and N fertilizer to grain yield, *Canadian Journal of Plant Science*, 86, 927-939, 2006.
- Jantalia, C. P., dos Santos, H. P., Urquiaga, S., Boddey, R. M., and Alves, B. J.: Fluxes of nitrous oxide from soil under different crop rotations and tillage systems in the South of Brazil, *Nutrient Cycling in Agroecosystems*, 82, 161-173, 2008.
- Jung, M., Henkel, K., Herold, M., and Churkina, G.: Exploiting synergies of global land cover products for carbon cycle modeling, *Remote Sensing of Environment*, 101, 534-553, 2006.

- Kaizzi, K. C., Byalebeka, J., Semalulu, O., Alou, I. N., Zimwanguyizza, W., Nansamba, A., Odama, E., Musinguzi, P., Ebanyat, P., and Hyuha, T.: Optimizing smallholder returns to fertilizer use: Bean, soybean and groundnut, *Field Crops Research*, 127, 109-119, 2012.
- Karlen, D., Hunt, P., and Matheny, T.: Fertilizer 15nitrogen recovery by corn, wheat, and cotton grown with and without pre-plant tillage on Norfolk loamy sand, *Crop science*, 36, 975-981, 1996.
- Klein Goldewijk, K., Beusen, A., Doelman, J., and Stehfest, E.: Anthropogenic land use estimates for the Holocene–HYDE 3.2, *Earth System Science Data*, 9, 927, 2017.
- Kunzová, E. and Hejcman, M.: Yield development of winter wheat over 50 years of FYM, N, P and K fertilizer application on black earth soil in the Czech Republic, *Field Crops Research*, 111, 226-234, 2009.
- Kurokawa, J., Ohara, T., Morikawa, T., Hanayama, S., Janssens-Maenhout, G., Fukui, T., Kawashima, K., and Akimoto, H.: Emissions of air pollutants and greenhouse gases over Asian regions during 2000–2008: Regional Emission inventory in ASia (REAS) version 2, *Atmospheric Chemistry and Physics*, 13, 11019-11058, 2013.
- Liu, M. and Tian, H.: China's land cover and land use change from 1700 to 2005: Estimations from high-resolution satellite data and historical archives, *Global biogeochemical cycles*, 24, 2010.
- Lopez-Bellido, R. J., Lopez-Bellido, L., Benítez-Vega, J., and Lopez-Bellido, F. J.: Tillage system, preceding crop, and nitrogen fertilizer in wheat crop, *Agronomy journal*, 99, 59-65, 2007.
- Lu, C. and Tian, H.: Global nitrogen and phosphorus fertilizer use for agriculture production in the past half century: shifted hot spots and nutrient imbalance, *Earth System Science Data*, 9, 181, 2017.
- Lu, C., Tian, H., Liu, M., Ren, W., Xu, X., Chen, G., and Zhang, C.: Effect of nitrogen deposition on China's terrestrial carbon uptake in the context of multifactor environmental changes, *Ecological Applications*, 22, 53-75, 2012.
- Mahajan, G., Chauhan, B., Timsina, J., Singh, P., and Singh, K.: Crop performance and water- and nitrogen-use efficiencies in dry-seeded rice in response to irrigation and fertilizer amounts in northwest India, *Field Crops Research*, 134, 59-70, 2012.
- Massad, R.-S., Nemitz, E., and Sutton, M.: Review and parameterisation of bi-directional ammonia exchange between vegetation and the atmosphere, *Atmospheric Chemistry and Physics*, 10, 10359-10386, 2010.
- Matthews, E.: Nitrogenous fertilizers: global distribution of consumption and associated emissions of nitrous oxide and ammonia, *Global biogeochemical cycles*, 8, 411-439, 1994.
- Melaj, M. A., Echeverría, H. E., Lopez, S. C., Studdert, G., Andrade, F., and Bárbaro, N. O.: Timing of nitrogen fertilization in wheat under conventional and no-tillage system, *Agronomy Journal*, 95, 1525-1531, 2003.
- Morris, M., Kelly, V. A., Kopicki, R. J., and Byerlee, D.: Fertilizer use in African agriculture: Lessons learned and good practice guidelines, *The World Bank*, 2007.
- NASS, U., 2010. 2010.
- Nemitz, E., Sutton, M. A., Schjoerring, J. K., Husted, S., and Wyers, G. P.: Resistance modelling of ammonia exchange over oilseed rape, *Agricultural and Forest Meteorology*, 105, 405-425, 2000.

- Nishina, K., Ito, A., Hanasaki, N., and Hayashi, S.: Reconstruction of spatially detailed global map of NH₄⁺ and NO₃⁻ application in synthetic nitrogen fertilizer, *Earth System Science Data*, 9, 149, 2017.
- Nyi, T., Mucheru-Muna, M., Shisanya, C., Lodi-lama, J., Mutuo, P., Pypers, P., and Vanlauwe, B.: Effect of delayed cassava planting on yields and economic returns of a cassava-groundnut intercrop in the Democratic Republic of Congo, 2014. 2014.
- Olivier, J. G. J., Jm, B., Peters, J. A., Bakker, J., Visschedijk, A. J., and Bloos, J. J.: Applications of EDGAR emission database for global atmospheric research, 2002. 2002.
- Ottman, M.: Nitrogen Fertilizer requirement of feed and malting barley compared to wheat, 2011, *Forage and Grain: A College of Agriculture and Life Sciences Report*, 2012. 2012.
- Pan, S., Tian, H., Dangal, S. R., Yang, Q., Yang, J., Lu, C., Tao, B., Ren, W., and Ouyang, Z.: Responses of global terrestrial evapotranspiration to climate change and increasing atmospheric CO₂ in the 21st century, *Earth's Future*, 3, 15-35, 2015.
- Pinder, R. W., Adams, P. J., and Pandis, S. N.: Ammonia emission controls as a cost-effective strategy for reducing atmospheric particulate matter in the eastern United States, *Environmental science & technology*, 41, 380-386, 2007.
- Pinder, R. W., Strader, R., Davidson, C. I., and Adams, P. J.: A temporally and spatially resolved ammonia emission inventory for dairy cows in the United States, *Atmospheric Environment*, 38, 3747-3756, 2004.
- Piva, J. T., Dieckow, J., Bayer, C., Zanatta, J. A., de Moraes, A., Pauletti, V., Tomazi, M., and Pergher, M.: No-till reduces global warming potential in a subtropical Ferralsol, *Plant and Soil*, 361, 359-373, 2012.
- Potter, P., Ramankutty, N., Bennett, E. M., and Donner, S. D.: Characterizing the spatial patterns of global fertilizer application and manure production, *Earth Interactions*, 14, 1-22, 2010.
- Reese, P. and Buss, G.: Response of dryland soybeans to nitrogen in full-season and doublecrop systems, *Journal of production agriculture*, 5, 528-531, 1992.
- Reis, S., Pinder, R., Zhang, M., Lijie, G., and Sutton, M.: Reactive nitrogen in atmospheric emission inventories, *Atmospheric Chemistry and Physics*, 9, 7657-7677, 2009.
- Ren, W., Tian, H., Tao, B., Huang, Y., and Pan, S.: China's crop productivity and soil carbon storage as influenced by multifactor global change, *Global change biology*, 18, 2945-2957, 2012.
- Riddick, S., Ward, D., Hess, P., Mahowald, N., Massad, R., and Holland, E.: Estimate of changes in agricultural terrestrial nitrogen pathways and ammonia emissions from 1850 to present in the Community Earth System Model, *Biogeosciences*, 13, 3397-3426, 2016.
- Rozas, H. R. S., Echeverría, H. E., and Barbieri, P. A.: Nitrogen balance as affected by application time and nitrogen fertilizer rate in irrigated no-tillage maize, *Agronomy Journal*, 96, 1622-1631, 2004.
- Sacks, W. J., Deryng, D., Foley, J. A., and Ramankutty, N.: Crop planting dates: an analysis of global patterns, *Global Ecology and Biogeography*, 19, 607-620, 2010.
- Schlesinger, W. H. and Hartley, A. E.: A global budget for atmospheric NH₃, *Biogeochemistry*, 15, 191-211, 1992.
- Schmitt, M. A., Lamb, J. A., Randall, G. W., Orf, J. H., and Rehm, G. W.: In-season fertilizer nitrogen applications for soybean in Minnesota, *Agronomy Journal*, 93, 983-988, 2001.
- Seitzinger, S. P. and Kroeze, C.: Global distribution of nitrous oxide production and N inputs in freshwater and coastal marine ecosystems, *Global biogeochemical cycles*, 12, 93-113, 1998.

- Sutton, M. A., Reis, S., Riddick, S. N., Dragosits, U., Nemitz, E., Theobald, M. R., Tang, Y. S., Braban, C. F., Vieno, M., and Dore, A. J.: Towards a climate-dependent paradigm of ammonia emission and deposition, *Philosophical Transactions of the Royal Society of London B: Biological Sciences*, 368, 20130166, 2013.
- Tian, H., Banger, K., Bo, T., and Dadhwal, V. K.: History of land use in India during 1880–2010: Large-scale land transformations reconstructed from satellite data and historical archives, *Global and planetary change*, 121, 78-88, 2014.
- Tian, H., Lu, C., Ciais, P., Michalak, A. M., Canadell, J. G., Saikawa, E., Huntzinger, D. N., Gurney, K. R., Sitch, S., Zhang, B., Yang, J., Bousquet, P., Bruhwiler, L., Chen, G., Dlugokencky, E., Friedlingstein, P., Melillo, J., Pan, S., Poulter B., Prinn, R., Saunio, M., Schwalm, C., and Wofsy, S.: The terrestrial biosphere as a net source of greenhouse gases to the atmosphere, *Nature*, 531, 225-228, 2016.
- Tian, H., Xu, X., Lu, C., Liu, M., Ren, W., Chen, G., Melillo, J., and Liu, J.: Net exchanges of CO₂, CH₄, and N₂O between China's terrestrial ecosystems and the atmosphere and their contributions to global climate warming, *Journal of Geophysical Research: Biogeosciences*, 116, 2011.
- Wei, Y., Liu, S., Huntzinger, D., Michalak, A., Viovy, N., Post, W., Schwalm, C., Schaefer, K., Jacobson, A., and Lu, C.: The North American carbon program multi-scale synthesis and terrestrial model intercomparison project—part 2: environmental driver data, *Geoscientific Model Development Discussions*, 6, 5375-5422, 2013.
- Wood, C., Torbert, H., and Weaver, D.: Nitrogen fertilizer effects on soybean growth, yield, and seed composition, *Journal of Production Agriculture*, 6, 354-360, 1993.
- Xu, P., Liao, Y., Lin, Y., Zhao, C., Yan, C., Cao, M., Wang, G., and Luan, S.: High-resolution inventory of ammonia emissions from agricultural fertilizer in China from 1978 to 2008, *Atmospheric Chemistry and Physics*, 16, 1207-1218, 2016.
- Xu, P., Zhang, Y., Gong, W., Hou, X., Kroeze, C., Gao, W., and Luan, S.: An inventory of the emission of ammonia from agricultural fertilizer application in China for 2010 and its high-resolution spatial distribution, *Atmospheric Environment*, 115, 141-148, 2015.
- Xu, R., Pan, S., Chen, J., Chen, G., Yang, J., Dangal, S., Shepard, J., and Tian, H.: Half-Century Ammonia Emissions From Agricultural Systems in Southern Asia: Magnitude, Spatiotemporal Patterns, and Implications for Human Health, *GeoHealth*, 2, 40-53, 2018.
- Xu, R., Tian, H., Lu, C., Pan, S., Chen, J., Yang, J., and Bowen, Z.: Preindustrial nitrous oxide emissions from the land biosphere estimated by using a global biogeochemistry model, *Climate of the Past*, 13, 977-990, 2017.
- Yan, X., Akimoto, H., and Ohara, T.: Estimation of nitrous oxide, nitric oxide and ammonia emissions from croplands in East, Southeast and South Asia, *Global change biology*, 9, 1080-1096, 2003.
- Zhang, X., Davidson, E. A., Mauzerall, D. L., Searchinger, T. D., Dumas, P., and Shen, Y.: Managing nitrogen for sustainable development, *Nature*, 528, 51-59, 2015.
- Zhang, Y., Dore, A., Ma, L., Liu, X., Ma, W., Cape, J., and Zhang, F.: Agricultural ammonia emissions inventory and spatial distribution in the North China Plain, *Environmental Pollution*, 158, 490-501, 2010.
- Zhang, Y., Luan, S., Chen, L., and Shao, M.: Estimating the volatilization of ammonia from synthetic nitrogenous fertilizers used in China, *Journal of environmental management*, 92, 480-493, 2011.

- Zhou, F., Ciais, P., Hayashi, K., Galloway, J., Kim, D.-G., Yang, C., Li, S., Liu, B., Shang, Z., and Gao, S.: Re-estimating NH₃ Emissions from Chinese Cropland by a New Nonlinear Model, *Environmental science & technology*, 50, 564-572, 2016.
- Zou, J., Huang, Y., Lu, Y., Zheng, X., and Wang, Y.: Direct emission factor for N₂O from rice–winter wheat rotation systems in southeast China, *Atmospheric Environment*, 39, 4755-4765, 2005.

Chapter 8. Rise of future ammonia emissions from global croplands

Abstract

Ammonia (NH₃) volatilization from synthetic nitrogen (N) application in croplands not only can lead to the formation of aerosols (PM_{2.5}) causing adverse health effects on human beings, but also can alter soil and water chemistry through increased amount of N deposition and hence reduce biological diversity. Previous studies mainly focused on investigating NH₃ emissions in the historical and contemporary period through using multiple approaches. The Bi-directional NH₃ exchange module (Bi-NH₃) from the Community Multi-scale Air Quality (CMAQ) model has been coupled with the Dynamic Land Ecosystem Model (DLEM) to examine NH₃ emissions due to increased N fertilizer use with consideration of multiple environmental factors (typically climate) at crop-type, regional, and global scales during the period of 1986-2005 at a spatial resolution of 0.5° × 0.5°. Results indicate that global NH₃ emissions from N fertilizer use were average of 12.4 Tg N yr⁻¹. The projected NH₃ emissions would increase by 15%-31% by the end of this century for three Representative Concentration Pathway (RCP) projections of global warming, as compared with levels during 1986-2005. The Northern Hemisphere would experience a substantial increase of NH₃ emissions by 2099, especially North America and southern Asia, under the RCP8.5 scenarios. Thus, effective mitigation strategies should be implemented by national governments to raise nitrogen use efficiency (NUE) and reduce NH₃ emissions in the future.

1. Introduction

The increasing global food demand is a stimulator to the synthetic nitrogen (N) fertilizer production and its application in agricultural systems, especially in croplands (Lassaletta et al., 2014b; Lu and Tian, 2017; Xu et al., 2019a). Previous study has indicated that N loss is more than 50% of the total N inputs (Lassaletta et al 2014), resulting in approximately 100 Tg N surplus in 2010 (Zhang et al., 2015). Synthetic N fertilizer application rates in agriculture is expected to be 260 Tg N yr⁻¹ by 2050 in the shared socioeconomic pathways of fragment scenario (SSP3) (Mogollon et al., 2018). Xu et al. (2018, 2019) have indicated that NH₃ volatilization is one of the major outlets for N losses from agricultural activities. Agriculture not only affects the Earth's radiation budget contributing N₂O emissions to atmosphere (Tian et al., 2016; Tian et al., 2018; Tian et al., 2019), but also causes adverse health effects (Lelieveld et al., 2015) and biodiversity loss (Clark and Tilman, 2008; Vitousek and Farrington, 1997). Due to the enormous NH₃ output from soils, the reaction of atmospheric NH₃ with other precursor gases forms aerosol, that is PM_{2.5}, a component that leads to 3.3 (1.61-4.81) million premature deaths per year worldwide, predominantly in Asia.

Sutton and Howard (2018) pointed out that NH₃ emissions from many countries, especially with intensive agricultural activities, would increase by 1.3 Tg N by 2030, relative to 2005. Recent results have shown that NH₃ emissions would increase 40% assuming a 5°C warming (Sutton et al., 2013). Later, Riddick et al. (2016) indicated that every 1°C increase would enhance global NH₃ emissions by up to 1 Tg N. The process-based model is an effective approach for estimating NH₃ emissions. For instance, The Flow of Agricultural Nitrogen (FAN) process model has been combined within the Community Land Model 4.5 to compute the reactive N flows and NH₃ emissions (Riddick et al., 2016). Our previous studies have incorporated the bi-directional NH₃ exchange module in CMAQ within the Dynamic Land Ecosystem Model (DLEM, Tian et al.

(2011)) (DLEM-Bi-NH₃) and applied this model to estimate NH₃ emissions from Asian and global croplands during the period of 1961–2014 (Xu et al., 2018a; Xu et al., 2019b). Previous studies mainly provide estimates of historical and contemporary NH₃ emissions. Here, driving by three different projection climate datasets, the current study applied the DLEM-Bi-NH₃ module to predict NH₃ emissions in global croplands, and investigate its spatial variations under three different scenarios during the rest of the 21st century.

2. Methodology

2.1 Input datasets and experimental design

Input datasets for the DLEM-Bi-NH₃ simulations include a natural vegetation map, land use change (LUC), synthetic N fertilizer application, atmospheric CO₂ concentration, and time series of climate at a spatial resolution of 0.5° × 0.5° during 1961-2005. These datasets for historical simulations have been described in (Xu et al., 2018b). Future climate input data are at daily steps with a spatial resolution of 0.5° × 0.5° during 2006-2099. These projection datasets include Representative Concentration Pathways (RCPs) emission scenarios: RCP2.6, RCP6.0, and RCP8.5, provided based on the Coupled Model Intercomparison Project Phase 5 (CMIP5) output of GFDL-ESM2M, IPSL-CM5A-LR, and MIROC5. The detailed description of these three datasets are documented in Frieler et al. (2017) and are also available through the Inter-Sectoral Impact Model Intercomparison Project (ISIMIP) website (<https://www.isimip.org/gettingstarted/#input-data-bias-correction>). We made bias corrections in climate variables included in these three GCMs and kept the inter-annual variations and long-term trends during 2006-2099. This implementation allows us to run simulations for two hundred years with no gap between 2005 and 2006 as the historical simulation (1900-2005) was driven by daily

climate data obtained from the Climatic Research Unit (CRU) and National Centers for Environmental Protection (NCEP) (CRU-NCEP).

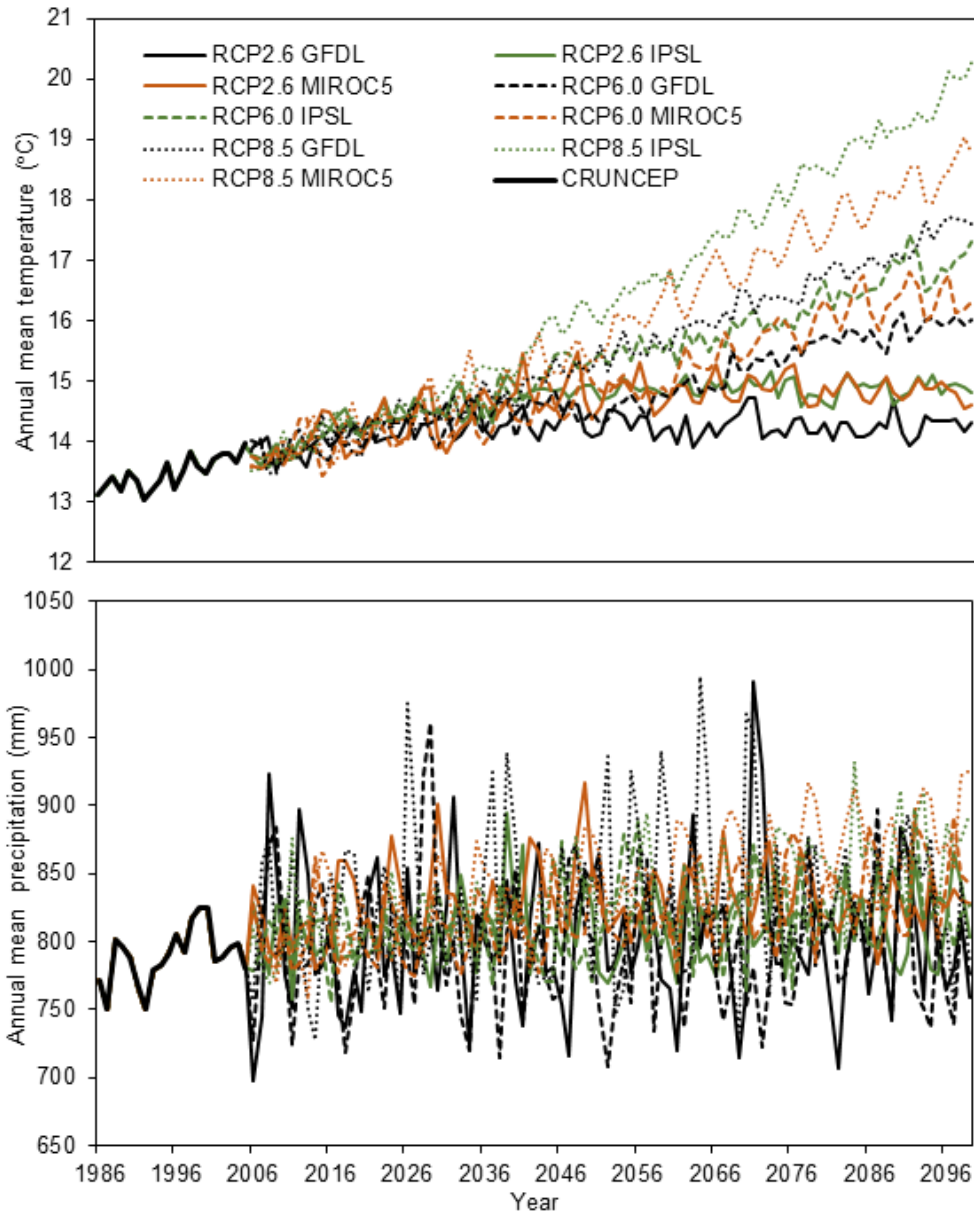


Figure 8-1. The historical and projected trends of climate changes (i.e., temperature and precipitation) in the RCP projection. Data were obtained from the CRU-NCEP and three Global Circulation Models (GCMs): GFDL-ESM2M, PSL-CM5A-LR, and MIROC5.

In the historical period, we conducted the simulation experiment driven by the CRU-NCEP climate, CO₂ concentration, N fertilizer, and LUC data during 1901-2005. Then, to investigate the climate impact, we conducted nine simulation experiments with climate projection datasets from 2006 to 2099 while holding all other input datasets at 2005 levels.

3. Results and discussions

3.1 Temporal changes of future NH₃ emissions

There appears to be a continuously increasing trend of NH₃ emissions in the RCP6.0 and RCP8.5 emission scenarios, but stabilized smaller increase in the RCP2.6 emission scenario during 2006–2099 (Figure 8-2). The modeled results indicated that NH₃ emissions would reach 16.2 ± 1.0 Tg N over the period of 2076-2099 in the RCP8.5 emission scenarios, the net average increase of which would be 3.8 ± 1.0 Tg N compared with the average value during 1986-2005. In contrast, NH₃ emissions in the RCP2.6 emission scenarios would reach up to 14.5 ± 1.1 Tg N with a net increase of 2.1 ± 1.1 Tg (16.7 % increase). This study provided evidence that climate change could significantly accelerate NH₃ emissions from the agricultural system in the coming decades in these three RCPs emission scenarios. Our estimates confirmed that global warming could significantly stimulate NH₃ volatilization from soils and worsen global air pollution in the future.

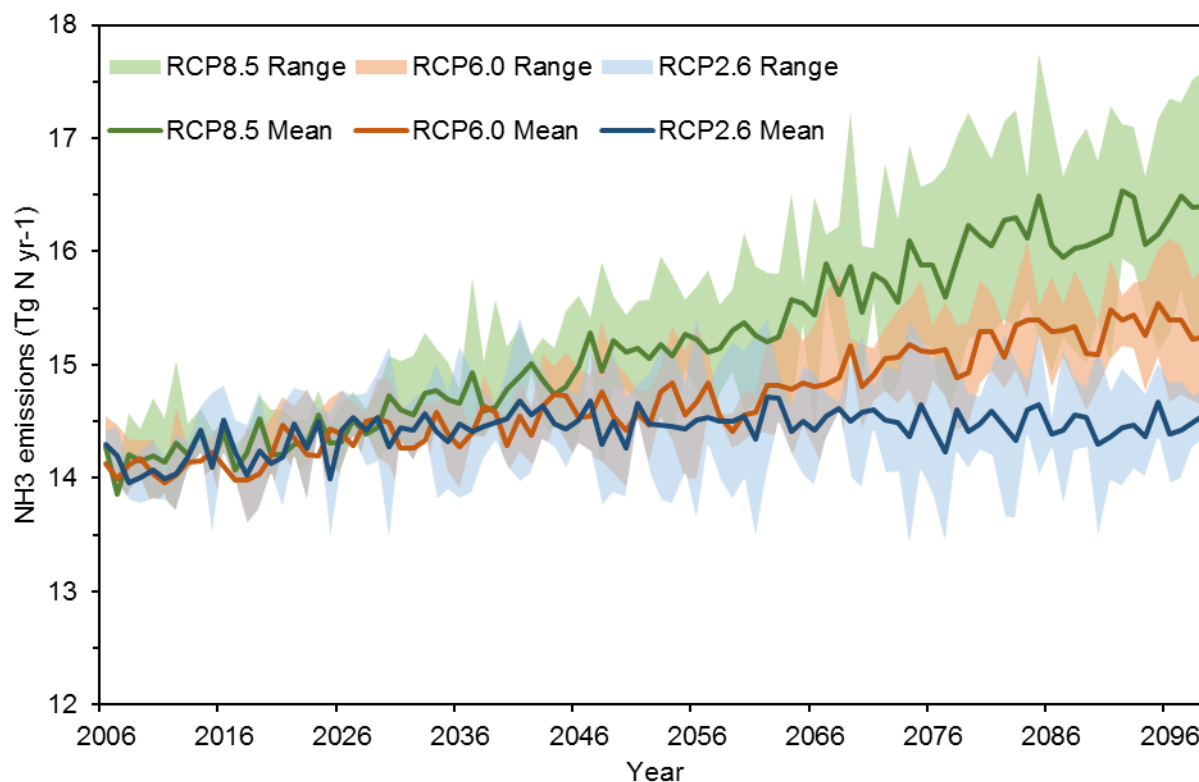


Figure 8-2. Projected global annual mean ammonia (NH_3) emissions over the period 2006-2099 driven by three GCMs. The green, orange, and blue shaded areas are 95% confidence intervals of mean NH_3 emissions driven by the RCP8.5, RCP6.0, and RCP2.6 emission scenarios, respectively.

Ammonia emission at the continental scales shows a large inter-annual variation (Figure 8-3). Southern Asia, North America and South America showed a large increase of NH_3 emissions during the period 2076-2099 in the RCP8.5 emission scenarios compared with that during 1986-2005, which was 2.6 Tg N, 0.6 Tg N, and 0.3 Tg N, respectively. In the RCP2.6 emission scenario, there still a significant increase of NH_3 emission detected in Southern Asia (1.9 Tg N) and South America (0.34 Tg N) during the period 2076-2099, while Europe shows a decline of emission (-0.3 Tg N) and North America sees a 0.07 Tg N emission. (Figure 8-3). The amount of NH_3 emissions in the RCP6.0 emission scenario is between the low RCP2.6 emission and high RCP8.5 emission scenarios. Although NH_3 emissions would increase at the end of 21st century compared

with the historical period, the amount in South America show a slight decline in these three emission scenarios during 2006-2099 (Figure 8-3).

Table 8-1. Estimates of global NH₃ emissions during 1986-2005 and over the 21st century in the three RCP scenarios. Unit: Tg N yr⁻¹

Historical (1986-2005)		12.4				
Future	RCP2.6	(+%)	RCP6.0	(+%)	RCP8.5	(+%)
2006-2025	14.2±0.9	14.5	14.2±0.4	14.1	14.3±0.4	15.0
2026-2050	14.5±1.0	16.7	14.5±0.5	16.8	14.8±0.7	19.1
2051-2075	14.5±1.2	17.1	14.8±0.6	19.4	15.5±0.9	24.6
2076-2099	14.5±1.1	16.7	15.3±0.6	23.2	16.2±1.0	30.5

3.2 Spatial pattern of future NH₃ emissions

At the global scale, most regions are expected to experience an increase in NH₃ emission, but with a large spatial heterogeneity in these three emission scenarios. Spatial results show that the entire Earth would show positive responses, in which the significant increase would occur in high latitudes in the RCP8.5 emission scenarios, especially in the Midwestern US, India, and the North China Plain. Southern Asia, typically India and China, would present a substantial increase of NH₃ emission at different level in these three different RCPs emission scenarios. Europe with declining NH₃ emissions in the RCP2.6 emission scenarios would shift to NH₃ sources in the RCP8.5 scenarios (Figure 8-4). The Great Plain in the United States would show a significant increase of NH₃ emissions in the RCP8.5 emission scenario.

It is of great importance that climate effects should be considered while estimating NH₃ emissions. Through performing the with/without climate and temperature-only simulations, we could evaluate the contribution of different climate factors to the increase in global NH₃ emission

during the historical period. Historical simulation results indicated that temperature was the dominant factor that boosted the emission increase (Xu et al. 2019). In terms of foreseeable future global NH₃ emissions, this study has provided the first series of projections based on the RCP2.6, RCP6.0, and RCP8.5 emission scenarios. We found that the annual temperature in RCP8.5 climate scenarios increased about 5°C in high latitudes (+50°), even larger in high latitude regions of North America, compared to that of RCP2.6 emission scenarios. Due to the enlarged warming effect in high latitudes, these regions could become larger sources of future NH₃ emissions, especially in North America and Europe. Sensitivity test conducted in Riddick et al. (2016) also supported that warming effect could accelerate global NH₃ emissions. Our prediction indicates that global NH₃ emission would continuously increase under the context of global warming in the remainder of the 21st century.

3.3 Uncertainty and future work

The projected NH₃ emission remains far from certain. In our projections, we only quantified the likely NH₃ emission patterns under future climate scenarios but did not consider the contributions of other changing environmental factors, such as land-use and land-management practices. We held the rates of N fertilizer unchanged since 2005 due to a lack of suitable future scenario data, which could cause large underestimation of NH₃ emissions in the rest of the 21st century. In future work, it is necessary to predict NH₃ emission within a multi-factor environmental change framework such as LUC and N fertilizer application (Tian et al., 2011).

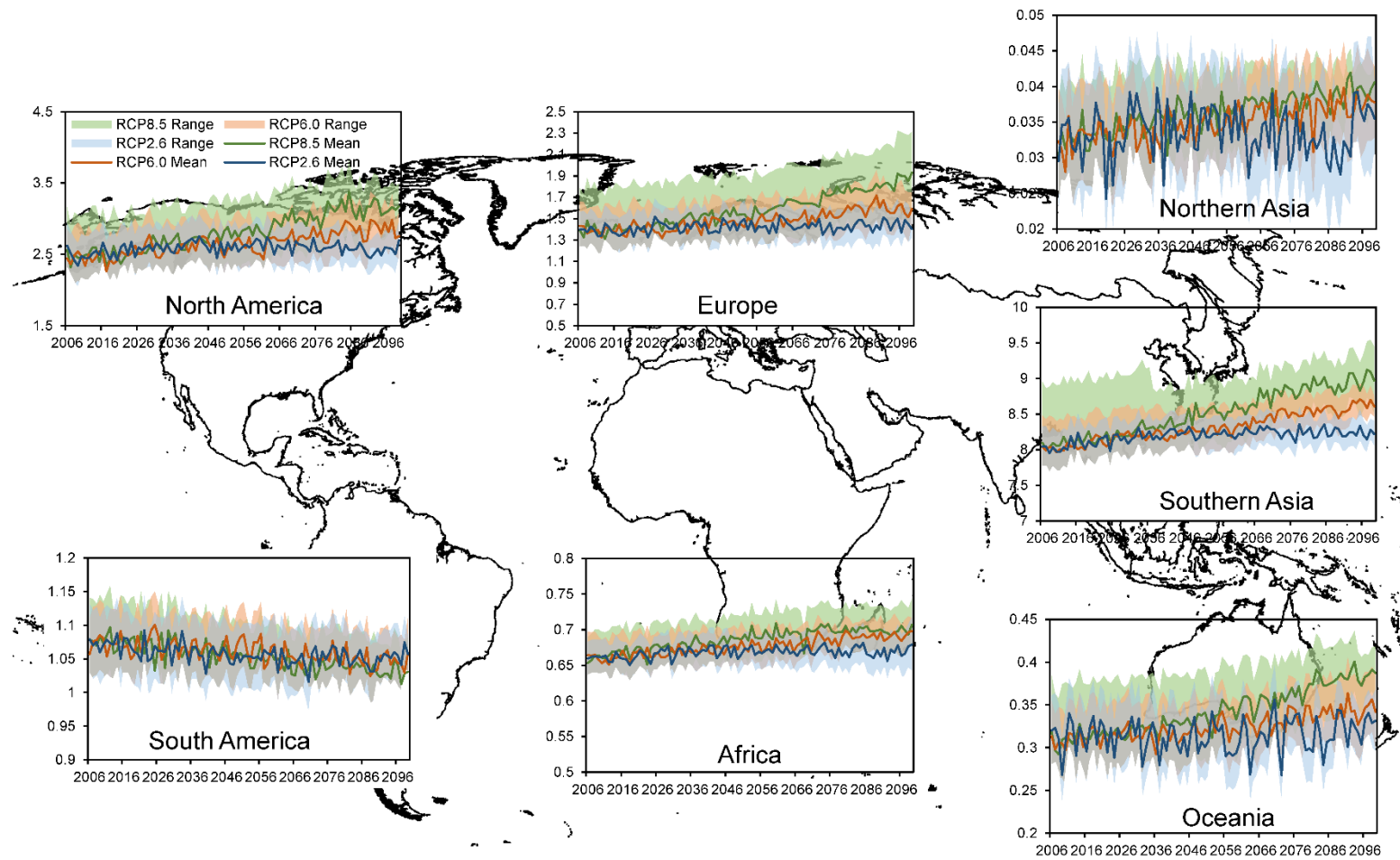


Figure 8-3. Estimates of NH₃ emission at continental scales during the period 2006-2099. All units are Tg N yr⁻¹.

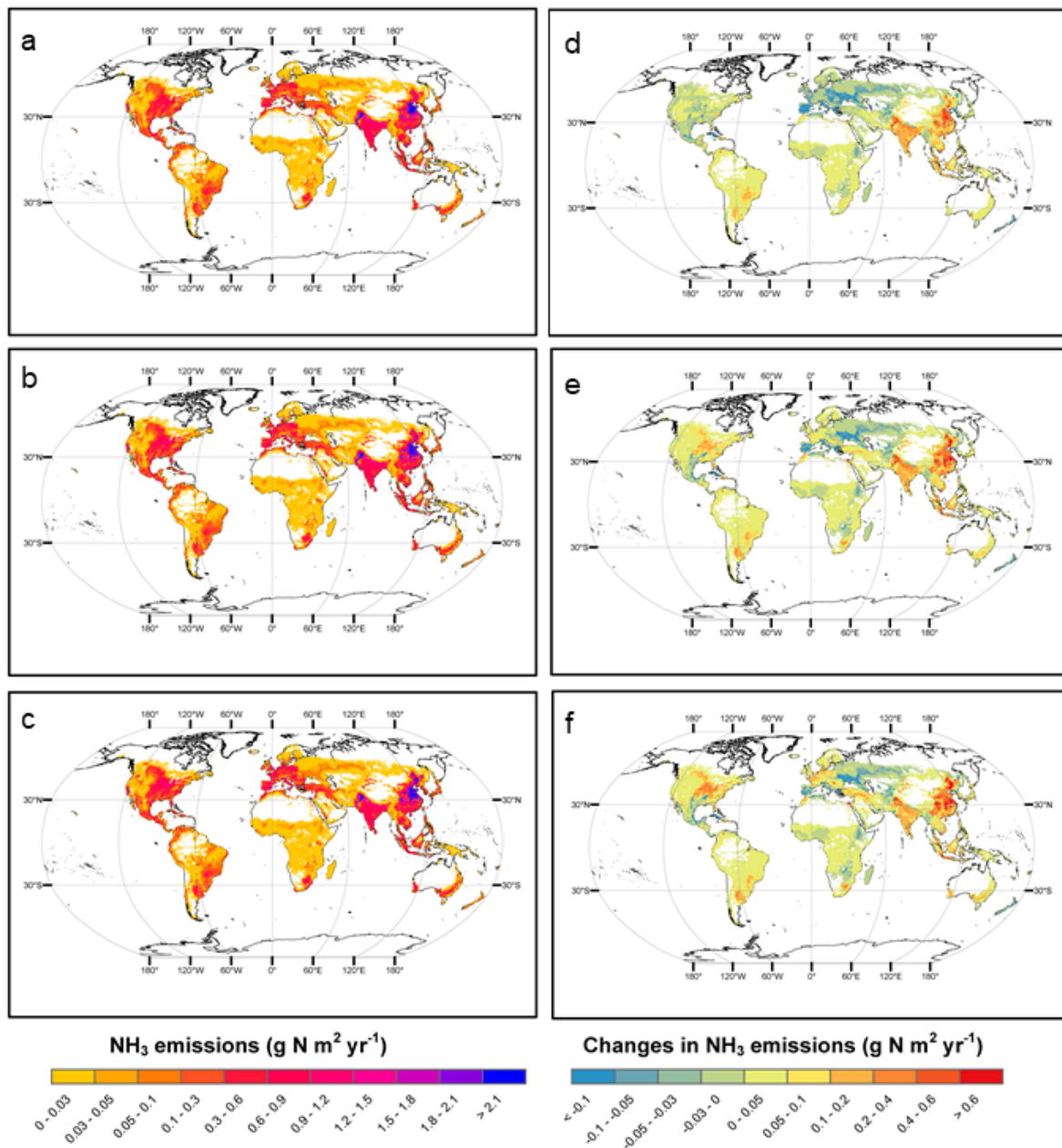


Figure 8-4. The spatial distribution of annual mean NH_3 emission (a, b, c) and the difference (d, e, f) between the future prediction and the period 1986-2005 forced by three GCMS in three RCPs emission scenarios.

4. Conclusion

Our projections based on the DLEM-Bi-NH₃ module pointed out that NH₃ emissions, solely driven by climate change, would continue to increase and be a major influence on the increase of N deposition and atmospheric aerosol concentration in this century. High latitudinal regions would be more sensitive to the effect of global warming; as a result, these regions could become larger sources for future NH₃ emissions, especially the Midwestern United States, and Europe. More model-model inter-comparisons and ground-based observations are needed to reduce uncertainties in quantifying global and regional NH₃ emissions in the 21st century. In terms of future projections, it is important to combine all environmental factors to accurately forecast NH₃ emissions.

References

- Clark, C. M. and Tilman, D.: Loss of plant species after chronic low-level nitrogen deposition to prairie grasslands, *Nature*, 451, 712-715, 2008.
- Frieler, K., Lange, S., Piontek, F., Reyer, C. P. O., Schewe, J., Warszawski, L., Zhao, F., Chini, L., Denvil, S., Emanuel, K., Geiger, T., Halladay, K., Hurtt, G., Mengel, M., Murakami, D., Ostberg, S., Popp, A., Riva, R., Stevanovic, M., Suzuki, T., Volkholz, J., Burke, E., Ciais, P., Ebi, K., Eddy, T. D., Elliott, J., Galbraith, E., Gosling, S. N., Hattermann, F., Hickler, T., Hinkel, J., Hof, C., Huber, V., Jägermeyr, J., Krysanova, V., Marcé, R., Müller Schmied, H., Mouratiadou, I., Pierson, D., Tittensor, D. P., Vautard, R., van Vliet, M., Biber, M. F., Betts, R. A., Bodirsky, B. L., Deryng, D., Frohking, S., Jones, C. D., Lotze, H. K., Lotze-Campen, H., Sahajpal, R., Thonicke, K., Tian, H., and Yamagata, Y.: Assessing the impacts of 1.5 °C global warming – simulation protocol of the Inter-Sectoral Impact Model Intercomparison Project (ISIMIP2b), *Geosci. Model Dev.*, 10, 4321-4345, 2017.
- Lassaletta, L., Billen, G., Grizzetti, B., Garnier, J., Leach, A. M., and Galloway, J. N.: Food and feed trade as a driver in the global nitrogen cycle: 50-year trends, *Biogeochemistry*, 118, 225-241, 2014.
- Lelieveld, J., Evans, J., Fnais, M., Giannadaki, D., and Pozzer, A.: The contribution of outdoor air pollution sources to premature mortality on a global scale, *Nature*, 525, 367-371, 2015.
- Lu, C. and Tian, H.: Global nitrogen and phosphorus fertilizer use for agriculture production in the past half century: shifted hot spots and nutrient imbalance, *Earth System Science Data*, 9, 181, 2017.
- Riddick, S., Ward, D., Hess, P., Mahowald, N., Massad, R., and Holland, E.: Estimate of changes in agricultural terrestrial nitrogen pathways and ammonia emissions from 1850 to present in the Community Earth System Model, *Biogeosciences*, 13, 3397-3426, 2016.
- Sutton, M. and Howard, C. M.: Ammonia maps make history, *Nature*, 2018. 2018.
- Sutton, M. A., Reis, S., Riddick, S. N., Dragosits, U., Nemitz, E., Theobald, M. R., Tang, Y. S., Braban, C. F., Vieno, M., and Dore, A. J.: Towards a climate-dependent paradigm of ammonia emission and deposition, *Philosophical Transactions of the Royal Society of London B: Biological Sciences*, 368, 20130166, 2013.
- Tian, H., Lu, C., Ciais, P., Michalak, A. M., Canadell, J. G., Saikawa, E., Huntzinger, D. N., Gurney, K. R., Sitch, S., Zhang, B., Yang, J., Bousquet, P., Bruhwiler, L., Chen, G., Dlugokencky, E., Friedlingstein, P., Melillo, J., Pan, S., Poulter B., Prinn, R., Saunio, M., Schwalm, C., and Wofsy, S.: The terrestrial biosphere as a net source of greenhouse gases to the atmosphere, *Nature*, 531, 225-228, 2016.
- Tian, H., Xu, X., Lu, C., Liu, M., Ren, W., Chen, G., Melillo, J., and Liu, J.: Net exchanges of CO₂, CH₄, and N₂O between China's terrestrial ecosystems and the atmosphere and their contributions to global climate warming, *Journal of Geophysical Research: Biogeosciences*, 116, 2011.

- Tian, H., Yang, J., Lu, C., Xu, R., Canadell, J. G., Jackson, R., Arneth, A., Chang, J., Chen, G., and Ciais, P.: The global N₂O Model Intercomparison Project (NMIP): Objectives, Simulation Protocol and Expected Products, *Bulletin of the American Meteorological Society*, 99, 1231-1251, 2018.
- Tian, H., Yang, J., Xu, R., Lu, C., Canadell, J. G., Davidson, E. A., Jackson, R. B., Arneth, A., Chang, J., and Ciais, P.: Global soil nitrous oxide emissions since the preindustrial era estimated by an ensemble of terrestrial biosphere models: Magnitude, attribution, and uncertainty, *Global Change Biology*, 25, 640-659, 2019.
- Vitousek, P. M. and Farrington, H.: Nutrient limitation and soil development: experimental test of a biogeochemical theory, *Biogeochemistry*, 37, 63-75, 1997.
- Xu, R., Pan, S., Chen, J., Chen, G., Yang, J., Dangal, S., Shepard, J., and Tian, H.: Half-Century Ammonia Emissions From Agricultural Systems in Southern Asia: Magnitude, Spatiotemporal Patterns, and Implications for Human Health, *GeoHealth*, 2, 40-53, 2018a.
- Xu, R., Tian, H., Pan, S., Dangal, S. R., Chen, J., Chang, J., Lu, Y., Skiba, U. M., Tubiello, F. N., and Zhang, B.: Increased nitrogen enrichment and shifted patterns in the world's grassland: 1860–2016, *Earth System Science Data*, 11, 175-187, 2019a.
- Xu, R., Tian, H., Pan, S., Prior, S. A., Feng, Y., Batchelor, W. D., Chen, J., and Yang, J.: Global ammonia emissions from synthetic nitrogen fertilizer applications in agricultural systems: empirical and process-based estimates and uncertainty, *Global Change Biology*, 25, 314-326, 2019b.

Chapter 9. Conclusions and future works

This study focuses on the perturbation of the global N cycle and aims to examine the N-containing gas emissions from natural and agricultural ecosystems. A process-based Dynamic Land Ecosystem Model (DLEM) was coupled with the bi-directional NH₃ exchange module (Bi-NH₃) to investigate N₂O emissions and NH₃ volatilizations from natural and agricultural soils over the historical and future periods. Multiple environmental factors (e.g., climate, land use change, atmospheric N deposition) together with synthetic N fertilizer and manure N application were used to drive the DLEM simulations. In the meanwhile, time-series gridded datasets for N fertilizer and manure N inputs were constructed to evaluate the amount of reactive N that was introduced into agricultural systems at regional and global scales during 1860-2016.

The major conclusions are as follows:

(1) Using the process-based land ecosystem model DLEM, we estimated that pre-industrial N₂O emission from the terrestrial biosphere is 6.20 Tg N yr⁻¹. Tropical ecosystem was the dominant contributor of global N₂O emissions. This estimate could be used as a reference to estimate net human-induced emissions in the contemporary period. Based on the study in the pre-industrial era, we provided a robust estimate of N₂O emissions from global croplands as the globally increasing food demand has boosted N₂O emissions to the atmosphere as the intensive agricultural inorganic/organic N inputs by humans. Across the globe, N₂O emissions due to N fertilizer increased from 0.3 to 2.3 Tg N yr⁻¹ during 1961–2014. Additionally, elevated CO₂,

atmospheric N deposition, and climate change caused the increase of N₂O emissions with different magnitudes.

(2) At the global scale, NH₃ emitted from N fertilizer applications in global croplands increased from 1.9±0.03 to 16.7±0.5 Tg N yr⁻¹ between 1961 and 2010. Southern Asia contributed to more than 50% of total global NH₃ emissions since the 1980s, followed by North America and Europe. In addition, results indicate that ignoring environmental factors in the empirical methods (constant emission factor in the IPCC Tier 1 guideline) could underestimate NH₃ emissions in the context of global warming, with the highest difference (i.e., 6.9 Tg N yr⁻¹) occurring in 2010. At the regional scale, together with manure N application in southern Asia, NH₃ emissions from N inputs to croplands reached 21.3±3.9 Tg N yr⁻¹. Ammonia emissions from China and India together accounted for 64% of the total amount in SA during 2000–2014. In the context of future climate change, global NH₃ emissions would increase by 15%-31% by the end of this century for three Representative Concentration Pathway (RCP) projections of global warming. The Northern Hemisphere would experience a substantial increase of NH₃ emissions by 2099, especially North America and southern Asia, under the RCP8.5 scenarios.

(3) Manure and fertilizer N inputs to permanent meadows and pastures (pastures and rangelands areas) globally have increased rapidly since the industrial revolution. This is the first study that has attempted to consider major sources of anthropogenic N inputs in permanent meadows and pastures and hence generated time-series gridded datasets of manure and fertilizer N application rates, and manure deposition rate during 1860–2016. The hotspots of grassland N application shifted from European countries to southern Asia, specifically China and India in the early 21st century.

Uncertainty along with future work needs are described in this study. In the pre-industrial era, although input datasets could play a significant role in the variety of the model output, it is difficult to obtain accurate datasets back to the year 1860. Large uncertainty still exists in the DLEM simulation associated with model structures and parameters applied in simulations. There are five key parameters (i.e., maximum nitrification and denitrification rates, N fixation rate, and the adsorption coefficient for soil NH_4^+ and NO_3^-) dominated N_2O production and fluxes in soils. For simulating N-containing gas emissions since the widely spread of N fertilizer and manure, large uncertainties associated with input data should be addressed. For example, the spatial variations of N fertilizer use rates are significantly divergent among datasets, which was mainly attributed to different land use datasets and methodologies that were used to generate these datasets. The concentration of NH_4^+ and NO_3^- is a significant factor that affects the production of $\text{N}_2\text{O}/\text{NH}_3$ in agricultural soils. The ratio of NH_4^+ and NO_3^- varied with different types of N fertilizer. Different N fertilizer types have different EFs, and thus could result in different rates of NH_3 emissions. A constant EF for NH_3 emissions from manure was used in this study, which might introduce more uncertainty in our estimate compared to other studies that have used region-based or animal species-based EFs. In addition, the N management strategies in croplands should be considered. Timing of N fertilizer application can also be a major factor that controls $\text{N}_2\text{O}/\text{NH}_3$ emissions from soils. Variation in N fertilizer/manure application timing could affect monthly $\text{N}_2\text{O}/\text{NH}_3$ emissions at regional scales. Few sites were available for studying N_2O emissions from manure application alone. Most sites collected for the calibration included not only manure application, but N fertilizer use. Thus, it is hard to separate the impact of N fertilizer from manure.

In our future work, more *in situ* experiments are needed for more accurate estimates of N fertilizer and manure N-induced $\text{N}_2\text{O}/\text{NH}_3$ emissions. For N-containing gases prediction, a multi-

factor environmental change framework is required to more accurately predict NH_3 emissions at global and regional scales. While improving N input datasets in agricultural systems, it is vital to better understanding land use changes and human management strategies. Meanwhile, other human-induced sources of N inputs to pastures and rangelands were not included in this study, which may underestimate total N received globally. More information is needed to improve these datasets in our further work.